

Telomere Length and Distribution in Three Developmental Stages

A thesis submitted to the University of Kent for the degree of

DOCTOR OF PHILOSOPHY

In the Faculty of Sciences

2014

Kara Jane Turner

School of Biosciences

Declaration

No part of this thesis has been submitted in support of an application for any degree or qualification of the University of Kent or any other University or Institute of learning.

Kara Jane Turner

Acknowledgements

First and foremost I would like to say a huge thank you to my friend and supervisor Professor Darren Griffin for his continued support and encouragement throughout my education and career so far. Darren has opened the door to several fantastic opportunities in the eight years that I've known him and I'll always be grateful of these.

A very special thanks to my collaborators, particularly Vimal Vasu whose ideas and contributions were pivotal to my work. My PhD would not have been possible without efforts from Vimal, Shermi George and John Greenall in newborn patient recruitment, Hannah Rouse and Colleen Lynch in polar body and embryo sample recruitment, and Dimitra Christopikou and Alan Thornhill in semen sample recruitment. Of course a big thank you also goes to all the patients whom participated in each study.

Thank you very much to all members of the Griffin lab both past and present, especially Katie Fowler, Becki Gould, Becky O'Connor, Maryam Sadraie, Gothami Fonseca, Pamela Lithgow, Mike Romanov and Claudia Rathje. You have all contributed in your own way to making a warm working environment, complete with a lot of laughs. An additional thanks goes to all of the people whom I have met over the years that have gone out of their way to help me, particularly Ben Skinner, Dan Mulvihill, Matt Johnson, Veryan Codd, Souraya Jaroudi, Maryam Ojani, Steven Trim and Steven Poon.

Thank you to the MRC, Digital Scientific UK, East Kent Hospitals Trust and the University of Kent for funding my PhD. I would especially like to thank Michael Ellis (Digital Scientific UK) for providing prompt solutions to my ridiculous imaging woes!

A special thanks to my closest friends Sarah and Michael Taylor, and Eimear and Paul Skeffington. You've all done a fantastic job of reassuring me when things haven't gone quite to plan, and helping me celebrate when they have!

An extra special thank you to my best friend and partner Dean Judge for putting up with me over the last four and a half years, and for being extremely supportive and understanding during what has been the biggest challenge of my career so far.

Finally, all my love and thanks to my parents Alan and Eileen Turner and my siblings Joanne Worsell and Steven Turner. I owe all of my achievements to your unconditional support and your indisputable belief in me. I know I can depend on you for absolutely anything, and for that I am extremely grateful.

Dedicated to my wonderful parents, Alan and Eileen

Table of Contents

Declaration.....	ii
Acknowledgements.....	iii
List of figures.....	xiii
List of tables	xxiii
List of equations	xxv
Abbreviations.....	xxvi
Abstract.....	xxx
1 Introduction: Telomere function and sexual reproduction.....	1
1.1 The structure, function and regulation of the telomere.....	1
1.1.1 The structure of the telomere.....	1
1.1.1.1 The sequence of the telomere.....	1
1.1.1.2 The T-loop.....	2
1.1.1.3 The shelterin complex	4
1.1.2 Telomere function.....	6
1.1.2.1 Telomere DNA replication: The ‘end replication problem’.....	6
1.1.2.1.1 Senescence.....	8
1.1.2.2 Telomeres and genome stability:.....	9
1.1.2.3 Telomeres and nuclear organisation.....	11
1.1.2.3.1 The Rab1 configuration.....	12
1.1.2.3.2 The ‘chromocentric’ model of nuclear organisation	14
1.1.2.3.3 Other models of nuclear organisation	14
1.1.2.4 Telomeres and cell division.....	15
1.1.3 Telomere length regulation.....	15
1.1.3.1 Telomerase mediated telomere maintenance	16
1.1.3.2 Alternative lengthening of telomeres	19
1.1.3.2.1 Telomere lengthening by homologous recombination.....	19
1.1.3.2.2 Telomere lengthening by retrotransposition.....	20
1.1.3.2.3 The telomere position effect.....	21
1.2 Normal and dysfunctional telomere homeostasis	22
1.2.1 Normal telomere homeostasis and ageing	22
1.2.1.1 Telomere homeostasis during embryogenesis.....	23
1.2.1.2 Telomere homeostasis during fetal development.....	25
1.2.1.3 Telomere homeostasis in the newborn	26

1.2.1.4	Telomere homeostasis beyond birth.....	27
1.2.1.5	Other factors affecting telomere homeostasis	28
1.2.1.6	Telomere homeostasis in premature ageing diseases	30
1.2.2	The role of abnormal telomere homeostasis in tumorigenesis	30
1.2.3	Dysfunctional telomere homeostasis and cancer	32
1.2.4	Dysfunctional telomere homeostasis in other diseases.....	32
1.3	Gametogenesis	35
1.3.1	Meiosis.....	35
1.3.2	Spermatogenesis	37
1.3.3	Oogenesis.....	38
1.4	Telomere function in gametogenesis	39
1.4.1	Sex specific telomere regulation in gametogenesis	41
1.4.1.1	Telomere distribution in male gametogenesis.....	41
1.4.1.2	Telomere homeostasis in spermatogenesis.....	43
1.4.1.3	Telomeres distribution in oogenesis.....	44
1.4.1.4	Telomere homeostasis in oogenesis	45
1.5	Telomere function beyond fertilisation.....	46
1.5.1	Telomere distribution in fertilisation and embryogenesis	47
1.5.2	Telomere homeostasis in fertilisation and embryogenesis	48
1.6	Infertility	49
1.7	Assisted reproductive technologies.....	51
1.7.1	Preimplantation genetic screening.....	53
1.7.1.1	Techniques in PGS	55
1.7.1.2	PGS controversy.....	57
1.8	Telomere assessment: A novel tool in PGS?	58
1.8.1	Telomere regulation in sperm of infertile males.....	58
1.8.1.1	Telomere distribution in male infertility	58
1.8.1.2	Telomere homeostasis in male infertility	60
1.8.2	Telomere regulation in oocytes of infertile females	61
1.8.2.1	Telomere distribution in female infertility	61
1.8.2.2	Telomere homeostasis in female infertility	61
1.8.2.3	Telomere length and the maternal age affect	63
1.8.3	Leukocyte telomere length and infertility.....	65
1.8.4	Telomere dynamics and developmental outcome in ART	66
1.8.5	Telomere length in pregnancy complications.....	68

1.8.5.1	Telomere length in the premature infant	70
1.9	Techniques for telomere assessment.....	71
1.9.1	Measuring telomere length	71
1.9.1.1	Telomere restriction fragment analysis	71
1.9.1.2	Slot blot analysis and hybridisation protection assay.....	73
1.9.1.3	Quantitative real-time polymerase chain reaction.....	74
1.9.1.4	Single telomere length analysis.....	76
1.9.1.5	Quantitative fluorescence in situ hybridisation	79
1.9.1.6	Primed in situ labelling.....	81
1.9.2	Measuring telomere distribution.....	82
1.10	Thesis rationale	84
1.11	Thesis Aims	85
2	Materials and Methods	86
2.1	Materials	86
2.2	Methods.....	87
2.2.1	Sperm sample preparation	87
2.2.2	Telomere detection in sperm: FISH.....	87
2.2.2.1	Slide preparation.....	88
2.2.2.2	Ageing of slides and pre-hybridisation washes	88
2.2.2.3	Probe preparation and DNA denaturation	88
2.2.2.4	Post-hybridisation washes and detection.....	89
2.2.2.5	Telomere detection after sperm nuclear decondensation	90
2.2.2.5.1	Sperm nuclear decondensation with dithiothreitol.....	90
2.2.2.5.2	Sperm nuclear decondensation with sodium hydroxide.....	90
2.2.2.6	2D image analysis of telomeric signals	90
2.2.2.7	3D image analysis	91
2.2.3	Immunofluorescence localisation of H2BFWT in sperm.....	92
2.2.3.1	2D H2BFWT signal localisation	93
2.2.3.2	3D H2BFWT signal localisation	94
2.2.4	Telomere and H2BFWT co-localisation.....	94
2.2.4.1	Telomere detection by FISH	94
2.2.4.2	H2BFWT detection by immunofluorescence.....	95
2.2.4.3	2D Fluorescence microscopy	95
2.2.5	Sperm chromomycin A ₃ staining.....	95
2.2.6	Optimisation of qRT-PCR relative telomere length analysis	96

2.2.6.1	Setting up qRT-PCR and cycling conditions	98
2.2.7	Agarose gel electrophoresis	99
2.2.8	qRT-PCR analysis of telomere length in single cells	100
2.2.8.1	qRT-PCR components.....	100
2.2.8.2	Setting up the qRT-PCR reaction.....	102
2.2.8.3	qRT-PCR cycling conditions.....	102
2.2.9	Validation of telomere length analysis in single cells	104
2.2.9.1	Whole genome amplification of control DNA.....	105
2.2.9.2	WGA product purification.....	106
2.2.9.3	Determination of relative telomere length.....	107
2.2.10	qRT-PCR analysis of relative telomere length in single cells	107
2.2.11	DNA extraction from whole blood	108
2.2.11.1	Red and white blood cell lysis.....	108
2.2.11.2	RNA degradation and protein precipitation	108
2.2.11.3	DNA precipitation	109
2.2.12	Average relative telomere length analysis in newborns	109
2.2.13	Lymphocyte metaphase preparation	110
2.2.14	L5178Y-R and LY5178Y-S cell culture.....	111
2.2.15	Quantitative Fluorescence <i>in situ</i> Hybridisation	111
2.2.15.1	Slide preparation.....	111
2.2.15.2	Ageing of slides and pre-hybridisation washes.....	112
2.2.15.3	Denaturation and hybridisation	112
2.2.15.4	Post-hybridisation washes and detection.....	113
2.2.15.5	QFISH control slide preparation	113
2.2.15.6	QFISH image analysis.....	113
3	Specific aim 1: To test the hypothesis that telomere distribution is altered in the sperm heads of males with severely compromised semen parameters.....	115
3.1	Background	115
3.2	Specific aims.....	117
3.3	Results.....	118
3.3.1	Specific aim 1a: To test the hypothesis that telomeres are non-randomly distributed (predominantly at the nuclear periphery) in the sperm heads of normally fertile males.....	118
3.3.1.1	Extrapolations of 2D data.....	118
3.3.1.2	Direct evidence from 3D preparations	120

3.3.2	Specific aim 1b. To test the hypothesis that an apparently altered telomere distribution can be artificially induced by inappropriate swelling of the sperm head	122
3.3.2.1	Extrapolations of 2D data.....	122
3.3.2.2	Direct evidence from 3D preparations	125
3.3.3	Specific aim 1c. To test the hypothesis that H2BFWT also clusters at the nuclear periphery (and, by implication, is anchored to the nuclear membrane) in the sperm heads of normally fertile males.....	126
3.3.4	Specific aim 1d. To test the hypothesis that H2BFWT and the TTAGGG motif co-localise thereby suggesting a functional interaction.....	129
3.3.5	Specific aim 1e. To test the hypothesis that nuclear (telomere) organisation is altered in infertile males compared to their normal counterparts	130
3.3.5.1	Telomere distribution using 2D telomere FISH.....	131
3.3.5.2	Proportion of cells with > 16 signals.....	133
3.3.6	Specific aim 1f. To test the hypothesis that any alteration in nuclear organisation between fertile and infertile males may be related to the degree of chromatin packaging	134
3.4	Discussion	136
3.4.1	Telomeres are located at the nuclear periphery in human sperm heads	136
3.4.2	H2BFWT is also located at the nuclear periphery but not in association with telomeres	137
3.4.3	Nuclear (telomere) organisation as a marker for male infertility	137
3.4.4	The role of CMA3 staining and telomere distribution	139
3.4.5	Differences between 2D and 3D analyses	140
3.4.6	Conclusions	141
4	Specific aim 2: To optimise a qRT-PCR approach for assaying telomere length using small quantities of starting material	143
4.1	Background.....	143
4.2	Specific aims:.....	144
4.3	Results.....	145
4.3.1	Specific aim 2a. To optimise a multiplex qRT-PCR assay for telomere length analysis from low quantities of genomic DNA template extracted from whole blood from newborns, using the Rotor-gene Q real-time PCR machine.	145
4.3.2	Specific aim 2b. To optimise a singleplex qRT-PCR assay for telomere length analysis from whole genome amplified DNA from single cells using the Rotor-Gene Q real-time PCR machine.....	149

4.3.3	Specific aim 2c. Verification of faithful representation of telomere and reference sequences after whole genome amplification using the SurePlex DNA amplification kit	154
4.4	Discussion	155
4.4.1	Multiplex qRT-PCR for telomere length analysis	155
4.4.2	Singleplex qRT-PCR for telomere length analysis in single cells.....	156
4.4.3	Faithful representation of the DNA template following WGA	157
4.5	Conclusion	158
5	Specific aim 3: To investigate the telomere theory of reproductive ageing in women by addressing a series of hypotheses pertaining to telomere length in first polar bodies and cleavage stage embryos, in relation to maternal age and generation of aneuploidy.....	159
5.1	Background	159
5.2	Specific aims	161
5.3	Results.....	162
5.3.1	Specific aim 3a. To test the hypothesis that telomere length is significantly shorter in first polar bodies from women of advanced maternal age (over the age of 35) compared to their younger counterparts	164
5.3.2	Specific aim 3b. To test the hypothesis that telomere length is significantly shorter in blastomeres derived from women of advanced maternal age (over the age of 35) compared to their younger counterparts	166
5.3.3	Specific aim 3c. To test the hypothesis that telomere length is significantly shorter in first polar bodies that are involved in chromosome segregation errors compared to sibling euploid first polar bodies	169
5.3.4	Specific aim 3d. To test the hypothesis that telomere length is significantly shorter in aneuploid blastomeres compared to euploid blastomeres from sibling embryos.....	170
5.4	Discussion	172
5.4.1	Telomere length in relation to maternal age in polar bodies	172
5.4.2	Telomere length in relation to maternal age in embryos	173
5.4.3	Telomere length and aneuploidy in first polar bodies compared to sibling euploid first polar bodies	175
5.4.4	Telomere length and aneuploidy in blastomeres	176
5.5	Conclusion	177
6	Specific aim 4: To test the hypothesis that preterm babies have significantly reduced telomere length by term equivalent age compared their term born counterparts	178
6.1	Background	178
6.2	Specific aims	180

6.3	Results.....	181
6.3.1	Specific aim 4a. To recruit up to 30 preterm infants and sample their blood at birth and “at term” age and to recruit an equivalent number of term-born healthy infants as controls	181
6.3.2	Specific aim 4b. To use the qRT-PCR protocol developed in specific aim 2 to test the hypothesis that the telomeres of preterm infants are significantly shorter than they were at the time that they were born	183
6.3.3	Specific aim 4c. Using the same methodology to test the hypothesis that at term equivalent age, preterm infants have reduced average relative telomere length compared to term born controls.....	184
6.3.4	Specific aim 4d. To test the hypothesis that, in each of the three groups (preterm at birth; preterm at term; term born controls) overall telomere length correlates to gestational age, birth weight, maternal age, maternal body mass index and/or mode of delivery	185
6.3.5	Specific aim 4e. To test the hypothesis that individual telomeres are prematurely shortened in preterm infants at term equivalent age	187
6.4	Discussion	192
6.4.1	Recruitment of preterm infants and term born healthy controls.....	192
6.4.2	Relative telomere length in preterm infants at birth compared to preterm infants term equivalent age.....	192
6.4.3	Relative telomere length in preterm infants at term equivalent age compared to term born controls.....	194
6.4.4	Correlation of telomere length with gestational age, birth weight, maternal age, maternal BMI and mode of delivery	195
6.4.5	Telomere lengths of individual chromosome arms	196
6.5	Conclusion	197
7	General discussion.....	198
7.1	Biomarkers of ageing and age-related disorders.....	199
7.2	Diagnostics in male infertility.....	201
7.3	Does assessment of telomere length or distribution have a role in the future of preimplantation genetic screening (PGS)?.....	202
7.4	The future of telomere studies	204
7.5	Future studies arising from this thesis	205
7.6	Personal perspectives and concluding remarks.....	206
8	References	208
9	Supplementary data	253
10	Publications and activities arising from this thesis.....	260
10.1	Publications.....	260

10.2	Manuscripts in preparation	260
10.3	Poster and oral presentations	260

List of figures

- Figure 1.1: The human telomere. Telomeres are made up of repetitive sequences of DNA associated with specialised proteins, present at the end of each chromosome arm. Terminal DNA is organised into a loop formation, with the single stranded G-rich 3' overhang invading the double stranded duplex (Kovacic et al., 2011).....2
- Figure 1.2: The T-loop and the D-loop. The 3' end of the G rich strand protrudes as a single stranded extension of the telomere. This G-strand overhang loops back to form a T-loop, and invades the 5' double stranded telomeric duplex, forming a D-loop.4
- Figure 1.3: The Shelterin Complex. Shelterin is made up 6 associated proteins; TRF1, TRF2, RAP1, TIN2, TPP1, POT1. Diagram taken from (Oeseburg et al., 2010).5
- Figure 1.4: The Rab1 configuration. Centromeres (coloured in red) cluster at one pole of the nucleus via interactions with the nuclear membrane through Csi1 and Sad1. Chromosome arms (coloured in blue) are attached to lamins of the nuclear matrix via matrix attachment regions (MARs). Telomeres (coloured in green) are orientated towards the opposite pole of the nucleus to centromeres and attach to lamins of the nuclear matrix via TRF1, TRF2 and TIN2. Telomeres are additionally anchored at the nuclear envelope via associations with lamins which in turn bind to nuclear membrane spanning lamin associated proteins (LAPs), or via interactions with the nuclear pore.....13
- Figure 1.5: Diagrammatic representation of the chromocentric model of nuclear organisation, whereby centromeres (red) form a chromocentre deep within the nuclear volume and telomeres (green) from clusters at the nuclear periphery.14
- Figure 1.6: Leading strand telomere lengthening by telomerase. (A) Recruitment of telomerase to the telomere by ATM promotes primer annealing (B) and initiates reverse transcriptase activity of the TERT component, using the TERC RNA template. Telomerase elongates the leading strand (C) and is then transferred to another telomere for the process to repeat again (D) (Gavory et al., 2002). ...18
- Figure 1.7: Alternative lengthening of telomeres by homologous recombination. RAD51 and RAD52 regulate invasion of the 3' overhang into the T-loop of a telomere present on a separate chromosome. This forms a structure similar to a replication fork, allowing synthesis and addition of more telomeric repeats by DNA polymerase. Taken from (Verdun and Karlseder, 2007).20
- Figure 1.8: Telomere length changes following fertilisation through embryogenesis and fetal development. Telomere length declines after fertilisation through cleavage and morula stages, then drastically increases at the blastocyst stage. Current literature has not explored telomere length at the earliest stages of gastrulation and development, however between weeks six and seven of gestation telomere length appears to decline. This decline in telomere length continues between weeks seven and eight, however it is less pronounced. All other developmental stages tested (weeks nine to 19 and weeks 23 to 36) show steady maintenance

- of telomere length. Fetal images adapted from http://homepage.smc.edu/wissmann_paul/anatomy2textbook/.25
- Figure 1.9: Telomere length decline is correlated with the process of ageing. Furthermore, telomere attrition rate appears to be more rapid during early life, as indicated by a steeper decline in the data points (Lansdorp, 2008).28
- Figure 1.10: Events during prophase I of meiosis. Chromosomes begin to condense in leptotene followed by chromosome pairing and synaptonemal complex formation in zygotene. Next, in pachytene crossing over occurs between sister homologous chromosomes. Chiasma remain through the following stages of diplotene, when the chromosomes begin to align along the equator and synaptonemal complex begins to disappear. Finally in diakinesis chromosomes are fully aligned at the equator, the synaptonemal complex disappears and the nuclear envelope begins fragmentation. Green spots represent telomeres. Image modified from <https://study-biology.wikispaces.com/meiosis>.36
- Figure 1.11: Events during Meiosis I and II. During prophase chromosomes pair and decondense and the meiotic spindle begins to form. This is followed by metaphase, in which chromosomes align along the equator of the nucleus and attach to spindle fibres. Chromosomes are then pulled apart in anaphase. During telophase, chromosomes arrive at opposite poles in the cell. Meiosis completes with cytokinesis, when the nuclear envelope pinches between the newly formed nuclei to produce two daughter cells. Image taken from <http://www.ib.bioninja.com.au/higher-level/topic-10-genetics/101-meiosis.html>.36
- Figure 1.12: The process of spermatogenesis. In the seminiferous tubules (within the testis) spermatogonia undergo mitotic division to produce haploid primary spermatocytes, which in turn undergo the first meiotic division to produce secondary spermatocytes. Following meiosis II, round spermatids are produced which differentiate first into elongating spermatids and then elongated spermatids before finally differentiating into mature spermatozoa. Sertoli cells support this process of gametogenesis. Image taken from <http://intanriani.files.wordpress.com/2009/03/spermatogenesis.jpg>38
- Figure 1.13: The process of oogenesis. The primary oocyte surrounded by a single layer of flat granulosa cells makes up a primordial follicle. These granulosa cells become cuboidal, and the primary oocyte begins meiosis I, marking differentiation into a primary follicle. As granulosa cells increase in numbers and theca cells are recruited, the primary follicle differentiates into a secondary follicle, which develops several antra that eventually fuse to become one antrum in the Graafian follicle. At this point meiosis resumes in the primary oocyte to produce a secondary oocyte. Meiosis is arrested in metaphase II however. The secondary oocyte is expelled from the Graafian follicle along with a surrounding layer of cumulus cells in the process of ovulation. The remaining corpus luteum then degrades. Image taken from <https://www.repropeedia.org/sites/repropeedia/files/ovulation-final.jpg>.39
- Figure 1.14: The 'bouquet' configuration. Telomere led bouquet arrangement of chromosomes during meiosis. Centromeres (shown in red) are positioned at one

- end of the nucleus, whilst telomeres (shown in green) cluster at the inner nuclear envelope, tethering chromosomes in place.40
- Figure 1.15: Telomere redistribution during prophase I of spermatogenesis. Telomeres (green) are randomly distributed throughout the nucleus prior to the onset of prophase, however they redistribute to the nuclear periphery by late preleptotene. At the leptotene stage, telomeres adopt the bouquet configuration, before beginning to uncluster once more at the early zygotene stage. In late zygotene and Pachytene, telomeres redistribute once more to the entire nuclear periphery.42
- Figure 1.16: Telomere anchoring at the nuclear periphery in mature sperm. H2BFWT binds double stranded telomeric DNA repeats and allows interaction of the telomere with the nuclear membrane. This sperm specific H2B variant makes up part of STBP, which is involved in the clustering of telomeres.43
- Figure 1.17: Embryogenesis: Following fertilisation, male and female pronuclei fuse and mitotic division produces two daughter blastomeres during cleavage stage. These further divide into 4, then 8 blastomeres. At 16-32 blastomeres, the embryo is called a morula. Further divisions of blastomeres produces trophoblasts and the inner cell mass, which marks differentiation into the blastocyst (http://www.maxhealthcare.in/newsletter/2010/january/ivf-simpler.html?utm_source=ivf-simpler&utm_medium=Facebook&utm_campaign=FB).47
- Figure 1.18: Intracytoplasmic sperm injection (ICSI). A single sperm cell is sucked into the end of a needle, which is then used to pierce the oocyte zona pellucida. The sperm cell is injected directly into the oocyte to allow fertilisation. Taken from <http://www.goivf.com/treatment-options/ivf-process/male-factor-icsi-tese/>. .52
- Figure 1.19: Sample biopsy for PGS using a pipette. Top left shows first polar body removal, top right shows second polar body removal, bottom left shows first and second polar body removal, bottom right shows blastomere biopsy from a cleavage stage embryo (Verlinsky and Kuliev, 2005).55
- Figure 1.20: Fluorescence in situ hybridisation with a biopsied blastomere. Blastomere(s) are fixed to a glass slide and a fluorescently labelled probe is applied. The probe and the blastomere DNA are denatured at high temperature before allowing hybridisation at cooler temperature (usually 37°C). After counterstaining the nucleus and mounting, the blastomere may be visualised and assessed for aneuploidy using a fluorescence microscope.56
- Figure 1.21: aCGH. Top describes to aCGH principle: Test DNA labelled green and reference DNA labelled red are allowed to hybridise to an array containing a number of genomic DNA fragments. The ratio of red to green labelling indicates chromosome copy number, or single gene copy number. Taken from <http://www.ncbi.nlm.nih.gov/dbvar/content/overview/>. Bottom shows an example of an output from aCGH. The log ratio of reference DNA to test DNA (y axis) is plotted for each chromosome position on each chromosome (x axis). Peaks above the line indicate gains and peaks below the line indicate losses. Partial monosomy of chromosome five and partial trisomy of chromosome 8 is indicated by black arrows. Red arrows indicate monosomy for chromosomes 12, 21 and 22 (Fiorentino et al., 2011).57

- Figure 1.22: Representation of non-telomeric sequences inclusive in telomere restriction fragment analysis that may contribute to variability among individuals. Green represents true TTAGGG telomere repeats, yellow represents telomere repeat variants, red represents sub-telomeric sequences and blue represents the rest of the chromosome arm (Turner et al., 2014).72
- Figure 1.23: Molecular basis of single telomere length analysis. (1.) Shows annealing of a ‘telorette’ linker to the G-rich 3’ overhang of the telomere, which is ligated to the C-rich 5’ strand. (2.) A ‘teltail’ primer and a primer specific to the sub-telomere region primes synthesis of the telomere in a PCR reaction. Finally telomere length is quantificatied by gel electrophoresis and southern blotting (Turner et al., 2014).77
- Figure 1.24: Molecular basis of universal single telomere length analysis. (1) Restriction enzyme digest creates sticky ends in both the telomere-containing fragment and the intragenomic DNA fragment. (2) Linkers are then ligated to these sticky ends, and fillers are subsequently ligated to the linkers. A ‘telorette’ linker is then annealed to the 3’ overhang and ligated to the 5’ strand before PCR amplification of the telomere-containing fragment. (3) In the first stage of each PCR cycle, dsDNA is denatured into single strands. (4) This allows formation of stable hairpin structures of the intragenomic fragment due to complimentary sequences in the linker and filler, such that in the second stage of the PCR cycle, amplification of intragenomic sequences is inhibited, whilst amplification of the telomere-containing fragment is permitted. Synthesis is primed using a ‘teltail’ primer designed to anneal to the ‘telorette’ linker, and a primer designed to anneal to the filler sequence (Turner et al., 2014).78
- Figure 1.25: Example of a Q-FISH image. Chromosomes are stained blue, whilst telomeres are stained green.80
- Figure 1.26: 2D analysis of signal distribution within the sperm nucleus. A: Longitudinal distribution of basal (b), medial (m) and apical (a) regions of the sperm nucleus (Olszewska et al., 2008). B: Spatial distribution where L and l represent the long and short axes of the nucleus, L’-L represents the symmetry of the long axis, D is the distance from the tail attachment point to the signal and H is the distance from the signal to the long axes (Zalenskaya and Zalensky, 2004). C: Radial distribution where the nucleus is split into five shells of equal area, and the signal position is determined by assessing which shell the signal lies within (Finch et al., 2008).83
- Figure 2.1: The ImageJ macro is able to split the nucleus into separate channels, convert the blue channel to a binary mask, and then apply five rings of equal area to the blue channel.91
- Figure 2.2: Diagramatic representation of distances measured for analysis of telomere distribution. A: Blue represents DAPI staining on the nucleus, red represents telomere staining, D1 represents distance 1 (the distance between the centre of the telomere signal and the centre of the nucleus), D2 represents distance 2 (the distance between the centre of the telomere signal and the nuclear periphery). B: Calculation of telomere position within the 3D nucleus.92
- Figure 2.3: Cycling conditions of the multiplex qRT-PCR for relative telomere length analysis.99

- Figure 2.4: PCR cycling conditions for telomere amplification in WGA samples from cell line DNA or biopsied single cells.103
- Figure 2.5: Cycling conditions for amplification of the multicopy reference gene from WGA cell line DNA and biopsied single cells.104
- Figure 3.1: Distribution of telomeres in sperm nuclei of normal males. Example images acquired following FISH experiments using a pan telomere probe (red) and DAPI staining of the sperm nucleus (blue). Although spots appear anywhere in the nucleus, the majority of telomere spots are localised at the nuclear periphery.118
- Figure 3.2: 2D telomere distribution in normal males as determined by FISH and following mathematical compensation of 2D representation of 3D objects using DAPI density (left) and volumetric (right) models. Both models confirm a preferentially peripheral distribution of telomeres, as determined p values < 0.05 following χ^2 analysis.119
- Figure 3.3: Gallery of example images depicting ‘random’ pattern of telomere localisation (red) in a subpopulation of sperm nuclei (blue). The number of telomere spots is much greater than other sperm nuclei, and no preference for peripheral localisation is evident.119
- Figure 3.4: Still images from 180° rotation of 3D sperm cell image showing the 3D distribution of telomeres (red) within the sperm nucleus (blue) as determined by analysis using Nemo.121
- Figure 3.5: 3D distribution of telomeres in normal fertile males determined by FISH. p value represents statistical significance of a peripheral localisation of telomeres following χ^2 analysis.121
- Figure 3.6: Example images of telomere distribution (red) in sperm nuclei (blue) of non-swollen sperm (a), 10mM DTT swollen sperm (b) and 0.5M NaOH swollen sperm (c). While telomere staining patterns appear to be similar in non-swollen and 10mM DTT swollen sperm, 0.5M NaOH swollen sperm show a more random distribution of signals, with a much higher overall number of telomere signals.122
- Figure 3.7: 2D telomere distribution patterns in non-swollen (no treatment), 10mM DTT swollen and 0.5M NaOH swollen sperm nuclei, as determined by FISH analysis and using DAPI density (left) and volumetric (right) models. χ^2 p values are shown in each graph representation. Both models show a preferentially peripheral distribution of telomeres in non-swollen and 10mM DTT swollen sperm, however 0.5M NaOH swollen sperm show a random distribution of telomeres.123
- Figure 3.8: Comparison of average number of telomere signals (left) and percentage of nuclei with greater than 15 telomere signals (right) in non-swollen sperm (blue), 10mM DTT swollen sperm (red) and 0.5M NaOH swollen sperm (orange). Non-swollen and 10mM DTT swollen sperm possess an equal number of average telomere signals, however 10mM DTT swollen sperm possess twice the percentage of cells belonging to a sub-population of sperm nuclei with above 16 telomere signals. 0.5M NaOH swollen sperm possess a much greater average number of telomere signals than both other groups, and almost all cells possess 16 or more telomere signals.124

- Figure 3.9: 3D telomere distribution in non-swollen, 10mM DTT swollen and 0.5M NaOH swollen sperm nuclei, as determined by FISH analysis. Statistical significance of a non-random distribution of telomeres is confirmed by χ^2 analysis (p values shown in each graphical representation of telomere distribution).....126
- Figure 3.10: H2BFWT distribution in human sperm as determined by immunofluorescence experiments. H2BFWT (green) shows almost exclusively peripheral localisation at the nuclear membrane (nucleus stained blue).127
- Figure 3.11: 2D H2BFWT localisation in sperm of normal males as determined by immunofluorescence experiments using DAPI density (left) and volumetric (right) compensation models and χ^2 analysis to determine statistical significance of non-random distribution (p values shown in graphical representation). While the general trend representing H2BFWT localisation is slightly different among the two models, the median position shows peripheral location in both models.....128
- Figure 3.12: Graphical representation of 3D analysis of H2BFWT localisation as determined by immunofluorescence experiments and χ^2 analysis to determine statistical significance of non-random, peripheral distribution (p value shown in graph).....128
- Figure 3.13: Still images from 180° rotation of 3D sperm cell image showing the 3D distribution of H2BFWT (green) within the sperm nucleus (blue) as determined by analysis using Nemo.128
- Figure 3.14: Example images depicting telomere localisation (red) in relation to H2BFWT (green) localisation within the sperm nucleus (blue). The top row of images display only H2BFWT staining, the middle row of images display telomere staining only, while the bottom row of images show H2BFWT staining over-laid with telomere staining. As can be seen in the bottom row of images, whilst both telomeres and H2BFWT are predominantly located at the nuclear periphery in close proximity to one another, few signals overlap indicating that H2BFWT does not directly interact with the telomere.....129
- Figure 3.15: 2D telomere distribution in sperm of infertile males (lower graphs) as determined by FISH followed by analysis using DAPI density (left) and volumetric (right) compensation models. p values represent statistical analysis of a non-random position of telomeres using χ^2 . Both are compared to controls (upper graphs – repeat of figure 3.2). In both analyses, control males showed non-random patterns and a preference for the nuclear periphery, infertile males showed patterns not statistically different from random.132
- Figure 3.16: 3D telomere distribution in pooled data from sperm of infertile males. p value represents χ^2 statistical significance of non-random, preferentially peripheral distribution of telomeres.....132
- Figure 3.17: Comparison of overall average number of telomere signals (a), and percentage of nuclei with greater than 16 telomere signals (b) in pooled control (blue) and infertile males (red) males. The average number of telomere signals is increased in sperm nuclei of infertile males, and a greater percentage of nuclei make up the subpopulation of sperm cells with a large number of randomly distributed telomere signals in infertile males.134

- Figure 3.18: Example images of negatively stained (a) and positively stained (b) sperm nuclei after chromomycin A3 (CMA3) staining. b: Graphical representation of the percentage of positively stained sperm nuclei in fertile controls (blue) compared to sperm nuclei of infertile males (red) following CMA3 staining. Infertile males possess a higher percentage of positive CMA3 staining (error bars represent standard error).135
- Figure 4.1: Melting curve analysis following cycling conditions using 150nm each telomere and reference sequence primer pair for multiplex qRT-PCR analysis of relative telomere length. The peaks to the far left and right of the graph represent the expected melting profiles of the telomere and single copy reference sequence amplicon respectively, however the peak in the middle represents formation of a primer complex in the no template control reaction.146
- Figure 4.2: Reaction efficiencies (shown in the red boxes) for telomere (left) and reference sequence (right) following multiplex qRT-PCR conditions using 150nm for each telomere and reference sequence primer pair. Both reactions show over-efficiencies (118% for telomere and 113% for reference sequence respectively).....147
- Figure 4.3: Melt curve analysis following thermal cycling for multiplex amplification of the telomere and single copy gene sequences. Both the telomere amplicon peak (left) and the single copy reference sequence amplicon peak (right) are in line with those reported by Cawthon et al 2009.147
- Figure 4.4: Reaction efficiencies (shown in the red box) of telomere amplification (left) and single copy reference sequence amplification (right). Both are within acceptable range (102% and 100% respectively) and approximately equal..148
- Figure 4.5: Gel electrophoresis of products formed following multiplex qRT-PCR. Two bands are present representing the expected sizes of the telomere and single copy reference sequence amplicons (79bp and 106bp respectively).....149
- Figure 4.6: Reaction efficiencies (detailed within the red boxes) of telomere amplification (left) and multicopy reference gene (right). Reaction efficiencies are close to 100% and are approximately equal, confirming optimal amplification conditions for quantitative analysis of relative telomere length.152
- Figure 4.7: An example of poor reaction conditions resulting in an over-efficient reaction of 136% (calculated by the Rotor-Gene Q software and shown in the red box to the top right of the graph) for the multicopy reference sequence. This particular reaction was carried out using the Rotor-Gene SYBR® Green PCR Kit, with primer concentrations at 100nm each and a cycling condition as follows: Polymerase activation at 95°C for 5 mins, melting at 95°C for 15 secs, annealing at 60°C for 60 secs and signal acquisition at 70°C for 10 sec.152
- Figure 4.8: Melt curve analysis following amplification of the multicopy reference sequence (top) and the telomere sequence (bottom). On both graphs the y axis represents the change in fluorescence units divided by the change in temperature plotted against the temperature of signal acquisition (°C) on the x axis. Both melt curves indicate a single peak representing specific amplification of a single product.153

- Figure 4.9: Agarose gel electrophoresis of alu reference (left) and telomere (right) PCR products. Both show amplification of a single product that matches the size expected for the amplicon (79bp and 127bp respectively).153
- Figure 4.10: Verification of the faithful representation of relative telomere length following whole genome amplification using the SurePlex DNA amplification kit. The graph shows a good correlation between relative telomere length in unamplified DNA and relative telomere length in WGA DNA, indicating acceptable representation of telomeres in the WGA process.154
- Figure 5.1: Relative telomere lengths in first polar bodies from women under the age of 35. Error bars represent standard error from the mean.....164
- Figure 5.2: Relative telomere lengths in first polar bodies from women aged over 35. Error bars represent standard error from the mean.165
- Figure 5.3: Average relative telomere length of all first polar bodies from women 35 years old or under compared to women of advanced maternal age. Results show that telomere length is slightly shorter in first polar bodies from women above 35 years old, however this difference is not statistically significant ($p = 0.48$). Error bars represent standard error from the mean.....165
- Figure 5.4: Relative telomere lengths of aneuploid and euploid first polar bodies in relation to maternal age. Results indicate no correlation between relative telomere length of first polar bodies and maternal age.....166
- Figure 5.5: Relative telomere length in blastomeres of cleavage stage embryos from women under the age of 35. Error bars represent standard error from the mean.167
- Figure 5.6: Relative telomere length in blastomeres of cleavage stage embryos from women over the age of 35. Error bars represent standard error from the mean.167
- Figure 5.7: Average relative telomere length in all blastomeres from younger women compared to those from women of advanced maternal age. Relative telomere length is slightly shorter in blastomeres derived from couples in which women were younger however this difference was not statistically significant ($p = 0.37$) (bottom). Error bars represent standard error from the mean.168
- Figure 5.8: Telomere length in blastomeres from cleavage stage embryos in relation to maternal age. Results show no correlation.168
- Figure 5.9: Average relative telomere length of two aneuploid first polar bodies compared to two sibling euploid first polar bodies from the same woman. Error bars represent standard error between the two aneuploid or euploid polar bodies assessed.....169
- Figure 5.10: Overall average relative telomere length of all aneuploid first polar bodies in comparison to all euploid first polar bodies assessed in all women. Error bars represent standard error among each group.170
- Figure 5.11: Average relative telomere length of blastomeres biopsied from two euploid embryos, compared to average relative telomere length of blastomeres biopsied from two sibling aneuploid embryos generated from the same couple in the same IVF cycle. Error bars represent standard error between the two euploid and two aneuploid blastomeres assessed.171

- Figure 5.12: Overall average relative telomere length of all euploid and all aneuploid blastomeres assessed from all couples. Error bars represent the standard error within the study group.171
- Figure 6.1: Average relative telomere length (as determined by T/S ratio following qRT-PCR) in preterm infants sampled at birth (top left) and preterm infants sampled at term equivalent age (top right). Mean telomere length is longest in preterm infants sampled at birth (bottom), however this difference is not significant ($p = 0.10$). Error bars represent standard error of the mean.....184
- Figure 6.2: Average relative telomere length (as determined by T/S ratio following qRT-PCR) in preterm infants sampled at term equivalent age (top left) compared to term born controls (top right). Mean telomere length is longest in preterm infants (bottom), however this difference is not significant ($p = 0.07$). Error bars represent standard error.185
- Figure 6.3: Correlation between gestational age (top left), birth weight (top right), maternal body mass index (bottom left) and maternal age (bottom right) with relative telomere length (T/S ratio) as determined by qRT-PCR in preterm infants sampled at birth. No correlation is present amongst any of the variables tested.186
- Figure 6.4: Correlation between gestational age (top left), birth weight (top right), maternal body mass index (bottom left) and maternal age (bottom right) with relative telomere length (T/S ratio) as determined by qRT-PCR in preterm infants sampled at term equivalent age. No correlation is present amongst any of the variables tested.186
- Figure 6.5: Correlation between gestational age (top left), birth weight (top right), maternal body mass index (bottom left) and maternal age (bottom right) with relative telomere length (T/S ratio) as determined by qRT-PCR in term infants. No correlation is present amongst any of the variables tested.....187
- Figure 6.6: Example of an image acquired following QFISH procedures (top left) and detection of chromosomes and telomeres for fluorescence analysis of telomere spots in TFL-Telo (top right). The raw QFISH image was karyotyped with the aid of SmartType 2 (bottom) in order to assign chromosome number to each measured chromosome.188
- Figure 6.7 Average absolute telomere lengths of individual p and q arms from each chromosome in preterm infants sampled at birth (blue), preterm infants sampled at term equivalent age (yellow) and term born controls (red). Among all individual p and q arms from each chromosome, telomere length is consistently approximately equal between preterm infants sampled at birth and preterm infants sampled at term equivalent age. Similarly, telomere length is consistently longer in term controls compared to both other groups regardless of the chromosome or the chromosome arm. Therefore these results show no chromosome specific effect on telomere length among the different groups. Error bars represent standard error of the mean.190
- Figure 6.8: Normalised average absolute telomere lengths of individual p and q arms from each chromosome in preterm infants sampled at birth (blue), preterm infants sampled at term equivalent age (yellow) and term born controls (red).

Among all groups, telomere lengths of individual p and q arms are similar. Error bars represent standard error of the mean.....191

List of tables

Table 1.1: Lifestyle factors affecting telomere length and appropriate references.	29
Table 1.2: The role of telomere dysfunction in the pathogenesis of other disease process.	34
Table 1.3: Examples of genetic aberrations leading to infertility, their effects and some examples. N/A is not applicable.	50
Table 2.1: Primer design for amplification of the single copy gene beta-globin for qRT-PCR analysis of relative telomere length in infants.....	97
Table 2.2: Different mastermixes tested during optimisation of qRT-PCR analysis of relative telomere length.	97
Table 2.3: Different primer concentrations trialled (in nm) during optimisation of multiplex qRT-PCR analysis of average relative telomere length.	97
Table 2.4: Components of multiplex qRT-PCR set up for relative telomere length analysis in infants.	98
Table 2.5: Primer design for amplification of a multicopy reference gene from single cells.	100
Table 2.6: Different mastermixes tested during optimisation of qRT-PCR analysis of relative telomere length from single cells.....	101
Table 2.7: Primer concentrations tested for amplification of the mutlicopy reference sequence for telomere length analysis by qRT-PCR in single cells.	101
Table 2.8: Primer concentrations tested for amplification of the telomere in telomere length analysis by qRT-PCR from single cells.....	101
Table 2.9: Reaction contents for telomere or multicopy reference sequence amplification from single cells for relative telomere length analysis.....	102
Table 2.10: Different cycling conditions attempted for the amplification of the multicopy reference gene for relative telomere length analysis in WGA DNA derived from single cells.....	103
Table 2.11: SurePlex preamp cycling conditions used for whole genome amplification of cell line DNA.....	105
Table 2.12: SurePlex amplification cycling conditions for whole genome amplification of cell line DNA.....	106
Table 3.1: Percentage of nuclei representing a sub-population of sperm cells with 16 or more telomere signals dispersed throughout the nucleus.	120
Table 3.2: Statistical analyses of telomere distribution in sperm treated with either 10mM DTT or 0.5M NaOH compared to non-treated sperm as ascertained by FISH and using DAPI density or volumetric models. Values indicated represent p values derived from chi ² analysis. While telomere distribution is not altered in 10mM DTT swollen sperm nuclei compared to non-treated sperm, telomere distribution in 0.5M NaOH swollen sperm nuclei is significantly difference to both other groups. These observations are true for both DAPI density and volumetric models of analysis.	124
Table 3.3: Semen parameters of males included in the infertile cohort.	130
Table 3.4: Percentage of nuclei with a larger number of dispersed telomere signals in sperm of infertile males.	133

Table 4.1: Different mastermixes tested for optimisation of multiplex qRT-PCR analysis of average relative telomere length. The mastermix highlighted in bold gave the best performance and therefore this was used in subsequent analyses.	145
Table 4.2: Different primer concentrations trialled (in nm) during optimisation of multiplex qRT-PCR analysis of average relative telomere length. The concentration combination highlighted in bold performed the best and therefore this concentration was used in subsequent analyses.....	146
Table 4.3: PCR mastermixes trialled for qRT-PCR analysis of relative telomere length from WGA DNA. The kit highlighted in bold generated the best reaction performance therefore this was used in subsequent reactions.	150
Table 4.4: Primer concentrations trialled for amplification of the telomere sequence. Details highlighted in bold generated the best performance and were therefore included in all subsequent reactions.	150
Table 4.5: Primer concentrations trialled for amplification of the multicopy reference sequence. Details highlighted in bold generated the best performance and were therefore included in all subsequent reactions.....	150
Table 4.6: Different cycling conditions attempted for the amplification of the multicopy reference gene for relative telomere length analysis in WGA DNA derived from single cells. Cycling conditions highlighted in bold gave the best reaction performance.	151
Table 5.1: Anonymised patient details and results of aneuploidy screening in first polar bodies following assessment using the 24 Sure preimplantation genetic screening kit. ‘complex’ refers to aneuploid results involving four or more chromosomes, ‘n/a’ is not applicable (i.e. no aneuploid polar body available).	162
Table 5.2: Patient details and results of aneuploidy screening in blastomeres biopsied from cleavage stage embryos following assessment using the 24 Sure preimplantation genetic screening kit. ‘complex’ refers to aneuploid results involving four or more chromosomes, ‘n/a’ is not applicable (i.e. no embryo available), ‘del’ refers to a deletion with the chromosome involved identified in the first set of brackets and the portion deleted identified in the second brackets, ‘dup’ refers to a duplication with the chromosome involved identified in the first set of brackets and the portion duplicated identified in the second brackets.	163
Table 6.1: Patient information and relative telomere length (T/S ratio). CS (labour) refers to delivery by caesarean section following labour, CS (non-labour) refers to caesarean section in the absence of labour. Where a ‘-’ is present, no information was available.....	182

List of equations

Equation 2.1: Comparative method for fold change calculation between a reference and an unknown sample. ‘tel’ refers to the telomere sequence amplification reaction, ‘alu’ refers to the multicopy sequence reaction, ‘ref’ refers to the reference DNA amplification and ‘Ct’ is the cycle threshold.107

Abbreviations

aCGH	Array comparative genomic hybridisation
ALT	Alternative lengthening of telomeres
AMA	Advanced maternal age
ANOVA	Analysis of variance
AR	Androgen receptor
ART	Assisted reproductive technologies
ATM	Ataxia telangiectasia mutated
ATP	Adenosine triphosphate
ATR	Ataxia telangiectasia and Rad3-related protein
AZF	Azoospermic factor
BMI	Body mass index
CCD	Charge coupled device
CDK1	Cyclin dependent kinase 1
CDKN1A	Cyclin dependant kinase inhibitor 1A
CDKN2A	Cyclin dependant kinase inhibitor 2A
CFTR	Cystic fibrosis trans-membrane conductance regulator
CHO	Chinese hamster ovarian
CMA3	Chromomycin A3
Csi1	Cop9 Signalosome Interactor 1
Cy3	Cyanine 3
DAPI	4'-6,diamidino-2-phenylindole
Dax1	Dosage-sensitive sex reversal, adrenal hypoplasia critical region, on chromosome X, gene 1
ddH2O	Double distilled water
DMSO	Dimethylsulfoxide
DNA-PK	DNA protein kinase
DSB	Double strand break
DTT	Dithiothreitol
EDTA	Ethylenediaminetetraacetic acid

ERCC1	Excision repair cross-complementing
FISH	Fluorescence in situ hybridisation
FITC	Fluorescein isothiocyanate
GFP	Green fluorescent protein
HAB	Hyaluronic A binding
H2BFWT	Histone 2B family member W testis-specific
HDR	Homology directed repair
HFEA	Human fertilisation and embryology authority
HP1	Heterochromatin protein 1
HPA	Hybridisation protection assay
HTT	Huntingtin
ICSI	Intracytoplasmic sperm injection
IMS	Industrial methylated spirit
IMSI	Intracytoplasmic morphological sperm injection
INSL3	Insulin like factor 3
IUGR	Intra-uterine growth restriction
IUI	Intra-uterine insemination
IVF	<i>in vitro</i> fertilisation
KAL1	Kallmann syndrome I
KASH	Klarsicht, adenine nucleotide carrier 1, syne homology
LAPs	Lamin associated proteins
LINE-1	Long interspersed elements
MARs	Matrix attachment regions
MMqRT-PCR	Multiplex monochrome quantitative real-time polymerase chain reaction
MRE11	Meiotic recombination 11
MRN	MRE11/RAD50/NBS1
MSUC	Meiotic silencing of unsynapsed chromatin
NBSI	Nibrin
NHEJ	Non-homologous end joining
NTC	No template control

OAT	Oligoasthenoteratozoospermia
OB	Oligonucleotide/oligosaccharide binding
PARP	Poly adenosine diphosphate ribose polymerase
PBS	Phosphate buffered saline
PCR	Polymerase chain reaction
PGD	Preimplantation genetic diagnosis
PGS	Preimplantation genetic screening
PNA	Protein nucleic acid
POF	Premature ovarian failure
POT1	Protector of telomeres 1
PRINS	Primed <i>in situ</i> labelling
PRM1	Protamine 1
PRM2	Protamine 2
QEQMH	Queen Elizabeth Queen Mother Hospital
QFISH	Quantitative fluorescence in situ hybridisation
qRT-PCR	Quantitative real-time polymerase chain reaction
RAD3	Radiation 3
RAD 52	Radiation 52
RAD50	Radiation 50
RAD51	Radiation 51
RAP1	Repressor/activator protein 1
RB	Retinoblastoma
Rif2	Repressor/activator protein 1 interacting factor 2
ROS	Reactive oxygen species
RPA	Replication protein A
RPMI	Roswell park memorial institute medium
RTEL1	Regulator of telomere length 1
Sad1	sn RNP assembly defective 1
SFE	Signal free ends
Sir	Silent information regulator

Sir4	Silent information regulator 4
Sn RNP	Small nuclear ribonucleic particles
SNP	Single nucleotide polymorphism
SPAM1	Sperm adhesion molecule 1
SSC	Sodium saline citrate
STBP	Sperm telomere binding protein
STELA	Single telomere length analysis
SUN1	Sad1 and uncoordinated 84 domain containing protein 1
SUN2	Sad1 and uncoordinated 84 domain containing protein 2
TAE	Tris-acetate ethylenediaminetetraacetic acid
TBS	Tris buffered saline
TE	Tris diaminoethane-tetraacetic acid
TERB1	TRF1-binding protein
TERC	Telomerase RNA component
TERRA	Telomeric repeat-containing RNA
TERT	Telomerase reverse transcriptase
TIN2	TRF1 interacting nuclear factor 2
TPE	Telomere position effect
TPP1	TIN2-POT1 interacting protein 1
TRF	Telomere restriction fragment
TRF1	Telomere repeat factor 1
TRF2	Telomere repeat factor 2
TRFH	Telomere repeat factor homology
UKC	University of Kent
U-STELA	Universal single telomere length analysis
WGA	Whole genome amplification
WHH	William Harvey Hospital
WHO	World health organisation
XPF	Xeroderma pigmentosum group F

Abstract

Telomeres are specialised nucleoprotein structures present at the ends of each chromatid that function to maintain genome stability. It is well established that a gradual decline in telomere length is associated with the process of cellular ageing, and thereby to the pathobiology of age-related diseases. In addition, the localisation of the telomere at the nuclear periphery plays an important role in the spatio-temporal organisation of the genome and in ensuring faithful segregation of chromosomes during meiosis. The aims of this thesis were to investigate telomere localisation in the nucleus, and telomere length in three hitherto early stages of development, gametogenesis, preimplantation embryogenesis and the neonatal period. Specifically:

1. To test the hypothesis that telomeres localised at the nuclear periphery in sperm cells and that this organisation was altered in sub-fertile men
2. To optimise a means of assessing average telomere length using DNA from small sample sizes and using whole genome amplified DNA from single cells
3. To investigate the role of telomere length in reproductive ageing and aneuploidy generation in women by testing the hypothesis that telomere length is significantly shorter in the first polar bodies and cleavage stage embryos of older women
4. To test the hypothesis that “preterm at term” babies (i.e. premature babies assessed at the time of their due date) displayed genetic signs of premature ageing (as manifested by significantly shorter telomeres than their term born counterparts) alongside the already established clinical signs (characterised by hypertension, diabetes and altered body fat distribution)

Results confirmed the peripheral distribution of telomeres in the sperm heads of normally fertile males (using both 2D and 3D imaging) plus the novel finding that telomere distribution patterns are altered in the sperm heads of infertile males. Secondly, a reliable means of measuring telomere length was optimised in order to assess average telomere length using DNA from small sample volumes (down to single cells). Using this technology, average telomere length analysis in polar bodies and embryos found no evidence to support the hypothesis that telomere length is associated with either advanced maternal age or aneuploidy generation. Similarly, results suggest that telomere length is not significantly shorter in “preterm at term” infants compared to term born controls, thus providing no evidence that telomere attrition is involved in the pathobiology of the ‘aged phenotype’ observed in preterm infants. Taken together, results from this thesis provide some novel insights into the function of these highly important features of the genome, but also highlight that a great deal remains to be uncovered in the complex molecular mechanisms that contribute to the regulation of telomere length and nuclear distribution.

1 Introduction: Telomere function and sexual reproduction

Telomeres are highly conserved, nucleoprotein structures present at the ends of each chromosome arm. Since their discovery in the late 1930s, a growing level of interest has been paid to the function and complex regulation of the telomere, which appears to be an essential feature of the genome. Following pioneering studies by Watson, Olovnikov and Hayflick (discussed in section 1.2), the majority of these studies have focused on the relationship between telomere function and the process of cellular senescence (which may be linked to the process of ageing) and immortality (which may be linked to the process of tumorigenesis). In more recent decades however, the role of telomere function in sexual reproduction and early development has begun to attract investigation.

1.1 The structure, function and regulation of the telomere

The term ‘telomere’ is derived from the Greek words ‘telo’ meaning end, and ‘mero’ meaning part, and was first coined by Hermann Muller in 1938 from his study of fruit fly chromosomes. Telomeres are complex, highly specialised structures present on the chromosomes of eukaryotes and some prokaryotes. They are made up of repetitive sequences of non-coding double stranded DNA, associated with a number of proteins (Figure 1.1)(Calado and Young, 2009).

1.1.1 The structure of the telomere

The structure of the telomere is highly conserved and although differences exist from one organism to the next, there are many common features across even phylogenetically diverse genomes. These important structural features are described hereafter.

1.1.1.1 The sequence of the telomere

In all eukaryotes, telomeres are made up of double stranded tandem repeat sequences: a G rich strand and a complementary C rich strand. It was first discovered that telomeres are made up of repetitive sequences in 1978, when Elizabeth Blackburn noted that the *Tetrahymena thermophila* telomere contained repeats of the sequence

TTGGGG (Blackburn and Gall, 1978). Although the precise sequence of the telomere may vary from one organism to the next, in general the 5' → 3' G rich strand contains various numbers of repeats of the sequence (T/A/TA)₁₋₄(G)₁₋₈ (Blackburn and Szostak, 1984; Meyne et al., 1989). Moreover, highly divergent species may share the same sequence despite vast differences in chromosome size and number. For example in humans and all other vertebrates studied, the telomere sequence consists of a TTAGGG hexameric repeat (Meyne et al., 1989; Moyzis et al., 1988). This sequence is also common among fungi, slime moulds and phylogenetically diverse groups of algae (Podlevsky et al., 2008). Indeed it has been postulated that this may be the ancestral motif of eukaryotic telomeres (Fulneckova, 2014).

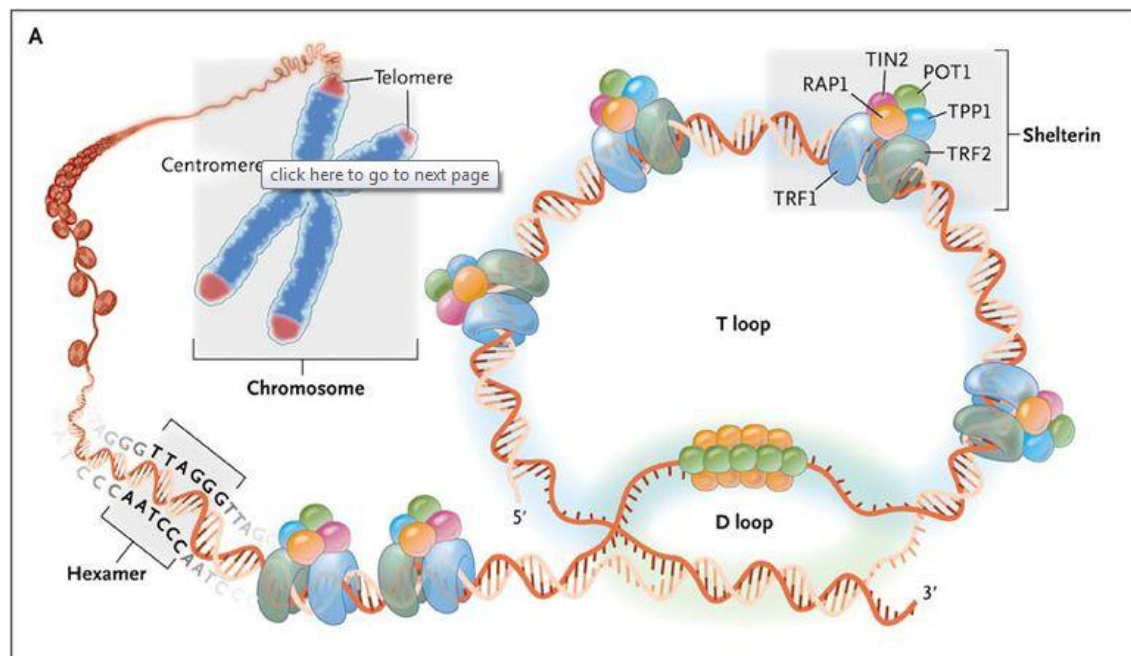


Figure 1.1: The human telomere. Telomeres are made up of repetitive sequences of DNA associated with specialised proteins, present at the end of each chromosome arm. Terminal DNA is organised into a loop formation, with the single stranded G-rich 3' overhang invading the double stranded duplex (Kovacic et al., 2011).

1.1.1.2 The T-loop

At the extreme termini of the chromosome, the G rich 3' end of the telomere protrudes as a single stranded extension, often termed the G-strand overhang. This single stranded extension varies in length from species to species but is shorter than the double stranded tract and loops back to invade the double stranded duplex. This is known as a T-loop. At the base of the T-loop, the G-strand overhang displaces the double stranded duplex, forming a displacement loop, or D-loop (De Lange, 2004) (figure 1.2). This D-loop

formation is thought to be similar to D-loop formation during initiation of homologous recombination (Verdun and Karlseder, 2006). Therefore, it is thought that the 5' strand may be involved in this invasion process, by creating a structure similar to a Holliday junction (a structure involved in homologous recombination) (De Lange, 2004) from guanine rich G-quadruplexes (a structure formed from tetrads of hydrogen bonded guanine bases) (Bochman et al., 2012; Webb et al., 2013; Williamson et al., 1989). G-quadruplexes at the telomere may form from single strands, double strands or four strands of DNA, and may be parallel or anti-parallel. Depending on their conformation, they may function to promote or hinder telomerase (an enzyme involved in telomere length regulation discussed in section 1.1.3.1) (Webb et al., 2013; Zahler et al., 1991; Zaug et al., 2005) and to cap telomeres (Smith et al., 2011). It is thought that regulation of the Holliday junction by regulator of telomere length 1 (RTEL1) ensures that the 3' overhang forms a D-loop only along lengths of DNA belonging to the same chromosome (as oppose to creating tangles between telomeres belonging to separate chromosomes). RTEL1 is an essential helicase that has been shown to be involved in both DNA damage repair and telomere length maintenance. Indeed RTEL1 deficiency results in shortened telomere length and genomic instability. However, the exact mechanisms that enable RTEL1 inhibition of D-loop formation remain to be discovered (Uringa et al., 2010). In addition, it is thought that Rap1 plays a key role in inhibiting inappropriate non-homologous end joining (NHEJ) mechanisms which could result in telomere-telomere fusions. In the yeast model this activity is mediated by repressor/activator protein 1 interacting factor 2 (Rif2) and silent information regulator 4 (Sir4), however again, the exact mechanisms of their actions are unknown (Jain and Cooper, 2010).

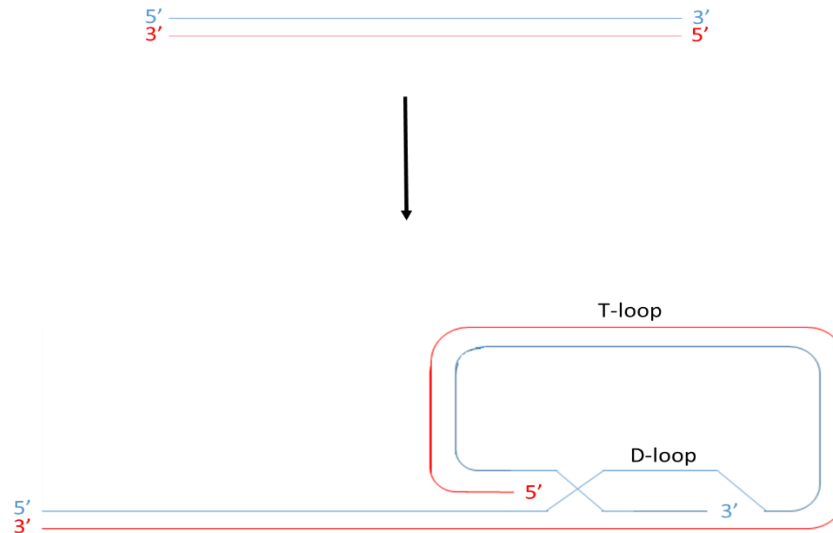


Figure 1.2: The T-loop and the D-loop. The 3' end of the G rich strand protrudes as a single stranded extension of the telomere. This G-strand overhang loops back to form a T-loop, and invades the 5' double stranded telomeric duplex, forming a D-loop.

Although absent in many plant species (or present but very short) (Webb et al., 2013), the G-rich overhang appears to be a conserved feature across many species, however the size of this overhang is variable. In humans it is approximately 100-280 nucleotides (Makarov et al., 1997; Wright et al., 1997) however in budding yeast it varies between 12-14 nucleotides up to 50-100 nucleotides during S-phase of the cell cycle, when genome replication occurs (Wellinger et al., 1993). Similarly the number, and identity of the proteins that are involved in its formation may vary considerably (Wei and Price, 2003). These proteins are known as the shelterin complex, and are discussed in more detail in the next section.

1.1.1.3 The shelterin complex

In mammals, the shelterin complex is made up of six proteins that are associated with telomeric sequences to form the telosome: telomere repeat factor 1 (TRF1), telomere repeat factor 2 (TRF2), telomere interacting protein 2 (TIN2), protection of telomeres 1 (POT1), TIN2-POT1 interacting protein 1 (TPP1) and repressor/activator protein 1 (RAP1) (figure 1.3). These proteins together with the TTAGGG motif form the structure of the telosome, and protect it from DNA repair machinery that might otherwise recognise it as a double strand break. They are also responsible for telomere maintenance by regulating the action of telomerase. While TRF1, TRF2 and POT1

directly interact with the TTAGGG repeat of mammalian telomeres, others interact via association with these highly specific proteins. RAP1 is associated with TRF2 and is responsible for regulating telomere length, whereas TIN2 may associate with TRF1, TRF2, TPP1 and POT1. TIN2 is therefore responsible for tethering of TPP1 and POT1 to TRF1 and TRF2, and for tethering TRF1 to TRF2, which stabilises the association of TRF2 with the telomere (de Lange, 2005a).

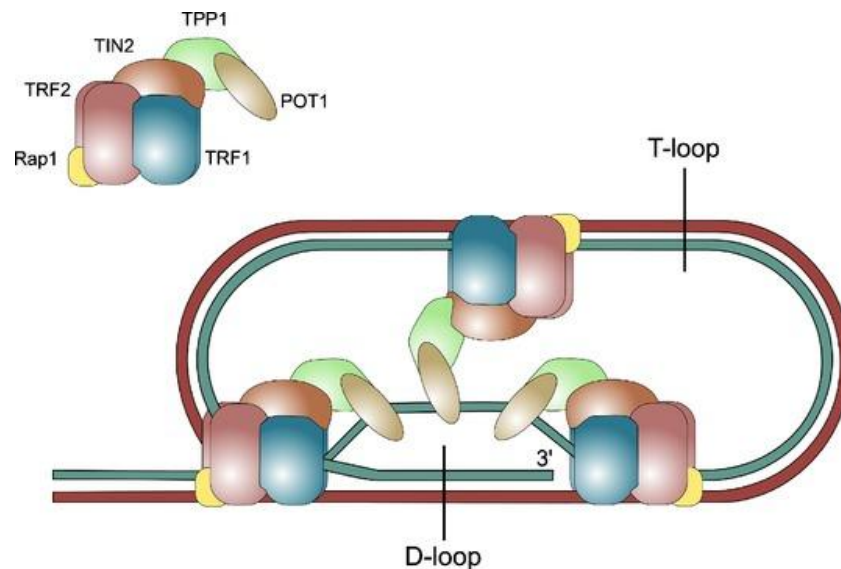


Figure 1.3: The Shelterin Complex. Shelterin is made up 6 associated proteins; TRF1, TRF2, RAP1, TIN2, TPP1, POT1. Diagram taken from (Oeseburg et al., 2010).

The unique high specificity of the shelterin complex for the telomere sequence stems from multiple recognition folds within the complex. TRF1 and TRF2 each have two recognition sites for double stranded telomeric DNA, and may form homodimers or higher oligomers, mediated by a telomere repeat factor homology (TRFH) domain. The carboxy-terminal Myb domains in these two telomeric proteins are essential features for binding to the telomere duplex. Although TRF1 and TRF2 are related proteins that share sequence similarity, their functions differ. TRF1 is thought to be involved in the regulation of telomere length and spans a large sequence, whereas TRF2 is involved in stabilisation of the T-loop, by binding at the double strand and single strand junction (Xin et al., 2008).

POT1 binds with strong specificity for single stranded telomere repeats at the 3' and internal end (de Lange, 2005a), via two oligonucleotide/oligosaccharide binding folds (OB folds) (Lei et al., 2004). Although TPP1 is thought to play a role in enhancing

POT1 binding to DNA via association with TPP1, TPP1 does not interact with the telomere sequence. Thus POT1 is the only protein that is able to bind to single stranded telomere DNA. Similarly to TRF2, POT1 is responsible for capping telomeres and inhibiting the DNA damage response. Interestingly, it has become apparent that although these proteins fulfil similar roles, they are responsible for the regulation of separate signalling pathways. While TRF2 is involved in regulating DNA repair mechanisms via the ataxia telangiectasia mutated (ATM) response, POT1 is involved in regulation of DNA repair mechanisms via the ataxia telangiectasia and radiation 3 (RAD3) related protein (ATR) response (Xin et al., 2008). This is discussed further in section 1.1.1.3.1.

An additional role of POT1/TPP1 heterodimers is their ability to regulate telomere length via regulation of the enzyme telomerase. TPP1 is required for recruitment of telomerase, and to aid telomerase processing. Furthermore, POT1 has been shown to inhibit G-quadruplex formation. Therefore it is likely that POT1 and TPP1 function together to regulate telomere length (Xin et al., 2008).

Another important feature of TPP1 is its interaction with TIN2. TIN2 is involved in the negative regulation of telomere length, and plays a key role in maintaining the interactions of the telosome. Since TIN2 also interacts with TRF1 and TRF2, it provides a key link to associations with TPP1 and POT1 (Xin et al., 2008).

1.1.2 Telomere function

Since their discovery in the late 1930s, it has been clear that telomeres are essential for the maintenance of genome stability. Firstly they protect genes near the ends of chromosome arms from degradation following each round of replication. Secondly they play a significant role in maintaining genome stability by preventing chromosome fusion events. Thirdly, telomeres play an essential role in nuclear organisation, and in genome segregation during mitosis and meiosis.

1.1.2.1 Telomere DNA replication: The ‘end replication problem’

During DNA replication double stranded DNA is denatured into single strands with the aid of helicases and topoisomerases. This permits access of DNA replication

machinery, and most importantly DNA polymerase, the enzyme responsible for catalysing the synthesis of new DNA.

Polymerase forms a new DNA molecule made up of one original DNA strand, and one new DNA strand. For this reason DNA synthesis is described as semiconservative. However, DNA polymerase may only function in 5' → 3' direction, and with the aid of RNA primers (formed by the enzyme primase). The action of polymerase works in the same direction as the progression of the replication fork using the 3' → 5' DNA strand as a template. This results in the continuous synthesis of new DNA in the 5' → 3' direction, hence this is known as the leading strand (Meselson and Stahl, 1958; Ohki et al., 2001; Waga and Stillman, 1998). However, since DNA exists as two antiparallel strands, the complementary strand is orientated against the direction of polymerase action. Synthesis of this strand, known as the lagging strand, is therefore discontinuous as it requires repeated synthesis of RNA primers which are elongated into short fragments (called Okazaki fragments). These are subsequently ligated to form the new DNA strand (Ogawa and Okazaki, 1980; Okazaki et al., 1968; Sakabe and Okazaki, 1966). Consequently, a length of DNA at least the size of the RNA primer is lost at the 5' end of the lagging strand when the RNA primer is removed following replication (Watson, 1972). In reality however, evidence shows lengths of DNA longer than the size of an RNA primer missing at the 5' end of the lagging strand. Such an observation implicates priming failure, resulting in lack of polymerase activity and causing a loss of sequences at the extreme end of the telomere (Ohki et al., 2001). Alternatively, replication fork stalling due to the presence of TRF1/TRF2 complexes (Ohki and Ishikawa, 2004), or fork slipping due to the presence of G-quadruplexes (Kruisselbrink et al., 2008; Lopes et al., 2011; Webb et al., 2013) may also contribute to telomere loss during replication of the genome.

An additional problem in DNA replication lies with the fact that DNA polymerase produces a blunt end at the terminus of the leading strand at one end of the chromosome. As mentioned before, a G-rich overhang is an important structural feature of telomeres, therefore to solve this problem, the complementary C-rich strand of the blunt end must be degraded in order to generate a G-rich overhang (Lingner et al., 1995; Webb et al., 2013; Wellinger et al., 1996). This is brought about in part by nucleolytic activity of the meiotic recombination 11 (MRE11)/radiation 50 (RAD50)/nibrin (NBS1) complex (the MRN complex, which also produces single stranded overhangs

during the process of DNA damage repair) under the control of cyclin dependent kinases (Longhese, 2008). More specifically, this is achieved via MRE11, which possesses four N-terminal phosphoesterase motifs, single stranded DNA endonuclease, 3'-5' DNA exonuclease and DNA annealing and unwinding activities (Williams et al., 2007). Furthermore Apollo possesses a 5'-3' DNA exonuclease activity and therefore it is thought that it is this activity specifically that is able to resect the C rich strand (Lenain et al., 2006). Regulation of the resection process by nucleolytic activity to produce a G rich overhang is considered to occur via members of the shelterin complex. More specifically it has been shown that TRF2 is able to physically interact with Apollo in order to perform this function (Lenain et al., 2006).

Collectively, the phenomena described above are known as the end replication problem, as the length of DNA is shortened following each replication event. Since telomeres are non-coding sections of DNA repeats, no vital genetic information is lost, therefore in this way telomeres function to protect genes near the ends of chromosome arms from degradation. Instead, the loss of telomeric sequences following each replication event ensues, until eventually the length is reduced to such an extent that it reaches critical telomere length. At this point, the cell leaves the cell cycle in G1 and undergoes senescence, which is described in more detail in section 1.1.2.1.1. This phenomenon was first described by Leonard Hayflick in 1961, and therefore the finite replicative capacity of the cell is known as the Hayflick limit (Hayflick and Moorhead, 1961) (discussed in section 1.2). It is now well established that this process of telomere shortening and inevitable cellular senescence is positively correlated with the process of ageing (Olovnikov, 1973).

1.1.2.1.1 Senescence

Senescence describes a process in which the cell leaves the cell cycle and ceases to divide (Hayflick, 1976; Sasaki et al., 1994). It is defined by irreversible cessation of cell division, alongside a number of hallmark characteristics, including: morphological changes (flattened and enlarged cells), changes in expression profiles (upregulation of tumour suppressors, cell cycle inhibitors and DNA damage markers), presence of heterochromatic foci, secretion of signalling molecules, absence of proliferation markers and senescence associated β galactosidase activity (Muñoz-Espín and Serrano, 2014). Senescence is an extremely important cellular response to damage, since it

prevents the replication and spreading of damaged cells and promotes their clearance by immune cells. This is vital in ensuring the prevention of tumorigenesis. In addition senescence plays an essential role during embryogenesis and tissue renewal by limiting the amount of tissue that is produced (Muñoz-Espín and Serrano, 2014). Interestingly it appears that both senescence and apoptosis (which describes programmed cell death) function to perform very similar roles during embryogenesis and tissue renewal. However the mechanisms controlling their inter-activity and the mechanisms which dictate whether the cell will undergo senescence or apoptosis is currently unknown (Vicencio et al., 2008). There are a number of stimuli that induce cellular senescence, however in the context of telomere function, it is known that a loss of telomere repeats (either due to damage or due to the end replication problem described in section 1.1.2.1) elicits a DNA damage response mediated by ATM or ATR pathways. In turn, this leads to phosphorylation of p53, expression of p21 and inhibition of cyclin dependant kinases that permit progression through the cell cycle (Muñoz-Espín and Serrano, 2014). It is thought that an accumulation of senescent cells drives the process of ageing due to a reduction in the number of mitotically active progenitor cells, alongside the release of degradative proteases, growth factors and inflammatory cytokines, which impact upon non-senescent neighbouring cells (Vicencio et al., 2008). Under normal circumstances, the release of these components would stimulate immune clearance of senescent cells, however as the immune system ages, its ability to clear senescent cells is impaired (Muñoz-Espín and Serrano, 2014).

1.1.2.2 Telomeres and genome stability:

Under normal circumstances, a break in DNA would result in the recruitment and action of DNA repair mechanisms. In Herman Muller's experiments with *Drosophila* in 1938, an important observation that led him to the discovery of telomeres, was that inversion events never involved the very end of the telomere fusing with another chromosome. Furthermore, Barbara McClintock confirmed this important function of telomeres in 1939, shortly after Muller. Her observations of maize chromosomes showed that fusion events only occurred in broken chromosomes, not unbroken ends. These pioneering observations led to the idea that telomeres are required to maintain genome stability, and that the cells ability to recognise telomeres as normal features, rather than double strand breaks, is essential to avoid inappropriate action of DNA

repair mechanisms (McClintock, 1939; Muller, 1938). Since these experiments, it has been established that the ability of the telomere to evade a DNA damage response is orchestrated through tightly controlled interactions between the shelterin complex and proteins involved in DNA repair. These DNA repair proteins are made up of those involved in ATM and ATR mediated repair pathways via NHEJ and homologous recombination respectively (Longhese, 2008).

The mechanisms by which the shelterin complex is able to inhibit DNA repair pathways are largely unknown, but current evidence suggests that inhibitory action is predominantly brought about through the shelterin complex physically blocking access of DNA damage proteins at telomeric sequences (Longhese, 2008). For example, POT1 physically blocks the recruitment and accumulation of replication protein A (RPA) along the single stranded 3' overhang, which would otherwise result in ATR mediated homologous recombination based repair (Lei et al., 2004; Lei et al., 2005). Similarly, TRF2 possesses the ability to remodel telomeric DNA in order to favour 5' strand invasion by the 3' overhang leading to T-loop formation (Amiard et al., 2007). This hides the single stranded DNA overhang from accumulation of RPA resulting in ATR mediated repair. Furthermore, the formation of the T-loop inhibits the accumulation of Ku70-Ku86 complexes, which stabilise broken DNA ends in close proximity to one another and stimulates fusion via DNA ligase IV (Costantini et al., 2007; Ramsden and Gellert, 1998). Thus TRF2 is able to inhibit both homologous recombination and NHEJ mediated repair via ATR and ATM pathways respectively. Interestingly, TRF2 is additionally able to inhibit ATM induction of cell cycle arrest via direct binding. Although the exact mechanism in which this occurs is unclear, it is thought that TRF2 is able to block ATM autophosphorylation by directly binding to its Ser1981, which in turn blocks ATM activation (Bakkenist and Kastan, 2003; Denchi and de Lange, 2007; Karlseder et al., 2004). Indeed, loss of TRF2 leads to ATM activation and upregulation of p53, leading to p21 mediated cell cycle arrest via inhibition of cyclin dependant kinase 1 (CDK1) and subsequent inhibition of retinoblastoma (RB) (Karlseder et al., 1999).

Several other proteins that are involved in ATM and ATR mediated DNA repair are found in association with the telosome, therefore the presence of an intact telomere structure is extremely important in order to avoid inappropriate action. Most notably,

these include DNA protein kinase (DNA-PK) (which is made up of Ku and a protein kinase catalytic subunit), tumour suppressor protein p53, poly adenosine diphosphate ribose polymerase (PARP), Tankyrase 1 and 2, excision repair cross-complementing associated with xeroderma pigmentosum group F (ERCC/XPF), radiation 51 (RAD51), werner (WRN), and bloom (BLM) (Bailey et al., 2001; Bailey et al., 1999; Bailey and Murnane, 2006; di Fagagna et al., 1999; Hande et al., 1999; Hsu et al., 2000; Lansdorp, 2000; Samper et al., 2000; Zhu et al., 2000). Many of these are also involved in regulating telomere length; for example Mre11 of the MRN complex (which associates with TRF2) is involved in the generation of a 3' overhang which acts as a substrate for telomerase (an enzyme responsible for telomere lengthening, discussed in more detail in section 1.1.3.1) (Bailey and Murnane, 2006; Lansdorp, 2000; Verdun et al., 2005; Zhu et al., 2000). Similarly, ATM (which is recruited by MRN) may phosphorylate TRF1 resulting in its dissociation from the telomere and enabling access of telomerase to allow telomere elongation (Wu et al., 2007). Indeed ATM knockout mice possess drastically shortened telomeres and a large number of extrachromosomal telomeric circles (Hande et al., 2001). Maintaining telomere length is extremely important in forming a functional telomere, since shortened telomeres cannot support the telosome and therefore chromosome fusion events ensue (as demonstrated in the mouse model) (Blasco et al., 1997). Thus DNA damage response proteins are responsible for both preventing and causing genomic instability events, and therefore it is essential that they are tightly controlled by members of the shelterin complex.

Despite the risks associated with chromosome fusion events, it must be appreciated that such events can be 'normal' and produce sustainable products. Chromosome fusion events play vital roles in evolution of the genome. An example of this is evident in the divergence of avian genomes which show several fusion events (Voss et al., 2011), and indeed the human genome, which shows fusion of ancestral chromosomes 12 and 13 to give rise to human chromosome 2 (Ijdo et al., 1991; Kasai et al., 2000). Furthermore, the normal association of telomeres with one another and with components of the nucleus plays a vital role in genome organisation and cellular division.

1.1.2.3 Telomeres and nuclear organisation

Since early observations from Carl Rabl and Theodor Boveri at end of the 19th century, the hypothesis that nuclear organisation is non-random has been frequently tested. It

is now well established that chromosomes occupy discrete territories (Cremer et al., 1993; Lichter et al., 1988; Manuelidis and Borden, 1988), dependent on the stage in the cell cycle and the cell type (Funabiki et al., 1993; Mayer et al., 2005). Such highly specific nuclear organisation has been shown to be conserved in eukaryotes (Neusser et al., 2007; Tsend-Ayush et al., 2009), and therefore it is unsurprising that it serves a functional role. Several studies have shown that nuclear organisation plays a pivotal role in ensuring that appropriate regions of the genome are positioned in proximity to replication and transcriptional cues. Furthermore, it is considered that nuclear organisation is highly important in ensuring the correct orientation of chromosomes within the nucleus, which is important during cell division. Therefore strict nuclear organisation acts to regulate normal functioning of the genome (Cremer and Cremer, 2001), and deviation from this strict pattern of nuclear organisation is known to result in several pathologies including cancer (Kuroda et al., 2004) and laminopathies (Mewborn et al., 2010). There are several models of nuclear organisation, which are each discussed below.

1.1.2.3.1 The Rabl configuration

In interphase cells of many species including plants, animals and single cell eukaryotes, telomeres cluster at one pole of the nucleus on the opposite side to the centromeres (Funabiki et al., 1993; Hilliker and Appels, 1989; Hiraoka et al., 1990; Mathog et al., 1983; Sperling and Luedtke, 1981). This is known as the Rabl configuration (shown in figure 1.4), and is thought to begin at anaphase and persist into interphase (however this appears to be species and cell type specific) (Cremer et al., 1982; Rabl, 1885). This conformation is thought to be vital for ensuring the correct orientation of chromosomes, which aids in the maintenance of genome integrity (Manders et al., 1999; Parada and Misteli, 2002).

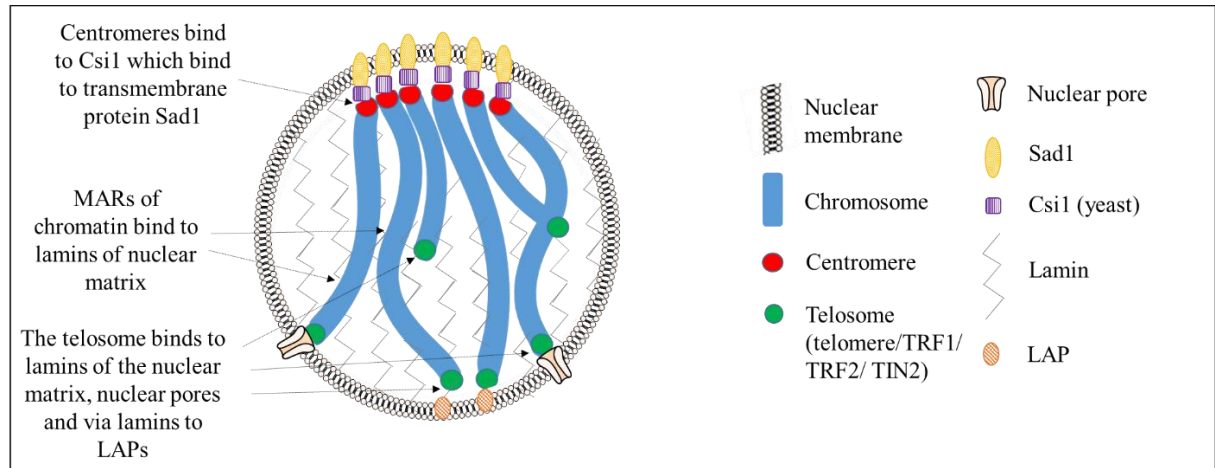


Figure 1.4: The Rab1 configuration. Centromeres (coloured in red) cluster at one pole of the nucleus via interactions with the nuclear membrane through Csi1 and Sad1. Chromosome arms (coloured in blue) are attached to lamins of the nuclear matrix via matrix attachment regions (MARs). Telomeres (coloured in green) are orientated towards the opposite pole of the nucleus to centromeres and attach to lamins of the nuclear matrix via TRF1, TRF2 and TIN2. Telomeres are additionally anchored at the nuclear envelope via associations with lamins which in turn bind to nuclear membrane spanning lamin associated proteins (LAPs), or via interactions with the nuclear pore.

Centromere interactions with the nuclear membrane is essential for anchoring chromosomes in the Rab1 Configuration. In yeast, this occurs via interactions with Cop9 Signalosome Interactor 1 (Csi1), which in turns binds to membrane spanning protein small nuclear ribonucleic particles (sn RNP) assembly defective 1 (Sad1). In addition, it has been proposed that telomeres have a significant role in the organisation of chromosomes into the Rab1 orientation by providing further anchorage points. Tight association of the telomere sequence with lamins of the nuclear matrix has previously been demonstrated, and has been shown to involve TRF1 and TRF2 proteins as well as TIN2 (de Lange, 1992; Kaminker et al., 2009; Luderus et al., 1996; Weipoltshammer et al., 1999). Indeed disruption to nuclear lamins results in telomere redistribution (De Vos et al., 2010; Gonzalez-Suarez et al., 2009; Raz et al., 2008). Furthermore, interactions of telomeres with lamin associated proteins (LAPs) via lamins plays a key role in anchoring telomeres in place (Dechat et al., 2004; Ludérus et al., 1992; Novo and Londoño-Vallejo, 2013; Shoeman and Traub, 1990). In addition, several studies have implicated the nuclear pore complex in tethering of telomeres to the nuclear periphery, which may be chromosome specific, and dependent upon the stage in the cell cycle, and different telomere states (Bukata et al., 2013). The association of telomeres to form clusters at the nuclear periphery has been noted in several cell types, and is thought to play a crucial role in the 3D organisation of chromosomes. Finally,

the Rabl configuration also relies on chromosome-chromosome interactions, chromosome interactions with lamins via matrix attachment regions (MARs) and chromosome interactions with the nuclear envelope via lamins (Cowan et al., 2001).

1.1.2.3.2 The ‘chromocentric’ model of nuclear organisation

In addition to telomere involvement in the Rabl configuration, the chromocentric model of nuclear organisation (shown in figure 1.5) proposes a model in which centromeres localise in the interior of the nucleus to form a chromocenter, whereas telomeres cluster at the nuclear periphery (Jennings and Powell, 1995; Zalensky et al., 1993). First described in sperm nuclei (which will be discussed in more detail in section 1.4.1.1), the chromocentric model of nuclear organisation has been seen in retinal cells of several nocturnal mammals (Solovei et al., 2009), *Saccharomyces cerevisiae* (Bupp et al., 2007), *Drosophila melanogaster* salivary glands (Hochstrasser et al., 1986; Mathog et al., 1983) and in mouse lymphocytes (Weierich et al., 2003).

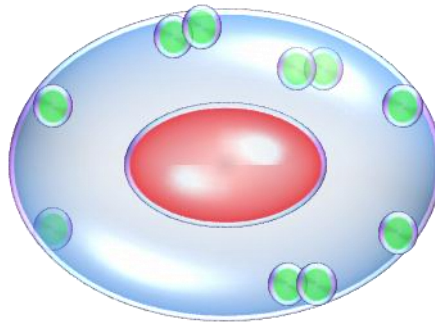


Figure 1.5: Diagrammatic representation of the chromocentric model of nuclear organisation, whereby centromeres (red) form a chromocentre deep within the nuclear volume and telomeres (green) from clusters at the nuclear periphery.

1.1.2.3.3 Other models of nuclear organisation

Aside from the Rabl and chromocentric models of nuclear organisation (which specifically involve telomeres) there are two other main models of nuclear organisation which are not dependent upon the telomere. These include the size dependant model and the gene density model. The size dependant model describes a system whereby smaller chromosomes occupy the interior regions of the nucleus and larger ones the periphery (Sun et al., 2000). This has been observed in human lymphocytes (Sun et al., 2000) and in human and chicken fibroblasts (Bolzer et al., 2005; Cremer et al., 2001; Habermann et al., 2001). Alternatively a gene density model has been proposed, in

which gene rich chromosomes occupy the interior regions of the nucleus and gene poor ones the periphery, irrespective of size (Cremer et al., 1993; Croft et al., 1999). This model has been shown in human lymphoblasts and dermal fibroblasts (Boyle et al., 2001; Cremer et al., 2003; Croft et al., 1999; Lukasova et al., 1999), and in porcine lymphocytes (Federico et al., 2004) and primate lymphoblasts (Tanabe et al., 2004; Tanabe et al., 2002). Of course, evidence shows that some cell types fit both of these models, including chicken fibroblasts and porcine genomes (Foster and Bridger, 2005; Habermann et al., 2001), and that others including some murine models fit neither (Meaburn and Misteli, 2008). Nonetheless, it is widely considered that genome organisation is non-random, and is functionally relevant for gene expression patterns (Cremer and Cremer, 2001).

1.1.2.4 Telomeres and cell division

During meiosis, telomeres cluster under the nuclear envelope positioned toward the centriole at the early leptotene stage of prophase I, with centromeres dispersed across the nuclear periphery at the opposite pole. This results in a ‘bouquet’ appearance of chromosomes within the nucleus, and is dependent upon telomere association as a group. It is thought that this telomere led bouquet formation of chromosomes within the nucleus is essential for chromosomes pairing and the formation of the synaptonemal complex (a protein matrix that reinforces the interaction between homologous pairs) and meiotic recombination in mice and humans (Kohli, 1994; Rasmussen and Holm, 1978; Scherthan et al., 1996). Therefore, such organisation of telomeres indicates an important role of telomeres in the segregation of the genome into daughter cells during meiotic divisions (Blackburn and Szostak, 1984). This will be discussed in section 1.4.

1.1.3 Telomere length regulation

With the above information in mind, it is clear that the telomere serves several important functions, which ultimately results in maintenance of genome stability, correct nuclear architecture and faithful segregation of chromosomes in cell division. In order for this to be efficiently and accurately achieved, a fully functional telomere is required. The major limiting factor of a fully functional telomere, is the length of the repeat sequence itself. Telomeres that have shortened beyond a threshold level can no longer perform their roles, due to their inability to associate with the many proteins that

are involved in their regulation and function. In normal cells, loss of telomeres beyond the critical length leads to cell senescence, where the cell exits the cell cycle in G1 and ceases to divide (the Hayflick limit) (Hayflick and Moorhead, 1961). However, failure of the cell to recognise this critical point leads to a number of detriments resulting from chromosome instability.

Thus it is clear that telomere length must be maintained and regulated in some way in order to perform normal function. There are two ways in which this may be achieved: The first and most prominent contributor in telomere length maintenance is via telomerase, a key enzyme responsible for the synthesis of new telomere repeats (Greider and Blackburn, 1985) (section 1.1.3.1). The second method of telomere length maintenance is via alternative telomere lengthening (ALT) strategies (1.1.3.2), which can be sub-divided into recombination based ALT, retrotransposon involvement, and epistasis.

1.1.3.1 Telomerase mediated telomere maintenance

The discovery of telomerase was a major breakthrough in the study of telomeres and eventually led to the award of a Nobel prize for Elizabeth Blackburn and her team in 2009. Telomerase is a ribonucleoprotein complex, made up of RNA subunits (telomerase RNA component (TERC)) and a reverse transcriptase catalytic subunit (telomerase reverse transcriptase (TERT)). Telomerase synthesises new repeats to the strand running in the 5'→3' direction toward the chromosome end, and thus synthesises the 3' single stranded overhang of the telomere. The TERT catalytic subunit does this by copying the short RNA template sequence in its TERC subunit (Greider and Blackburn, 1989), which is also responsible for recognition of the telomere sequence itself. Synthesis of the complementary strand, is thought to occur via normal lagging strand DNA synthesis using DNA polymerase (Chan and Blackburn, 2004), depicted in figure 1.6 on page 18.

Regulation of telomerase activity at the telomere is thought to be controlled by DNA damage response pathways, further supporting a role for their existence at the telomere. These damage response proteins are in turn regulated by members of the telosome. The majority of studies that have unravelled telomerase regulation pathways have been carried out in yeast models. These have identified that ATM and ATR DNA damage

checkpoint proteins promote telomerase activity. The recruitment of telomerase through ATM, is via the MRN damage complex, of which NBS1 (a substrate for ATM (Craven et al., 2002; Kastan et al., 2001). The MRN complex, has endonuclease activity on DNA, which converts the DNA strand into a substrate for telomerase (Tsukamoto et al., 2001). Thus the current model suggests that uncapping of telomeres as a result of telomere sequence loss, leads to recognition by the DNA damage response pathway. This in turn acts on the telomere structure, and promotes synthesis of new telomere sequences via the recruitment and action of telomerase (Chan and Blackburn, 2004; Chan et al., 2001). The length of the telomere itself therefore plays a key role in telomerase regulation, since loss of telomere sequence in turn results in loss of the telosome. The fact that short telomeres are more likely to be extended by telomerase than longer ones provides support of this (Bianchi and Shore, 2007; Sabourin et al., 2007). Furthermore, in yeast, RAP1 interacting factor 2 (Rif2) preferentially binds to long telomeres and inhibits ATM (McGee et al., 2010).

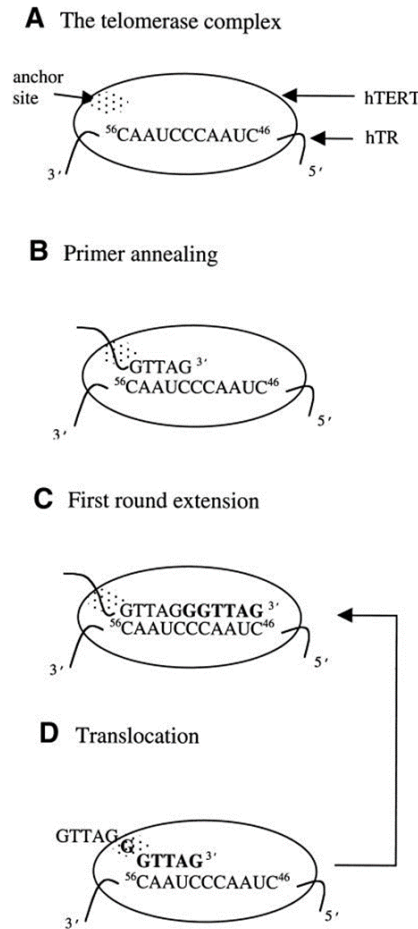


Figure 1.6: Leading strand telomere lengthening by telomerase. (A) Recruitment of telomerase to the telomere by ATM promotes primer annealing (B) and initiates reverse transcriptase activity of the TERT component, using the TERC RNA template. Telomerase elongates the leading strand (C) and is then transferred to another telomere for the process to repeat again (D) (Gavory et al., 2002).

Alternatively, telomerase may be inhibited by telomeric repeat-containing RNA (TERRA). This non-coding RNA is expressed from sub-telomere and telomere sequences of all chromosomes, and is associated with telomeres (Azzalin et al., 2007). TERRA may act on telomerase in order to suppress activity by acting as a competitive inhibitor (Redon et al., 2010), or be inhibited by telomerase depending on their feedback on one another (Arnoult et al., 2012). This regulation of telomerase by TERRA remains to be further characterised (Luke and Lingner, 2009).

The complex interplay between telomerase and other components of the telosome means that regulation of telomere length by telomerase is extremely tightly controlled. Furthermore, although telomerase is inactivated in most somatic cells, those that are highly proliferative have been shown to exhibit telomerase activity, such as cells of the

immune system, skin, hair follicles and intestinal lining .Therefore telomerase serves a significant function, not only in cancerous cells, germ cells and embryogenesis as originally thought, but also in normal somatic cell turnover (Blackburn, 2000; Masutomi et al., 2003).

1.1.3.2 Alternative lengthening of telomeres

In organisms where telomerase is not present, or when telomerase expression is repressed, synthesis of telomeric repeats must occur by some other means. The main ALT strategies are via homologous recombination, retrotransposons and epistasis (Biessmann and Mason, 1997).

1.1.3.2.1 Telomere lengthening by homologous recombination

Telomere lengthening by homologous recombination occurs in many cell types where telomerase expression is repressed (e.g. tumour cells). In these cells, telomeres are often heterogeneous in length (Biessmann and Mason, 1997). Although telomere elongation using this system has been fairly well studied, the exact mechanisms are not fully understood. It has been hypothesised that the 5' overhang of the telomere belonging to one chromatid may invade the T-loop of the telomere belonging to the homologous chromatid. This resembles a replication fork, which may be recognised by polymerase, resulting in extension of the telomere (shown in figure 1.7). It is thought that this process is regulated by RAD51, radiation 52 (RAD52) and replication protein A (RPA) as well as the MRN complex (Henson et al., 2002).

Interestingly, homologous recombination at telomeres may also serve to reduce telomere length in cases where telomerase is present and telomeres are exceptionally long. In yeast, an MRN dependent mechanism generates T-circles by homologous recombination mediated deletion of T-loops, significantly reducing telomere length back to wild type length (Li and Lustig, 1996). These extra chromosomal T-circles can in turn act as templates for homologous recombination mediated telomere lengthening (Cesare and Griffith, 2004; Natarajan and McEachern, 2002). A similar mechanism has also been shown in mammals (Wang et al., 2004), however, under normal circumstances, Ku and TRF2 proteins regulate homologous recombination mediated telomere shortening (Celli et al., 2006; Sfeir et al., 2010).

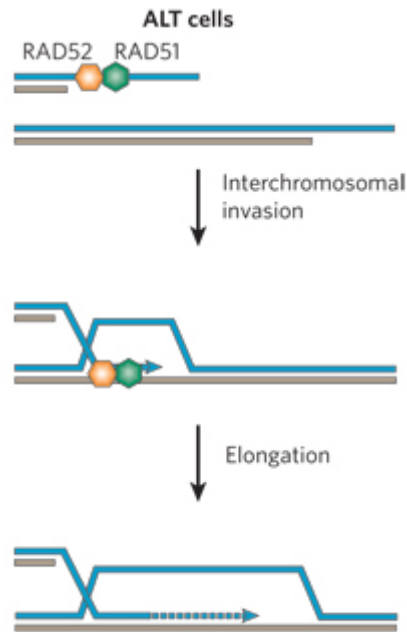


Figure 1.7: Alternative lengthening of telomeres by homologous recombination. RAD51 and RAD52 regulate invasion of the 3' overhang into the T-loop of a telomere present on a separate chromosome. This forms a structure similar to a replication fork, allowing synthesis and addition of more telomeric repeats by DNA polymerase. Taken from (Verdun and Karlseder, 2007).

1.1.3.2.2 Telomere lengthening by retrotransposition

Retrotransposon mediated ALT is predominantly a feature of the chromosome ends of *Drosophila*, which are made up of retrotransposed elements. The length of these elements are regulated by both homologous recombination and transposition (Levis, 1989). A single targeted transposition of several kilobases to the chromosome end occurs due to the loss of endonuclease activity of the retrotransposon (Mason et al., 2008). Thus it may only reposition to DNA ends. Evidence for this model of telomere lengthening is shown by the arrangements of huntingtin (HTT) elements at *Drosophila* chromosome ends, where tandem head to tail arrays with their 3' ends pointing to the chromosome end, possess variable 5' sequences. This proves that new transposons are placed at the chromosome end following different amounts of sequence loss before the arrival of a new sequence (Levis et al., 1993).

Interestingly telomere maintenance by transposition has been shown in rare cases in telomerase deficient yeast, where the subtelomeric Y' has been shown to move in an RNA mediated process (Maxwell et al., 2004). Similarly evidence shows that long interspersed elements (LINE-1) may move to dysfunctional telomeres in Chinese hamster ovary (CHO) cells deficient in TRF2 capping (Morrish et al., 2007).

1.1.3.2.3 The telomere position effect

In recent years, an increasing level of interest has been paid to epigenetic markers found at telomeres and subtelomeres. These chromatin modifications involving histones and DNA sequences at telomeres and subtelomeres, include DNA methylation, histone methylation and histone hypoacetylation. Such modifications have been shown to play a role in the silencing of genes that are in close proximity to the telomere. This phenomenon, known as the telomere position effect (TPE) was first observed in *Drosophila* (Baur et al., 2001; Gottschling et al., 1990; Levis et al., 1985).

TPE has also been shown in mammals, where it may regulate, and be regulated by telomere length (Baur et al., 2001). This is evident by the fact that loss of function of the proteins involved in TPE often results in telomere elongation (Schoeftner and Blasco, 2009). In turn, it has also been shown that the number of telomere repeats directly regulates chromatin modifications at the chromosome end, thus telomere elongation results in increased TPE chromatin modifications (Kyrion et al., 1993). Similarly, telomere shortening causes loss of histone methylation and increased histone acetylation.

Although it is unknown how chromatin modifications directly influence telomere length and structure, it is plausible that telomere length regulators are positively controlled by heterochromatin factors. Therefore heterochromatin disruption impedes their ability to regulate telomeres. This has been hinted towards in a handful of studies showing that TRF1 overexpression leads to TPE reversal (Koering et al., 2002), and that TIN2 is able to interact with heterochromatin protein 1 (HP1) (which promotes histone methylation) (Kaminker et al., 2005).

Furthermore, DNA and histone modifications by TPE also serve to maintain genome stability. Evidence shows that disruptions in chromatin modifications at the telomere leads to chromosome mis-segregation (Opravil et al., 2001).

Overall, it is clear that the telomere is a fundamentally important feature of the genome, which owes its diverse roles to its unique structure and location in both the metaphase and interphase nuclei. The complex interplay between components of the telosome, which serves to regulate telomere length, plays a vital role in telomere homeostasis in normal processes and disease initiation and progression.

1.2 Normal and dysfunctional telomere homeostasis

Normal telomere homeostasis is controlled by a complex balance between attrition and mechanisms of telomere lengthening. As discussed in section 1.2.1, telomere shortening following each round of replication is a normal part of telomere homeostasis and serves a functional role in preserving genome integrity. Many studies have linked this process to cellular ageing *in vitro* and highlighted a relationship between telomere length and normal organismal ageing *in vivo*. Should this balance become unstable however during abnormal conditions, aberrant telomere length homeostasis can lead to several undesired effects; most notably, tumorigenesis (section 1.2.2).

1.2.1 Normal telomere homeostasis and ageing

The study of how telomeres are related to the process of ageing is a subject that has received a great deal of attention. After their discovery more than 75 years ago, it was a further 40 years until Watson and Olovnikov proposed the idea of the end replication problem, and how this might be related to Leonard Hayflick's observation of the cells replicative capacity (Hayflick and Moorhead, 1961; McClintock, 1939; Muller, 1938; Olovnikov, 1973; Watson, 1972). However, no formal link between telomere length and cellular ageing was made until 1986, when Smith and Cooke showed evidence of longer telomeres on the sex chromosomes of sperm cells compared to adult somatic cells (Cooke and Smith, 1986).

Since this discovery, a number of others have confirmed the shortening of telomeres in association with replicative capacity *in vitro*, and in relation to chronological age *in vivo*. Calvin Harley was one of the first to show that telomere length in fibroblasts decreased with the number of passages, and that the total number of passages before entering senescence correlated with initial telomere length and donor age (Harley et al., 1990). A similar study by Allsopp also noted that telomere length of fibroblasts decreased with age, and that in agreement with Harley's observations, initial telomere length correlated strongly with replicative capacity in culture (Allsopp et al., 1992). These observations were extended in *in vivo* observations showing that telomere length was shortened as a function of age in both skin, colorectal and blood samples (Hastie et al., 1990; Lindsey et al., 1991).

Interestingly, these investigations have also highlighted that although telomere length generally declines as a function of age, in many studies the data is somewhat scattered, and therefore the correlation may be weak. This suggests that telomere length is highly variable from one individual to the next, and therefore is not solely dependent upon chronological age, but also in combination with other factors (Allsopp et al., 1992; Hastie et al., 1990). The correlation between telomere length and replicative capacity however, appears to be much stronger (Allsopp et al., 1992).

In light of this, Leonard Hayflick proposed the idea that telomere length is a more accurate measure of maximum longevity than the process of ageing. He hypothesised that telomeres may simply act as a buffer for a reserve capacity of physiological function to ensure survival beyond reproductive maturity. Since the process of ageing is stochastic, involving many physiological and molecular changes, whereas telomere attrition is not, the process of ageing may occur before the reserve capacity has been extinguished *in vivo*. Thus the process of ageing and inevitable death precedes complete telomere loss and the Hayflick limit (Hayflick, 1998, 2003). This is reiterated by the conflicting data that exists regarding telomere length and mortality. While some studies show that telomere length does provide a predictive measure of mortality (Cawthon et al., 2003), other studies do not (Honig et al., 2006; Martin-Ruiz et al., 2005).

Nonetheless, telomere shortening following each successive round of replication is a feature of normal functioning mitotic cells. Once telomeres have shortened to a critical length in normal cells, ATM/ATR, p53 and RB DNA damage response pathways are initiated, which results in senescence (Herbig et al., 2004; Shay, 2003). The question of whether shortened telomere length is the cause or the effect of the process of ageing (or both) has remained a subject of some debate. What is clear however, is that the two are related to one another (Allsopp et al., 1992; Harley et al., 1990; Hastie et al., 1990). This has provoked many to ask the question: At what point does telomere attrition begin? The next sections are therefore dedicated to what is known about telomere homeostasis from the earliest stages of life.

1.2.1.1 Telomere homeostasis during embryogenesis

As the genomes from the spermatozoon and ovum combine during fertilisation and undergo replication and division during embryogenesis, the regulation of telomere

length is paramount in order to produce a viable offspring in which telomere length is 'reset'. This ensures that the offspring have sufficient telomeric reserve to fulfil a normal and healthy lifespan.

Following fertilisation, telomere length appears reduced in the cleavage stage embryo compared to the oocyte (Turner et al., 2010). This possibly reflects telomere shortening during prolonged meiotic arrest, which becomes evident following DNA replication subsequent to fertilisation (Passos et al., 2007). After the cleavage stage, telomere length reduces further at the morula stage, then increases at the blastocyst stage (Turner et al., 2010) when embryonic genome activation occurs and therefore telomerase expression may increase (Liu et al., 2007; Wright et al., 2001). Changes to telomere length during embryogenesis is depicted in figure 1.8 on the next page.

Intriguingly, telomere lengths of individual blastomeres in cleavage stage, morula and blastocyst stage embryos show a high degree of variation (Turner et al., 2010). This is in line with observations that telomerase activity in individual blastomeres also show a high degree of variability (Wright et al., 2001). Alternatively, this might be a result of recombination based ALT (Liu et al., 2007; Turner et al., 2010; Wright et al., 2001), chromosomal mosaicism (which is common in embryos) (Delhanty et al., 1997) or differences in polarity and ability to activate the embryonic genome (Edwards, 2005; Tesarik, 1989).

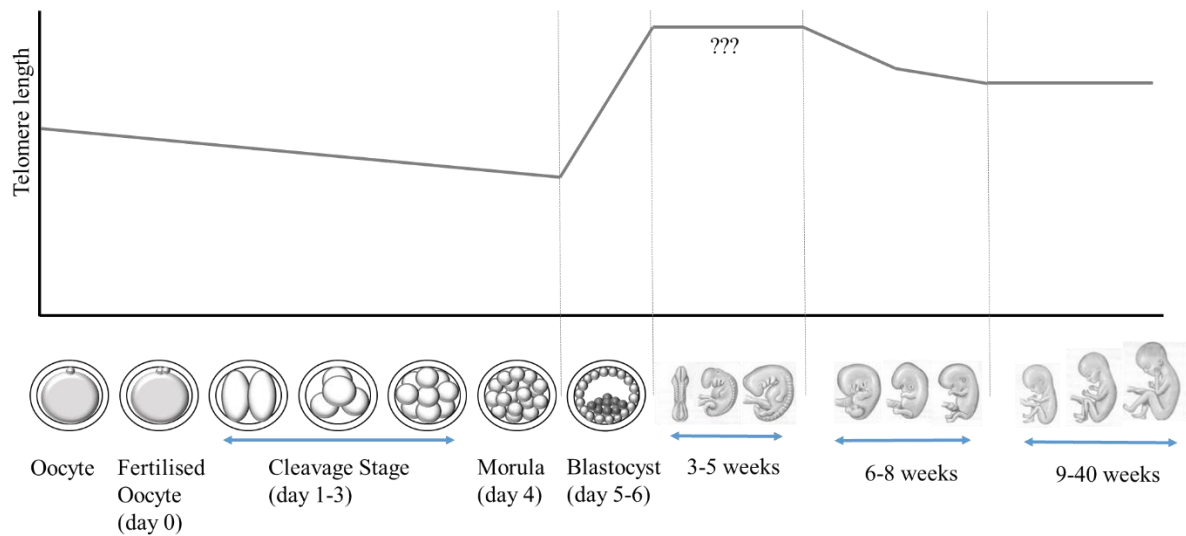


Figure 1.8: Telomere length changes following fertilisation through embryogenesis and fetal development. Telomere length declines after fertilisation through cleavage and morula stages, then drastically increases at the blastocyst stage. Current literature has not explored telomere length at the earliest stages of gastrulation and development, however between weeks six and seven of gestation telomere length appears to decline. This decline in telomere length continues between weeks seven and eight, however it is less pronounced. All other developmental stages tested (weeks nine to 19 and weeks 23 to 36) show steady maintenance of telomere length. Fetal images adapted from http://homepage.smc.edu/wissmann_paul/anatomy2textbook/.

1.2.1.2 Telomere homeostasis during fetal development

Very few studies have investigated telomere length in the developing fetus, due to limitations in sample material available. However a few important discoveries have been made and these are illustrated in figure 1.8. A study by Youngren *et al* was the first to measure telomere lengths in different tissues from fetuses between 15 and 19 weeks gestation. Results showed that telomere lengths were variable between fetuses, but this was not associated with gestational age. The authors also concluded that telomere length among different tissues are synchronous during fetal life, which is lost in extra-uterine life. Interestingly however, this study observed no correlation between telomere lengths of specific tissues and telomerase activity (Youngren *et al.*, 1998). Holmes *et al* went on to investigate this observation further and found that telomere length fluctuated during several time point intervals between 23 and 36 weeks gestation, but resulted in an overall increase in telomere length, or no detectable change (Holmes *et al.*, 2009).

Taken together, the above observations are in line with the finding that telomerase activity is present in many fetal tissues, including liver, lung, intestine, kidney, skin,

muscle and adrenal glands between 16 and 20 weeks gestation (Wright et al., 1996). Furthermore, a study by Ulaner and Giudice showed that telomerase activity is present in liver, lung, spleen, testis, brain, kidney and heart at eight weeks gestation. This is lost in the heart after 12 weeks, and in brain and kidney at 16 weeks, but is maintained up to the latest stage of testing at 21 weeks in all other tissues (Ulaner and Giudice, 1997). Furthermore, a later study by Cheng and colleagues 2013 confirmed findings by Holmes *et al* 2009, and provided further insight into telomere length dynamics during fetal development. In this study, telomere length and telomerase was measured from six weeks until eleven weeks gestational age, and compared with telomere lengths of full term infants. Results showed rapid telomere attrition between weeks six and seven, which then slowed between weeks eight and eleven. After this point, telomere length was slightly reduced, or not different to telomere lengths of full term infants at birth. Telomerase activity showed an inverse correlation such that a steady decrease in activity was observed from six weeks gestation until 11 weeks gestation (Cheng et al., 2013b; Holmes et al., 2009).

1.2.1.3 Telomere homeostasis in the newborn

Studies investigating telomere length in the newborn generally show that while telomere length is steady during fetal life, it begins to decline from birth. Indeed it has been postulated that events during birth itself may play a role in initiating telomere attrition. Evidence for this has been shown in a study by Holmes *et al.* 2009, in which it was found that preterm infants showed a steady decline in telomere length following birth, whereas telomere lengths of age matched fetuses *in utero* remained constant (Holmes et al., 2009). It is thought that this maintenance of telomere length during normal gestation is important in ensuring a supportive environment for development. Indeed it has been postulated that short telomere length resulting from increased oxidative stress can lead to premature rupture of amniotic membrane and premature birth. This was demonstrated in a study by Menon and colleagues 2012, which found that fetal leukocyte and placental telomere lengths were shortened in preterm infants born following preterm rupture of amniotic membrane in comparison to preterm infants born with intact amniotic membrane and term born infants (Menon et al., 2012). Taken together these two studies highlight that the maintenance of a steady telomere length in the fetus is important to ensure that the full gestation period is completed, and that this

maintenance of telomere length is specific to life *in utero* in normal pregnancies. Following birth telomere attrition ensues regardless of whether the infant was carried to full term. Interestingly, a key study by Okuda showed that telomere length in the newborn is highly variable among individuals (Okuda et al., 2002). This is not surprising given that telomere lengths of fetuses (Youngren et al., 1998) and embryos (Turner et al., 2010) are also highly variable. Furthermore, Okuda *et al.* 2002 found that telomere lengths of different tissues are highly synchronised, in keeping with observations in the fetus (Okuda et al., 2002; Youngren et al., 1998).

1.2.1.4 Telomere homeostasis beyond birth

The majority of studies investigating telomere dynamics throughout life have focused primarily on telomere length from young adulthood to old age. However, a minority of studies have investigated the rate of telomere attrition since birth, which have provided valuable insights in to telomere dynamics throughout a lifetime.

The first study to do so was carried out by Frenck and colleagues in 1998; this study investigated telomere lengths of newborns compared to a group of infants between five and 48 months, young adults and older individuals. Results from peripheral blood sampling showed that telomere attrition is most pronounced in the first years of life up to approximately age four. The rate of telomere loss then declines into young adulthood, and further still in older individuals. Moreover, it was also noted that telomere lengths in newborns showed a narrower range compared to adults, indicating that telomere lengths of individual chromosomes are less variable in newborns (Frenck et al., 1998). This pattern also held true when telomere lengths of newborns were compared to their parents, grandparents and great-grandparents. The largest difference in telomere length was seen between the newborn and the parents. This difference was reduced between parents and grandparents and further still between grandparents and great grandparents. The authors propose that this accelerated telomere attrition during early life is due to high proliferation of hematopoietic progenitor cells to form mature cells (Frenck et al., 1998).

Similar observations were seen in a study by Zeichner *et al* 1999, who found that average telomere attrition rates were higher between ages 0 and 36 months compared to telomere attrition over 8-10 years (Zeichner et al., 1999). Furthermore, Rufer *et al*

also showed this characteristic pattern of higher average telomere attrition rate up to age four, and a decline in telomere attrition rate thereafter in lymphocytes and granulocytes (Rufer et al., 1999). Similar observations were shown by Lansdorp *et al* 2008 as illustrated in figure 1.9, and it appears that this pattern is consistent among other cell types including hepatocytes (Takubo et al., 2000) and esophageal mucosa (Takubo et al., 1999). In addition, the percentage of long telomeres appears to decrease over time (Guan et al., 2007; Iwama et al., 1998).

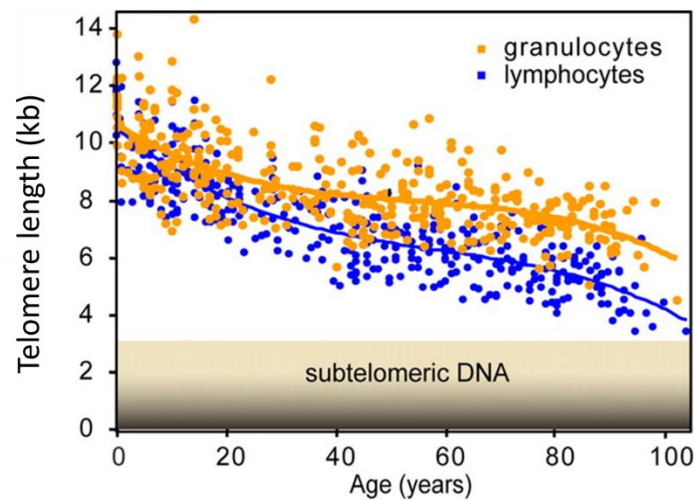


Figure 1.9: Telomere length decline is correlated with the process of ageing. Furthermore, telomere attrition rate appears to be more rapid during early life, as indicated by a steeper decline in the data points (Lansdorp, 2008).

In studies that have investigated telomere attrition in longitudinal studies beyond young adulthood, many have found that telomere attrition appears to occur most prominently in those that have higher telomere length at baseline (Aviv et al., 2009; Benetos et al., 2013; Nordfjäll et al., 2009).

1.2.1.5 Other factors affecting telomere homeostasis

Telomere length is known to be highly variable among individuals, which is likely reflective of both genetic and environmental influences (Slagboom et al., 1994). Aside from the association of age related telomere shortening, telomere length is also affected by many other factors and in some instances, many of these factors may not be mutually exclusive. Some of these are listed in table 1.1 on the next page.

Factors influencing telomere length	General observations	References
Gender	Women possess longer telomeres than men. This may be a result of higher levels of estrogen, which has anti-inflammatory and antioxidant properties, and is known to promote telomerase expression.	(Kang et al., 1999; Kyo et al., 1999; Simoncini et al., 2000; Willeit et al., 2010a)
Ethnicity	White individuals have slightly longer telomeres than black and Hispanic individuals. However, this difference is subtle and therefore not statistically significant unless also adjusted for other factors including age, sex, socio-economic background and lifestyle factors (diet and smoking)	(Diez Roux et al., 2009)
Level of psychosocial stress	High levels of psychosocial stress are associated with shortened telomeres due to increased oxidative stress and decreased telomerase activity. Telomere length is also inversely correlated with major depressive disorder due to increased inflammatory factors leading to increased oxidative stress.	(Epel, 2009; Epel et al., 2004; Simon et al., 2006; Wolkowitz et al., 2011)
Level of physical activity	Those that engage in higher levels of physical activity possess longer telomeres. Higher levels of physical activity is associated with improved physical and psychological wellbeing, therefore it is likely that the effects of physical activity are two-fold on the positive correlation with telomere length.	(Cherkas et al., 2008; Ludlow et al., 2008; Puterman et al., 2010)
Obesity	Increased adipose tissue in obese individuals increases inflammatory modulators, which leads to oxidative stress and telomere shortening. Furthermore, increased body mass leads to higher blood volume, stimulating proliferation of blood cells and telomere shortening. Telomere length is also correlated with body mass index (BMI).	(Das, 2004; Furukawa et al., 2004; Gardner et al., 2005; Rupnick et al., 2002; Valdes et al., 2005)
Smoking	Telomere length is shorter in smokers and ex-smokers, and negatively associated with the amount of cigarettes smoked per year.	(McGrath et al., 2007; Valdes et al., 2005)
Alcohol consumption	Telomere lengths are shorter in alcohol abusers compared to controls after age, gender, BMI, diet, job, genotoxic exposure and smoking habit adjustments. A negative correlation exists between telomere length and the number of units consumed per day.	(Pavanello et al., 2011)

Table 1.1: Lifestyle factors affecting telomere length and appropriate references.

Although these studies have highlighted valid possible origins of highly inter-individual telomere length, many studies show highly conflicting data (Adams et al., 2007; Batty et al., 2009; Shiels et al., 2011). Furthermore, transparent information is difficult to deduce from studies that have reported telomere lengths that are corrected for several parameters.

Interestingly a study in newborns identified that no sex specific differences are present at birth. Thus the author postulated that the longer telomeres in adult women observed in many studies must arise as a result of reduced telomere attrition in women compared

to men. Furthermore, no difference in telomere length was observed among different ethnic groups at birth. This further suggests that individual specific differences in telomere homeostasis must occur after birth (Okuda et al., 2002). This is likely a result of a combination of both genetic and environmental influences (Slagboom et al., 1994).

The above findings highlight that further research remains to be undertaken in order to elucidate how the complex relationship between telomere attrition and chronological age drives the process of aging. Until then, the currently available information detailing telomere length in age-related disease processes provides some valuable insights.

1.2.1.6 Telomere homeostasis in premature ageing diseases

Given the evidence of telomere shortening with each cell division and therefore the association of telomere shortening with ageing, it is perhaps unsurprising that sufferers of premature ageing diseases also display aberrant telomeres. Examples of these include telomere shortening in patients with Hutchinson-Gilford Progeria Syndrome (Allsopp et al., 1992; Benson et al., 2010; Decker et al., 2009), Nijmegen breakage Syndrome (Ranganathan et al., 2001; Shiloh, 1997), Cockayne Syndrome (Batenburg et al., 2012), Dyskeratosis Congenita (Alter et al., 2007; Mitchell et al., 1999; Savage et al., 2008; Vulliamy et al., 2006; Walne et al., 2007; Yamaguchi et al., 2005), Ataxia Thelanogaster (Metcalf et al., 1996), and Down's Syndrome (Vaziri et al., 1993). Furthermore, although shortened telomeres were not observed in Werner Syndrome or Bloom Syndrome, an acceleration in telomere length decline has been observed (Baird et al., 2004; Schulz et al., 1996; Yankiwski et al., 2000). Moreover, telomere loss from individual chromatids has also been observed in Werner Syndrome cells. Thus, while overall telomere length may not be reduced, genomic instability from critically short telomeres of individual chromosomes may lead to pathogenesis (Bai and Murnane, 2003; Crabbe et al., 2007; Crabbe et al., 2004).

1.2.2 The role of abnormal telomere homeostasis in tumorigenesis

The fact that cells have a limited replicative capacity, and that they will eventually enter senescence, is considered to play an essential role in the prevention of cancer development (Wright et al., 1989). The development of cancer cells is characterised by chaotic genome instability, which manifests as dysfunctional cells that are able to

circumvent normal protective measures, leading to immortality. Due to the fact that the eventual attrition of telomeres beyond a critical level induces cellular senescence, telomeres are considered to play an important role in ensuring genome stability and preventing tumorigenesis. The ability of cancer cells to overcome senescence due to the loss of normal telomere function is thought to be a key feature in tumorigenesis. This occurs in a three step process: The first is the shortening of telomeres or the loss of telomere structure (i.e. telomere uncapping by loss of association with its protein complex, or loss of t-loop formation). Loss of telomere structure is becoming increasingly recognised as a key contributor in tumorigenesis over loss of telomere sequence length (Bellon et al., 2006; Crabbe and Karlseder, 2005; Karlseder et al., 2002; Oh et al., 2005; Yamada et al., 2001). However, telomeric repeat sequences accommodate these structures, thus, arguably, the length of the telomere is fundamental in its function. Regardless, ultimately, a loss of telomere length and/or structure leads to the second stage of cancer development, known as the crisis stage. In this stage, due to the inappropriate action of NHEJ or homology directed repair (HDR) mechanisms, chromosome instability ensues. These may lead to duplication of whole chromosomes (leading to aneuploidy), gene amplification, translocations, inversions or deletions (De Lange, 2005b; Zhu et al., 2003). Such complex chromosomal rearrangements, can add further oncogenic potential via deregulation of oncogenes, or altered gene dosage (Albertson et al., 2003; Cheung and Deng, 2008; Nowell, 1997; Rowley, 1999). This second stage further drives malignant transformation via the ability to evade apoptosis mechanisms (Wright and Shay, 1992). In addition, as more successive divisions occur, telomeres shorten further, encouraging an accumulation of genomic instability (De Lange, 2005b). Finally, in the third stage, in order for such unstable cells to survive, the activation of telomere lengthening mechanisms must occur. This is usually achieved by the expression of telomerase, however in some cases it is achieved by ALT (Cerone et al., 2001; Muntoni and Reddel, 2005; Shay et al., 1991). Indeed, telomerase (which is not usually expressed in somatic cells) is expressed in 90% of tumours (Kim et al., 1994), and the amount of telomerase expression often correlates with malignant potential and cancer stage (Falchetti et al., 1999; Langford et al., 1997).

It is widely accepted therefore that telomere shortening is a key underlying cause of chromosome instability leading to cancer (Davoli et al., 2010). More recently however, emphasis has been placed on critical telomere length of specific chromosomes, rather

than reduced average telomere length as a whole (De Lange, 1995; Deng et al., 2003; der-Sarkissian et al., 2004). Such a hypothesis is supported by the observation that chromosome fusions and structural aberrations were observed in the shortest telomeres in pre-crisis cells (Deng et al., 2003; Hemann et al., 2001b). Furthermore, increasing levels of interest have been paid to the role of stochastic uncapping of telomeres, leading to a change in telomere structure and tumorigenesis (Blackburn, 2000). Taken together, evidence implies that telomeres are both protectors and initiators of tumorigenesis. Whether cancer develops is dependent on the key roles played by DNA damage and cell cycle checkpoint proteins, and telomere elongation mechanisms (Shay, 1995).

1.2.3 Dysfunctional telomere homeostasis and cancer

Many research articles describe the association of telomere length and cancer development, and the association of telomere length with degree of malignancy. To summarise, shorter telomeres have been implicated in many cancers, however there are exceptions to this rule. In a recent meta-analysis of several types of cancer, it was found that the literature reported a significant association of shortened telomere length in bladder, esophageal, gastric, head and neck, ovarian and renal cancers. Studies assessing telomere length and non-Hodgkin's lymphoma, breast, lung and colorectal cancer were inconclusive, while studies on endometrial, prostate and skin cancer found no association with telomere length (Wentzensen et al., 2011)(and references therein). A separate study, which found that shorter telomere length was associated with a range of cancers, also noted that degree of malignancy and prognosis was also associated (Willeit et al., 2010b).

1.2.4 Dysfunctional telomere homeostasis in other diseases

The relationship between telomere length and the process of ageing and development of cancer has sparked much interest in the association of telomere length with other disease conditions. These are outlined in Table 1.2 on page 34. Many of these, as is also the case with most cancers, are considered to be age related diseases. Therefore, they reflect the complex interplay between telomere homeostasis and age-related cellular processes. Furthermore, telomere length has been identified as an indicator of the severity of such diseases (Cawthon et al., 2003; Kitada et al., 1995; Willeit et al.,

2010a), and with mortality (Cawthon et al., 2003; Fitzpatrick et al., 2007; Honig et al., 2006).

Taken together, the wealth of evidence that associates telomere length with aging, and the development of disease lends further emphasis to the important role of these highly conserved structures. This has led to a great deal of interest in how the balance between telomere attrition and telomere lengthening mechanisms are maintained throughout the lifetime of an individual, which ultimately begins with the fusing of male and female gametes during fertilisation. To begin understanding these processes, it is important to consider events in normal sexual reproduction and how telomere dynamics during gametogenesis are implicated in fertility and embryogenesis.

Disease	Telomere Aberration	Additional Information	References
Cardiovascular Disease	Short telomeres are associated with incidence of cardiovascular disease: Specifically atherosclerosis, hypertension, vascular dementia and coronary heart disease	Telomere length is associated with risk of stroke, myocardial infarction and mortality due to cardiovascular disease	(Aviv and Aviv, 1997, 1999; Cawthon et al., 2003; Fitzpatrick et al., 2007; Minamino et al., 2002; Okuda et al., 2000; Salpea and Humphries, 2010; Samani et al., 2001; Serrano and Andrés, 2004; Von Zglinicki et al., 2000; Wang et al., 2011)
Lung Disease	Short telomeres are associated with idiopathic pulmonary fibrosis and idiopathic interstitial pneumonias	In most cases the cause is unknown but thought to be heritable. 15% cases possess inherited mutation in telomerase.	(Alder et al., 2008; Cronkhite et al., 2008; de Leon et al., 2010; Gribbin et al., 2009; Tsakiri et al., 2007)
Liver Disease	Patients with chronic hepatitis or liver cirrhosis possess shorter telomeres	Degree of telomere shortening is associated with disease progression	(Kitada et al., 1995; Wiemann et al., 2002)
Diabetes	Telomeres are shorter in patients with type 1 and type II diabetes	Degree of telomere shortening is associated with insulin sensitivity and level of glycaemic control in sufferers	(Adaikalakoteswari et al., 2007; Salpea et al., 2010; Salpea and Humphries, 2010; Uziel et al., 2007)
Alzheimer's Disease	Leukocyte and T cell telomere lengths are reduced, however hippocampus telomere lengths are lengthened in Alzheimer's patients, suggesting altered telomere length maintenance in these individuals	Telomere length may also be related to mortality in Alzheimer's patients	(Hochstrasser et al., 2012; Honig et al., 2006; Panossian et al., 2003; Thomas et al., 2008b; Valdes et al., 2010)
Dementia	Telomere shortening has been observed in those suffering with dementia	The risk of developing dementia and its severity including eventual mortality has been associated with telomere length in stroke survivors	(Grodstein et al., 2008; Martin-Ruiz et al., 2006; Zekry et al., 2010)
Parkinson's Disease	Average telomere length is unrelated to risk of, or the presence and severity of Parkinson's disease. However, the range of telomere lengths is altered	Rapid age-related telomere shortening occurs in Parkinson's disease patients. This correlates with oxidative stress levels	(Guan et al., 2008; Wang et al., 2008; Watfa et al., 2011)

Table 1.2: The role of telomere dysfunction in the pathogenesis of other disease process.

1.3 Gametogenesis

An essential feature of sexual reproduction is the ability of an organism to produce haploid gametes (spermatozoa or oocytes) in the process of gametogenesis. To begin this process, precursor cells (primary spermatocytes or primary oocytes) initially undergo a pre-meiotic division in which DNA replicates. Following completion of this pre-meiotic division, meiosis may then ensue.

1.3.1 Meiosis

Meiosis is characterised by two cellular divisions such that four genetically distinct haploid products arise from one diploid cell (Kleckner, 1996). The first division is reductional (meiosis I) resulting in a product containing half the genetic complement of the mother cell, and the second is equational (meiosis II). Cellular division in this way plays a central role in the shuffling of maternal and paternal genomes, resulting in the inheritance of a random combination of genes in the offspring. This is achieved by the random segregation of chromosomes into daughter cells, programmed DNA recombination and crossing over events (Terasawa et al., 2007). The latter of these characterises the importance of the lengthy prophase stage during the first meiotic division, which is further sub-divided into separate stages: Leptotene, zygotene, pachytene, diplotene and finally diakinesis (Kleckner, 1996; Roeder, 1997). These are illustrated in figure 1.10 on the next page.

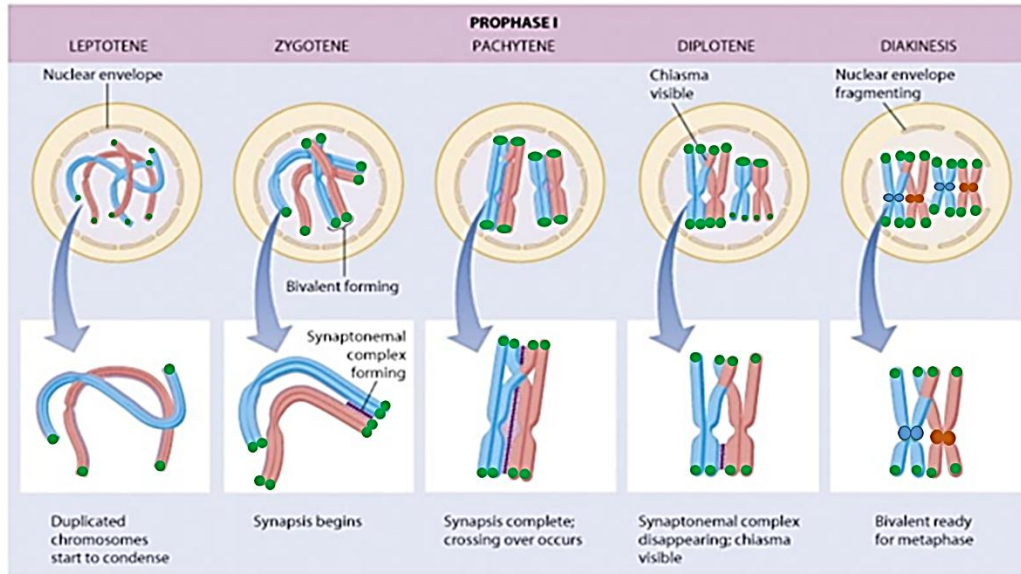


Figure 1.10: Events during prophase I of meiosis. Chromosomes begin to condense in leptotene followed by chromosome pairing and synaptonemal complex formation in zygotene. Next, in pachytene crossing over occurs between sister homologous chromosomes. Chiasma remain through the following stages of diplotene, when the chromosomes begin to align along the equator and synaptonemal complex begins to disappear. Finally in diakinesis chromosomes are fully aligned at the equator, the synaptonemal complex disappears and the nuclear envelope begins fragmentation. Green spots represent telomeres. Image modified from <https://study-biology.wikispaces.com/meiosis>.

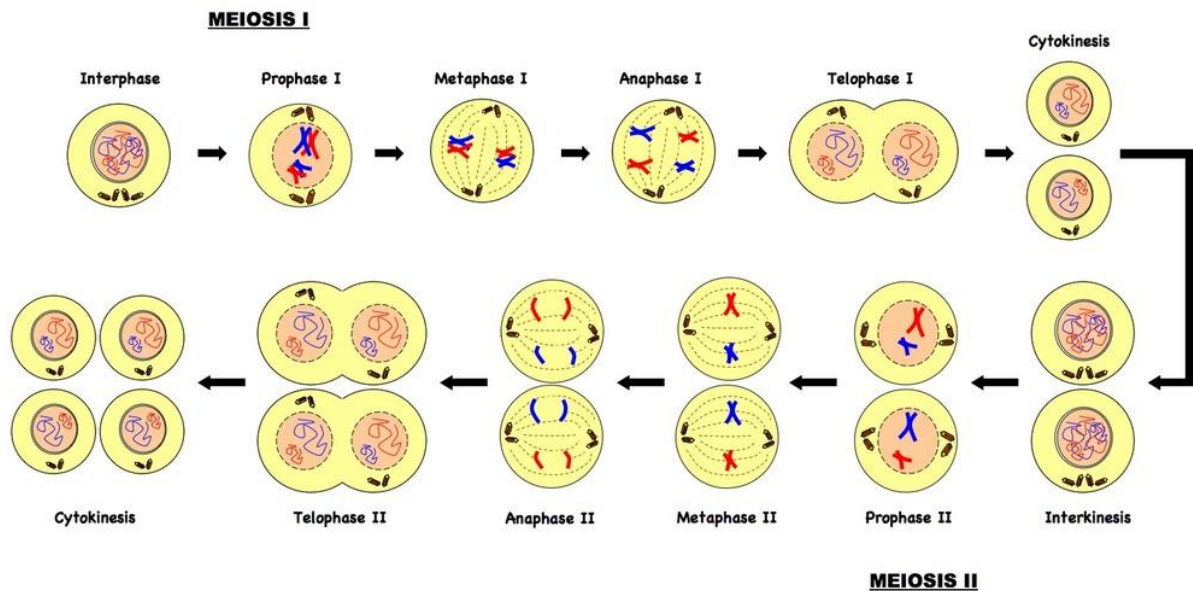


Figure 1.11: Events during Meiosis I and II. During prophase chromosomes pair and decondense and the meiotic spindle begins to form. This is followed by metaphase, in which chromosomes align along the equator of the nucleus and attach to spindle fibres. Chromosomes are then pulled apart in anaphase. During telophase, chromosomes arrive at opposite poles in the cell. Meiosis completes with cytokinesis, when the nuclear envelope pinches between the newly formed nuclei to produce two daughter cells. Image taken from <http://www.ib.bioninja.com.au/higher-level/topic-10-genetics/101-meiosis.html>.

In the second meiotic division, sister chromatids are separated and migrate to opposite poles of the cell. Therefore following both meiotic divisions, one diploid parental cell is able to produce four genetically distinct haploid daughter cells (Chen et al., 2008; Jones, 2008; Kleckner, 1996) (shown in figure 1.11). The result of these specialised cellular divisions is the production of sperm or oocytes (Hassold and Hunt, 2001).

1.3.2 Spermatogenesis

Spermatogenesis is characterised by three different phases: The proliferative phase, the meiotic phase and the differentiation phase. In the proliferative phase, diploid spermatogonia undergo mitotic division to produce diploid primary spermatocytes. These then form two secondary spermatocytes following meiosis I, which in turn each produce two haploid round spermatids following meiosis II. Round spermatids then enter the differentiation phase, which involves the tight packaging of DNA, the formation of the acrosome, removal of unnecessary organelles and excess cytoplasm, formation of a tail and the ability to become motile. This differentiation occurs during phases of transition from round to elongating spermatids and from elongating to elongated spermatids, which finally differentiate into fully mature spermatozoa (Achi et al., 2000; Clermont, 1972; Russell et al., 1993; Tanemura et al., 2005). In males, the process of gametogenesis to produce mature sperm (which is illustrated in figure 1.12 on the next page) occurs just prior to puberty. Spermatozoa are continuously produced and therefore meiosis I and II occur immediately consecutive to one another (Hilscher, 1974). As described in the next section, the timing of gametogenesis is altered in females.

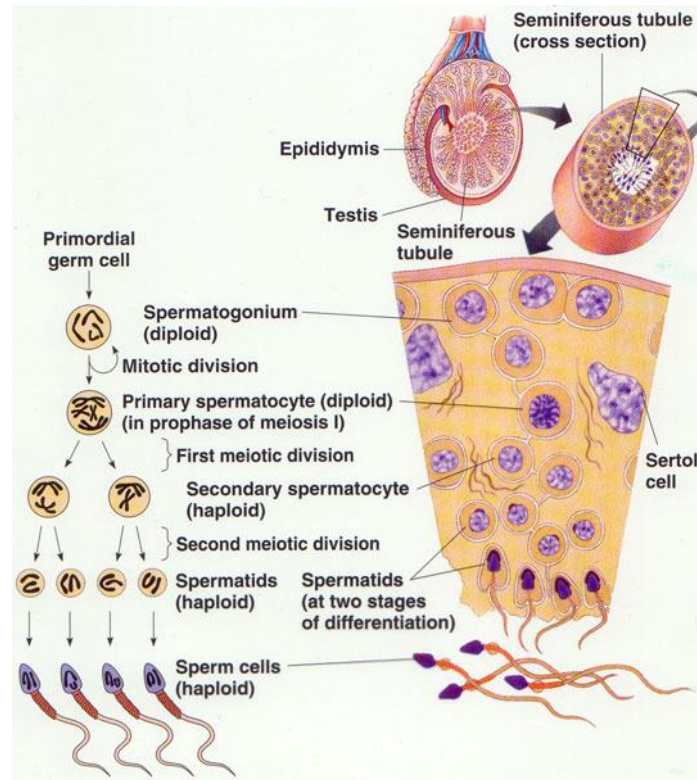


Figure 1.12: The process of spermatogenesis. In the seminiferous tubules (within the testis) spermatogonia undergo mitotic division to produce haploid primary spermatocytes, which in turn undergo the first meiotic division to produce secondary spermatocytes. Following meiosis II, round spermatids are produced which differentiate first into elongating spermatids and then elongated spermatids before finally differentiating into mature spermatozoa. Sertoli cells support this process of gametogenesis. Image taken from <http://intanriani.files.wordpress.com/2009/03/spermatogenesis.jpg>

1.3.3 Oogenesis

The production of female gametes involves a highly complex process (shown in figure 1.13 on the next page), which begins with mitotic division of primordial germ cells to produce oogonia in weeks four to eight of gestation. Oogonia then divide mitotically to produce primary oocytes in weeks nine to 20, which become surrounded by a single layer of granulosa cells between weeks 10 and 30 to form primordial follicles. These give rise to primary follicles, as granulosa cells become cuboidal and the oocyte grows a zona pellucida. The primary oocyte then begins ootidogenesis by undergoing meiosis I, however it is arrested in the diplotene stage of prophase I until ovulation following puberty. At the start of the menstrual cycle, 12-20 primary follicles form secondary follicles, however the majority of these follicles undergo follicular atresia, leaving one dominant follicle to develop into a graafian follicle. Ootidogenesis resumes in the graafian follicle and the primary oocyte continues through meiosis I to produce a secondary oocyte and a first polar body. This secondary oocyte immediately enters

meiosis II, but is arrested in metaphase until fertilisation occurs. At around day 13, the oocyte (now called the ovum) is expelled from the graafian follicle along with a complement of cumulus cells in the process of ovulation. If the ovum is fertilised in the fallopian tube, completion of meiosis II ensues, creating a zygote and a second polar body (Ohno et al., 1962; Sadler, 2011).

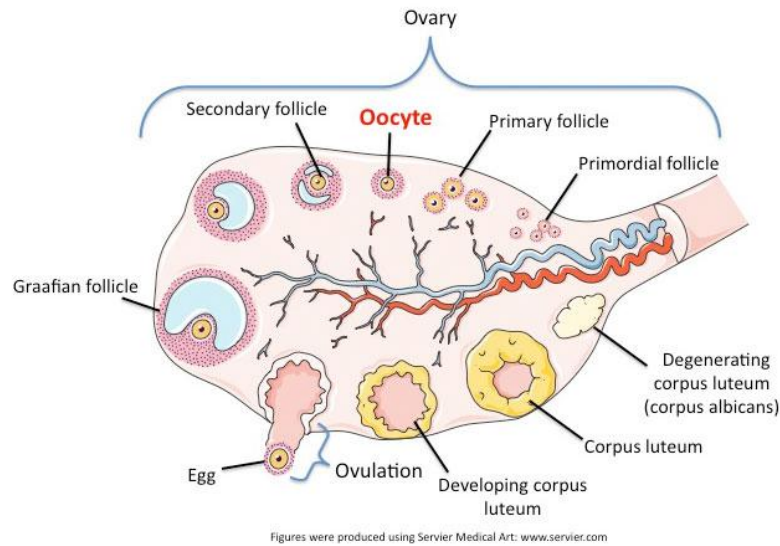


Figure 1.13: The process of oogenesis. The primary oocyte surrounded by a single layer of flat granulosa cells makes up a primordial follicle. These granulosa cells become cuboidal, and the primary oocyte begins meiosis I, marking differentiation into a primary follicle. As granulosa cells increase in numbers and theca cells are recruited, the primary follicle differentiates into a secondary follicle, which develops several antra that eventually fuse to become one antrum in the Graafian follicle. At this point meiosis resumes in the primary oocyte to produce a secondary oocyte. Meiosis is arrested in metaphase II however. The secondary oocyte is expelled from the Graafian follicle along with a surrounding layer of cumulus cells in the process of ovulation. The remaining corpus luteum then degrades. Image taken from <https://www.reproedpedia.org/sites/reproedpedia/files/ovulation-final.jpg>.

1.4 Telomere function in gametogenesis

During gametogenesis, telomere distribution plays a functional role in leading the ‘bouquet formation’ in meiosis. This is characterised by the clustering of telomeres at one pole under the nuclear envelope and the dispersion of centromeres at the opposite pole, somewhat resembling a bouquet of flowers (figure 1.14 on the next page).

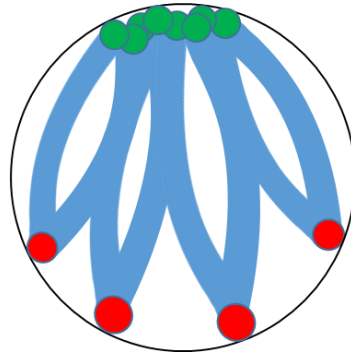


Figure 1.14: The 'bouquet' configuration. Telomere led bouquet arrangement of chromosomes during meiosis. Centromeres (shown in red) are positioned at one end of the nucleus, whilst telomeres (shown in green) cluster at the inner nuclear envelope, tethering chromosomes in place.

There are three stages in telomere led bouquet formation: Nuclear attachment, clustering of telomeres and finally movement of telomeres (Bhalla and Dernburg, 2008). Little is known about this process in humans, however in mice, telomere movement along the nuclear envelope to form bouquet structures is mediated by a meiosis specific protein known as TRF1 binding protein (TERB1). TERB1 possesses a Myb domain, and is therefore able to form a heterocomplex with TRF1 at the telomere. This interaction facilitates telomere association with Sad1 and uncoordinated protein 84 (Unc84) domain containing protein 1 (SUN1), and Sad1 and Unc84 domain containing protein 2 (SUN2) proteins, which span across the nuclear envelope. In turn, SUN proteins may interact with the cytoplasmic motor protein Klarsicht, adenine nucleotide carrier 1 (ANC-1), syne homology (KASH) (forming a SUN-KASH complex) and in doing so, this interaction transmits forces to the nucleus for chromatin remodelling (Haque et al., 2006; Schmitt et al., 2007; Stewart and Burke, 2014). Furthermore, TERB1 recruits and binds to cohesin, which supports structural rigidity. Mutation in TERB1 results in infertility in both males and females (Shibuya et al., 2014).

Telomere led bouquet formation as described above, is thought to be essential for chromosome pairing, recombination and synapsis (Liu et al., 2004), which is in turn essential for fertility in males in particular (Gillies, 1989). It is thought that asynapsis leads to an accumulation of double strand break (DSB) repair proteins, which are recognised at cell checkpoints, leading to apoptosis. In addition, meiotic silencing of unsynapsed chromatin (MSUC) leads to silencing of autosomal genes essential for survival (Burgoyne et al., 2009).

In addition to its distribution during gametogenesis, several lines of evidence have shown that the length of the telomere also plays an important role in meiosis. Concordance in telomere length among homologous chromosomes appears to play a functional role in synapsis, homologous recombination and segregation (Cooper et al., 1998; Dernburg et al., 1995; Nimmo et al., 1998). Several studies utilising telomerase knockout mice have shown that telomere shortening results in meiotic arrest, segregation errors, aneuploidies and apoptosis. More specifically, telomere loss causes senescence and apoptosis in spermatocytes, and meiotic arrest in oocytes (Hemann et al., 2001a; Lee et al., 1998; Liu et al., 2004).

1.4.1 Sex specific telomere regulation in gametogenesis

Although telomere distribution during gametogenesis is largely similar between spermatocytes and oocytes, subtle differences exist between. Furthermore, the regulation of telomere length appears to be sex specific in gametes. These topics are outlined hereafter.

1.4.1.1 Telomere distribution in male gametogenesis

During spermatogenesis, telomeres lead the ‘bouquet’ formation of chromosomes throughout the leptotene stage of prophase I. In mice, rats and humans, telomeres redistribute following mid preleptotene, such that any interior telomeres move to peripheral positions. Therefore at late preleptotene, telomeres are exclusively localised at the nuclear envelope. During leptotene through to zygotene, these peripheral telomeres form tight clusters as chromosomes adopt the bouquet formation. By mid zygotene telomeres of some cells remain clustered, however it is at this stage that telomeres begin to disperse once again. In pachytene, telomeres remain fully dispersed at the nuclear periphery (Meyer-Ficca et al., 1998; Scherthan et al., 1996; Tanemura et al., 2005). Telomere movements during prophase in human spermatogenesis is illustrated in figure 1.15 on the next page. Interestingly, in cattle, telomeres remain clustered in the bouquet orientation until late zygotene (Pfeifer et al., 2001).

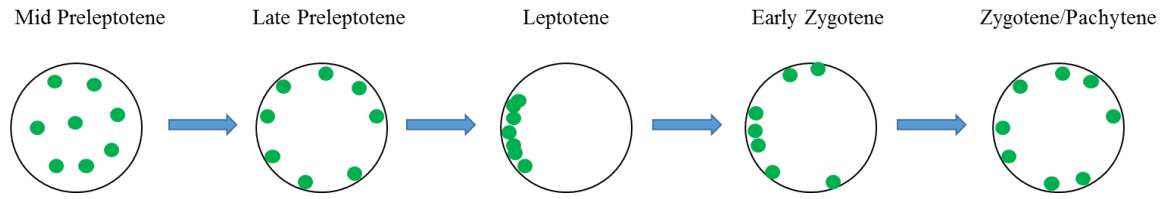


Figure 1.15: Telomere redistribution during prophase I of spermatogenesis. Telomeres (green) are randomly distributed throughout the nucleus prior to the onset of prophase, however they redistribute to the nuclear periphery by late preleptotene. At the leptotene stage, telomeres adopt the bouquet configuration, before beginning to uncluster once more at the early zygotene stage. In late zygotene and Pachytene, telomeres redistribute once more to the entire nuclear periphery.

As previously mentioned, studies in mouse have shown that during meiosis, SUN1 is essential in anchoring telomere clusters to the nuclear periphery. This serves a pivotal role in ensuring homologous chromosome alignment, recombination and synapsis. Indeed deletion of SUN1 results in disruption to bouquet formation during meiosis and result in infertility in males and females (Ding et al., 2007).

During maturation, telomere distribution in sperm appears to alter from peripheral in spermatocytes, to a more central clustering around the nucleolus in round spermatids, finally moving back to the periphery after the elongating spermatid stage (Tanemura et al., 2005).

Once a mature spermatozoon is produced, it is well established that human sperm (and many other mammalian sperm including mice, rats, pigs, cattle and horses) adopt a chromocentric model of nuclear organisation (Ioannou and Griffin, 2010; Jennings and Powell, 1995; Zalensky et al., 1995; Zalensky et al., 1993). This is achieved via chromosome bending into hairpin structures, such that centromeres are localised in the nuclear interior forming a chromocenter, and telomeres attach to the nuclear periphery in dimer and tetramer clusters (Zalensky et al., 1995). This clustering occurs via intra chromosomal telomere-telomere associations (Solov'eva et al., 2004; Zalensky et al., 1995), aided by a sperm specific telomere binding protein (STBP) complex (Zalensky et al., 1997). Furthermore, the interaction of telomeres with the nuclear membrane in mature sperm is brought about with the aid of histone 2B family member W testis-specific (H2BFWT). This sperm specific histone 2B (H2B) variant is a key component of STBP and is responsible for binding to the telomeric DNA repeat (Churikov et al., 2004) (shown in figure 1.16 on the next page). The exact attachment points for telomeres on the nuclear membrane currently remains unknown, however it has been

speculated that telomeres may interact with lamins, which may in turn interact with nuclear membrane spanning lamin associated proteins (Gineitis et al., 2000). Strict nuclear organisation in this way anchors chromosome territories in place, and provides important replication and transcriptional cues during fertilisation and embryogenesis (Sotolongo and Ward, 2000; Ward et al., 1999; Zalenskaya et al., 2000).

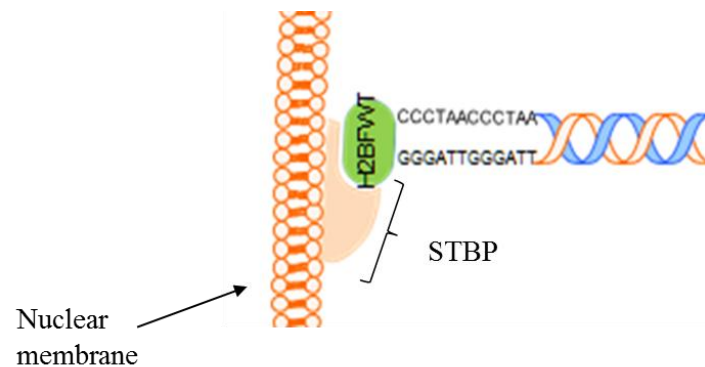


Figure 1.16: Telomere anchoring at the nuclear periphery in mature sperm. H2BFWT binds double stranded telomeric DNA repeats and allows interaction of the telomere with the nuclear membrane. This sperm specific H2B variant makes up part of STBP, which is involved in the clustering of telomeres.

The above information along with the findings from several other studies that have assessed centromere positioning in sperm of infertile males (Finch et al., 2008; Ioannou and Griffin, 2010), justify investigation into whether altered telomere distribution can act as a marker of male infertility. However, to date few have addressed this hypothesis, particularly in humans. Our current knowledge on this topic can be found in section 1.8.

1.4.1.2 Telomere homeostasis in spermatogenesis

Telomere length in sperm is known to be extremely diverse (Baird et al., 2006; Turner and Hartshorne, 2013) and exceptionally long compared to somatic cells. Moreover, sperm telomere length appears to increase with age (Allsopp et al., 1992; Baird et al., 2006; Cooke and Smith, 1986; De Lange et al., 1990; Kimura et al., 2008).

Interestingly, several lines of evidence have suggested that telomere length in the offspring is paternally inherited, proposing a vital role for telomere length in male gametes (Aviv et al., 2009; Njajou et al., 2007; Unryn et al., 2005). This heritability of

telomere length was shown to be cumulative in a study investigating telomere length in offspring from older fathers and grandfathers (Eisenberg et al., 2012).

It is thought that telomerase expression in early germ cell precursors accounts for such long telomeres in sperm. Levels of telomerase expression increases from spermatogonia to primary spermatocytes, but then decreases in secondary spermatocytes. Telomerase is not expressed in spermatids or mature spermatozoa (Bekaert et al., 2004; Eisenhauer et al., 1997; Yashima et al., 1998). Thus, although mature spermatozoa possess longer telomeres than spermatogonia, an inverse relationship has been found between telomerase activity and sperm maturity (Achi et al., 2000; Eisenhauer et al., 1997; Fujisawa et al., 1998). It is hypothesised that telomere lengthening during maturation is predominantly mediated by homologous recombination based ALT. The fact the telomeres cluster in dimers or tetramers at the nuclear periphery, is thought to induce recombination mechanisms, therefore this plays a key role in telomere lengthening in sperm (Wright et al., 1996).

1.4.1.3 Telomeres distribution in oogenesis

Telomeres also play a key role in meiosis during oogenesis, by leading bouquet formation of chromosomes. In humans and cattle, reorganisation of telomeres during female meiosis is largely similar to that of male meiosis (Bojko, 1983). In the preleptotene stage telomeres show no apparent order in the nucleus, however at the leptotene stage telomeres are localised at the nuclear periphery. During leptotene, peripherally localised telomeres begin to cluster, until they are tightly associated at one pole in the bouquet arrangement by late leptotene/early zygotene. Throughout zygotene and into pachytene, telomere clustering becomes loosened, until once again they are dispersed at the nuclear periphery at late pachytene. Finally, in diplotene/dictyotene oocytes in the primordial follicle, telomeres are scattered throughout the nucleus (Roig et al., 2004).

This reorganisation of telomeres in female meiosis differs from telomere reorganisation in male meiosis, in that telomeres persist in the bouquet formation until later stages. This implies that recombination and synapsis occurs later in female meiosis, which is confirmed by distribution patterns of synaptonemal complex staining (Pfeifer et al., 2003). Interestingly, synapsis appears to occur at both terminal and interstitial sites of

female meiotic chromosomes in cattle. In male cattle however, synapsis seems to occur exclusively terminally (Pfeifer et al., 2003; Pfeifer et al., 2001).

1.4.1.4 Telomere homeostasis in oogenesis

In contrast to spermatogenesis, telomere length reduces through oogenesis (Turner and Hartshorne, 2013; Turner et al., 2010). Such an effect may be explained in part by the fact the mitochondrial load is altered and adenosine triphosphate (ATP) production is increased during oocyte maturation. This could potentially lead to oxidative stress induced telomere attrition in the maturing oocyte (Duran et al., 2011).

Unlike spermatogenesis, telomerase is expressed in all stages of oogenesis. Wright *et al* observed a trend showing that telomerase expression is highest in immature oocytes, then reduces through the maturation and fertilisation process (Wright et al., 2001). This observation was confirmed in a later study by Turner *et al* 2013, and has also been observed in cattle and rats (Betts and King, 1999; Eisenhauer et al., 1997; Xu and Yang, 2000). It is postulated that the higher levels of telomerase in immature oocytes is important for maintaining telomere lengths in these cells in order to ensure proper telomere led synapsis and recombination events during meiosis (Betts and King, 1999).

Investigations into telomere lengths and telomerase activity of cells supporting oogenesis are sparse, however some information is available in bovine and porcine models. In cattle, telomere lengths of immature and mature cumulus cells are shorter than those of immature and mature oocytes respectively (Meerdo et al., 2005). Furthermore, studies have shown that telomerase activity is absent in pre-granulosa cells of primordial follicles, but becomes active when follicles begin to grow. It is at its highest levels in pre-antral and small antral follicles in line with these being the most proliferative, and then reduces again in later stages of follicular development (Lavranos et al., 1999).

In pigs, telomerase expression is seen in granulosa cells and immature oocytes of primordial and preantral follicles. During antral differentiation, only cumulus cells and somatic cells in close proximity to the antrum maintain telomerase expression. This observation was correlated with elongating telomeres only in those cells expressing telomerase during folliculogenesis. Expression of TERT appeared to redistribute to the cytoplasm of the oocyte during preantral to antral differentiation events of

folliculogenesis, in line with observations that telomere length remains stable during this time (Russo et al., 2006). This redistribution of TERT to the ooplasm remains evident in MII oocytes, which is thought to provide a stock of telomerase proteins to the zygote following fertilisation (Russo et al., 2006; Xu and Yang, 2000).

1.5 Telomere function beyond fertilisation

Following penetration of sperm through cumulus cells (via hyaluronidase activity of the sperm membrane protein sperm adhesion molecule 1 (SPAM1)) (Lin et al., 1994), fertilisation begins when a spermatozoon makes contact with the zona pellucida of an ovulated ovum. This contact results in acrosome reaction, which releases hyaluronidase and acrosin, allowing digestion of the zona pellucida and fusion of the sperm and ovum plasma membranes. In addition, this action prevents other sperm from penetrating the ovum (a phenomenon known as polyspermy) (Lambert, 1986). After sperm penetration into the ovum, maternal and paternal pronuclei can be seen and the ovum is activated resulting in a calcium influx (Mengerink and Vacquier, 2001). This causes a signalling cascade and the completion of meiosis II, and finally the two haploid nuclei fuse to form a diploid zygote (Dupont, 1998).

Following fertilisation, the zygote begins to migrate through the fallopian tube toward the uterus. During this time it undergoes mitotic division to produce two daughter cells called blastomeres, which continue to divide to produce four and then eight cells by day three post fertilisation. At this stage, known as the cleavage stage, no growth occurs. By the fourth day, a morula is formed, which consists of 16 - 32 blastomeres, and on the fifth day the embryo begins to differentiate into a blastocyst. This is evident by the presence of a trophectoderm from which the placenta will form, and the inner cell mass from which the fetus will develop (Ambartsumyan and Clark, 2008) (outlined in figure 1.17 on the next page).

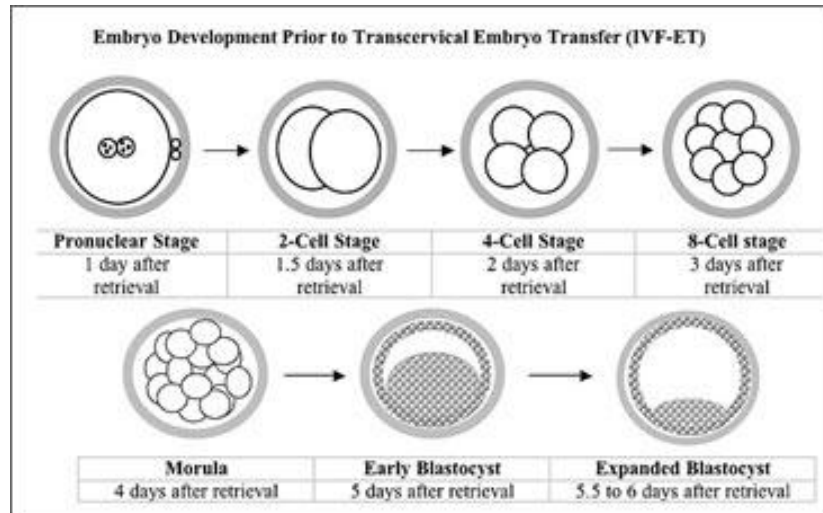


Figure 1.17: Embryogenesis: Following fertilisation, male and female pronuclei fuse and mitotic division produces two daughter blastomeres during cleavage stage. These further divide into 4, then 8 blastomeres. At 16-32 blastomeres, the embryo is called a morula. Further divisions of blastomeres produces trophoblasts and the inner cell mass, which marks differentiation into the blastocyst (http://www.maxhealthcare.in/newsletter/2010/january/ivf-simpler.html?utm_source=ivf-simpler&utm_medium=Facebook&utm_campaign=FB).

During the blastocyst stage the zona pellucida disintegrates resulting in hatching, allowing attachment of the trophectoderm to the uterine wall in the process of implantation. Embryogenesis then continues with the process of gastrulation, in which the three germ layers; the endoderm, mesoderm and ectoderm of the embryo are formed. These give rise to various specific tissues and organs in the process of neurulation and organogenesis. At nine weeks gestation, recognisable features have formed along with functional organs, and from this point the developing infant is called a fetus (Sadler, 2011).

1.5.1 Telomere distribution in fertilisation and embryogenesis

Telomere distribution during fertilisation events and embryogenesis is a largely understudied subject. Indeed, only one such study has reported telomere distribution and association patterns in human embryos derived from IVF cycles. In this study, the number of telomere signals at different stages of preimplantation embryos was recorded. These data show that the number of telomere signals appears to decrease from oocyte to two cell stage, increase through the three and four cell stage and decrease again at the six cell stage. The number of telomere signals then increases again through the seven cell stage and morula, before finally decreasing slightly in the

blastocyst (Turner et al., 2010). These changes in the number of signals could represent changing patterns of telomere association during development, which warrants further investigation.

1.5.2 Telomere homeostasis in fertilisation and embryogenesis

Although many have hypothesised that telomere lengthening during sperm maturation plays a functional role in the paternal inheritance of telomere length in the offspring, telomere length of the female pronuclei have been shown to be longer than that of the male pronuclei following fertilisation. This is in agreement with the observation that telomere lengths of mature oocytes are in fact longer than those of sperm (Turner 2013), contradicting the notion that longer telomere length in sperm compensates for short telomeres in the oocyte (Kalmbach et al., 2013). Given that oocytes are known to repair damaged DNA of spermatozoa following fertilisation (Derijck et al., 2008; Menezo, 2006), it is possible that in fact the opposite scenario may be true (Turner and Hartshorne, 2013). Furthermore, somatic cell telomere length is known to be generally longer in females compared to males (Cherif et al., 2003; Mayer et al., 2006). Therefore the assumption that telomere length in sperm is longer than that of oocytes based on comparisons between sperm and somatic cell telomere length, and oocytes compared to somatic cell telomere length (Allsopp et al., 1992; Kimura et al., 2008; Liu et al., 2007) might not necessarily be true.

Following fertilisation, telomere length decreases through the cleavage and morula stages, however at the blastocyst stage, telomere length is significantly increased (Turner et al., 2010). These observations are in line with conclusions drawn from studies investigating telomerase activity in the developing embryo (Wright et al., 2001). During human embryogenesis, telomerase activity appears to show a decline following oocyte maturation at the zygote stage, and through all cleavage stages (two to 16 cell) and the morula stage. At the blastocyst stage however, a sharp increase in telomerase activity has been observed, which coincides with embryonic genome activation. However, this data was produced from whole embryos. When telomerase activity was calculated on a cell-by-cell basis throughout different stages of embryogenesis however, a trend existed showing a decline in activity from the immature oocyte through to the blastocyst stage (Wright et al., 2001).

Overall, the findings outlined in the above sections suggest a vital role for functional telomeres in normal gametogenesis, fertilisation and embryogenesis. In support of this, evidence showing that dysfunctional telomeres might be involved in fertility complications is becoming increasingly apparent. With this in mind, it is possible that telomere length and/or distribution patterns could act as a valuable tool in the fertility clinic. The next section is therefore dedicated to this topic, and how telomere biology may prove a useful aid in the detection and diagnosis of fertility complications.

1.6 Infertility

Infertility is defined as a failure to achieve and maintain pregnancy following one year of regular unprotected intercourse. According to statistics from the World Health Organisation (WHO), infertility affects around one in six couples, with 38% arising from maternal origin, 27% arising from contributions from both parents and 20% arising from paternal origin. The remaining 15 to 20% are idiopathic, in which the exact cause is unknown (Comhaire, 1987; Seli and Sakkas, 2005), and therefore the main aim of fertility research is to reduce this number. However, reports of male and female contributions to infertility are highly variable within the literature. While some indicate that the male contribution to infertility is over 50% (Seli and Sakkas, 2005), others report that male contribution accounts for around 40% of infertility cases (Sharma et al., 1999). This is likely due to difficulty in differentiating true infertility (in which the couple will never achieve pregnancy) and sub-fertility (in which fertilisation is possible, but difficulties are experienced). Since the causes of infertility may be complex, it is also often difficult to identify a true cause from which contributions from either partner can be ascertained. Furthermore, population based studies are difficult to conduct. Indeed most statistics regarding infertility have been derived from clinics, which may underestimate the prevalence of infertility, since only those whom have sought help are included in the data (Irvine, 1998).

Infertility may occur due to a number of reasons, including physiological causes (Hull et al., 1985), hormonal dysfunction (Baird et al., 2002), infection (Baird et al., 2002; Paavonen and Eggert-Kruse, 1999), lifestyle factors (Homan et al., 2007; Medicine, 2004; Pasquali et al., 2007) and age (Baird et al., 2002). Furthermore, there are several known genetic causes of infertility, including numerical aberrations, reciprocal

translocations, micro-deletions and DNA damage (Evenson et al., 2002; Liebaers et al., 2014; O'Flynn O'Brien et al., 2010; Shah et al., 2003; Zini et al., 2002) (summarised in table 1.3).

Genetic aberration	Cause of infertility	Examples	References
Numerical	Hormone imbalance	Down's syndrome (trisomy 21), Klinefelter syndrome (47, XXY), Turner syndrome (45, X), Hyper Y (47, XYY)	(Egozcue et al., 1997; Ferlin et al., 2007; Onalan et al., 2011; Shah et al., 2003)
Structural	Impaired gametogenesis due to meiotic pairing deficiency and reduced crossing over	Reciprocal translocations, inversion events	(Belangero et al., 2009; Griffin and Finch, 2005; Mikelsaar et al., 2012)
Single gene disorders	Reviewed in O'Flynn O'brien 2010	Cystic fibrosis trans membrane conductance regulator (CFTR), androgen receptor (AR), insulin like factor 3 (INSL3), orphan nuclear receptor dosage-sensitive sex reversal, adrenal hypoplasia critical region, on chromosome X, gene 1 (dax1), Kallmann syndrome I (KAL1)	(O'Flynn O'Brien et al., 2010; Shah et al., 2003)
Micro-deletion	Impaired gametogenesis due to meiotic pairing defects, aneuploidy, hormonal imbalances, reduced sperm quality	Y chromosome micro-deletion in the azoospermic factor (AZF) interval	(Antonelli et al., 2011; Ferlin et al., 2007; Khan et al., 2010; O'Flynn O'Brien et al., 2010; Pandey et al., 2010; Yamada et al., 2010)
DNA damage	Improper chromatin packaging (reduced protamination in sperm), oxidative stress, apoptosis leading to impaired fertilisation and developmental potential	N/A	(Aitken and De Iuliis, 2010; Aitken and De Iuliis, 2006, 2007)
Asynapsis	Apoptosis due to meiotic silencing of unpaired chromatin (MSUC), causing repression of autosomal genes essential for survival, and/or failure of meiotic sex chromosome inactivation (MSCI) in males.	N/A	(Mahadevaiah et al., 2008; Turner et al., 2004a; Turner et al., 2004b; Vincent et al., 2001)

Table 1.3: Examples of genetic aberrations leading to infertility, their effects and some examples. N/A is not applicable.

In addition, a growing level of interest is being paid to the role of functional telomeres in fertility. Given the importance of telomeres in organising and protecting the genome

during gametogenesis and embryogenesis (discussed in sections 1.4 and 1.5), it stands to reason that telomere length and distribution (which may not be entirely mutually exclusive) could be involved in fertility. Furthermore, functional telomeres may be implicated in the health of the infant during development *in utero*, at birth and throughout life. Evidence to support this hypothesis are discussed in sections 1.5 and 1.8.5. For this reason, it is possible that telomere localisation and/or length may be a useful role in assisted reproductive technologies, which is discussed hereafter.

1.7 Assisted reproductive technologies

Advancements in our understanding of human sexual reproduction has led to several different treatment options for couples experiencing infertility, which offer solutions to a variety of reproductive complications. Collectively these are termed assisted reproductive technologies (ART), and include techniques such as intrauterine insemination (IUI), *in vitro* fertilisation (IVF), intracytoplasmic sperm injection (ICSI), cryopreservation, preimplantation genetic diagnosis (PGD) and preimplantation genetic screening (PGS) (Cooke and Fleming, 2009).

In situations where the cause of infertility is of male origin (e.g. where impotence is the cause) or in cases involving sperm donors, IUI offers a simple straightforward solution. In this case, semen is inserted directly into the recipient and fertilisation occurs *in vivo*.

In cases where the cause of infertility is more complex, IVF may be necessary. In this instance a women is usually hyperstimulated by daily injections of gonadotrophins in order to achieve super-ovulation (where many oocytes are ovulated in one cycle). The effectiveness of this is assessed by transvaginal ultra-sonography and if successful, oocytes may be retrieved by ultrasound-guided transvaginal aspiration of follicular fluid. From this, a mature oocyte may be isolated and co-incubated with sperm (which will have been assessed for fertility potential prior to co-incubation), permitting *in vitro* fertilisation. The zygote is often allowed to develop to the blastocyst stage (at around day five post-fertilisation) before implantation into the uterus (Van Voorhis, 2007).

Alternatively, in cases where sperm concentration or motility is low, or in situations where the sperm is unable to penetrate the oocyte, ICSI may provide a suitable solution. Following oocyte retrieval as described above, sperm is injected directly into the oocyte

in order to achieve fertilisation. This process is illustrated in figure 1.18. The zygote is once again allowed to develop to blastocyst stage *in vitro* before implantation into the recipient (Cooke and Fleming, 2009).

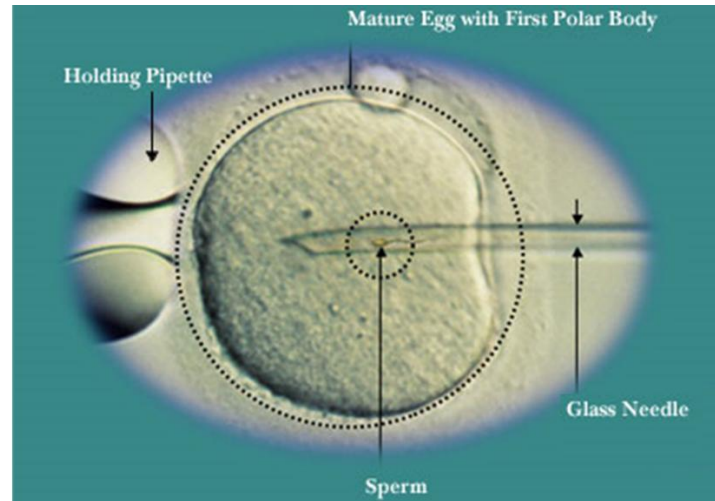


Figure 1.18: Intracytoplasmic sperm injection (ICSI). A single sperm cell is sucked into the end of a needle, which is then used to pierce the oocyte zona pellucida. The sperm cell is injected directly into the oocyte to allow fertilisation. Taken from <http://www.goivf.com/treatment-options/ivf-process/male-factor-icsi-tese/>.

Following IVF or ICSI it is possible to cryopreserve embryos, which allows the transfer of a reduced number of embryos in any one given cycle, whilst retaining excess embryos for subsequent attempts at implantation should the initial attempt fail. Similarly, in situations where individuals are likely to lose fertility potential prematurely (e.g. as a result of cancer treatment or premature ovarian failure) it is possible to cryopreserve gametes in order to improve the chances of achieving a pregnancy (Cooke and Fleming, 2009). In addition, cryopreservation of embryos undergoing PGS or PGD is sometimes carried out in order to allow sufficient time for analysis of test results and consultation with the parents prior to implantation (Ciotti et al., 2000).

In addition to the above technologies, genetic analysis of sperm, polar bodies (which represent genetic complement of the oocyte) or embryos may be performed. This enables PGD for couples at risk of transmitting a heritable genetic disorder, as evidenced by diagnosis in either or both parents, or affected relatives. A list of such disorders that can be tested for in PGD can be found at the following website: <http://guide.hfea.gov.uk/pgd/>, however with new and emerging technologies in the

field, this list is ever-evolving (Collins, 2013; Handyside et al., 2009). Similarly, genetic analysis may also be offered to couples experiencing recurrent miscarriage, recurrent implantation failure or in women of advanced maternal age (AMA) in order to improve the chances of having a healthy baby. This is known as preimplantation genetic screening and predominantly involves the detection of aneuploidy by one of several techniques (Keltz et al., 2013; Rubio et al., 2013). Given the role of telomeres in preventing genomic instabilities leading to aneuploidy and in appropriate chromosome pairing and synapsis during meiosis (discussed in section 1.4), it is possible that telomere assessment might prove useful in PGS. For this reason, current practices in PGS and the potential for telomere biology to form a part of this are described in the following sections.

1.7.1 Preimplantation genetic screening

PGS offers a means to which chromosomally normal embryos may be produced and selected for transfer following IVF and ICSI procedures, in order to improve the chances of achieving and maintaining pregnancy in infertile couples. There are several sources of biopsied sample material for PGS that will reflect the genetic complement of the developing embryo, each with their strengths and limitations. These include the first and/or second polar bodies derived from the maturing oocyte, a single blastomere from the cleavage stage embryo, or a trophoctoderm biopsy from the blastocyst stage embryo. Illustrations of polar body and blastomere biopsies can be seen in figure 1.19 on page 55. Although PGS is not able to be carried out on sperm (since techniques in PGS render the sample unable to fertilise an oocyte) screening the sperm of an ejaculate sample can provide a useful indication of the level of aneuploidy.

Analysis of the first polar body has the advantage that it avoids removing embryonic cells, which is prohibited in some parts of the world (Fiorentino et al., 2008; Harton et al., 2011; K pker et al., 2001). This technique provides information on the chromosome number of the biopsied oocyte, which highlights whether non-disjunction has occurred during meiosis I of oogenesis that could ultimately lead to aneuploidy in the embryo. Since aneuploidy is thought to be largely due to errors in maternal meiosis I (Gabriel et al., 2011; Hassold et al., 1996; Hassold and Hunt, 2001, 2009; Kuliev et al., 2005), first polar body analysis provides a useful tool. This being said, aneuploidy rescue has been observed in several cases in the developing embryo (Kuliev and

Verlinsky, 2004). Furthermore, analysis of the first polar body ignores potential meiosis II errors, which could also result in an aneuploid embryo.

Use of the second polar body in PGS in addition to the first polar body, circumvents the detrimental implications of missing maternal meiosis II errors (Kuliev et al., 2005; Kuliev et al., 2011). However again, discarding of affected oocytes eliminates the chance of aneuploidy rescue (Kuliev et al., 2005) and the potential for a successful pregnancy with the birth of a healthy individual. Furthermore, biopsy of either the first or second polar body ignores potential paternal origins of aneuploidy (Harton et al., 2011).

Biopsy of up to two blastomeres on day three post fertilisation, offers a solution to this problem by enabling the investigation of both maternal and paternal contributions to the chromosomal complement of the developing embryo. Although conflicting data has been reported with regard to the safety of embryo biopsy (De Vos et al., 2009; Hardarson et al., 2008; Mastenbroek et al., 2007; Munné et al., 2007; Munné et al., 2003), in general evidence shows that removal of one blastomere has no harmful effects of the developmental potential of the embryo (De Vos et al., 2009; Goossens et al., 2008). However again, the embryo is deprived of the opportunity to correct for extra or missing chromosomes. Furthermore, it is well established that blastomeres of cleavage stage embryos may not be chromosomally identical, but can be highly mosaic (Colls et al., 2007; DeUgarte et al., 2008; Hanson et al., 2009; Harton et al., 2011). This means that while one blastomere might show aneuploidy, this may not be indicative of the embryo as a whole.

Analysis of biopsied material from the trophectoderm of the blastocyst on day five post fertilisation enables the embryo more time to correct for chromosomal errors originating from the maternal or paternal genomes (Johnson et al., 2010). Furthermore, rather than analysis of one or two cells, several cells may be analysed allowing for more confidence in the results generated (Harton et al., 2011). However, blastocyst stage embryos may also be highly mosaic in chromosome complement (Bielanska et al., 2002), and the analysis of the trophectoderm, which will go on to produce the placenta, may not be reflective of the inner cell mass, which will go on to produce the fetus (Kalousek and Dill, 1983).

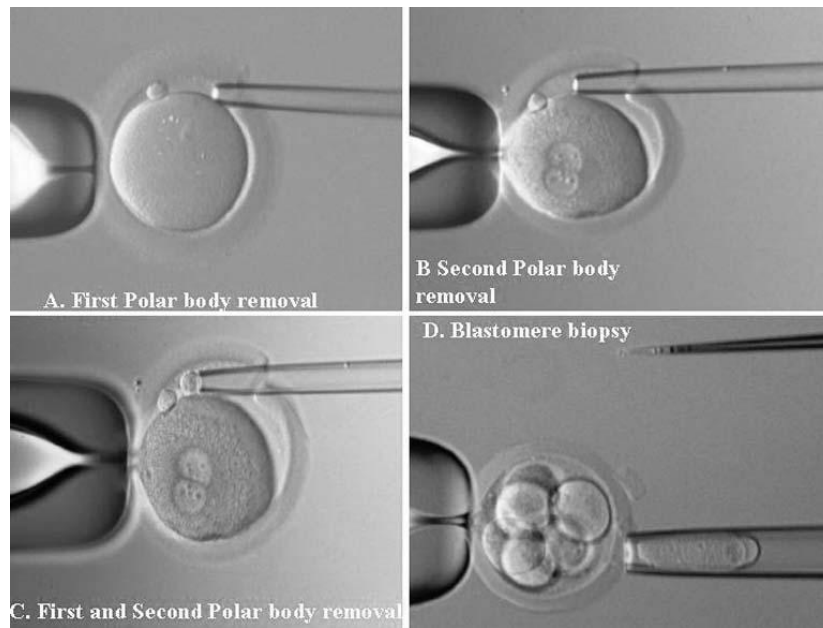


Figure 1.19: Sample biopsy for PGS using a pipette. Top left shows first polar body removal, top right shows second polar body removal, bottom left shows first and second polar body removal, bottom right shows blastomere biopsy from a cleavage stage embryo (Verlinsky and Kuliev, 2005).

1.7.1.1 Techniques in PGS

Until recently, the most common techniques employed in PGS were fluorescence *in situ* hybridisation (FISH) and array comparative genomic hybridisation (aCGH). Both techniques are based around similar principles. While in FISH, generally up to five or six chromosomes are detected at a time (although this may be repeated several times until all chromosomes are detected, but this is a lengthy process (Ioannou and Griffin, 2010)), aCGH allows detection of all chromosomes in one test, with a relatively fast turnaround time.

FISH involves the application of fluorescently labelled probes that are complimentary to specific sequences on particular chromosomes of interest. Biopsied cells must first be fixed to a slide before application of these probes, which are then allowed to hybridise before finally detecting chromosome copy number by visualising the signals using a dedicated fluorescence microscope (Harper and SenGupta, 2012). This is shown in figure 1.20 on the next page. FISH was first used for PGD in 1994 (Griffin et al., 1993) and quickly adopted for PGS (Munné et al., 2005). However, many subsequent studies have shown that the FISH technique in PGS is not beneficial (Jansen et al., 2008; Mastenbroek et al., 2007; Schoolcraft et al., 2009; Staessen et al., 2004; Staessen et al., 2008). This is thought to be due mainly due to technical errors and the

fact that usually only three or five chromosomes may be assessed rather than the whole chromosome complement (Harper and SenGupta, 2012). Since then several other options have been developed.

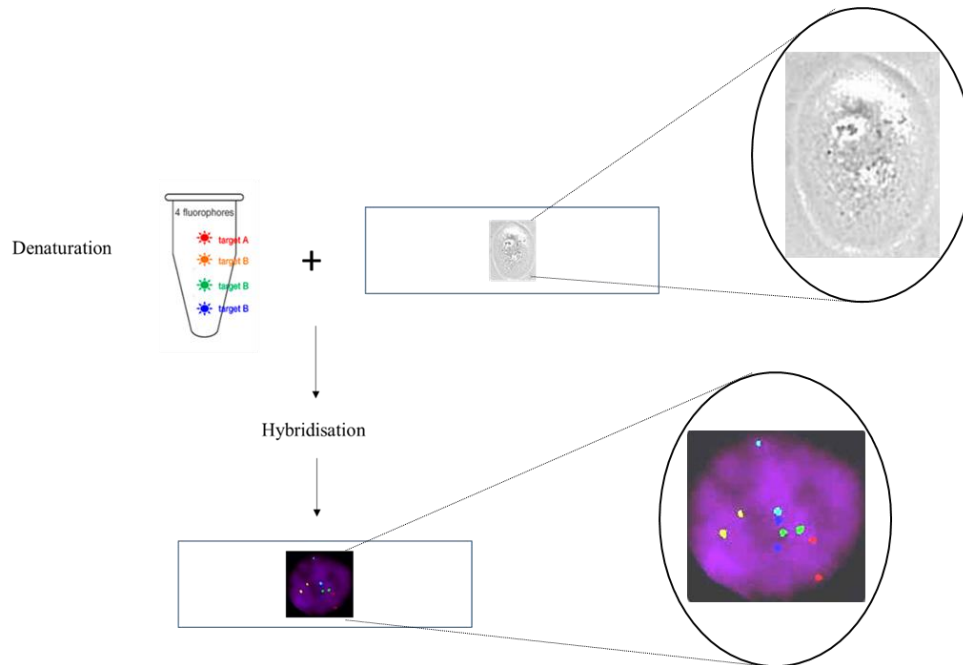


Figure 1.20: Fluorescence *in situ* hybridisation with a biopsied blastomere. Blastomere(s) are fixed to a glass slide and a fluorescently labelled probe is applied. The probe and the blastomere DNA are denatured at high temperature before allowing hybridisation at cooler temperature (usually 37°C). After counterstaining the nucleus and mounting, the blastomere may be visualised and assessed for aneuploidy using a fluorescence microscope.

aCGH involves whole genome amplification of biopsied single cells followed by fluorescent labelling of both the test DNA sample (usually labelled green) and a reference DNA sample (usually labelled red) (De Ravel et al., 2007). These samples are then allowed to hybridise to selected spots of genomic fragments (an array), and the colour ratio is determined in order to identify copy number of whole chromosomes and/or specific sequences within the test sample (depicted in figure 1.21 on the next page). Therefore aCGH allows for aneuploidy screening as well as identification of deletions and duplications of specific genes in PGS (Fishel et al., 2010; Le Caignec et al., 2006; Traversa et al., 2011; Vanneste et al., 2009).

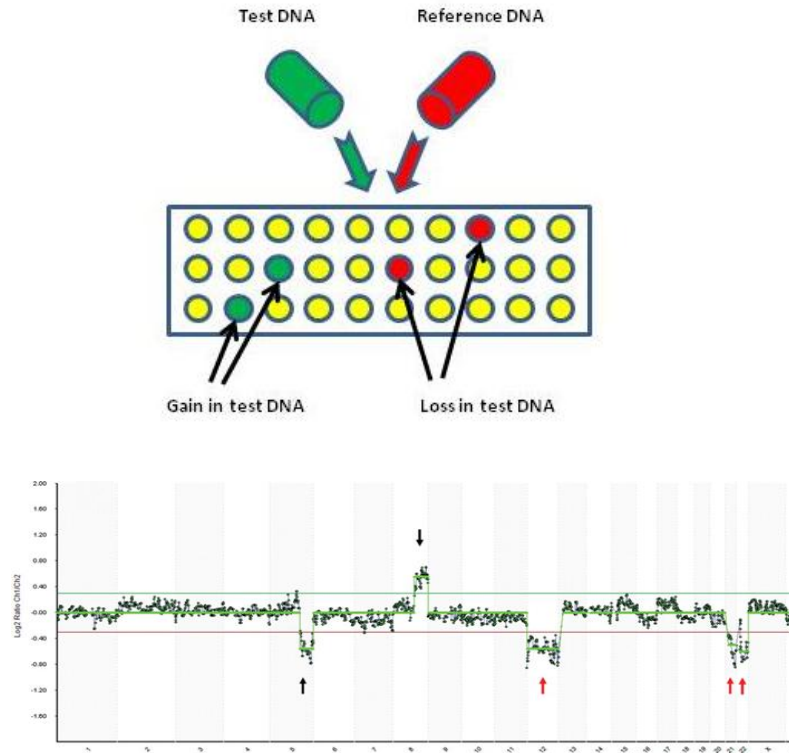


Figure 1.21: aCGH. Top describes to aCGH principle: Test DNA labelled green and reference DNA labelled red are allowed to hybridise to an array containing a number of genomic DNA fragments. The ratio of red to green labelling indicates chromosome copy number, or single gene copy number. Taken from <http://www.ncbi.nlm.nih.gov/dbvar/content/overview/>. Bottom shows an example of an output from aCGH. The log ratio of reference DNA to test DNA (y axis) is plotted for each chromosome position on each chromosome (x axis). Peaks above the line indicate gains and peaks below the line indicate losses. Partial monosomy of chromosome five and partial trisomy of chromosome 8 is indicated by black arrows. Red arrows indicate monosomy for chromosomes 12, 21 and 22 (Fiorentino et al., 2011).

More recently, other approaches have evolved with the aim of increasing accuracy of PGS. These include single nucleotide polymorphism (SNP) microarrays (Treff et al., 2010a; Treff et al., 2010b), multiplex qRT-PCR based approaches (Treff and Scott Jr, 2013; Treff et al., 2012), and next generation sequencing (Treff et al., 2013).

1.7.1.2 PGS controversy

Much controversy continues to surround the use of PGS in ART in terms of its effectiveness in improving pregnancy rates. While some studies report that PGS does improve success rates, other studies report the opposite or indeed negative effects of PGS. This debate remains very active to date (Anderson and Pickering, 2008; Gleicher et al., 2014; Harper et al., 2010; Harper and Harton, 2010; Harton et al., 2013; Jansen et al., 2008; Mastenbroek et al., 2008; Scott Jr et al., 2013) and as a result, the search for new tools in ART continues. In light of the findings from earlier studies

investigating the effects of telomere attrition and/or telomere mislocalisation on the reproductive potential in the mouse model (Liu et al., 2002a; Liu et al., 2004; Ward et al., 1999), it is possible that these important features of telomere function may act to provide a novel PGS tool in human ART.

1.8 Telomere assessment: A novel tool in PGS?

Following on from the observations made regarding telomere homeostasis in normal reproduction (outlined in sections 1.4 and 1.5), several investigators have sought to determine whether telomere function is altered in couples experiencing fertility complications (Moskovtsev et al., 2010; Turner and Hartshorne, 2013). As outlined in the following sections, telomere dysfunction in infertile individuals lends support to the idea that telomere distribution patterns and/or telomere length evaluation may prove a useful tool in PGS.

1.8.1 Telomere regulation in sperm of infertile males

1.8.1.1 Telomere distribution in male infertility

The non-random distribution of chromatin into discrete chromosome territories is well characterised in many cell types (Cremer and Cremer, 2001; Foster and Bridger, 2005), and is known to play an important role in controlling gene expression patterns forming a functional nuclear landscape. Indeed evidence shows that normal regulation of gene expression via strict nuclear organisation plays a functional role during the process of differentiation (Cremer and Cremer, 2010; Foster et al., 2005; Kosak and Groudine, 2004; Kuroda et al., 2004). Furthermore, disruption of this strict level of nuclear organisation is known to be involved in the pathogenesis of many disease conditions, of which cancers and laminopathies have been particularly well studied (Boyle et al., 2001; Bridger and Kill, 2004; Cremer et al., 2003; Marella et al., 2009; Meaburn and Misteli, 2008). Given the importance of nuclear organisation during differentiation and in normal cellular function, a small number of studies have addressed whether altered nuclear organisation is implicated in relation to male infertility. During mammalian spermatogenesis, a highly ordered set of nuclear reorganisation events leads to a chromocentric model of nuclear organisation in the mature spermatozoa (Haaf and

Ward, 1995; Hazzouri et al., 2000; Mudrak et al., 2005; Zalensky et al., 1995). As discussed in section 1.4.1.1, this proposes a model whereby the centromeres are clustered in the nuclear interior, and the telomeres reside in dimers or tetramers at the nuclear periphery (Solov'eva et al., 2004; Zalensky et al., 1995; Zalensky et al., 1993). It is thought that this is important for providing replication and transcriptional cues during fertilisation and embryogenesis (Sotolongo and Ward, 2000; Ward et al., 1999; Zalenskaya et al., 2000), and therefore it is possible that aberrant nuclear organisation might represent an underlying cause of infertility. Given that impaired spermatogenesis is implicated in many cases of male infertility (Ioannou and Griffin, 2010), it is plausible that disruption to normal events in nuclear reorganisation might occur, leading to aberrant nuclear architecture. Similarly, it is possible that aberrant nuclear organisation is involved in the etiology of the 15-20% reported cases of idiopathic male infertility (Seli and Sakkas, 2005).

Indirect evidence from the mouse model lends support to this hypothesis, since chemically induced disruption to the organisation of chromatin in the sperm nucleus results in failed embryogenesis (Ward et al., 1999). Furthermore, mutation of SUN1 (which is responsible for guiding telomere led bouquet formation of chromosomes during meiosis) results in impaired synapsis and crossing over events, and ultimately apoptosis (Ding et al., 2007). In addition, indirect evidence supporting the hypothesis that nuclear organisation is important for male fertility in humans comes from studies showing that loss of telomere-telomere interactions (which are also a vital component of telomere led bouquet formation in meiosis) is associated with infertility (Moskovtsev et al., 2010; Mudrak et al., 2005; Turner and Hartshorne, 2013). Moskovtsev *et al* 2010 hypothesised that loss of telomere-telomere interactions may either be the cause or the result of loss of telomere repeats and/or their associated proteins, which induces a DNA damage response resulting in senescence or apoptosis (Karlseder, 2003; Moskovtsev et al., 2010; Zhang et al., 2007). Finally, it has also been shown that single nucleotide polymorphisms in H2BFWT, which is thought to be responsible for anchoring telomeres to the nuclear periphery in mature sperm (Churikov et al., 2004), are associated with spermatogenesis impairment and idiopathic male infertility (Lee et al., 2009; Ying et al., 2012).

Although the above represent some insightful findings, direct evidence of altered nuclear organisation in relation to male infertility in humans is sparse in the current

literature. While one study showed altered distribution of sex chromosomes by analysis of centromeres (Finch et al., 2008), another showed that centromere distribution remains remarkably stable with impaired spermatogenesis (Ioannou and Griffin, 2010). Moreover, to date none have directly addressed whether telomere localisation is altered in the infertile male, which is one avenue that may be worthy of investigation.

1.8.1.2 Telomere homeostasis in male infertility

In the telomerase deficient mouse model, previous studies have shown that there exists a relationship between telomere length and male infertility. These mice show shortened telomeres in sperm and a decline in litter size with successive generations until eventual sterility (Liu et al., 2002a; Liu et al., 2002b; Liu et al., 2004). Furthermore, a reduction of telomere length as a result of telomerase deficiency is associated with reduced sperm motility and sperm concentration in mice (Liu et al., 2002b). This is unsurprising given that extensive apoptosis prior to the onset of prophase I is associated with telomere shortening in early germ cell precursors of telomerase deficient mice (Hemann et al., 2001a; Lee et al., 1998). These conclusions are further supported by the observation that critically short telomeres are also positively correlated with DNA sperm fragmentation in male mice (Rodríguez et al., 2005). Interestingly, the shortening of telomeres in telomerase deficient mice has been shown to lead to both peripheral and dispersed patterns of telomere distribution in the pachytene and diplotene stages of prophase I. This in turn leads to inefficient tethering of chromosomes to the nuclear membrane, which results in similar consequences to those described in SUN1 mutants and stalling of meiotic progression (Liu et al., 2002a; Liu et al., 2004). Therefore these studies provide evidence that the length of the telomere is additionally important for the localisation of the telomere within the sperm nucleus, which as mentioned above, is likely important in the ability of the sperm to produce viable offspring.

Correlations between telomere length and male fertility in humans appears to be less transparent. While some studies have found a positive association between sperm fitness and telomere length, others have not. For example, a study by Santiso *et al* found that swim-up selected sperm had longer telomeres and less DNA damage (Santiso et al., 2010). Furthermore, studies have shown that telomere length is shorter in males with idiopathic infertility (Thilagavathi et al., 2013), and that the sperm of oligozoospermic males possess shorter telomeres compared to that of

normozoospermic males of the same age (Ferlin et al., 2013). Conversely however, other studies have found no association between overall telomere length in sperm and DNA fragmentation, or any semen parameter (Thilagavathi et al., 2013; Turner and Hartshorne, 2013). Although with that being said, interestingly one of these studies did highlight that some oligozoospermic males possessed a subpopulation of sperm with altered telomere length distributions. However again, the presence of this subset of sperm did not appear to correlate with sperm motility, morphology or DNA fragmentation index. Nonetheless, such a finding may be worthy of future investigation.

1.8.2 Telomere regulation in oocytes of infertile females

1.8.2.1 Telomere distribution in female infertility

Very little information is available detailing the role of telomere distribution in oocytes from women experiencing infertility, probably due to the fact that unlike sperm, oocytes are difficult to obtain for research purposes. Studies in mice have shown that, in similarity to males, SUN1 mutants (which lack the ability to orchestrate telomere movements during bouquet configuration formation) showed absence of mature oocytes and impaired chromosome alignment, recombination and synapsis. This is likely due to impaired meiotic events (Ding et al., 2007).

1.8.2.2 Telomere homeostasis in female infertility

Studies investigating shortened telomeres in telomerase deficient mice have concluded that telomere shortening leads to impaired oogenesis, reduced oocyte quality, improper synapsis and mis-segregation, resulting in increased aneuploidy in oocytes (Liu et al., 2004). In addition, short telomeres may be responsible for directly initiating a DNA damage response leading to the observed increase in apoptosis in oocytes, which may be exacerbated by mis-segregation events. Indeed, ovarian atrophy in telomerase deficient mice and failure to ovulate despite exogenous hormone stimulation might be explained by apoptosis resulting from telomere loss (Liu et al., 2002a). All of these features ultimately lead to reduced litter size and eventual sterility in late generation telomerase deficient mice (Herrera et al., 1999; Lee et al., 1998), highlighting the

importance of functional telomere length regulation and ultimately functional telomeres. Telomerase activity therefore likely plays a vital role in maintaining functional telomeres and preventing apoptosis. This is presumably true in cells supporting germ cell production and maturation (such as granulosa cells) as well as the oocyte itself (Lavranos et al., 1999; Liu et al., 2002a). In support of this, reduced telomerase activity has been observed in granulosa cells of large atretic follicles in rats, suggesting that telomerase levels in these cells is critical for healthy folliculogenesis (Yamagata et al., 2002).

In humans, oocytes with shorter maximum telomere length have been associated with cytoplasmic fragmentation in embryos from women undergoing IVF. This led the authors to hypothesise that oocyte telomere length is predictive of embryo development potential (Keefe et al., 2007; Keefe et al., 2005). Interestingly, however this study showed no association between average telomere length and embryo fragmentation, which is in agreement with findings from others (Turner and Hartshorne, 2013). Furthermore, telomere lengths were assessed in spare eggs that were not exposed to sperm, therefore the embryos assessed were derived from other eggs retrieved from the same patient.

To circumvent this problem, it is possible to assess telomere lengths in polar bodies which can act as a representative of oocyte genetic complement. Indeed, telomere length has been found to be reduced in aneuploid polar bodies compared to sibling euploid polar bodies, which supports the notion that oocytes with shortened telomeres may be prone to chromosome segregation errors, as seen in the mouse model (Treff et al., 2011b). In line with this hypothesis, older mothers who have given birth to children affected with Down's syndrome (caused by trisomy 21) are known to possess significantly shorter telomeres than age matched controls (Dorland et al., 1998b; Ghosh et al., 2010).

Given that telomerase is known to be expressed in oocytes (Wright et al., 2001), it is possible that impaired mechanisms of telomere length regulation might play a role and/or exacerbate the observations described above. In point of fact, telomerase splice variants, which have been found in several immortal cell types and tumours, are also expressed in abnormal oocytes and embryos (Brenner et al., 1999). Although these variants are present in some normal tissues in addition to commonly spliced telomerase,

the majority of normal tissues do not express these variants (Kilian et al., 1997; Nakamura et al., 1997). It is possible that the presence of these splice variants might impact telomere length maintenance in oocytes, contributing to their attrition and resulting in genomic instability. In order for this to be ascertained however, it would be necessary to investigate the presence of these splice variants alongside telomere length analysis, and in relation to developmental potential of oocytes and embryos in future experiments.

As mentioned above, telomerase activity and/or telomere length in cells supporting the oocyte may also have a part in the developmental potential of the oocyte given that these cells are responsible for communication and nourishment during gametogenesis and ovulation. In support of this, it has been shown that telomere lengths in cumulus cells of fertilised oocytes that go on to produce good quality embryos are longer than those that go on to produce poor quality embryos (Cheng et al., 2013a). In addition, a reduction of telomerase activity and telomere length in granulosa cells is associated with occult ovarian insufficiency and a reduction in the number of follicles produced in IVF cycles (Butts et al., 2009). This offers explanation to the reduced replicative capacity and increased apoptosis of granulosa cells in women with occult ovarian insufficiency (Seifer et al., 1996; Seifer et al., 1993).

1.8.2.3 Telomere length and the maternal age affect

All of the features associated with telomere shortening in mice oocytes described above appear to mirror reproductive ageing in humans (Keefe and Liu, 2008; Liu et al., 2002b; Liu et al., 2004). This has led to the telomere theory of reproductive ageing in women (Keefe et al., 2006). Telomeres of oocytes are consistently shorter than somatic cells (Liu et al., 2007; Wright et al., 1996; Wright and Shay, 1992) and further shorten with age (Kalmbach et al., 2013). Thus the theory of reproductive ageing in women hypothesises that oocytes in women of advanced maternal age possess shortened telomeres that are unable to support fertilisation and embryogenesis. It is thought that this age effect acts as a natural protective contraception against the high risks associated with pregnancy and childbirth (Kalmbach et al., 2013).

The maternal age affect describes the decreased reproductive potential experienced by women in association with advanced maternal age (defined as above age 35). Indeed,

a sharp decline in natural conception occurs beyond age 35 in women. This is thought to be caused by a number of factors including a depletion in the number of oocytes and a reduction in oocyte quality (Dorland et al., 1998a; Hassold and Hunt, 2001; Munné et al., 2005; Navot et al., 1991). Indeed, oocytes from older women are significantly more likely to carry errors from meiosis, leading to aneuploid offspring. This is known to be the leading cause of first trimester pregnancy loss in humans (Boué et al., 1977; Hassold et al., 1980).

Given the vital role of telomeres in synapsis, recombination and segregation events during meiosis (Cooper et al., 1998; Dernburg et al., 1995; Liu et al., 2004; Nimmo et al., 1998), it is thought that telomere dysfunction represents a significant contribution to reproductive ageing in women. Current understanding suggests that there are two main mechanisms that cause this phenomenon: Firstly, it has been demonstrated that oocytes are ovulated in the order that they are produced during fetal oogenesis (therefore those that are produced first are ovulated first and those that are produced last are ovulated last). Those that are ovulated last are therefore produced from primary cells that have undergone many more mitotic divisions, and have therefore lost a greater number of telomere repeats due to the end replication problem (Edwards, 1970; Polani and Crolla, 1991). Secondly, female gametes are exposed to a prolonged interval between oogenesis and ovulation, during which time oxidative stress due to reactive oxygen species (ROS) (originating in part from mitochondria) may have accumulated. The fact that telomeres reside at the nuclear periphery in gametes may also render them particularly susceptible to lipid peroxidation (Passos and von Zglinicki, 2005). Since telomeres are G rich (and G rich sequences are known to be particularly susceptible to oxidative damage), it stands to reason that as women age, oxidative stress induced telomere shortening leads to a decline in reproductive potential (Kawanishi and Oikawa, 2004; Oikawa and Kawanishi, 1999; Sastre et al., 2002; Tarín et al., 2002; Tatone et al., 2008). This has been demonstrated in a study showing that telomere attrition, leading to chromosome fusions and apoptosis, is associated with mitochondrial dysfunction (Lansdorp, 1996). Furthermore, decreased telomerase activity and telomere length in meiosis II oocytes has been associated with higher levels of reactive oxygen species in oocytes of older mice compared to younger mice (Yamada-Fukunaga et al., 2013).

Similar observations of reduced telomerase activity have been seen in ovaries of older women compared to younger women, and in relation to follicle depletion (Kinugawa et al., 2000), in agreement with findings from animal models (Yamada-Fukunaga et al., 2013). However, evidence of telomere length attrition and reproductive ageing in women is not so clear-cut. One study that assessed telomere lengths in oocytes found no correlation between telomere length and maternal age (Turner and Hartshorne, 2013), however a second study that measured telomere lengths in cumulus cells found that overall telomere length is negatively correlated with age (Cheng et al., 2013a). Furthermore, telomere lengths in cumulus cells from meiosis I oocytes were shown to be longer than those from meiosis II oocytes in younger women, whereas this pattern was not seen in older women. In fact telomere lengths were not significantly different in meiosis I and II oocyte cumulus cells in older women (Cheng et al., 2013a). The latter study is perhaps unsurprising given that cumulus cells are mitotically active, but nonetheless provides a valuable insight into telomere length involvement in human female fertility. Further studies will be required in the future to ascertain whether the reproductive ageing due to telomerase deficiency and/or telomere attrition observed in mice is indeed part of reproductive ageing in women.

1.8.3 Leukocyte telomere length and infertility

In addition to the study of how gamete telomere length and localisation is related to fertility, a number of studies have investigated leukocyte telomere length in relation to fertility. Interestingly, average telomere length measured from peripheral blood is associated with reproductive life span (Aydos et al., 2005). Furthermore, leukocyte telomere lengths of both males and/or females are shorter in couples experiencing idiopathic recurrent miscarriage (Hanna et al., 2009; Thilagavathi et al., 2013). Interestingly however, average leukocyte telomere length is increased in women suffering with premature ovarian failure (POF). The authors conclude that the latter finding may be an error due to low sample size, or that these patients experience an overall slower rate of proliferation leading to a reduced number of gametes, but an increase in telomere length. Alternatively abnormal hormonal control in these individuals might positively influence telomere length (Hanna et al., 2009). Indeed, long-term hormone replacement therapy in postmenopausal women has been shown to

reduce the rate of telomere shortening (Lee et al., 2005) and estrogen has been shown to reduce oxidative damage to DNA and promote telomerase activity (Kyo et al., 1999).

Overall, in recent years the role of telomeres in fertility has received an increasing level of interest. Although much still remains unclear, some interesting and important observations have been made. One of the key outcomes from the current data is the potential use of telomere length as a biomarker for fertility potential in gametes and developmental potential in embryos.

1.8.4 Telomere dynamics and developmental outcome in ART

Increased interest in the role of telomeres in reproduction and fertility potential over the last few years has sparked a small number of studies to investigate the importance of functional telomeres in developmental outcome.

Telomere distribution patterns in the developing human embryo is a largely understudied area, which is largely due to ethical constraints. Furthermore, information from natural conceptuses is impossible to achieve, therefore studies in human embryos are limited to use of those not implanted from couples undergoing infertility treatments. The use of telomere distribution patterns in embryo quality assessment is thus currently negligible, but may warrant investigation given the observations in a study by Turner *et al* 2010 whom showed varying degrees of telomere clustering in the preimplantation embryo (discussed in section 1.5.1) (Turner et al., 2010).

A larger amount of information is available regarding the relationship between telomere length and developmental potential of the embryo. Information on this subject area obtained from model organisms shows that, compared to wild type mice, third and fourth generation telomerase null mice exhibit a reduction in the percentage of fertilised ova reaching cleavage stage. Embryos are also slower to develop into morulae and blastocyst stage, and fewer cells are present in blastocyst embryos. Furthermore, the rate of cytofragmentation is increased in telomerase null mice compared to wild type controls and largely coincides with the presence of only one pronucleus at fertilisation (Liu et al., 2007). These phenotypes can be attributable to telomere length deficiency as opposed to a direct effect of telomerase deficiency, since first generation telomerase null mice exhibit normal fertility and embryogenesis potential.

In studies that have assessed telomere length in relation to embryo quality in humans, it has been found that telomeres are shortened in blastomeres of cleavage stage embryos that are aneuploid compared to blastomeres of cleavage stage embryos that are euploid. Interestingly however, evidence shows that no difference exists in telomere lengths of trophoctoderm biopsies of blastocysts that are aneuploid compared to those of euploid blastocysts. It is proposed that this is a by-product of telomerase mediated telomere lengthening that occurs following genome activation of blastocyst stage embryos (Treff et al., 2011b). Similarly, no difference has been observed in blastocyst stage embryos compared to embryos that arrested prior to blastocyst stage, suggesting that telomere length does not play a role in the selection for developmentally competent embryos (Mania et al., 2014; Treff et al., 2011b). Thus the presence of senescent cells in these embryos, which may contribute to developmental arrest, cannot be attributed to telomere shortening. Perhaps instead, it is possible that a loss of telomere structure may have resulted in cellular senescence and developmental arrest (Hemann et al., 2001b; Mania et al., 2014; Stewart et al., 2003) however this remains to be investigated. Interestingly, evidence shows that while telomere lengths of abnormal cells within blastocysts are not different to normal cells from the same blastocyst, telomere length is shortened in abnormal cells of morulae that have arrested prior to blastocyst stage compared to normal cells from the same embryo (Mania et al., 2014). However, since overall no difference in telomere length exists between developmentally normal and arrested embryos, the significance of this has yet to be uncovered.

Mania *et al* 2014 also noted that embryos from couples classified under advanced maternal age or recurrent miscarriage had shorter telomeres than those classified under repeated IVF failure (Mania et al., 2014). This association of shorter telomere length in embryos from couples experiencing recurrent miscarriage correlates with reduced leukocyte telomere length in parents (Hanna et al., 2009).

Studies assessing telomerase activity in relation to embryo quality in humans have found that telomerase splice variants are associated with poor embryo development in cleavage stage embryos and blastocysts. Thus, although the overall level of telomerase expression may not be altered, the presence of splice variants may affect its function (Brenner et al., 1999). This hypothesis confirms findings by Wright *et al*, who showed that although telomerase activity in polypronuclear zygotes was significantly lower than normal pronuclear zygotes, biopsied blastomeres from embryos that arrested did

not show significantly altered telomerase activity compared to blastomeres that went on to develop into blastocysts. Therefore the level of telomerase activity is not associated with embryo development potential (Wright et al., 2001).

Overall, findings outlined in the above sections indicate that functional telomeres are required for gametogenesis, fertilisation and embryogenesis. This provides evidence to suggest that some form of telomere analysis (e.g. analysis of telomere length and/or nuclear distribution patterns) may possibly be used in future PGS strategies to screen for chromosomally, genetically and developmentally normal embryos. Furthermore, the above findings, along with evidence showing a relationship between dysfunctional telomere homeostasis and disease processes (described in section 1.2.4), provoke thoughts on how telomeres may function in the health of the developing fetus.

1.8.5 Telomere length in pregnancy complications

As mentioned in section 1.5, telomere length appears to be established during the blastocyst stage of embryogenesis and remains stable during fetal development. However, studies assessing the effects that a complicated growth environment during gestation might have on infant telomere length are limited. During pregnancy, several complications can arise including gestational diabetes, high blood pressure, pre-eclampsia, infection, intrauterine growth restriction (IUGR) and preterm labour (<https://www.womenshealth.gov/pregnancy/you-are-pregnant/pregnancy-complications.html>). Given that aberrant telomere length maintenance is associated with altered tissue function in several disease processes (outlined in section 1.2.4), it is possible that telomere length is altered in association with pregnancy complication. In point of fact, evidence shows that telomere length is involved in the pathogenesis of pregnancies complicated by IUGR. In cases where IUGR is caused by placental insufficiency or pre-eclampsia, reduced telomere lengths have been shown in placental trophoblasts. It is thought that this is the result of oxidative stress, which may contribute to increased telomere loss and increased cellular senescence in the placenta, ultimately leading to growth restriction of the fetus (Biron-Shental et al., 2010; Davy et al., 2009; Toutain et al., 2013). Interestingly the above observation does not result in telomere length alterations in the infant, as telomere length in small for gestational age babies resulting from IUGR appear to be unaffected compared to appropriately grown infants (Akkad et al., 2006).

Also worthy of mention on this topic is the fact that in many cases, placental chromosomal mosaicism is associated with IUGR (Grati et al., 2005; Lestou and Kalousek, 1998; Robinson et al., 1997). Given the role of telomeres in guiding chromosome pairing and segregation events (Manders et al., 1999; Parada and Misteli, 2002), it is tempting to speculate that a link may be found between these two observations. It has also been noted that telomere aggregates are present in placentas of women experiencing pre-eclampsia during pregnancy. These telomere aggregates appear to form independently of telomere length, but represent dysfunctional telomeres, which can lead to breakage-bridge-fusion cycles and eventually apoptosis or senescence (Suknik-Halevy et al., 2009). It is possible that this may also be linked to chromosomal mosaicism in the placentas of pregnancies complicated by IUGR.

Conversely, evidence shows that diabetes during pregnancy does not affect telomere length. Cord blood telomere lengths from mothers with type I, type II or gestational diabetes are not altered compared to mothers who do not suffer with diabetes (Cross et al., 2010). These findings are in agreement with the observation that telomere lengths are not altered in young adults born to mothers suffering type I diabetes or gestational diabetes compared to controls (Cross et al., 2009). Interestingly however, telomerase activity is up-regulated in cord blood from mothers with type I or gestational diabetes compared to controls. It is possible that this observation reflects altered telomere homeostasis, which might explain the lack of altered telomere length in cord blood samples (Cross et al., 2010).

One of the most important risk factors associated with pregnancy complications is that of premature birth, however the effects of preterm birth on newborn telomere length is largely unknown. One study has shown that telomere lengths of preterm infants born with intact membrane is altered compared to preterm infants born following preterm rupture of the membrane. It is proposed that this difference is due to the multiple risk factors associated with oxidative stress leading to membrane rupture, which might in turn reduce telomere lengths in these infants. Therefore, it is postulated that preterm rupture of the membrane significantly impacts telomere length in the newborn (Menon et al., 2012). However, what effect this might impose on the newborn is generally unknown. The next section is therefore dedicated to what is currently known about telomere lengths in preterm infants and what this might mean in terms of subsequent health outcome.

1.8.5.1 Telomere length in the premature infant

Telomere length in the preterm infant represents an interesting topic. While telomere length in the fetus is highly synchronised and tightly maintained, telomere length rapidly declines after birth. This poses the question: Does telomere attrition occur as a result of an extrauterine growth environment, or is it programmed to begin at a defined stage of maturity (i.e. at full gestational age)? If the former is correct then how might this affect telomere length in the preterm infant?

Evidence from the current literature suggests that although overall telomere lengths of preterm infants (born at less than 37 weeks gestation) are not different to full term controls, correlative data shows a reduction in telomere length with increasing gestational age (Friedrich et al., 2001; Menon et al., 2012). Furthermore, correlative data shows a rapid and significant decline in telomere length among preterm infants born between 27 and 32 weeks gestational age (Friedrich et al., 2001). Moreover, a longitudinal study that assessed telomere lengths at different time points in the same preterm infants found a significant decline in telomere length in the weeks following birth (Holmes et al., 2009). This represents an interesting finding, since in addition to the well-established morbidities associated with preterm birth (namely respiratory and neurocognitive disorders), a number of others are emerging which characterise an ‘aged’ phenotype in the preterm infant. This is evidenced by altered adipose tissue partitioning (Modi et al., 2009; Uthaya et al., 2005; Vasu V and N, 2009), ectopic fat deposition as intrahepatocellular lipid (Thomas et al., 2008a; Vasu et al., 2013), hypertension (Bhat et al., 2012; VanDeVoorde and Mitsnefes, 2014) and insulin resistance (Tinnion et al., 2013). These morbidities are strongly associated with metabolic syndrome (Liu et al., 2010; Parkinson et al., 2013), morbidity and mortality (Jacobs et al., 2010; Koster et al., 2008), imposing a significant public health concern. Since telomere length is associated with the process of ageing and with several disease conditions (including those listed above), it is possible that early telomere attrition might represent the underlying cause of the ‘aged’ phenotype observed in the preterm infant. With this in mind, it is possible that telomere length might act as a novel tool for predicting health outcome in the preterm infant, which could in turn provoke improved health management regimes in those identified as at risk of developing subsequent morbidities. However, although the aforementioned information from the current literature provides the basis for this rationale, to date none have explored

telomere length in the preterm infant by term equivalent age. Studies addressing this in the future might therefore provide some valuable information for assessing health outcome in this vulnerable study population.

1.9 Techniques for telomere assessment

To summarise the sections covered so far, telomeres represent an essential feature of the genome, as evidenced by the key roles that they fulfil, their conservation across phylogenetically diverse organisms, and by the presence of complex regulatory mechanisms controlling their structure. While the gradual loss of functional telomeres are a part of normal homeostasis, disruption to normal control mechanisms resulting in aberrant telomere homeostasis may have devastating effects. These include but are not limited to tumorigenesis, premature ageing disorders, fertility complications and pregnancy complications which may in turn impact on telomere length in the newborn. These observations provide rationale for the potential use of telomere assessment as a biomarker of health status, and as a tool in PGS. However, in order for this to be effective, suitable methodologies must be employed to do so.

1.9.1 Measuring telomere length

Measurement of telomeres is challenging, owing to their unique, complex structure. This is further complicated when the sample size for telomere length analysis is limited, such as in single cells for PGS, or small samples from newborns. Several methodologies exist for the measurement of telomere length, each with its own advantages and disadvantages, which must be appreciated when interpreting results. The next section is therefore devoted to evaluating the currently available methodologies for telomere length analysis, which is an important consideration for their use as tools in PGS, or as biomarkers of health status.

1.9.1.1 Telomere restriction fragment analysis

In the early 1990s Calvin Harley developed the first technique to measure average telomere length, by measuring telomere restriction fragments. The process involves restriction digest of non-telomeric DNA, leaving the telomere sequence intact. Telomere containing DNA fragments are then separated according to their size by gel

electrophoresis, and detected by standard southern blotting technique (Allshire et al., 1989; Harley et al., 1990).

Advantages of TRF analysis include its relative ease and simplicity, and the fact that minimal specialised equipment is required, which reduces the costs involved. Furthermore, several kits based on this technique are now commercially available, meaning very little optimization is necessary. Lastly, TRF analysis provides information detailing the distribution of telomere lengths within the sample as well as the average telomere length, which is represented as a smear of telomeric DNA fragments.

Disadvantages of TRF analysis however, include that it is reliant on the separation of telomere fragments on an agarose gel, which poses two main problems: Firstly, complete DNA digestion is imperative in order to avoid over-estimating telomere length. Secondly, the inclusion of non-telomeric sequences adjacent to the telomere but downstream of the restriction site will impact on the resolving capabilities of digested fragments (figure 1.22). Therefore, any variation identified in telomere length may in fact be attributable to sequences other than the telomere itself. One of the sources of this variation arises from the highly dynamic nature of the sub-telomeric region, resulting in variable quantities of repeat sequences, which may be anywhere between 2.5 and 6 Kbp (Levy et al., 1992). Furthermore, hypervariable regions within the sub-telomere create restriction site polymorphisms (Mefford and Trask, 2002). Finally, variable numbers of telomere repeat variants exist at the proximal 1kb of the telomere (Baird et al., 1995). Taken together, these factors may impose a strong influence on the resolving capability of the TRF fragment, thus it is important that these are taken in to consideration when results are interpreted (Riethman et al., 2005).

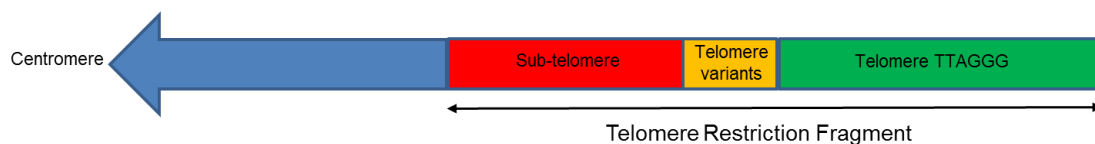


Figure 1.22: Representation of non-telomeric sequences inclusive in telomere restriction fragment analysis that may contribute to variability among individuals. Green represents true TTAGGG telomere repeats, yellow represents telomere repeat variants, red represents sub-telomeric sequences and blue represents the rest of the chromosome arm (Turner et al., 2014).

The most notable drawback of this methodology however, is that it requires a relatively large quantity (usually one microgram) of good quality DNA. Therefore other assays may prove better suited in studies where low sample volumes are available. Finally, TRF analysis is time consuming and labour intense. The entire procedure takes around three days to complete, and the number of samples that can be analysed at any one time is restricted by the size of the agarose gel. Therefore it is necessary to perform a large number of experiments in order to study a population.

1.9.1.2 Slot blot analysis and hybridisation protection assay

A solution to some of the shortcomings of TRF analysis was offered by the development of a slot blot based methodology in 1997. In this technique, DNA is blotted directly onto a nylon membrane, without prior need for restriction enzyme digest or agarose gel electrophoresis. A telomere specific probe is subsequently applied to the membrane, which is then exposed, so that the intensity of the telomere signal may be recorded. The telomere probe is washed off following exposure, and a second centromere specific probe is then applied, exposed and the signal recorded in the same way. A telomere to centromere (T/C) ratio can then be calculated from the intensities of the two signals measured (Bryant et al., 1997).

Similar to this assay is the hybridisation protection assay (HPA). In this instance, rather than measuring centromeric DNA content, a family of repetitive sequences known as alu sequences are used instead, to generate a ratio of telomere to alu DNA (Nakamura et al., 1999).

The advantage of these techniques is that only the telomeric DNA sequence is targeted in telomere intensity measurements. Thus this avoids artefacts that may arise from a non-telomeric component of telomere restriction fragments. Furthermore, calculation of T/C ratios (or telomere/alu ratios) circumvents any inaccuracies in quantitation of DNA before loading, or incomplete transfer of DNA onto the nylon membrane. However, for this to be true it must be assumed that the hybridisation efficiencies of the two probes are equal. Furthermore, high quality DNA is not essential for accurate quantification of telomere length by slot blot or HPA analysis. Indeed fragmented DNA still produces a signal representative of an intact sample, which is not the case for other telomere length techniques such as TRF analysis (Bryant et al., 1997).

In addition, this technique is well suited to studies where sample size is limited, since 10-20 nanograms of DNA is enough to produce a signal. Alternatively, it is possible to perform slot blot analysis using whole cells if the number of cells available is too low for DNA extraction (Norwood and Dimitrov, 1998). Therefore since slot blot analysis negates the need for DNA extraction, restriction enzyme digest and agarose gel electrophoresis, it is less labour intensive than other telomere length analysis techniques.

However, the disadvantage of these techniques is that they lack sensitivity and reproducibility. In repeat experiments using the same sample, variations of up to 1Kb have been reported (Norwood and Dimitrov, 1998).

1.9.1.3 Quantitative real-time polymerase chain reaction

Quantitative real-time polymerase chain reaction (qRT-PCR) enables the quantification of the number of copies of a sequence of interest. The cycle threshold (Ct) of the reaction (defined as the point at which the amplification curve raises above baseline) is determined from an amplification curve, and is directly proportionate to the number of copies of target sequence present in the sample to begin with.

In 2002 Richard Cawthon developed a novel and increasingly popular qRT-PCR approach for telomere length analysis (Cawthon, 2002). Cawthon's qRT-PCR approach is able to determine relative telomere length by ascertaining the T/S ratio, which represents the factor by which the sample under investigation differs from a reference DNA sample in its ratio of telomere sequence copy number (T) to a single copy gene copy number (S). This is determined by a standard qRT-PCR reaction using two pairs of primers in two separate amplification reactions; one pair to amplify the telomere sequence and one pair to amplify the single copy gene. Alternatively, it is possible to amplify both sequences within the same reaction using a multiplex approach developed subsequently to Cawthon's original protocol. The main advantages of the multiplex qRT-PCR procedure is that it significantly reduces inaccuracies due to inter assay plate-to-plate variation, and it reduces the total time and cost of the assay (Cawthon, 2009).

The advantages of using qRT-PCR over other telomere length analysis techniques include the clear and objective interpretation of T/S ratios. Furthermore, in similarity

to slot blot and HPA analyses, there are no contributions of non-telomeric sequences to relative telomere length calculated, since the primers included are specific to the sequence of interest. This means that any differences in T/S ratios observed between individuals are solely accountable to differences in telomere length and not sub-telomere length variation. In addition, qRT-PCR is highly sensitive, and therefore it can be carried out with as little as five nanograms of DNA, which makes this technique accessible to studies where sample size is limited (Treff et al., 2011b). Lastly, qRT-PCR is a relatively speedy technique. The assay completes in around three hours from setting up of reactions to completion of the amplification cycling programme, and as many as 42 duplicate samples can be run at once (assuming a multiplex approach is adopted). This makes the turnaround of results much faster than traditional techniques.

Disadvantages of this method however, include the fact that substantial optimisation is usually required, which requires a high level of expertise, and may take several weeks to achieve. It is imperative that this is carried out in order to gain acceptable reaction efficiencies that are similar for both primer pairs. Failure to do so will result in inaccurate data. Furthermore, it is important to appreciate that the reference gene may be subject to copy number variation within a population, which will significantly impact the relative telomere length results calculated. Lastly, qRT-PCR is fairly limited in the information that it generates. It cannot provide absolute telomere length in base pairs, or any details regarding telomere lengths of individual chromosomes, or the distribution of telomere lengths within a sample.

That being said, it has been proposed that it is possible to determine absolute telomere length from T/S ratios provided that a serial dilution of standards with known numbers of repeats for both the telomere and the single copy gene are included in the assay. One can then plot two standard curves for each reaction: One including the cycle thresholds of each of these knowns against the telomere DNA content in base pairs, and one of the cycle thresholds of each of these knowns against copy number of the single copy gene. From these standard curves, the researcher can extrapolate absolute telomere length per copy of the genome of unknowns (O'Callaghan and Fenech, 2011).

1.9.1.4 Single telomere length analysis

Single Telomere Length Analysis (STELA) is a ligation polymerase chain reaction (PCR) approach, developed specifically to measure telomere lengths of individual chromosomes. Unlike the qRT-PCR method, the PCR step in STELA is a standard PCR reaction, and therefore does not require intercalating dyes or labelled probes. Instead telomere length is quantified from the PCR products by southern blotting. The process of STELA is described in figure 1.23 on the next page. Briefly, it involves the annealing of a 'telorette' linker to the G rich 3' overhang of the telomere, which is comprised of 7 bases complementary to the telomere hexameric repeat followed by 20 non-telomere bases. The linker is then ligated to the C rich complementary 5' strand, creating a permanent tag at the telomere. This permits PCR amplification of the telomere, using a 'teltail' primer to prime synthesis at the non-telomere component of the telorette, and a second primer specific to the sub-telomere upstream. Following PCR amplification, the products are resolved according to size on an agarose gel and quantified by southern blotting (Baird et al., 1995; Baird et al., 2003).

In previous studies, STELA has proved successful for measuring telomeres of several specific chromatids including: XpYp, 2p, 11q, 12q and 17p (Baird et al., 2003; Britt-Compton et al., 2006; Xing et al., 2009). One of the advantages of STELA, is that it is able to identify the range of telomere lengths of a chromatid of interest within a given population, as well as the overall mean telomere length for that particular chromatid. The disadvantage of STELA however, is that it may only be used for chromosomes in which the sub-telomere is extensively characterised, and these may not be reflective of overall critical telomere length. In addition, it is not possible to accurately determine telomere lengths above 20kbp due to limitations of the amplification step (Baird et al., 2003). As a result, the accuracy of average telomere length calculated using this technique is questionable.

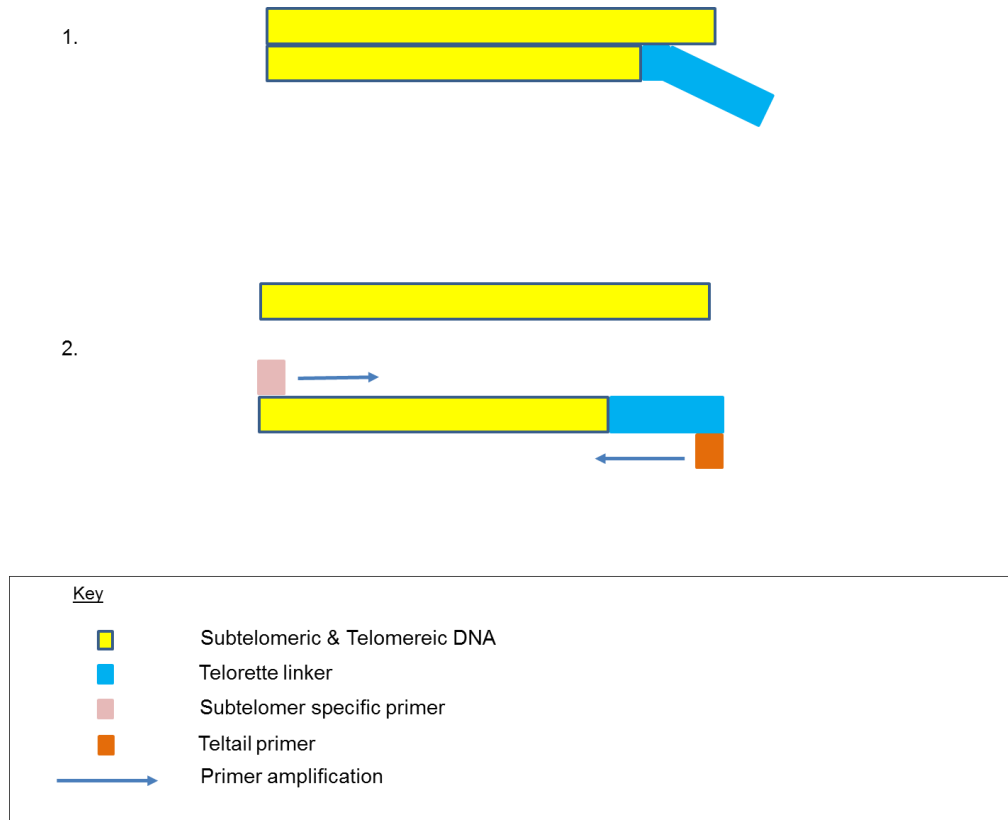


Figure 1.23: Molecular basis of single telomere length analysis. (1.) Shows annealing of a 'telorette' linker to the G-rich 3' overhang of the telomere, which is ligated to the C-rich 5' strand. (2.) A 'teltail' primer and a primer specific to the sub-telomere region primes synthesis of the telomere in a PCR reaction. Finally telomere length is quantificated by gel electrophoresis and southern blotting (Turner et al., 2014).

In order to solve the restricted use of STELA to the chromosomes of well characterised sub-telomeres, U-STELA (universal single telomere length analysis) was developed for the measurement of all telomeres in a single assay. This method, illustrated in figure 1.24, involves use of restriction enzymes to create telomere restriction fragments, followed by ligation PCR and finally southern blotting. Briefly, restriction enzyme digest of upstream sub-telomeric regions creates sticky ends in both the telomere containing fragment and the intra-genomic fragment. Both of these fragments are ligated to a linker sequence at their sticky ends, and the distal end of the telomere-containing fragment is annealed and ligated to a telorette linker. A filler sequence is then ligated to the linkers, which tags the ends of the sub-telomere and the intra-genomic fragments. This filler sequence is complimentary to the earlier ligated linker tags. Therefore upon denaturation of the double strands in subsequent PCR, a stable hairpin structure is formed in the intra-genomic sequence, inhibiting the amplification of the intra-genomic fragment, but permitting amplification of the telomere-containing

fragment. This is because neither the telorette linker nor the G rich telomeric 3' overhang are complimentary to the filler sequence and therefore no hairpin structure is formed (Bendix et al., 2010).

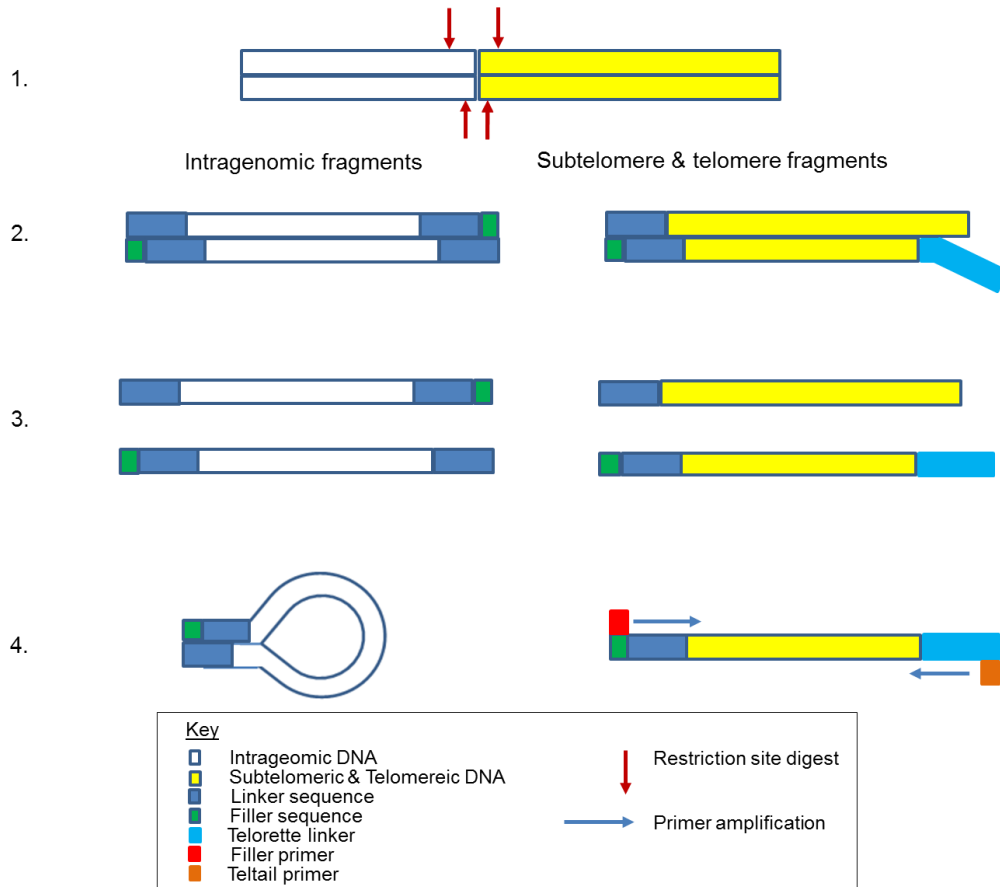


Figure 1.24: Molecular basis of universal single telomere length analysis. (1) Restriction enzyme digest creates sticky ends in both the telomere-containing fragment and the intragenomic DNA fragment. (2) Linkers are then ligated to these sticky ends, and fillers are subsequently ligated to the linkers. A 'telorette' linker is then annealed to the 3' overhang and ligated to the 5' strand before PCR amplification of the telomere-containing fragment. (3) In the first stage of each PCR cycle, dsDNA is denatured into single strands. (4) This allows formation of stable hairpin structures of the intragenomic fragment due to complimentary sequences in the linker and filler, such that in the second stage of the PCR cycle, amplification of intragenomic sequences is inhibited, whilst amplification of the telomere-containing fragment is permitted. Synthesis is primed using a 'teltail' primer designed to anneal to the 'telorette' linker, and a primer designed to anneal to the filler sequence (Turner et al., 2014).

The benefit of U-STELA, is that it is able to evaluate the amount of material below the threshold of critically short telomeres, as represented by all chromosomes in a population of cells. However, one must first identify what that threshold is. Current literature represents uncertainty on the threshold of telomere length, which is likely a reflection on the limitations of the various methodologies used to measure telomere

length over the years, as well as limited knowledge regarding other contributions to induced cellular senescence.

The main disadvantage however, is that it is prone to insufficient amplification of longer telomeres combined with preferential amplification of short telomeres, which renders U-STELA unsuitable for measuring mean telomere length (Bendix et al., 2010). Furthermore, the contributions of sub-telomere variation must additionally be considered when using this technique (Brown et al., 1990; Ijdo et al., 1992; Riethman, 2009; Rudd, 2014) (Levy et al., 1992; Mefford and Trask, 2002).

Taken together, the advantage of both STELA techniques is that they do not require large quantities of DNA; approximately 10 nanograms is sufficient. However, significant optimisation is necessary for STELA, which requires a great deal of expertise. Plus, it is labour intensive, which makes it unsuitable for high throughput studies.

1.9.1.5 Quantitative fluorescence in situ hybridisation

Quantitative Fluorescence *in situ* Hybridisation (Q-FISH) offers a modification of standard Fluorescent *in situ* Hybridisation (FISH) techniques developed in the 1980s, such that the amount of the sequence of interest may be quantified. In standard FISH, fluorescently labelled DNA probes that are complimentary to a sequence of interest allow the researcher to confirm the presence of the sequence of interest, and to visualise where that sequence is in the genome. Telomere length analysis by Q-FISH however, utilises a protein nucleic acid (PNA) probe complimentary to the telomere sequence. The uncharged backbone of the probe (as opposed to a charged DNA probe backbone) linked by peptide bonds offers more stable duplex formation with target DNA. This is because hybridisation of the probe with the DNA strand is favoured, whilst reannealing of denatured DNA is disfavoured, resulting in increased hybridisation efficiencies over standard FISH (Egholm et al., 1993; Lansdorp et al., 1996; Nielsen et al., 1991). As a result, the amount of telomere sequence present is easily quantified, since it is positively correlated with the intensity of the fluorescent signal generated (figure 1.25).

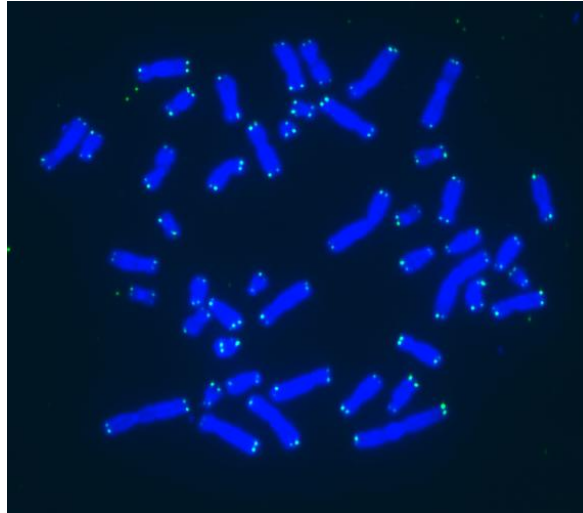


Figure 1.25: Example of a Q-FISH image. Chromosomes are stained blue, whilst telomeres are stained green.

Q-FISH is an attractive technique for telomere length analysis, since it enables analysis of telomere lengths from each individual chromosomes in a population of cells, allowing the researcher to address whether specific telomeres on specific chromosomes are affected under the conditions of the research area of interest. Secondly the probe is complimentary to the telomere sequence only, therefore sub-telomeric regions are excluded. Perhaps the most notable advantage in direct comparison with other technologies available however, is that Q-FISH is inclusive of long telomeres. Indeed it is the preferred method of choice in the study of mouse telomeres, which are known to be very long. Furthermore, it does not require large sample sizes; image capture and analysis of ten metaphase cells (Poon et al., 1999), or 40-200 interphase cells is considered acceptable (however telomere length of individual chromosomes cannot be ascertained in interphase cells) (De Pauw et al., 1998).

One of the disadvantages of Q-FISH for telomere length analysis however, is that it requires highly specialised and costly equipment. Secondly, by definition Q-FISH is hybridisation reliant. Improper assay optimisation and/or poor technique results in signal free ends (SFE), which lead to underestimation of telomere length. Secondly, and arguably more importantly, telomeres of individual chromosomes may only be detected in cells that may be metaphase induced, which is only possible in actively dividing cells. Furthermore, production of good quality metaphase preparations is a fine tuned skill in itself, as is the ability to accurately karyotype. Even when these skills

are available to the researcher, although denaturation and hybridisation of the probe is a speedy process, image capture and analysis is lengthy, particularly when one considers the time taken to properly calibrate the experiment. This is imperative in the accurate determination of telomere length, since inherent variations between experiments can occur due to altered optical alignment, variable hybridisation efficiencies and the age of the microscope lamp (Ourliac-Garnier and Londoño-Vallejo, 2011; Poon et al., 1999; Wong and Slijepcevic, 2004; Zijlmans et al., 1997). These inherent variation are likely the cause of the highly variable results generated by Q-FISH (Poon et al., 1999).

The development of high throughput Flow FISH experiments offers advantages over standard Q-FISH in that it greatly reduces the time taken to capture and analyse images. Indeed it was the first telomere length method utilised as a clinical tool (Alter et al., 2007). In this case, cells are hybridised with the PNA probe in suspension (as opposed to being fixed on a slide as in standard Q-FISH), and the intensity of the fluorescent signals is quantified using flow cytometry. Such a technique is semi-automated and therefore enables the analysis of many cells at one time (Baerlocher et al., 2006). Furthermore, simultaneous Q-FISH and antibody staining techniques allows the researcher to identify telomere lengths of different cell types within a population of cells (Baerlocher and Lansdorp, 2003). However, this requires extreme care as the unfixed cells are considerably more fragile. Furthermore, the cytoplasm must be left intact, which often results in difficulties in telomere length determination, due to non-specific hybridisation of the probe to components of the cytoplasm (Wieser et al., 2006).

1.9.1.6 Primed *in situ* labelling

Primed *in situ* labelling is a technique that combines Q-FISH and qRT-PCR techniques for telomere length analysis. Oligonucleotide sequences that are complimentary to the telomere sequence are annealed to denatured metaphase chromosomes or interphase cells. DNA polymerase then extends these oligomers using fluorescently labelled nucleotides. Fluorescent signals may then be measured using a fluorescent microscope and appropriate computer software (Lavoie et al., 2003; Therkelsen et al., 1995). Primers may extend telomeres simultaneously, however, this does not guarantee even coverage and therefore some telomeres may not show sufficient signal for detection

(Lavoie et al., 2003). This has led to several modifications of the protocol including multiple cycles of amplification (Musio and Rainaldi, 1997) and double stranded PRINS, where primers for both the forward and reverse telomere strands are included in the reaction (Yan et al., 2004).

The advantage of PRINS over Q-FISH, is that it is quicker and more cost effective (Gosden and Lawson, 1994; Koch et al., 1991; Wilkens et al., 1997). However disadvantages include that specialised equipment such as a programmable flat plate thermocycler is required. It is possible to carry out the reaction using water baths, however the stringency is greatly reduced due to non-specific primer annealing and extension (Gosden and Hanratty, 1993).

In conclusion, it is clear that the method of choice for telomere length analysis is dependent upon the sample type and sample size available. All techniques have their advantages and disadvantages, and it is important that these are considered in assay design, and in the analysis of the data obtained. Furthermore, it is important to appreciate that the cell type(s) present in the sample to be analysed may play a significant role in the contribution of telomere length. Since different cell types are known to have different telomere lengths and different telomere length maintenance regimes, these contributions cannot be ignored (Hoffmann et al., 2009; Spyridopoulos et al., 2008).

1.9.2 Measuring telomere distribution

As discussed in sections 1.1.2.3, 1.4. and 1.8, telomere distribution within the nucleus plays an important role in cellular function. Aberrant telomere distribution may therefore lead to loss of cellular function as a result of altered gene expression profiles and/or impaired synapsis during meiosis. It is possible therefore that a loss of cell function can be determined by assaying for telomere distribution within the nucleus, which might prove a useful tool. The most effective way in which this can be achieved is through FISH experiments using a pan-telomeric probe. The basis of this procedure is the same as that outlined in section 1.9.1.5, however cells are assayed in interphase as oppose to metaphase. Furthermore, it is not necessary to calibrate the experiment, since no quantitative measurements of fluorescence intensity are required. Images can either be acquired from the central plane of focus for 2D analysis, or images can be

acquired throughout several planes of depth through the nucleus, and subsequently rebuilt into a 3D image. 2D images can be assessed for telomere localisation using several different models. With particular reference to analysis of sperm nuclei for PGS, in which the tail attachment region offers a useful tool in determining the orientation of the nucleus, telomere localisation can be assayed using longitudinal (Olszewska et al., 2008; Sbracia et al., 2002), spatial (Zalenskaya and Zalensky, 2004), or radial (Boyle et al., 2001; Croft et al., 1999; Finch et al., 2008; Ioannou and Griffin, 2010; Skinner et al., 2009) analysis, as depicted in figure 1.26.

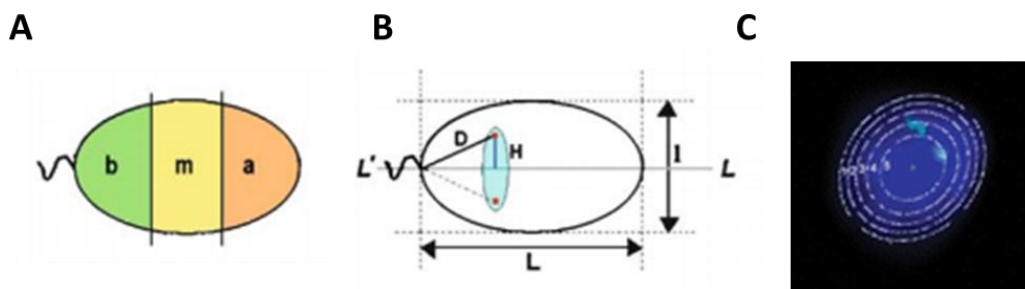


Figure 1.26: 2D analysis of signal distribution within the sperm nucleus. A: Longitudinal distribution of basal (b), medial (m) and apical (a) regions of the sperm nucleus (Olszewska et al., 2008). B: Spatial distribution where L and l represent the long and short axes of the nucleus, $L'-L$ represents the symmetry of the long axis, D is the distance from the tail attachment point to the signal and H is the distance from the signal to the long axes (Zalenskaya and Zalensky, 2004). C: Radial distribution where the nucleus is split into five shells of equal area, and the signal position is determined by assessing which shell the signal lies within (Finch et al., 2008).

Similarly, 3D images may be analysed by longitudinal or radial positioning (Alladin et al., 2013). In this analysis, the edges of the nucleus are determined using software able to detect the edge of nuclear staining, and from this measurements can be made including the volume of the nucleus and where the centre of the nucleus lies. From these measurements the position of the signal can be ascertained (for examples of freely available software able to perform these measurements see (Iannuccelli et al., 2010), (Gué et al., 2005).

The advantage of 2D analysis is that it provides a fast means of assaying nuclear organisation. However the main disadvantage is that information from a 3D object is flattened into a 2D image and therefore its accuracy is compromised. There are mathematical models designed to compensate for this effect (Boyle et al., 2001; Skinner et al., 2009), however ultimately a 3D approach likely offers the best solution. That being said, the disadvantage of 3D image analysis is that it is highly labour intense

and therefore the number of cells that can feasibly be analysed is often dramatically reduced.

1.10 Thesis rationale

Telomere biology specifically in relation to fertility and early life in humans is becoming an increasingly popular topic, however information remains limited to a few studies. Most studies have utilised mouse models to study telomere length and distribution in gametes, and during development. In humans however, although the telomere theory of reproductive ageing in women has been hypothesised, limited data is available in support of this. Similarly in males, few studies have investigated telomere length in relation to fertility. Moreover, to the best of my knowledge, none have attempted to study telomere distribution patterns in sperm. Given the importance of telomere distribution during meiosis and mitosis, coupled with evidence from mouse models, this represents an interesting topic worthy of investigation. Furthermore, how telomere biology is regulated during embryogenesis, and how this might implicate telomere biology in the newborn is largely understudied. Therefore, future studies would benefit from a deeper understanding of how these complex structures are involved in the process of ageing, the pathogenesis of disease and in fertility. Such information might shed light on the validity of telomere length and/or distribution patterns as indicators of fertility potential, and as biomarkers for infant health outcome.

1.11 Thesis Aims

With the aforementioned rationale in mind, the specific aims of this thesis were as follows:

1. To test the hypothesis that telomere distribution is altered in the sperm heads of males with compromised semen parameters
2. To optimise a qRT-PCR approach for assaying telomere length using small quantities of starting material
3. To investigate the telomere theory of reproductive ageing in women by addressing a series of hypotheses pertaining to telomere length in first polar bodies and cleavage stage embryos in relation to maternal age, and generation of aneuploidy
4. To test the hypothesis that preterm babies have significantly reduced telomere length by term equivalent age compared to their term born counterparts

2 Materials and Methods

2.1 Materials

In order to assess chromatin packaging, telomere distribution and telomere interactions with proteins at the nuclear membrane in sperm (specific aim 1), control semen samples were recruited from The Bridge Fertility Centre (London, UK) from 13 normal fertile males. In addition to this, semen samples from six infertile males were recruited from Embryogenesis (Athens, Greece). Patients were identified as fertile or infertile based on analysis of semen parameters by trained andrologists at The Bridge Fertility Centre or Embryogenesis respectively. Those with a sperm concentration of ≤ 20 million/ml and/or % motility of $\leq 20\%$ and/or % normal morphology of $\leq 5\%$ were classified as infertile. All semen donors provided written and informed consent for use of their samples in research. This was carried out under human fertilisation and embryology authority (HFEA) license 0700/L700-18-c awarded to the Bridge Fertility Centre. Use of semen samples from both The Bridge Fertility Centre and Embryogenesis for research purposes was approved by the Research Ethics Committee of the University of Kent.

For the assessment of telomere length in first polar bodies and embryos in relation to maternal age and the incidence of aneuploidy (specific aim 3), whole genome amplified DNA from biopsied blastomeres and first polar bodies that were surplus to requirement were donated from couples undergoing IVF treatment at Genesis Genetics (Nottingham, UK). These samples underwent whole genome amplification using the SurePlex DNA Amplification System (Illumina), and were assessed for presence of aneuploidy using the SurePlex 24sure kit (Illumina) by personnel at Genesis Genetics. Leftover WGA material was then transported to the University of Kent (UKC) for PCR purification and relative telomere length analysis by qRT-PCR. All patients consented to biopsy procedures and aCGH analysis of chromosome copy number, and the use of surplus sample material for research purposes. This work was also approved by the Sciences Faculty Research Ethics Advisory Group.

In order to test the hypothesis that telomere length is reduced in preterm infants compared to term born controls (specific aim 4), eligible infants were recruited by

research staff from the William Harvey Hospital (Ashford, UK) (WHH) or the Queen Elizabeth Queen Mother Hospital (Margate, UK) (QEQMH) following ethics approval from Surrey Research Ethics committee (10/H1109/51) and informed consent. Sampling involved drawing an extra 1-1.5ml blood from preterm infants (born less than 32 weeks gestation) during routine blood testing. Full term infants (born after 37 weeks gestation) were eligible for sampling only if blood sampling was deemed necessary for other medical purposes (for example suspected jaundice). Blood sampling was carried out using standard phlebotomy techniques by research staff at WHH and QEQMH. Samples were anonymised by research nurses at WHH and QEQMH, and the study remained blinded until analysis of all patient samples was complete.

2.2 Methods

2.2.1 Sperm sample preparation

Sperm samples were prepared for subsequent procedures by firstly washing in sperm buffer (10mM NaCl/10mM Tris pH7), followed by centrifugation at 1900rpm for five minutes. The supernatant was removed taking care not to disturb the pellet, and the pellet was resuspended in sperm buffer. This process was repeated a further three to five times depending on the quality of the sample (assessed by the size and colour of the pellet). Following the final centrifugation, sperm samples were fixed by adding 6mls of ice cold 3:1 methanol:acetic acid in a drop wise fashion, whilst agitating the tube. The samples were centrifuged again at 1900rpm for five minutes, the supernatant was removed and the pellet was again resuspended and fixed. This was repeated a further two times. Samples were then stored at -20°C until they were used for telomere and H2BFWT detection and chromatin assessment experiments.

2.2.2 Telomere detection in sperm: FISH

In order to assess telomere distribution in sperm nuclei (specific aim 1a part one), semen samples stored in fixative at -20°C were centrifuged at 1900rpm for five minutes and the appropriate volume of supernatant was removed (dependant on the size of the pellet) to produce the desired concentration of cells.

2.2.2.1 Slide preparation

Glass poly-lysine slides (VWR) were cleaned by immersion in methanol and marked underneath with a diamond marker to indicate the location of the sample. The slide was labelled appropriately and 8µl of the sample was dropped onto the marked area, followed by 8µl of fresh fixative when the sample appeared grainy. This was carried out in order to ensure that sperm cells did not fix to the slide in clumps of cells, making subsequent analysis difficult. Finally, before proceeding with the FISH protocol, the slide was inspected using phase contrast microscopy to check for optimum density and quality of the sperm cells.

2.2.2.2 Ageing of slides and pre-hybridisation washes

Slides were aged on a hot plate for 1 hour at 70°C, then incubated in an ethanol series (70%, 80% then 100%) for two minutes each in order to dehydrate the sperm nuclei. After air-drying, slides were incubated in pre-warmed pepsin solution at 37°C for 20 minutes to remove proteins, allowing access of the probe to sperm DNA. Pepsin solution was made up of 49ml double distilled water (ddH₂O) plus 500µl of one molar hydrochloric acid (1M HCl). Addition of 500µl 10mg/ml of pepsin to this solution occurred immediately prior to use in order to maximise enzymatic activity. Following the pepsin wash, slides were incubated in phosphate buffered saline (PBS) for five minutes, and rinsed by brief immersion in ddH₂O. Next, slides were incubated in 4% paraformaldehyde (made up in PBS) at 4°C for 10 minutes, rinsed by brief immersion in ddH₂O, and incubated in PBS for five minutes. Slides were then incubated again in an ethanol series for two minutes each, and air-dried.

2.2.2.3 Probe preparation and DNA denaturation

During the preceding ethanol series, enough probe for 3µl per sample (plus 10% error margin volume) of biotin labelled ready to use StarFISH pan telomeric probe (Cambio) was pipetted into a PCR tube and placed in a thermocycler programmed to incubate at 37°C for five minutes followed by 85°C for 10 minutes. Once the programme was complete, the probe was kept on ice until use.

When slides were dry, sperm cell nuclei were denatured in 70% formamide (Sigma Aldrich) (made up in 2x saline sodium citrate (SSC)) pH 7-7.5, at 75°C for two minutes.

Immediately after this, slides were immersed in ice cold 70% ethanol for two minutes, followed by 80% and subsequently 100% ethanol for two minutes each at room temperature. This allowed the dehydration of sperm nuclei as well as promoting reannealing of short repetitive, non-specific sequences.

Once slides had air dried, 3µl of probe was applied to the marked area and covered with a 13mm round cover slip, which was sealed with fixogum rubber cement (www.amazon.co.uk). Slides were then placed into a humid chamber and incubated at 37°C overnight to allow hybridisation of the probe.

2.2.2.4 Post-hybridisation washes and detection

On the following day, rubber cement was carefully removed using tweezers, and the slide was incubated in 0.7x SSC plus 0.3% Tween until the cover slip floated off. Slides were subsequently washed in pre-warmed 0.7x SSC plus 0.3% Tween at 37°C for 10 minutes in order to remove any excess un-hybridised probe. After this, samples were washed in storage buffer (0.4x SSC plus 0.05% Igepal) for two minutes, before adding 90µl of detection mix (50µl 2x SSC plus 40mg/ml Marvel powdered milk, 50µl storage buffer and 3µl streptavidin-Cyanine3 (Cy3) (Amersham biotechnology)). A 22 x 50mm cover slip was applied, and slides were incubated in the dark in a humid chamber at 37°C for 45 minutes, before washing off excess un-bound detection mix in three five minute incubations in storage buffer. Lastly, slides were rinsed by brief immersion in ddH₂O, air-dried in the dark, and one drop of Vectashield® with 4',6-diamidino-2-phenylindole (DAPI) (Vector Labs) was applied. A 22 x 50mm coverslip was gently pressed on, and fluorescence microscopy ensued. 2D fluorescence microscopy was carried out using a BX61 Olympus microscope equipped with a charge coupled device (CCD) camera. Images were captured with the appropriate filters under a 100x objective using SmartCapture software (Digital Scientific). For each patient a total of 100 nuclei were captured and analysed. For 3D image capture, cells were inspected under an Olympus IX71 microscope equipped with a CCD camera, under a PlanApo 100x OTIRFM-SP 1.45 NA lens mounted on a PIFOC z-axis focus drive (Physik Instrumente, Karlsruhe, Germany). Cells were illuminated using LED light sources (Cairn Research Ltd, Faversham, UK) with appropriate filters (Chroma, Bellows Falls, VT). The best plane of focus for the centre of the cells was identified and 61 images

were captured in 0.1 μM step sizes through the cell (30 images either side of the central position) for each filter using Metamorph software.

2.2.2.5 Telomere detection after sperm nuclear decondensation

To assess the effect of sperm nuclear decondensation on telomere localisation (specific aim 1a part two), a control semen sample was selected at random and a FISH experiment was performed including an extra step in which sperm nuclei were decondensed following ageing but prior to ethanol dehydration. A control slide in which the sample was not decondensed was also included in the experiment.

2.2.2.5.1 Sperm nuclear decondensation with dithiothreitol

After slides were aged at 70°C for one hour, they were placed in a coplin jar containing 10mM dithiothreitol (DTT) (Melford) made up in 0.1M Tris pH 7, for 30 minutes in the dark. Following this, slides were rinsed by brief immersion in 2 X SSC and the rest of the FISH protocol ensued starting with dehydration in the first ethanol series.

2.2.2.5.2 Sperm nuclear decondensation with sodium hydroxide

Alternatively, sperm nuclei were decondensed in 0.5M sodium hydroxide (NaOH) for four minutes at room temperature. Slides were then washed by incubation in PBS for five minutes before continuing with the FISH protocol starting with dehydration in the first ethanol series.

2.2.2.6 2D image analysis of telomeric signals

Telomere signal positions were identified in at least 100 sperm cells from 13 control males and six infertile males using a custom designed macro (designed by Michael Ellis, Digital Scientific) in ImageJ (freely available from <http://imagej.nih.gov/ij/>) based on that of Croft *et al.* (Croft *et al.*, 1999). This macro is capable of splitting the area of the nucleus into five concentric rings of equal area (shown in figure 2.1). The number of signals in each ring was then manually counted and recorded in a Microsoft Excel spreadsheet. The proportion of signals in each ring was calculated by dividing the number of signals in each ring by the total number of signals within the nucleus. In order to account for the flattening of a 3D object into a 2D image, two mathematical

models were adopted: The volumetric model, which calculates the volume of the nucleus and includes compensation factors for the pressures applied to the nucleus during the FISH procedure and image capture; and the DAPI density model, which normalises the signals in each ring against the intensity of the DAPI stain in that given ring.

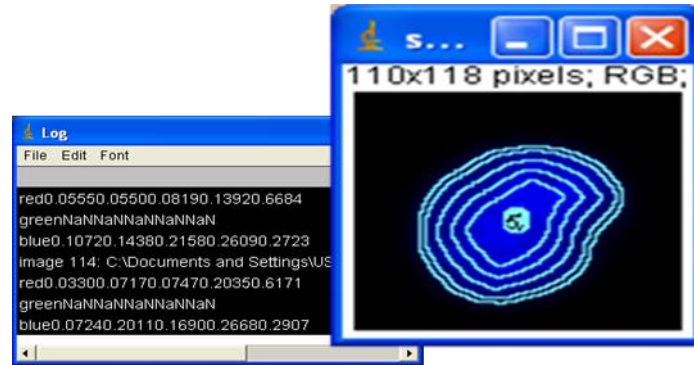


Figure 2.1: The ImageJ macro is able to split the nucleus into separate channels, convert the blue channel to a binary mask, and then apply five rings of equal area to the blue channel.

The mean percentage of signals in each ring was calculated for each patient using each model in order for clear comparisons to be drawn. A χ^2 test was performed to test the hypothesis that signals are distributed non-randomly within the sperm nucleus.

2.2.2.7 3D image analysis

Images for each filter were first deconvolved using the AutoQuant (Media Cybernetics) 3D deconvolution function, and then uploaded into a freely available software called Nemo for 3D analysis (Iannuccelli et al., 2010). Once opened in Nemo, each cell in the image was identified and analysed for several measurements. These measurements were exported into a Microsoft Excel spreadsheet for easy manipulation of data. The measurements of interest included: Distance from the centre of the telomere signal to the centre of the nucleus (distance 1) and distance from the centre of the telomere to the border of the nucleus (distance 2) (shown in figure 2.2). For each patient 30-50 sperm nuclei were analysed. Sperm samples from a total of six fertile control patients and five infertile patients were analysed in this way.

In order to confirm 2D localisation of telomeres by 3D image analysis, distance 1 was added to distance 2 and then distance 2 was divided by the sum of distance 1 and 2.

The resulting value was multiplied by 100. This was repeated for all telomere signals in all cells of all images. The results were then grouped into frequency bins of 0-20, 20.1-40, 40.1-60, 60.1-80 and 80.1-100 and the percentage of signals in each bin was calculated. This was plotted in a bar chart to represent the tendency of telomere localisation within the sperm nucleus, with values in the lower bins (0-20) reflecting peripheral localisation and those in the higher bins (80.1-100) reflecting a central localisation. Again, χ^2 statistical tests were performed to test the hypothesis that telomeres are distributed non-randomly within the sperm nucleus.

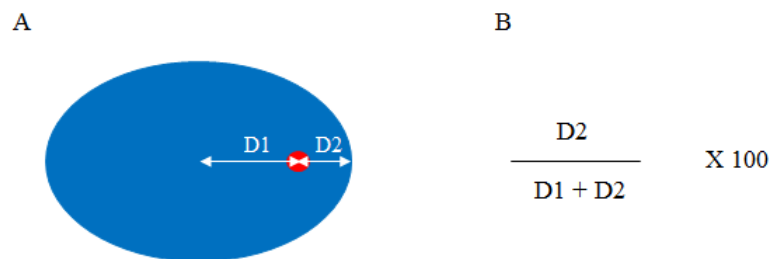


Figure 2.2: Diagrammatic representation of distances measured for analysis of telomere distribution. A: Blue represents DAPI staining on the nucleus, red represents telomere staining, D1 represents distance 1 (the distance between the centre of the telomere signal and the centre of the nucleus), D2 represents distance 2 (the distance between the centre of the telomere signal and the nuclear periphery). B: Calculation of telomere position within the 3D nucleus.

2.2.3 Immunofluorescence localisation of H2BFWT in sperm

To assess histone 2B family W testis specific (H2BFWT) distribution in sperm (specific aim 1a part three), semen samples stored in fixative at -20°C were prepared and dropped onto a clean poly-lysine glass slide as described in section 2.2.2.1. Each experiment included a positive control (a sample known to stain well) and a negative control (in which no primary antibody was applied). Following each incubation step, slides were allowed to mostly, but not completely dry in order to preserve nuclear membrane integrity.

Slides were first incubated in PBS for five minutes, then blocked by pipetting $150\mu\text{l}$ of 5% donkey serum (made up in PBS) onto the slide and applying a $22 \times 50\text{mm}$ coverslip. Blocking solution was washed off by immersion of the slide in PBS for 5 minutes, and subsequently $150\mu\text{l}$ of primary antibody solution (1:10 dilution of Santa Cruz H2BFWT (S-14) antibody plus 10% donkey serum in PBS) was applied (except for in the case of the negative control slide). After incubation for one hour, slides were

washed three times in PBS for five minutes each, and then 150µl secondary antibody solution was applied (1:100 dilution of Santa Cruz Fluorescein isothiocyanate (FITC) labelled donkey anti-goat IgG antibody plus 5% donkey serum in PBS). Slides were incubated for 45 minutes in the dark before washing a further three times in PBS for five minutes each. Finally slides were rinsed by brief immersion in ddH₂O and one drop of Vectashield® with DAPI was applied. A 22 x 50mm coverslip was applied, and for 2D analysis, slides were inspected under appropriate filters using a BX61 Olympus microscope equipped with a CCD camera under a 100x objective. For each patient 100 images equating to 100 nuclei were captured using SmartCapture3 software. For 3D analysis, cells were inspected under an Olympus IX71 microscope equipped with a CCD camera, under a PlanApo 100x OTIRFM-SP 1.45 NA lens mounted on a PIFOC z-axis focus drive (Physik Instrumente, Karlsruhe, Germany). Cells were illuminated using LED light sources (Cairn Research Ltd, Faversham, UK) with appropriate filters (Chroma, Bellows Falls, VT). The best plane of focus for the centre of the cells was identified and 61 images were captured in 0.1µM step sizes through the cell (30 images either side of the central position) for each filter using Metamorph software (Molecular devices).

2.2.3.1 2D H2BFWT signal localisation

H2BFWT localisation was determined in at least 100 cells from six control patients in a similar manner to that described in section 2.2.2.6, however a more automated process was adopted. Images were uploaded into ImageJ and an updated custom-made macro (described in detail by Ioannou *et al.* and Skinner *et al.* (Ioannou and Griffin, 2010; Skinner *et al.*, 2009)) was applied. Firstly, the image was split into green and blue channels representing H2BFWT signals and DAPI staining respectively. The macro then converted the blue image to a binary mask from which five rings of equal area were created. Finally, the proportion of signal in each ring in each channel, relative to the total signal was measured and the data was exported into Microsoft Excel for data manipulation in the same way that telomere signal positioning was determined. A chi² statistical test was carried out to test the hypothesis that H2BFWT localisation in the sperm nucleus is non-random.

2.2.3.2 3D H2BFWT signal localisation

3D localisation of H2BFWT was measured in 30 – 50 cells from six control patients in the same way that 3D telomere localisation was captured and analysed (described in section 2.2.2.7). Images for each filter were deconvolved using the AutoQuant 3D deconvolution function, and then uploaded into Nemo for 3D analysis (Iannuccelli et al., 2010). Again, measurements of the distance from the centre of the H2BFWT signal to the centre of the nucleus (distance 1), and distance from the centre of the H2BFWT signal to the border of the nucleus (distance 2) (shown in figure 2.2) were recorded and exported into a Microsoft Excel spreadsheet. Distance 1 was added to distance 2 and then distance 2 was divided by the sum of distance 1 and 2 (figure 2.2). The resulting value was multiplied by 100 and the results were grouped into the same frequency bins as described in section 2.2.2.7. Finally the percentage of signals in each bin was calculated and this was plotted in a bar chart to represent the tendency of telomere localisation within the sperm nucleus. A χ^2 statistical test was performed to test the hypotheses that H2BFWT is localised at the nuclear periphery.

2.2.4 Telomere and H2BFWT co-localisation

Semen samples stored in fixative at -20°C were prepared and dropped onto a clean poly-lysine glass slide as described in section 2.2.2.1. In order to detect both the telomere and H2BFWT, the FISH protocol was amended such that it would not impose implications on the subsequent immunofluorescence staining. All experiments included three controls using a sample known to stain well: Control one received only the FISH procedures with the telomere probe, control two received only the immunofluorescence procedures with the H2BFWT antibody plus secondary antibody and control three received both procedures, but no primary antibody incubation was included.

2.2.4.1 Telomere detection by FISH

Initially, all slides (except control two) were subjected to the FISH procedures described in section 2.2.2 (without nuclear swelling). However, steps following air drying after the first ethanol series until addition of the StarFISH pan telomeric probe were omitted so as to avoid detrimental effects on downstream processing. All other

steps were performed in exactly the same way. However following post hybridisation washing, slides were immediately washed in PBS for five minutes and allowed to almost, but not completely dry.

2.2.4.2 H2BFWT detection by immunofluorescence

Subsequent to FISH detection of telomeres, the immunofluorescence protocol ensued exactly as described in section 2.2.3 in order to detect H2BFWT, except in the case of control slide 1 (in which only telomere detection was carried out). All slides received the same treatment, apart from control slide three, in which no primary antibody incubation step was included.

2.2.4.3 2D Fluorescence microscopy

Images were captured as described in section 2.2.2.6 and analysed by overlaying images taken under the Cy3 filter (which detects telomeres) with images taken under the FITC filter (which detects H2BFWT), in order to observe whether telomeres co-localised with H2BFWT.

2.2.5 Sperm chromomycin A₃ staining

In order to assess chromatin packaging in human sperm nuclei (specific aim 1b part one), chromomycin A₃ (CMA3) staining was performed to test for protamine deficiency in sperm (a measure of chromatin packaging). Semen samples stored in fixative at -20°C were prepared and dropped onto a clean poly-lysine glass slide as described in section 2.2.2.1. A positive control sample was included in all experiments undertaken. In this positive control experiment sperm cells were decondensed by immersion of the slide in pre-warmed 200mM freshly made DTT (Melford) for 20 minutes at 37°C. The positive control slide was washed in PBS for five minutes, rinsed by briefly immersing in ddH₂O and air-dried. From thereafter all slides were treated in the same way.

Chromomycin A₃ from *Streptomyces griseus* was dissolved in McIlvane's solution (0.2M disodium orthophosphate heptahydrate, 0.1M citric acid, 10mM magnesium chloride (MgCl₂) pH7) to a final concentration of 0.25mg/ml. 100µl of this CMA3 solution was applied to each slide and a 22 x 50mm cover slip placed on top. After

incubation for 20 minutes in the dark, slides were incubated for 30 seconds in McIlvane's solution and allowed to dry (in the dark). One drop of Vectashield® (without DAPI) was applied to each slide and a 22 x 50mm cover slip was pressed on. Slides were inspected on a BX61 Olympus microscope equipped with a CCD camera and appropriate filter under a 100x objective. Images were captured using SmartCapture3 software. For each patient a total of 100 nuclei were captured, and the percentage of positively stained nuclei was calculated (indicated by bright yellow staining). A student's t-test was performed to test the hypothesis that infertile males possess a greater percentage of positively stained nuclei.

2.2.6 Optimisation of qRT-PCR relative telomere length analysis

In order to assess average relative telomere length from small starting quantities of DNA, a qRT-PCR protocol originally described by Cawthon 2009 was adapted and optimised for use with the Rotor-gene Q real-time PCR machine (specific aim 2a). In this reaction, relative telomere length is measured by determining the factor by which the DNA sample of interest differs from the reference DNA sample in its ratio of telomere sequence copy number (T) to the copy number of a single copy reference gene (S) (Cawthon, 2009).

Telg and Telc primers were used to amplify the telomere, and each reaction also contained primers designed to amplify part of a single copy gene sequence (beta-globin). The design of each primer is shown in table 2.1. Both primer pairs contain GC clamps in order to modify their melting temperature, such that multiplex qRT-PCR can be achieved with the use of SYBR Green®, negating the need for labelled primers.

Name	Design	Reference
Telg	ACACTAAGGTTTGGGTTTGGGTTTGGGTTTGGGTTAGTGT	(Cawthon, 2009)
Telc	TGTTAGGTATCCCTATCCCTATCCCTATCCCTATCCCTAACA	
Hbgu	CGGCGGCGGGCGGCGGGCTGGGCGGCTTCATCCACGTTACCTTG	
Hbgd	GCCCCGCCCGCCGCGCCCGTCCCCGCCGAGGAGAAGTCTGCCGTT	

Table 2.1: Primer design for amplification of the single copy gene beta-globin for qRT-PCR analysis of relative telomere length in infants.

In order to optimise reaction specificity and efficiency, several commercially available mastermixes were tested. These are outlined in table 2.2. In addition, a combination of different primer concentrations were trialled (outline in table 2.3 on the next page).

Mastermix	Supplier
SYBR® Green JumpStart™ Taq ReadyMix™	Sigma Aldrich
Power SYBR® Green Master Mix	Life Technologies
QuantiTect SYBR® Green PCR Kits	Qiagen
QuantiFast SYBR® Green PCR Kit	Qiagen
Rotor-Gene SYBR® Green PCR Kit	Qiagen
iQ™ SYBR® Green Supermix	Bio-Rad
LightCycler® 480 DNA SYBR Green I Master	Roche
SensiMix™ SYBR® No-ROX Kit	Bioline
SensiFast™ SYBR® No-ROX Kit	Bioline

Table 2.2: Different mastermixes tested during optimisation of qRT-PCR analysis of relative telomere length.

	Primer name			
	Telg	Telc	Hgbd	Hgbu
Primer concentration (nm)	150	150	150	150
	75	75	50	50
	50	50	75	75
	50	50	50	50
	25	25	50	50

Table 2.3: Different primer concentrations trialled (in nm) during optimisation of multiplex qRT-PCR analysis of average relative telomere length.

As discussed further in chapter 4, the optimum cycling conditions for multiplex qRT-PCR were achieved using the components outlined in table 2.4. Therefore all subsequent experiments were undertaken using these components.

Component	Supplier	Concentration	Volume (µl)	Final Concentration
Telg	Eurofins MWG Operon	1.25µM	1	50nM
Telc	Eurofins MWG Operon	1.25µM	1	50nM
Hbgu	Eurofins MWG Operon	1.25µM	1	50nM
Hbgd	Eurofins MWG Operon	1.25µM	1	50nM
2x SensiMix™ No Rox	Bioline	N/A	12.5	1x
PCR grade water	Qiagen	N/A	3.5	N/A
Patient DNA	N/A	5ng/µl	5	25ng
Reference DNA	N/A	20 – 0.625ng/µl	5	100 – 3.125ng

Table 2.4: Components of multiplex qRT-PCR set up for relative telomere length analysis in infants.

2.2.6.1 Setting up qRT-PCR and cycling conditions

In a pre-decontaminated PCR cabinet, enough mastermix was made up for all reactions and 20µl was dispensed into each 0.1ml tube (Qiagen). 5µl of PCR grade water was added to the no template negative control tubes, and the lids of these tubes were closed. The remaining tubes were transported to a different laboratory for the addition of 5µl DNA. A two-fold serial dilution of the reference DNA sample (AMS Biotechnology) was assayed in order to plot a standard curve of the log DNA concentration against the cycle threshold (an automatic function of the Rotor-gene Q software) to confirm acceptable reaction efficiency in each reaction (between 95-105% with an R² value above 0.95). Reference DNA was diluted to a concentration of between 10ng/µl to 0.3125ng/µl in ddH₂O immediately prior to setting up the reaction in order to give final amounts of between 50ng and 1.625ng of DNA upon addition of 5µl into each tube. All reactions were set up in triplicate. After addition of DNA to each reaction, the lids of the tubes were closed, and the samples were loaded into a Rotor-Gene Q 2 plex qPCR machine (Qiagen).

Cycling conditions are outlined in figure 2.3 on the next page. An initial hold temperature at 95°C promoted activation of the DNA polymerase, followed by two cycles at 94°C and 49°C for 15 seconds each to allow annealing and extension of Telg. In the subsequent 40 cycles Telc primed synthesis of the Telg product formed in the previous step via annealing at 62°C followed by extension at 74°C. Data was collected at 74°C under Cycling A in the Rotor-Gene Q Software. Although beta-globin amplification may occur at this temperature, the cycle threshold of this product is much later than that of the telomere, thus differentiating the two products. An incubation step

at 84°C melted the telomere product whilst still allowing annealing of Hgbu and Hgbd due to their high melt temperatures imposed by GC clamps. Extension and signal acquisition of the single copy gene product at 88°C was recorded in Cycling B in the Rotor-Gene Q Software. Finally a melt curve analysis was performed by incubating for one second and acquiring signals between 72°C and 95°C.

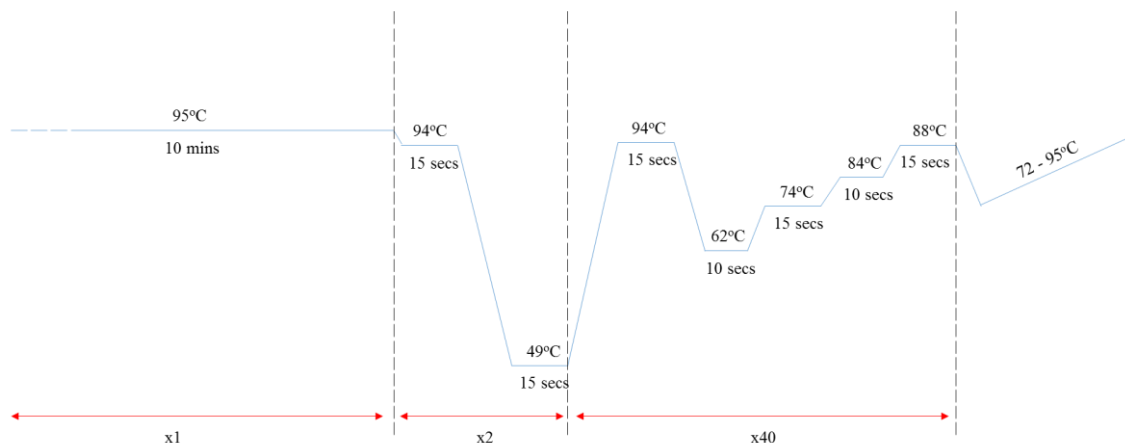


Figure 2.3: Cycling conditions of the multiplex qRT-PCR for relative telomere length analysis.

After completion of the cycle, the reaction efficiency was assessed using the Rotor-Gene Q Series Software. Furthermore, the melt curve was assessed to check that only the expected products had formed, and a 3% agarose gel was run for further confirmation of expected product sizes as described in the next section.

2.2.7 Agarose gel electrophoresis

In order to assess qRT-PCR product sizes, products were run on a 3% agarose gel. This was prepared by dissolving 1.35g Ultrapure™ Agarose (Invitrogen) in 45mls of Tris-acetate (40mM) Ethylenediaminetetraacetic acid (EDTA) (1mM) (TAE) by heating for 90 seconds in a microwave. After allowing the solution to cool slightly, 1µl SYBR safe (GE Healthcare) was added and the solution was mixed and poured into a cast containing a comb, and allowed to set. Once the gel was fully set, the comb was removed and the cast appropriately repositioned in the gel tank. Sufficient TAE was poured into the tank to cover the gel, and subsequently samples premixed with an appropriate volume of 6x loading buffer (Promega) were loaded into the wells. The outermost wells were loaded with 5µl of 500Kbp DNA ladder (Promega) premixed

with 1 μ l 6x loading dye. The gel was run for 45 minutes at 90V before assessing and photographing under a UV light on a transilluminator with a Kodak ID Camera (Carestream Health Inc., Rochester, New York, USA).

2.2.8 qRT-PCR analysis of telomere length in single cells

In order to assess telomere length in whole genome amplified DNA from single cells, a singleplex qRT-PCR protocol was adapted from Cawthon's multiplex qRT-PCR assay for telomere length analysis (described in section 2.2.6), and optimised for use with the Rotor-gene Q real-time PCR machine (specific aim 2b). In this assay, telomeres were amplified in a separate reaction to amplification of the reference sequence. Due to the fact that single cells contain only one copy of the genome, whole genome amplification (WGA) prior to qRT-PCR is necessary to generate the required input quantity of DNA. In order to reduce the risk of inaccuracies in telomere length quantitation as a result of allele dropout during WGA, and for differences in chromosome number, a multicopy reference gene (alu) was detected (Treff *et al.*, 2011) instead of a single copy reference gene (hgb), as utilised by Cawthon 2009 (Cawthon, 2009).

2.2.8.1 qRT-PCR components

Primer designs for amplification of the telomere is shown in table 2.1 in section 2.2.6. Primer designs for amplification of the multicopy reference gene are shown in table 2.5.

Name	Design	Reference
AluF	GACCATCCCGGCTAAAACG	(Treff et al., 2011b)
AluR	CGGGTTCACGCCATTCTC	

Table 2.5: Primer design for amplification of a multicopy reference gene from single cells.

In order to optimise specificity and efficiency of each amplification reaction, three of the best performing commercially available mastermixes identified in section 2.2.6 were trialled. These are described in table 2.6 on the next page. In addition, five different combinations of reference gene primer concentrations and three different

combinations of telomere primer concentrations were tested. These are outlined in tables 2.7 and 2.8.

Mastermix	Supplier
Rotor-Gene SYBR® Green PCR Kit	Qiagen
SensiMix™ SYBR® No-ROX Kit	Bioline
SensiFast™ SYBR® No-ROX Kit	Bioline

Table 2.6: Different mastermixes tested during optimisation of qRT-PCR analysis of relative telomere length from single cells.

	Primer name	
	AluF	AluR
Primer concentration (nm)	300	300
	200	200
	100	200
	100	100
	50	50

Table 2.7: Primer concentrations tested for amplification of the mutlicopy reference sequence for telomere length analysis by qRT-PCR in single cells.

	Primer name	
	Telg	Telc
Primer concentration (nm)	200	200
	100	100
	50	50

Table 2.8: Primer concentrations tested for amplification of the telomere in telomere length analysis by qRT-PCR from single cells.

As discussed in chapter 4, the optimum reaction conditions for amplification of the telomere and multicopy reference sequence are outlined in table 2.9. Each reaction run included six two-fold serial dilutions of a reference DNA in order to assess reaction efficiency (concentrations ranging from 10ng/µl to – 0.3125ng/µl in order to give a final input DNA ranging from 50ng – 1.625ng). All reference samples were run in triplicate.

Component	Supplier	Concentration	Volume (µl)	Final Concentration
Telg OR AluR	Eurofins MWG Operon	2.5µM	1	100nM
Telc OR AluF	Eurofins MWG Operon	2.5µM	1	100nM
2x Rotor Gene-Q SYBR Green PCR Kit	Qiagen	N/A	12.5	1x
PCR grade water	Qiagen	N/A	5.5	N/A
Patient DNA	N/A	5ng/µl	5	25ng
Reference DNA	N/A	20 – 0.625ng/µl	5	100 – 3.125ng

Table 2.9: Reaction contents for telomere or multicopy reference sequence amplification from single cells for relative telomere length analysis.

The multicopy reference gene amplification reaction was set up in exactly the same way as the telomere amplification reaction, however Telg and Telc primers were substituted for AluF and AluR primers (at the same concentration as Telg and Telc).

2.2.8.2 Setting up the qRT-PCR reaction

Each reaction was set up as described in section 2.2.6.1. One reaction (in triplicate) was set up containing primers designed to amplify the telomere and following completion of this run, a second reaction was set up containing primers designed to amplify the alu multicopy reference gene.

2.2.8.3 qRT-PCR cycling conditions

After the reaction was set up, the telomere sequence was amplified in a Rotor Gene-Q real-time PCR machine (Qiagen) under the cycling conditions outlined in figure 2.4. An initial hold temperature at 95°C promoted activation of the DNA polymerase, followed by two cycles at 94°C and 49°C for 15 seconds each. This allowed annealing and extension of Telg. In the subsequent 40 cycles, Telc is able to prime synthesis of the product formed in the previous step via annealing at 62°C followed by extension at 74°C. Data is collected at 74°C. A melt curve was performed at the end of the cycle.

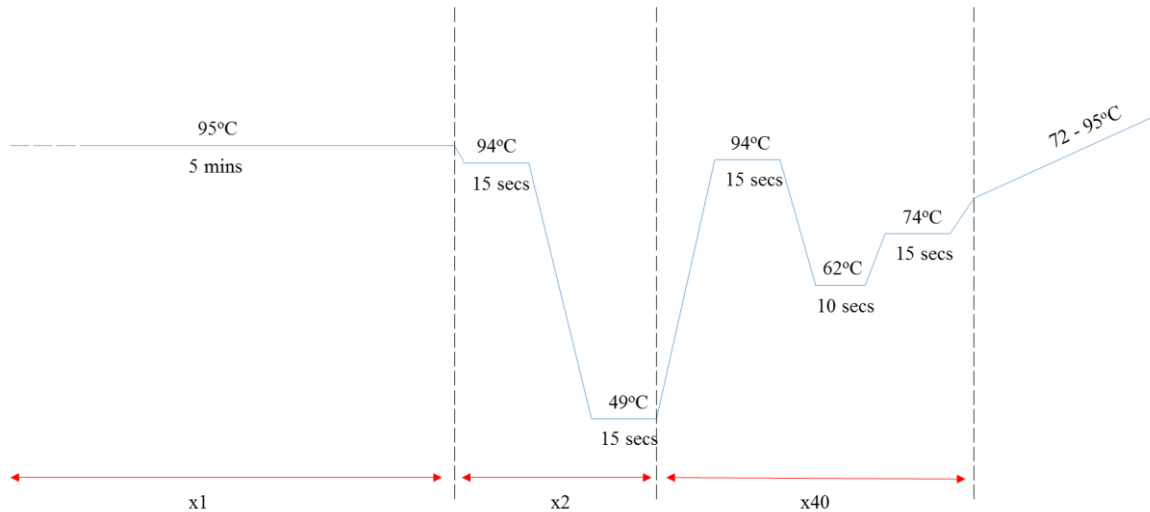


Figure 2.4: PCR cycling conditions for telomere amplification in WGA samples from cell line DNA or biopsied single cells.

In order to optimise cycling conditions for the amplification of the multicopy reference sequence, the cycling temperatures and durations outlined in table 2.10 on the next page were trialled.

Step	Temperatures tested °C	Hold duration time tested
Polymerase activation (as per manufacturer recommendation dependent upon mastermix used)	95	5 mins
		10 mins
Melting	95	15 secs
Annealing	60	60 secs
		30 secs
		15 secs
	64	30 secs
		15 secs
		10 secs
Extension and signal acquisition	70	10 sec
	75	
	77	

Table 2.10: Different cycling conditions attempted for the amplification of the multicopy reference gene for relative telomere length analysis in WGA DNA derived from single cells.

The optimum cycling conditions for multicopy reference gene amplification was achieved under the conditions outlined in figure 2.5 on the next page. Again, incubation at 95°C allowed for activation of the DNA polymerase. Subsequent cycling at 95°C,

60°C and 77°C allowed for denaturation of double stranded DNA, annealing of primers and polymerase extension respectively. A melt curve was performed at the end of the cycle in order to assess whether the products formed during the reaction matched the profiles of the expected product (presence of one peak at the expected melting temperature), thus indicating specific amplification of the desired sequence.

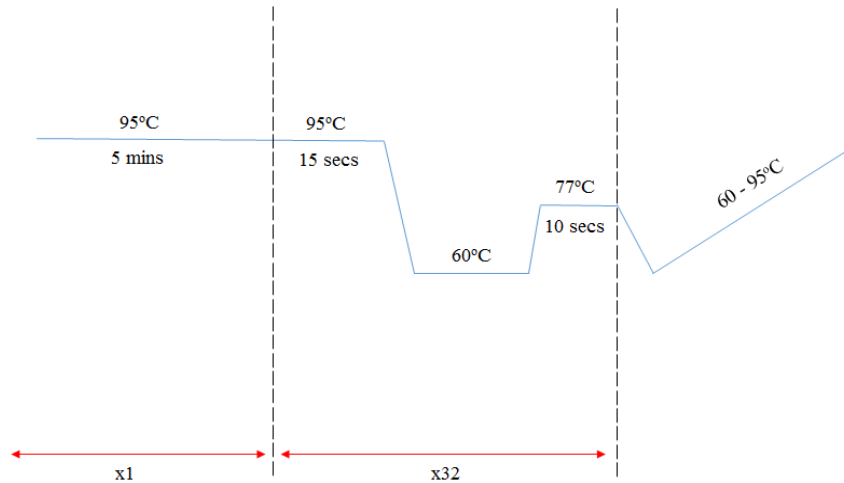


Figure 2.5: Cycling conditions for amplification of the multicopy reference gene from WGA cell line DNA and biopsied single cells.

Following completion of each cycle the reaction efficiency was assessed using the Rotor-Gene Q Series Software. The software performs this by plotting the log DNA concentration against the cycle threshold (Ct) for each of the serial dilutions included in the run. The slope of the line through the points indicates the reaction efficiency. Reaction products were also run on a 3% agarose gel following completion of the best performing run, in order to confirm reaction specificity. This was carried out as described in section 2.2.7.

2.2.9 Validation of telomere length analysis in single cells

Prior to analysis of telomere lengths in polar bodies and embryo biopsies (specific aim 4), it was necessary to ascertain whether whole genome amplification faithfully represented telomere DNA (specific aim 2c). To confirm true representation of telomere length following WGA, DNA samples from aneuploid cell lines (MCF-7 and A431) (AMS Biotechnology), euploid cell lines (male and female) and known trisomy 21 donor samples (Culture Collections) were amplified using the SurePlex

amplification system (Illumina). The correlation between pre WGA telomere copy number, and post WGA telomere copy number was then assessed.

2.2.9.1 Whole genome amplification of control DNA

Control DNA samples were first diluted to 15pg/ μ l in DNA free H₂O. 1 μ l of this was placed in a DNA free 0.2ml tube, and 4 μ l of cell extraction buffer was added. An extraction cocktail was then prepared by addition of 24 μ l extraction enzyme dilution buffer to 1 μ l cell extraction enzyme. Subsequently this extraction cocktail was mixed and 5 μ l added to each tube. Tubes were placed in a thermal cycler for incubation at 75°C for 10 minutes followed by 95°C for four minutes.

During this incubation time, a preamp cocktail was prepared and mixed, containing 24 μ l SurePlex preamp buffer and 1 μ l SurePlex preamp enzyme. After completion of the incubation steps, 5 μ l of preamp cocktail was added to each tube, and they were returned to the thermal cycler for cycling under the following conditions outlined in table 2.11:

Number cycles	Temperature (°C)	Time (seconds)
1	95	120
12	95	15
	15	50
	25	40
	35	30
	65	40
	75	40
1	4	Hold

Table 2.11: SurePlex preamp cycling conditions used for whole genome amplification of cell line DNA.

Once the preamp cycling was completed, samples were centrifuged briefly and placed on ice while the amplification cocktail components were prepared. This consisted of 25 μ l SurePlex amplification buffer, 0.8 μ l of SurePlex amplification enzyme and 34.2 μ l of nuclease free water. The amplification cocktail was mixed prior to adding 60 μ l to each tube. The entire solution was then mixed by pipetting before returning to the thermal cycler using cycling conditions outlined in table 2.12.

Number cycles	Temperature (°C)	Time (seconds)
1	95	120
14	95	15
	65	60
	75	60

Table 2.12: SurePlex amplification cycling conditions for whole genome amplification of cell line DNA.

Lastly, products were purified using the QIAquick PCR purification kit (Qiagen) as described in section 2.2.9.2, and DNA quantity and quality was then assessed using a Nanodrop spectrophotometer.

2.2.9.2 WGA product purification

After WGA, amplified products from validation cell lines were purified using the QIAquick PCR Purification kit (Qiagen). This was undertaken prior to telomere length analysis, to ensure that primers and reagents carried over into the WGA products did not interfere with downstream processes.

Initially, a volume of buffer PB equal to five times the volume of amplified product was added to each product. This resulted in a colour change in the SurePlex amplification products, indicating a sub-satisfactory pH, therefore 10µl 3M sodium acetate (Sigma) was added to each of these samples to ensure efficient binding of DNA to the purification columns, and maximum product retrieval following purification. One QIAquick spin column for each sample was assembled into a separate collection tube and each sample was added to a separate column. The columns were centrifuged at 13,000rpm for 60 seconds and the flow through was discarded. This allowed WGA products to bind to the column, whilst allowing carry-over reagents and primers to wash through the filter in the column as flow through. Columns were then re-assembled back into their collection tubes and 750µl of buffer PE was added to each one. They were then spun again at 13,000rpm for 60 seconds, to wash any residual WGA reagents from the DNA bound to the column filter. The flow through was again discarded and the collection tube was replaced back together with the column. A third centrifugation step at 13,000rpm for 60 seconds ensued, in order to remove all traces of buffer PE, which would affect the purity of the final product and in turn affect downstream telomere length analysis by qRT-PCR. After this, each column was assembled into a clean DNA

free Eppendorf tube and 30µl buffer EB was applied. The columns were left to stand at room temperature for 60 seconds to elute the bound DNA from the filter in the column, before finally centrifuging at 13,000rpm for 60 seconds. Eluted DNA was quantified using a Nanodrop spectrophotometer, and the purity was assessed by evaluating the A260/280 and A260/230 values. Those that fell within acceptable ranges (between 1.8 and 2, and between 2 and 2.2 respectively) were stored at -20°C until use in the qRT-PCR assay for telomere length analysis in single cells.

2.2.9.3 Determination of relative telomere length

qRT-PCR analysis of relative telomere length was carried out as described in section 2.2.8. Each DNA sample was assessed in triplicate. The amount of telomere sequence present was assessed by averaging the triplicate cycle threshold values for both the telomere and the reference gene reactions, before using the standard comparative method ($2^{-\Delta\Delta C_t}$) to determine the fold change in telomere copy number (representative of relative telomere length) between the reference sample and the unknown sample (Schmittgen and Livak, 2008). This was calculated using the formula in equation 2.1:

$$\text{Fold change} = 2^{-((\text{unknown tel } C_t - \text{unknown alu } C_t) - (\text{ref tel } C_t - \text{ref alu } C_t))}$$

Equation 2.1: Comparative method for fold change calculation between a reference and an unknown sample. 'tel' refers to the telomere sequence amplification reaction, 'alu' refers to the multicopy sequence reaction, 'ref' refers to the reference DNA amplification and 'Ct' is the cycle threshold.

2.2.10 qRT-PCR analysis of relative telomere length in single cells

To test the hypotheses that, overall, relative telomere length is altered in polar bodies and embryos in women of advanced maternal age (specific aims 3a and 3b), qRT-PCR analysis was performed using purified WGA DNA from first polar body and blastomere biopsies as described in section 2.2.8. Each sample was diluted to a concentration of 5ng/µl in buffer EB immediately prior to use, and 5µl was added to the reaction mix in the tube. All samples were assayed in triplicate, and all reaction runs included a two-fold serial dilution of reference DNA in order to monitor reaction efficiency. Relative telomere length was calculated using the cycle threshold values of the polar body or embryo sample and the cycle threshold values of the reference DNA

as 'ref' in equation 2.1. A student's t-test was performed to assess statistical significance of any differences observed.

2.2.11 DNA extraction from whole blood

For the analysis of average telomere length in newborns (specific aim 4a), DNA was extracted from whole blood sampled via standard phlebotomy techniques using Lithium Heparin Vacutainers™ (Becton Dickinson). Samples dedicated for DNA extraction were stored at -80°C for up to 1 week prior to DNA extraction. DNA was extracted from between 500µl and 1ml of whole blood using a DNA isolation kit from mammalian blood (Roche) following the manufacturer's protocol.

2.2.11.1 Red and white blood cell lysis

Red blood cell lysis was achieved by thawing the blood and allowing it to warm to room temperature, before pipetting 500µl of blood into a labelled DNA free 2ml tube (or two 2ml tubes when the volume was more than 500µl). 1.5ml of red cell lysis buffer was added to each sample and tubes were agitated gently at room temperature for 10 minutes. Next, the tubes were spun at 2000rpm for 10 minutes, and the supernatant was removed and discarded appropriately in Virkon® (VWR). In order to lyse white blood cells, the clear pellet remaining in the tube following centrifugation (representing white blood cells) was vortexed to dissolve the cells in the residual liquid, and 1ml of white cell lysis buffer was added to each tube. The tubes were incubated at 65°C for 10 minutes to allow complete lysis.

2.2.11.2 RNA degradation and protein precipitation

After white cell lysis, samples were allowed to cool to room temperature before addition of 5µl of 4mg/ml RNase (Promega) to each tube. Subsequently, tubes were incubated at 37°C for one hour so that any RNA in the sample was degraded. This was so that RNA could not interfere with subsequent telomere length analysis protocols. Next, 520µl of protein precipitation buffer was added to each tube, and the samples were vortexed for 25 seconds before centrifugation at 10,000rpm for 10 minutes. This

meant that precipitated protein was pelleted at the bottom of the tube, allowing recovery of DNA from the supernatant by subsequent DNA precipitation and purification.

2.2.11.3 DNA precipitation

600µl aliquots of the supernatant from section 2.2.11.2 were pipetted into fresh 2ml tubes. 1.2mls of 100% ethanol was then added to each aliquot, and tubes were inverted several times until the DNA had precipitated. Samples were centrifuged at 10,000rpm for 10 minutes to pellet the DNA, before washing the pellets in 1.5mls of ice cold 70% ethanol. Each tube was then centrifuged again at 10,000rpm for five minutes before air drying the pellet, and re-suspending it in 200µl Tris Diaminoethane-tetraacetic acid (EDTA) (TE). In order to dissolve the DNA, tubes were incubated at 65°C for 30 minutes. Samples were stored at 4°C until use.

2.2.12 Average relative telomere length analysis in newborns

To test the hypothesis that telomere length is reduced in preterm infants compared to term born controls (specific aim 4a and 4b), average relative telomere length analyses were performed using the MMqRT-PCR protocol optimised in section 2.2.6, with DNA extracted from whole blood as described in section 2.2.11. Prior to use in MMqRT-PCR, the DNA concentration and purity of each sample was assessed using a Nanodrop spectrophotometer. Samples were then diluted to a concentration of 5ng/µl in DNA free water, and 5µl was added to a reaction tube. Each patient DNA sample was assayed in triplicate. In addition, a two-fold serial dilution of reference DNA was also assayed in triplicate with each MMqRT-PCR run in order to monitor reaction efficiency. Relative telomere length (T/S ratios) of unknown patient samples were determined from the cycle thresholds of the telomere and single copy gene reactions using equation 2.1. However the 'unknown alu' and 'ref alu' were replaced with unknown single copy reference sequence cycle threshold and reference DNA single copy reference sequence cycle threshold respectively (Cawthon, 2009). Results were compared for statistical significance using a student's t-test.

2.2.13 Lymphocyte metaphase preparation

For the measurement of individual telomere lengths of p and q arms of each chromosome in newborns (specific aim 4c), metaphase preparations were made from whole blood drawn from infants recruited at WHH or QEPMH. Prior to setting up blood culture, a class 3 laminar flow cabinet was UV irradiated for 30 minutes, thoroughly wiped down with a Virkon® (VWR) soaked cloth, and then sprayed with 70% industrial methylated spirit (IMS) in order to sterilise the working area. All tip boxes, flasks, pipettes and other equipment were also sprayed with 70% IMS prior to entering the laminar flow cabinet.

500µl of blood was added to 9.5mls of pre-warmed PB Max™ Karyotyping media (Invitrogen™, Fischer Scientific) in a T25 tissue culture flask. This was then transferred to a 37°C incubator with 5.5% CO₂ for 72 hours in order to allow proliferation of lymphocytes and to ensure that cells were actively dividing (which is essential for metaphase preparation). Following incubation, metaphase preparations were produced by first re-suspending the cell layer formed at the bottom of the flask by gentle agitation, and subsequently addition of 100µl of 10µg/ml Demecolcine (Sigma Aldrich). The flask was then returned to the incubator for 40 minutes in order to arrest dividing cells in metaphase, before transferring the entire culture into a sterile 15ml falcon tube, and centrifuging at 1900rpm for five minutes.

After centrifugation, the supernatant was removed and disposed of appropriately, taking care not to disturb the pellet. The pellet was then re-suspended in a small residual volume of culture media, and a timer set at 12 minutes was started at the time of adding 6mls of pre-warmed hypotonic solution (0.075M KCl). Hypotonic solution was added in a drop wise fashion whilst agitating the tube, and then the tube was then returned to the incubator for the remainder of the 12 minutes in order to lyse cells, and promote proper spreading of chromosomes (which is essential for analysis of individual chromosomes).

Next, the tube was filled to the 14ml graduation line with ice cold 3:1 methanol:acetic acid, by gentle pipetting down the side of the tube in order to fix the chromosomes gently. The tube was inverted several times to mix the layers that had formed, and then centrifugation at 1900rpm for five minutes ensued. Subsequently the supernatant was removed, taking care not to disturb the pellet. The pellet was again re-suspended in a

small residual volume, before further addition of 6mls ice cold fixative in a drop wise fashion with gentle agitation. After this, the sample was centrifuged again at 1900rpm for five minutes and the process was repeated three to five times depending on the quality of the sample (assessed by the size and colour of the pellet). Samples were stored at -20°C in 6mls of fixative until use.

2.2.14 L5178Y-R and LY5178Y-S cell culture

Mouse lymphoma cell lines L5178Y-R and L5178Y-S with known telomere lengths were kindly donated by Predrag Slijepcevic (Brunel University UK) for use in the calibration of quantitative fluorescence *in situ* hybridisation (QFISH) telomere length analysis experiments (specific aim 4c). For both cell lines, 30-70,000 cells cryopreserved in liquid nitrogen (in 1ml cryopreservation media made from 90% fetal calf serum, 10% dimethylsulfoxide (DMSO) (Sigma)) were thawed at 37°C and seeded in 8ml pre-warmed Roswell Park Memorial Institute medium (RPMI) media (Sigma), supplemented with 1ml of newborn calf serum (Sigma) and 100µl of 10,000U/ml penicillin, 10mg/ml streptomycin (Gibco). Cells were incubated at 37°C with 5.5% CO₂ and passaged every 48-72 hours by removing 1ml of culture and placing it into 9ml of pre-warmed fresh media. Metaphase preparations were produced as described in section 2.2.13. All procedures were carried out following aseptic technique practices in a pre-sterilised class 3 laminar flow cabinet as described in section 2.2.13.

2.2.15 Quantitative Fluorescence *in situ* Hybridisation

To test the hypothesis that telomere lengths of individual chromosome ends are reduced in preterm infants compared to term born controls (specific aim 4c), patient lymphocyte metaphase preparations and calibration mouse lymphoma cell line metaphase preparations (L5178Y-R and L5178Y-S) were assessed by quantitative fluorescence *in situ* hybridisation (QFISH).

2.2.15.1 Slide preparation

Preparations stored in fixative at -20°C were centrifuged at 1900rpm for five minutes, and the appropriate volume of supernatant was removed in order to obtain a suitable concentration of cells (depending on the size of the pellet). A poly-lysine glass slide

was cleaned by immersing in methanol, dried, and marked with the diamond marker on the underside. The slide was labelled, and briefly passed through steam before dropping 8µl of sample onto the marked area. When the sample appeared grainy, a further 8µl of fresh fixative was dropped onto the marked area, and each slide was then immersed in 70% acetic acid (made up in methanol) for 10 seconds in order to fully spread the chromosomes and degrade cytoplasm. Following this, slides were immersed in an ethanol series (70%, 80% then 100%) for two minutes each, air dried and inspected under phase contrast to check the mitotic index, and the quality of the prep.

2.2.15.2 Ageing of slides and pre-hybridisation washes

Metaphase preparation slides were aged at 37°C overnight before proceeding with the manufacturer's instructions included in Telomere PNA FISH Kit (Dako). Briefly, slides were incubated in tris buffered saline (TBS) for two minutes in order to re-hydrate the samples, and then fixed in 3.7% formaldehyde (made in TBS) for two minutes, in order to preserve structure and ensure that samples were not lost from the slide during subsequent steps. Following fixation, slides were incubated twice in TBS for five minutes each, before incubation in pre-warmed pepsin solution (described in section 2.2.2.2) at 37°C for 10 minutes. This was carried out in order to remove cytoplasmic proteins, which may result in high background staining, and to allow efficient access of the probe to DNA sequences. The next step involved a further two washes in TBS for five minutes each, and subsequently incubation in an ice cold ethanol series for two minutes each in order to dehydrate the metaphase preparations.

2.2.15.3 Denaturation and hybridisation

After slides had air-dried, 5µl of FITC labelled PNA probe was pipetted onto the marked area and a cover slip was applied and sealed using Fixogum rubber cement. Chromosomes were then denatured on the heat block at 80°C for five minutes before allowing hybridisation of the probe at room temperature for between two and four hours. All procedures hereafter were carried out in the dark to avoid photobleaching of the probe.

2.2.15.4 Post-hybridisation washes and detection

After hybridisation, rubber cement was carefully removed with tweezers, and the cover slip allowed to float off in rinse solution. Excess un-hybridised probe was washed off in pre-warmed wash solution at 65°C for 10 minutes. Finally, slides were incubated in an ice cold ethanol series for two minutes each, air-dried, and mounted in 10µl of vectashield® with DAPI. A 22 x 50mm coverslip was pressed onto the slide, and sealed with nail varnish. Telomere signals were then visualised and captured as 16-bit images using a BX61 Olympus microscope equipped with a CCD camera and appropriate filters for DAPI and FITC detection under a 60x objective. At least 10 metaphases were captured per patient, and at least five metaphases were captured from each of the L5178Y-R and L5178Y-S control cell lines included with the experiment.

2.2.15.5 QFISH control slide preparation

Alongside each experiment, a control slide containing 3µl freshly dropped 0.2µM TetraSpeck™ microspheres (Life Technologies) diluted 1:5 in ddH₂O was prepared in order to calibrate against slight variation in capture system performance between experiments. These were prepared by simply pipetting the beads onto the slide, spreading the drop using the pipette tip, and allowing the slide to dry in the dark at room temperature for 2-3 hours. The beads were then mounted by pipetting 10µl of glycerol onto the slide and pressing a 22 x 50mm cover slip on top. The cover slip was then sealed using nail varnish and images were captured as described above.

2.2.15.6 QFISH image analysis

QFISH Images were analysed based on a previously published method (Wong and Slijepcevic, 2004). Briefly, QFISH was performed on six separate occasions using metaphases from mouse cell lines L5178Y-R and L5178Y-S previously shown to have telomere lengths of approximately 48kbp and 7kbp respectively (McIlrath et al., 2001). Following image capture of at least 10 metaphases, images were converted to 8-bit using ImageJ, and telomere fluorescence intensity values were measured using TFL-Telo software (freely available from <http://www.flintbox.com/public/project/502>). The average fluorescence values for each of the cell lines were then divided by their respective expected telomere length to provide two conversion factors. These conversion factors were averaged to produce a final conversion factor.

Images of the fluorescent beads were also converted to 8-bit using ImageJ and analysed using TFL-Telo, for each of the experiments performed with the mouse cell lines, and with patient samples. The average fluorescence values of the fluorescent beads captured in the experiments with the mouse cell lines, was then divided by the average fluorescent value of the fluorescent beads in the experiment with the patient samples, to give a correction value for day to day variations in the microscopy set up.

The conversion factor and the correction factor described above were then used to calibrate fluorescence values from unknown patient samples in order to calculate absolute telomere length. At least five metaphase images from unknown patient samples were converted to 8-bit using ImageJ, karyotyped with the aid of SmartType2 (Digital Scientific), and then imported to TFL-Telo for fluorescence intensity analysis. Raw fluorescence values for telomeres on the p and q arms of autosomes were exported into Microsoft Excel, multiplied by the calculated correction value, and then this corrected value was converted to absolute telomere length by dividing the value by the conversion factor. Following un-blinding of the study, telomere lengths of p and q arms from each autosomal chromosome in each patient were then grouped according to whether the patient belonged to the preterm cohort sampled at birth or at term equivalent age, or the term cohort. Measurements from these groups were then assessed using a multivariate analysis of variance (ANOVA) statistical test, in order to ascertain whether telomere lengths of specific arms from specific chromosomes were reduced in preterm infants compared to term born controls (specific aim 4c). Sex chromosome measurements were omitted from this analysis, since not all patients possessed a true homologous pair (some were males) therefore an average value for p and q arms was not possible.

3 Specific aim 1: To test the hypothesis that telomere distribution is altered in the sperm heads of males with severely compromised semen parameters

3.1 Background

Infertility, defined as the inability to conceive after one year of regular unprotected intercourse, affects around one in six couples wishing to start a family. Of these, at least 20% are solely attributable to male factors, and in many other cases, a male origin contributes to infertility alongside female factors (Seli and Sakkas, 2005). The causes of male factor infertility are complex, made up of physiological, hormonal, and genetic contributions. Genetic causes of infertility break down into monogenic, chromosomal and multifactorial categories (Shah et al., 2003), with chromosomal causes further subdivided into balanced translocations, inversions, Y chromosome deletions, sex chromosome trisomy and elevated levels of sperm disomy (Griffin and Finch, 2005). As pointed out in section 1.8.1, Ioannou and Griffin (Ioannou and Griffin, 2010) have also argued that another chromosomally related factor, that of nuclear organisation, should be altered in the sperm heads of a certain subset of infertile men. To date however there has been little direct evidence to support this hypothesis.

Male gametes represent a unique cell type in that they do not replicate, they are predominantly transcriptionally silent, and they are the smallest cell type in the body. The latter dictates that DNA must be packaged extremely tightly within the nucleus in order to deliver the paternal genome to the fertilised oocyte. This is mainly facilitated via replacement of the majority (90%) of histones with sperm specific protamines during spermatogenesis. This, tight packaging of the genome involves a highly ordered level of nuclear organisation within the sperm head, which has been extensively studied, and has been shown to adopt a chromocentric model. That is, centromeres cluster deep in the interior of the nucleus to form a chromocenter, and telomeres reside in dimers or tetramers at the nuclear periphery (Zalensky and Zalenskaya, 2007). Interestingly telomeres, at least in part, retain association with histones, which is thought to play a functional role in telomere attachment to the nuclear membrane (Gineitis et al., 2000; Zalenskaya et al., 2000). A sperm specific histone 2B variant

known as histone 2 family W testis-specific (H2BFWT) has been shown to be essential in facilitating this interaction (Churikov et al., 2004). Indeed, point mutations in H2BFWT have previously been associated with idiopathic male infertility (Lee et al., 2009; Ying et al., 2012).

This strict level of nuclear organisation is thought to be essential for fertilisation and embryogenesis, therefore it is reasonable to hypothesise that telomere organisation might play a key role in male fertility. Indeed, telomeres are thought to be the first part of the genome to respond to oocyte signals for male pronucleus development following fertilisation (Zalenskaya et al., 2000).

Current literature indicates uncertainty in the role of nuclear organisation in male factor infertility (as discussed in section 1.8.1.1). While one study has found altered sex chromosome positioning in the sperm of severely oligozoospermic males (Finch et al., 2008), another more recent study investigating the position of 18 chromosomes (including sex chromosomes) found that nuclear organisation in sperm is more robust, and is not altered in infertile males (Ioannou and Griffin, 2010). If the positions of the centromeres are largely unaltered in oligozoospermic males, and we accept the rationale that nuclear organisation *should* be altered in association with infertility then an obvious next place to look is the telomeres. Specifically it raises the hypothesis that the reported peripheral location of the telomeres is altered in infertile males and that the telomeric TTAGGG motif is associated with histone 2B variant H2BFWT differentially in fertile vs infertile males. To date however, information detailing telomere distribution and its role in nuclear organisation in relation to male fertility to the best of my knowledge has not been reported in the literature. This chapter therefore aims to test the hypothesis that telomere distribution is altered in males with severely compromised semen parameters compared to normal fertile controls.

3.2 Specific aims

With the above in mind the specific aims of this chapter were as follows:

1a. To test the hypothesis that telomeres are non-randomly distributed (predominantly at the nuclear periphery) in the sperm heads of normally fertile males:

- Using extrapolations of two dimensional data
- Using direct evidence from three dimensional preparations

1b. To test the hypothesis that an apparently altered telomere distribution can be artificially induced by inappropriate swelling of the sperm head

1c. To test the hypothesis that H2BFWT also clusters at the nuclear periphery (and, by implication, is anchored to the nuclear membrane) in the sperm heads of normally fertile males

1d. To test the hypothesis that H2BFWT and the TTAGGG motif co-localise thereby suggesting a functional interaction

1e. To test the hypothesis that nuclear organisation is altered in infertile males compared to their normal counterparts by assessment of telomere distribution, as assayed in aim 1a. That is, chromatin packaging and organisation of the sperm head is altered in males with compromised semen parameters and thus that altered nuclear organisation may be considered a marker of male infertility

1f. To test the hypothesis that any alteration in nuclear organisation between fertile and infertile males may be related to the degree of chromatin packaging

3.3 Results

3.3.1 Specific aim 1a: To test the hypothesis that telomeres are non-randomly distributed (predominantly at the nuclear periphery) in the sperm heads of normally fertile males

3.3.1.1 Extrapolations of 2D data

A biotin labelled pan-telomere sequence specific probe (TTAGGG_n) was used in 2D FISH experiments to detect the presence of the telomere specific sequence in sperm heads (see materials and methods section 2.2.2). Three dimensional extrapolations of 2D data were used (materials and methods section 2.2.2.6) to test the above hypothesis. Semen parameters (concentration, motility and morphology) were assessed and confirmed as within normal range by trained andrologists at The London Bridge Fertility Gynaecology and Genetics Centre.

Visual inspection of FISH images indicated that, while telomere spots may appear anywhere in the sperm nucleus, the majority of signals are seen towards a peripheral region. A gallery of example images for telomere distribution in normal males can be seen in figure 3.1.

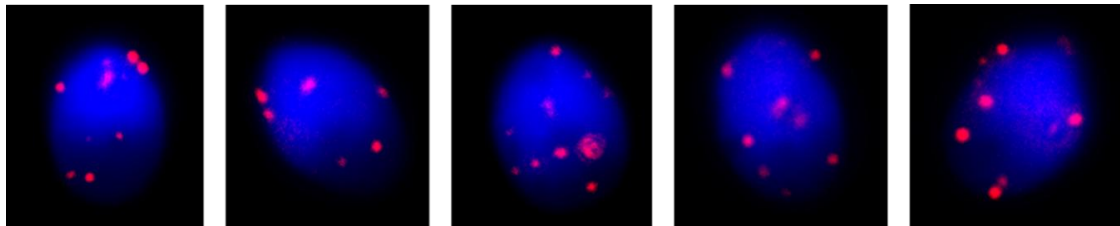


Figure 3.1: Distribution of telomeres in sperm nuclei of normal males. Example images acquired following FISH experiments using a pan telomere probe (red) and DAPI staining of the sperm nucleus (blue). Although spots appear anywhere in the nucleus, the majority of telomere spots are localised at the nuclear periphery.

Empirical evidence in support of this observation was provided when average telomere distribution was assessed following 2D analysis using the DAPI density and volumetric models (outlined in section 2.2.2.6). Figure 3.2 clearly indicates that telomeric sequences preferentially localise non-randomly and towards the nuclear periphery of

the sperm heads. Both models confirmed a highly statistically significant non-random distribution of telomeres ($p = <0.00001$), and this result was observed for all normozoospermic males, both individually (see supplementary data in section 9, figure 1), and when data was pooled (figure 3.2).

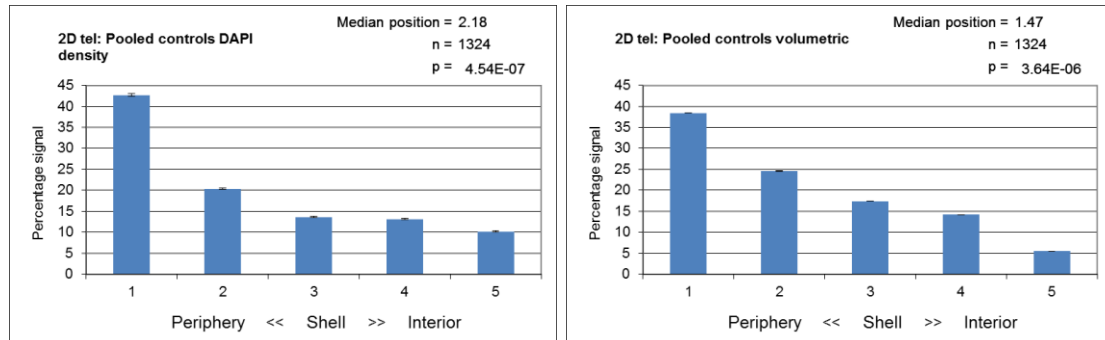


Figure 3.2: 2D telomere distribution in normal males as determined by FISH and following mathematical compensation of 2D representation of 3D objects using DAPI density (left) and volumetric (right) models. Both models confirm a preferentially peripheral distribution of telomeres, as determined p values < 0.05 following χ^2 analysis.

While both means of providing a 3D extrapolation of 2D data gave the same basic pattern, the medians (which indicate the overall tendency of signal localisation) were slightly different (2.18 and 1.47) respectively.

The average number of telomere signals observed in sperm of fertile males was 8, however, upon visual inspection of nuclei, it was clear that there was a subset of sperm nuclei where a significantly larger number of telomere signals were present. In each of these an apparently random pattern of staining was evident. A gallery of example images displaying this pattern of telomere distribution can be seen in figure 3.3 below:

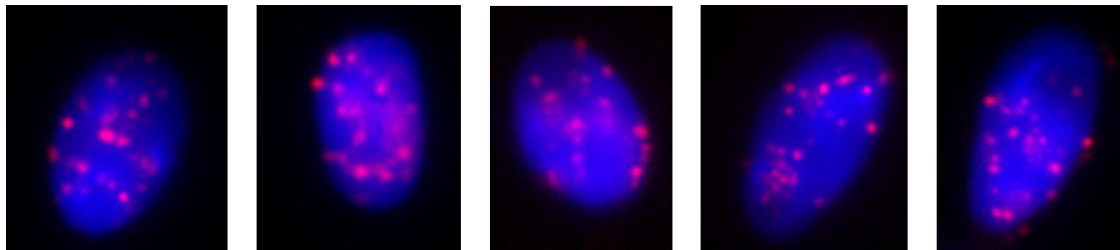


Figure 3.3: Gallery of example images depicting 'random' pattern of telomere localisation (red) in a subpopulation of sperm nuclei (blue). The number of telomere spots is much greater than other sperm nuclei, and no preference for peripheral localisation is evident.

In order to assess the proportion of cells in this subpopulation from each control male, the percentage of nuclei with 16 or more (twice the mean) telomere signals was calculated. Results among control males ranged from 0 to 20%, however all but three were below the mean of 5% (table 3.1).

Sample ID	% nuclei \geq 16 telomere signals
C1	0
C2	11
C3	2
C4	3
C5	2
C6	10
C7	2
C8	8
C9	1
C10	1
C11	1
C12	20
C13	2
Average	4.8 \pm 1.6

Table 3.1: Percentage of nuclei representing a sub-population of sperm cells with 16 or more telomere signals dispersed throughout the nucleus.

3.3.1.2 Direct evidence from 3D preparations

3D image capture and analysis of FISH was carried out in 30-50 cells for 6 control donors as described in sections 2.2.2 and 2.2.2.7. Telomere distribution was assessed in individual patients, and as a pooled group. In general terms both imaging and analysis of 3D data was several orders of magnitude more challenging than equivalent 2D work. Figure 3.4 shows a 3D preparation of telomere signals in a human sperm head. A movie can be found in the electronic appendix (movie 1).

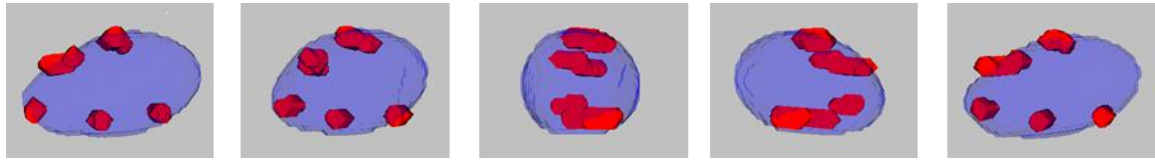


Figure 3.4: Still images from 180° rotation of 3D sperm cell image showing the 3D distribution of telomeres (red) within the sperm nucleus (blue) as determined by analysis using Nemo.

3D images of sperm nuclei were captured and analysed and largely confirmed the 2D data i.e. a tendency towards a peripheral localisation of telomeres. Visual inspection suggested that telomeres were located at the nuclear periphery (figure 3.4) and this was confirmed by empirical evidence confirming that the signals were non-randomly distributed ($p = <0.01$), and predominantly located on the nuclear periphery (median position 1.25) (figure 3.5). This was ascertained by analyses of distances between the center of each telomere spot and the nuclear periphery carried out using Nemo (described in section 2.2.2.7) in sperm nuclei from different individuals, and when data was pooled as a group.

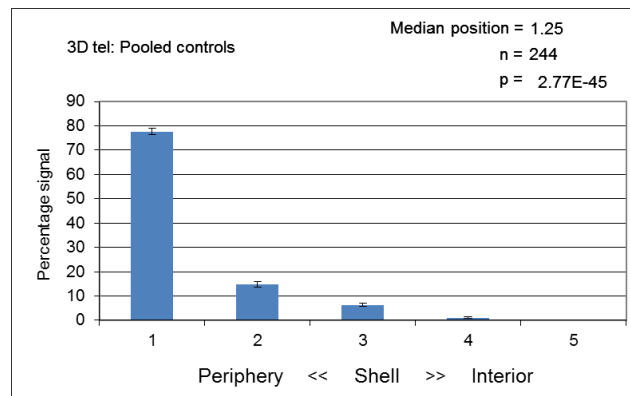


Figure 3.5: 3D distribution of telomeres in normal fertile males determined by FISH. p value represents statistical significance of a peripheral localisation of telomeres following χ^2 analysis.

Taken together therefore, both 2D and 3D data provides strong evidence that the telomeres are closely associated with the nuclear periphery (perhaps the nuclear membrane) in human sperm heads.

3.3.2 Specific aim 1b. To test the hypothesis that an apparently altered telomere distribution can be artificially induced by inappropriate swelling of the sperm head

As mentioned in section 3.1, nuclear organisation in the sperm head is dictated by the tight packaging of chromatin into highly organised domains. Evidence from specific aim 1a confirms that one feature of this ordered packaging is telomere distribution at the nuclear periphery. In order to investigate the effects of impaired chromatin packaging within the sperm nucleus on telomere distribution patterns, FISH experiments were performed on the sperm heads of one fertile patient selected at random with or without prior treatment with either one of two types of nuclear decondensation agents; 10mM DTT or 0.5M NaOH (materials and methods section 2.2.2.5). This allowed me to ask whether artificial disruption to the normal architecture of the sperm nucleus results in altered telomere distribution patterns.

3.3.2.1 Extrapolations of 2D data

Example images of telomere staining patterns in these sperm are shown in figure 3.6.

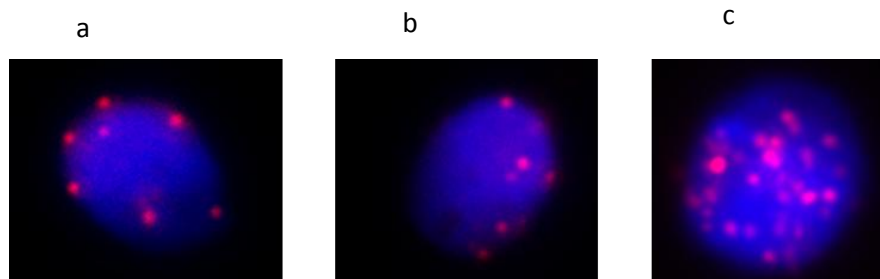


Figure 3.6: Example images of telomere distribution (red) in sperm nuclei (blue) of non-swollen sperm (a), 10mM DTT swollen sperm (b) and 0.5M NaOH swollen sperm (c). While telomere staining patterns appear to be similar in non-swollen and 10mM DTT swollen sperm, 0.5M NaOH swollen sperm show a more random distribution of signals, with a much higher overall number of telomere signals.

Following 2D analysis using DAPI density and volumetric compensation models, χ^2 analysis showed that while average telomere localisation in non-swollen (no treatment), and 10mM DTT swollen sperm heads were significantly different to random ($p = <0.01$), telomere localisation in 0.5M NaOH swollen sperm was not different to random ($p = >0.05$). Similar to observations in specific aim 1a, overall median localisation of telomeres in both non-swollen and 10mM DTT swollen sperm

was predominantly peripheral but with a higher median when the DAPI density model was used for analysis. Figure 3.7 shows the relative distributions of the two methods of analysis using the three means of preparation.

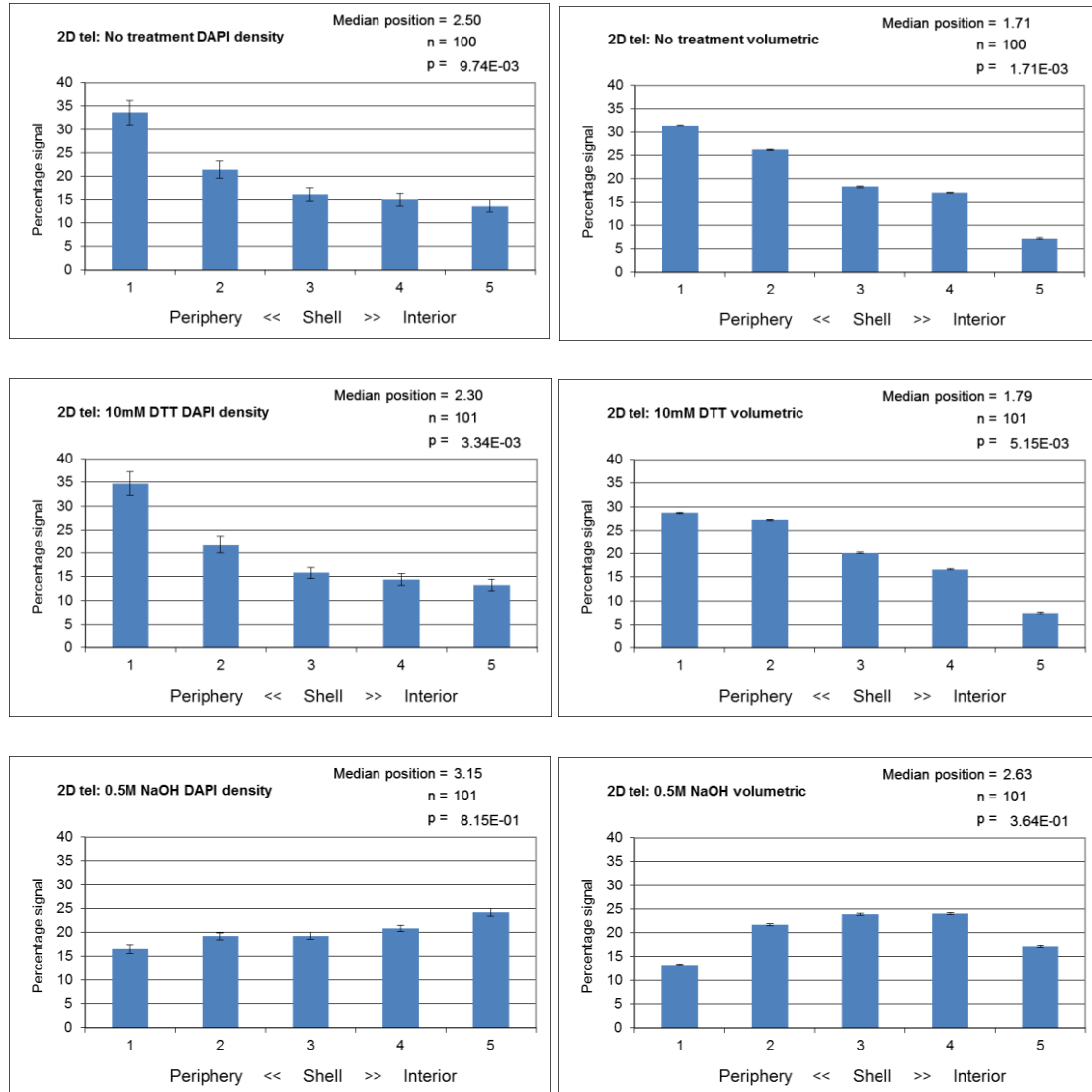


Figure 3.7: 2D telomere distribution patterns in non-swollen (no treatment), 10mM DTT swollen and 0.5M NaOH swollen sperm nuclei, as determined by FISH analysis and using DAPI density (left) and volumetric (right) models. Chi² p values are shown in each graph representation. Both models show a preferentially peripheral distribution of telomeres in non-swollen and 10mM DTT swollen sperm, however 0.5M NaOH swollen sperm show a random distribution of telomeres.

When compared to one another, telomere distribution in non-swollen sperm compared to 10mM DTT swollen sperm were not significantly different. This was true using both DAPI density and volumetric models (p values shown in table 3.4). However, when comparing telomere localisation in 0.5M NaOH swollen sperm to either of the two

other groups, telomere distribution was significantly different using analysis by both DAPI density and volumetric models (p values shown in table 3.2).

2D analysis model	No treatment vs. 10mM DTT	No treatment vs. 0.5M NaOH	10mM DTT vs. 0.5M NaOH
DAPI density	1	0.00006	0.00001
Volumetric	0.97	0.0000005	0.00002

Table 3.2: Statistical analyses of telomere distribution in sperm treated with either 10mM DTT or 0.5M NaOH compared to non-treated sperm as ascertained by FISH and using DAPI density or volumetric models. Values indicated represent p values derived from chi² analysis. While telomere distribution is not altered in 10mM DTT swollen sperm nuclei compared to non-treated sperm, telomere distribution in 0.5M NaOH swollen sperm nuclei is significantly difference to both other groups. These observations are true for both DAPI density and volumetric models of analysis.

When the average number of telomere signals was compared from each set, sperm that received no swelling treatment had a near identical number of signals as those treated with 10mM DTT. However, sperm treated with 0.5M NaOH possessed a much larger average number of telomere signals (figure 3.8). Interestingly, although the average number of telomere signals was not different between non-swollen and minimally swollen sperm, the percentage of sperm cells representing a subpopulation of cells with 16 or more telomere signals in 10mM DTT swollen sperm was twice that of non-swollen sperm. 0.5M NaOH swollen sperm had nearly all nuclei with 16 or more telomere signals (figure 3.8).

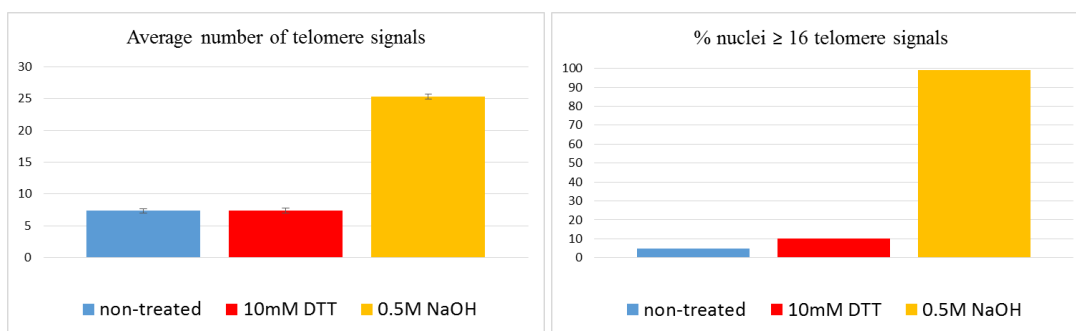


Figure 3.8: Comparison of average number of telomere signals (left) and percentage of nuclei with greater than 15 telomere signals (right) in non-swollen sperm (blue), 10mM DTT swollen sperm (red) and 0.5M NaOH swollen sperm (orange). Non-swollen and 10mM DTT swollen sperm possess an equal number of average telomere signals, however 10mM DTT swollen sperm possess twice the percentage of cells belonging to a sub-population of sperm nuclei with above 16 telomere signals. 0.5M NaOH swollen sperm possess a much greater average number of telomere signals than both other groups, and almost all cells possess 16 or more telomere signals.

3.3.2.2 Direct evidence from 3D preparations

Following 3D analysis in six of the control males, as with 2D analysis, a more pronounced peripheral localisation of telomeres was observed in all sperm (figure 3.9 on the next page). This was confirmed by an overall peripheral median position of telomeres in all sperm analysed. Although telomere distribution in 0.5M NaOH swollen sperm remained predominantly peripheral, this was not as pronounced as those of non-swollen or 10mM DTT swollen sperm. Following chi² analysis, the distribution of telomeres in non-swollen and 10mM DTT swollen sperm were not statistically significantly different from another ($p = 1$), however both were significantly different from that of 0.5M NaOH swollen sperm ($p = 0.0003$ and $p = 0.0005$ respectively).

In conclusion therefore, evidence from specific aim 1b shows that improper chromatin packaging as a result of artificial nuclear decondensation does indeed result in altered nuclear organisation, as determined by altered patterns of telomere staining. While the overall distribution of telomeres remains the same following treatment with 10mM DTT, the proportion of nuclei with an apparently random distribution of telomeres is doubled. Moreover, nuclear decondensation with 0.5M NaOH results in a significantly altered distribution of telomeres in almost all sperm nuclei.

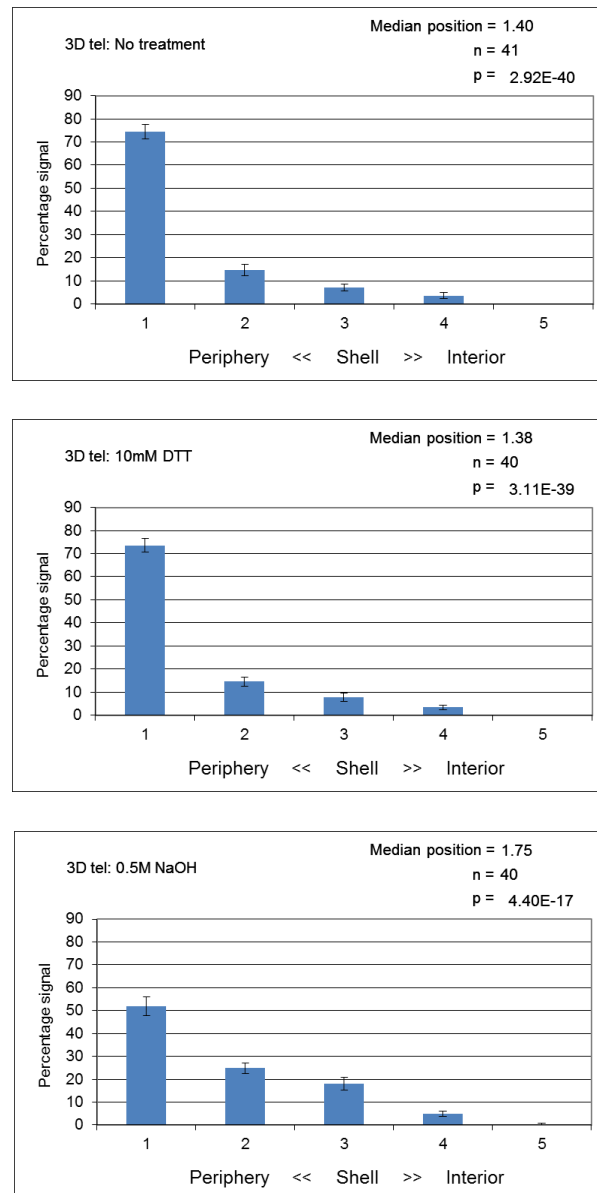


Figure 3.9: 3D telomere distribution in non-swollen, 10mM DTT swollen and 0.5M NaOH swollen sperm nuclei, as determined by FISH analysis. Statistical significance of a non-random distribution of telomeres is confirmed by χ^2 analysis (p values shown in each graphical representation of telomere distribution).

3.3.3 Specific aim 1c. To test the hypothesis that H2BFWT also clusters at the nuclear periphery (and, by implication, is anchored to the nuclear membrane) in the sperm heads of normally fertile males

In general, the expected number of telomere signals in the 3D sperm nucleus ought to be approximately 23 based on evidence of dimerization of telomeres in previous studies (Zalensky et al., 1993). However, it was noticed that the average number of telomere

signals present following 3D FISH in this study was 10. This may be reflective of the tight packaging of sperm DNA, which may not permit complete penetration of the telomere probe throughout the nucleus. However, it is additionally indicative of more complex clustering of telomeres within the sperm head. In order to investigate the potential role of H2BFWT in facilitating this clustering of telomeres at the nuclear periphery, this section addressed the *in vivo* localisation of H2BFWT.

H2BFWT localisation in sperm was assessed using immunofluorescence experiments with an antibody specific to the internal region of H2BFWT (Santa Cruz) (materials and methods section 2.2.3). At least 100 images were captured from sperm samples from six control males, and analysed using 2D and 3D methods described above. A gallery of example images can be seen in figure 3.10.

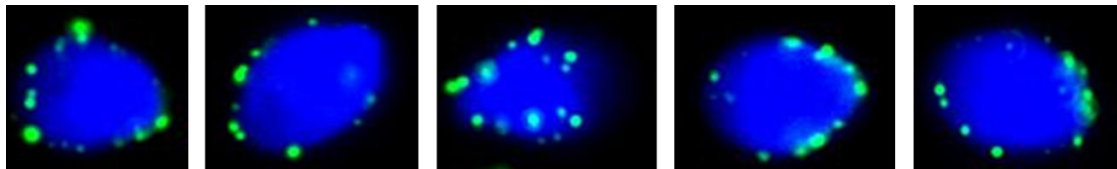


Figure 3.10: H2BFWT distribution in human sperm as determined by immunofluorescence experiments. H2BFWT (green) shows almost exclusively peripheral localisation at the nuclear membrane (nucleus stained blue).

Following 2D analysis, DAPI density and volumetric models produced different results (figure 3.11). While both showed a non-random distribution, the DAPI density model showed a clear preference for H2BFWT localisation at the nuclear periphery (~50% signals), with staining becoming increasingly reduced towards the nuclear interior. The volumetric model however showed staining predominantly present in mid to peripheral regions of the nucleus, with almost complete absence of staining at the nuclear interior. That being said, both models had similar median positions of H2BFWT at the nuclear periphery.

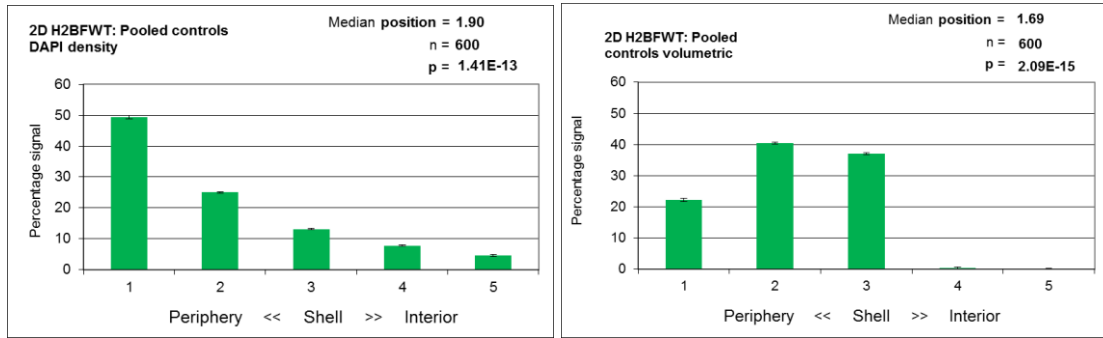


Figure 3.11: 2D H2BFWT localisation in sperm of normal males as determined by immunofluorescence experiments using DAPI density (left) and volumetric (right) compensation models and χ^2 analysis to determine statistical significance of non-random distribution (p values shown in graphical representation). While the general trend representing H2BFWT localisation is slightly different among the two models, the median position shows peripheral location in both models.

Following 3D analysis, H2BFWT localisation appeared almost exclusively peripheral (figure 3.12), which is in agreement with visual inspection of images (figure 3.13). A movie can be found in the electronic appendix (movie 2). Again, the overall median position of H2BFWT staining appeared to be peripheral.

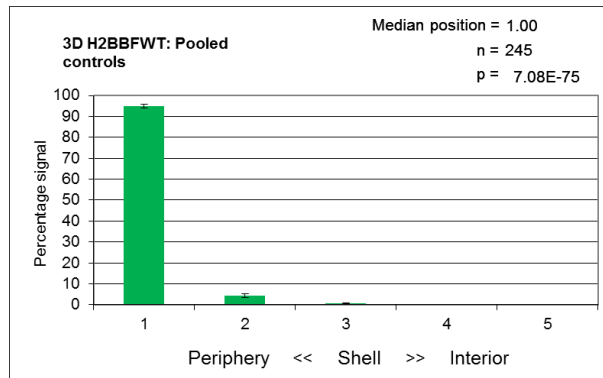


Figure 3.12: Graphical representation of 3D analysis of H2BFWT localisation as determined by immunofluorescence experiments and χ^2 analysis to determine statistical significance of non-random, peripheral distribution (p value shown in graph).

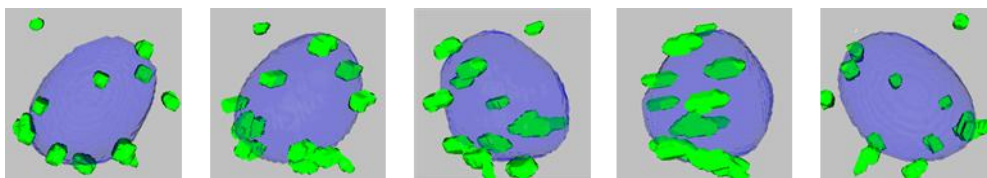


Figure 3.13: Still images from 180° rotation of 3D sperm cell image showing the 3D distribution of H2BFWT (green) within the sperm nucleus (blue) as determined by analysis using Nemo.

3.3.4 Specific aim 1d. To test the hypothesis that H2BFWT and the TTAGGG motif co-localise thereby suggesting a functional interaction

The previous observations show the presence of H2BFWT at the nuclear periphery and are in concordance with literature that suggest that H2BFWT is isolated in the nuclear membrane fraction isolated from human sperm cells. This, along with the affinity of H2BFWT for double stranded telomeric repeat sequences, supports the hypothesis that H2BFWT plays a functional role in anchoring telomeres to the nuclear membrane in sperm. However, to the best of our knowledge no studies as yet have directly investigated whether telomeres co-localise with H2BFWT in the human sperm nucleus. Therefore to address this, experiments were undertaken to detect telomeres using a pan-telomeric probe and H2BFWT using FISH and antibody staining simultaneously (materials and methods section 2.2.4). As shown in the example gallery of images (figure 3.14), although both telomeres and H2BFWT appear in close proximity to one another predominantly at the nuclear membrane, very few signals overlap.

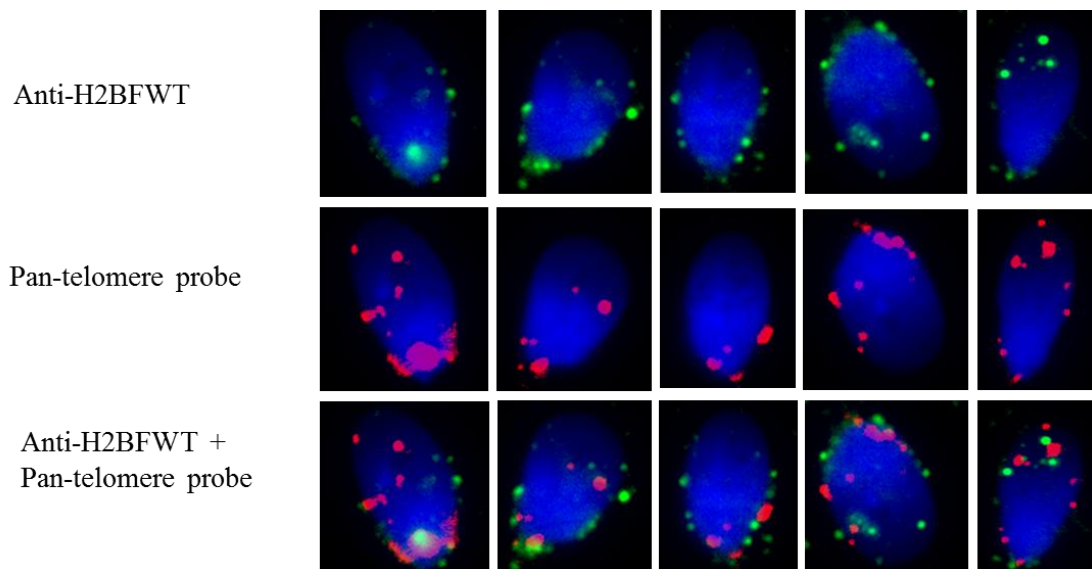


Figure 3.14: Example images depicting telomere localisation (red) in relation to H2BFWT (green) localisation within the sperm nucleus (blue). The top row of images display only H2BFWT staining, the middle row of images display telomere staining only, while the bottom row of images show H2BFWT staining over-laid with telomere staining. As can be seen in the bottom row of images, whilst both telomeres and H2BFWT are predominantly located at the nuclear periphery in close proximity to one another, few signals overlap indicating that H2BFWT does not directly interact with the telomere.

The evidence herein presented therefore does not support the hypothesis that H2BFWT has a direct role in anchoring the telomeres to the nuclear membrane.

3.3.5 Specific aim 1e. To test the hypothesis that nuclear (telomere) organisation is altered in infertile males compared to their normal counterparts

One of the reasons why Ioannou and Griffin (2010) argue strongly that nuclear organisation should be associated with male factor infertility is the association with elevated DNA damage in infertile males. In this study therefore DNA integrity in the sperm head and nuclear organisation were assessed in a cohort of infertile males with compromised semen parameters (sperm concentration ≤ 20 million per ml and/or percentage motility $\leq 20\%$ and/or percentage normal morphology $\leq 5\%$) and compared to that of normal fertile males (the same control semen samples from fertile males assessed in section 3.3.1). The rationale here is that, if there is an association with male infertility and altered nuclear organisation in the sperm heads of these males, then we might ultimately expect to observe a group of males with infertility status previously described as idiopathic (unexplained) that have altered nuclear organisation in their sperm heads. Semen parameters in the males included in this study were assessed by an experienced andrologist at Embryogenesis assisted reproduction unit, Athens; the details of which are summarised in table 3.3.

Sample ID	Sperm concentration (x10⁶/ml)	Percentage motility	Percentage progressivity	Percentage normal morphology
I1	20	20	10	5
I2	0.8	0	0	5
I3	18	20	5	2
I4	60	45	25	5
I5	2	5	0	5
I6	2	10	5	8

Table 3.3: Semen parameters of males included in the infertile cohort.

3.3.5.1 Telomere distribution using 2D telomere FISH

Nuclear organisation was assessed by investigating 2D telomere distribution patterns in the sperm heads of six infertile males, as assayed in section 3.3.1 (see specific aim 1a). When results from all patients were pooled following 2D analysis of telomere distribution, DAPI density and volumetric models gave results that suggested no statistical difference from a random distribution. Using the DAPI density model, although the pattern of the graph showed a preference for a peripheral pattern of telomere distribution, results did not reach the statistically significant value using χ^2 analysis suggesting a random distribution ($p = 0.062$) (figure 3.15). Similarly, when results from pooled infertile males were assessed using the volumetric model of analysis, results also indicated no significant difference from a random pattern ($p = 0.87$). Comparing these results to the control samples where p values were 0.00000045 and 0.0000036 for DAPI density and volumetric models respectively, the hypothesis that nuclear (telomere) organisation is altered in infertile males is thus supported. A difference in the median overall distribution of telomere signals was also observed using both modes of analysis: 2.66 (infertiles) compared to 2.18 (controls) using the DAPI density model; 2.29 versus 1.47 respectively using the volumetric model. Figure 3.15 illustrates the differences between both groups and both modes of analysis (the upper portion is a repeat of figure 3.2).

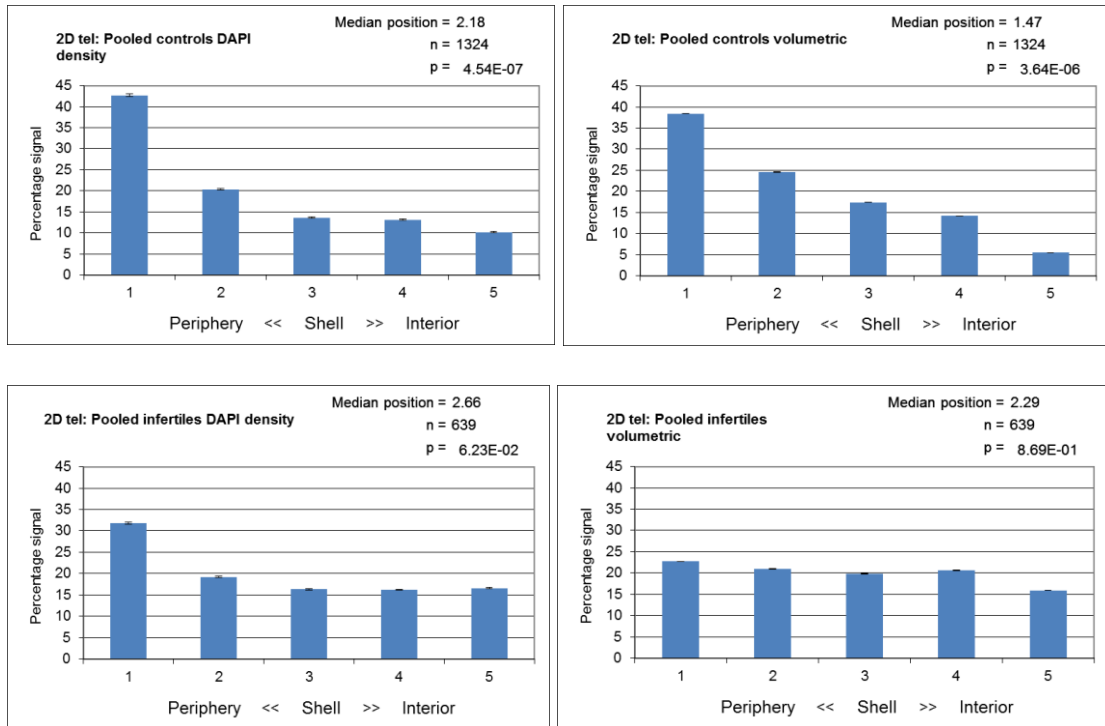


Figure 3.15: 2D telomere distribution in sperm of infertile males (lower graphs) as determined by FISH followed by analysis using DAPI density (left) and volumetric (right) compensation models. p values represent statistical analysis of a non-random position of telomeres using χ^2 . Both are compared to controls (upper graphs – repeat of figure 3.2). In both analyses, control males showed non-random patterns and a preference for the nuclear periphery, infertile males showed patterns not statistically different from random.

Surprisingly, after 3D analysis of telomere distribution in 30-50 sperm cells of five infertile males, pooled data showed that telomeres are localised predominantly at the nuclear periphery in these males (figure 3.16), similar to that of the six controls assessed.

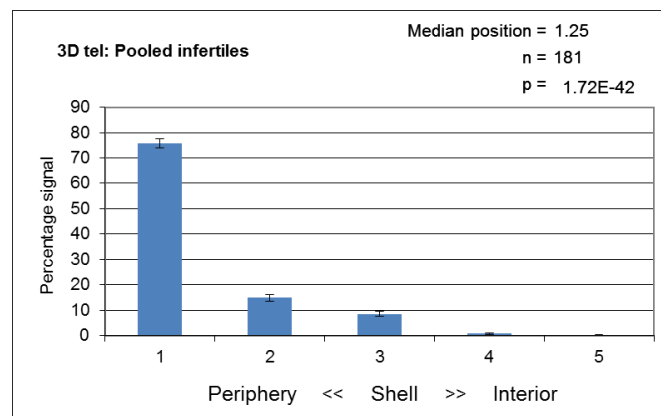


Figure 3.16: 3D telomere distribution in pooled data from sperm of infertile males. p value represents χ^2 statistical significance of non-random, preferentially peripheral distribution of telomeres.

3.3.5.2 Proportion of cells with ≥ 16 signals

In section 3.3.1 it was demonstrated that a proportion of cells show apparently random patterns and this can be visualised easily with at least twice the mean number of signals present in a proportion of the sperm heads. In section 3.3.2 it was demonstrated that an increased number of such cells were also manifested in a random distribution of signals throughout the nucleus. With this in mind therefore, we would expect the infertile males to show an increased number of cells with such patterns given the results of the previous section. As demonstrated in table 3.4, all six of the infertile males studied had >10% nuclei with this pattern compared to 3/12 in the control group. A third of these men had % of these nuclei >35 leading to a mean of 22.5% – more than four times that of the controls.

Sample ID	% nuclei ≥ 16 telomere signals
I1	11
I2	38
I3	13
I4	12
I5	12
I6	49
Average	22.5 \pm 6.8

Table 3.4: Percentage of nuclei with a larger number of dispersed telomere signals in sperm of infertile males.

An overall comparison between pooled infertile males and controls can be seen in figure 3.17. The average number of telomere signals in sperm nuclei of controls was significantly different to the average number of telomere signals in sperm nuclei of infertile males (11 vs 8, $p = 0.03$) when a student's t-test was employed. Similarly the percentage of nuclei with 16 or more signals was significantly different in controls compared to infertile males ($p = 0.002$) when a student's t-test was performed.

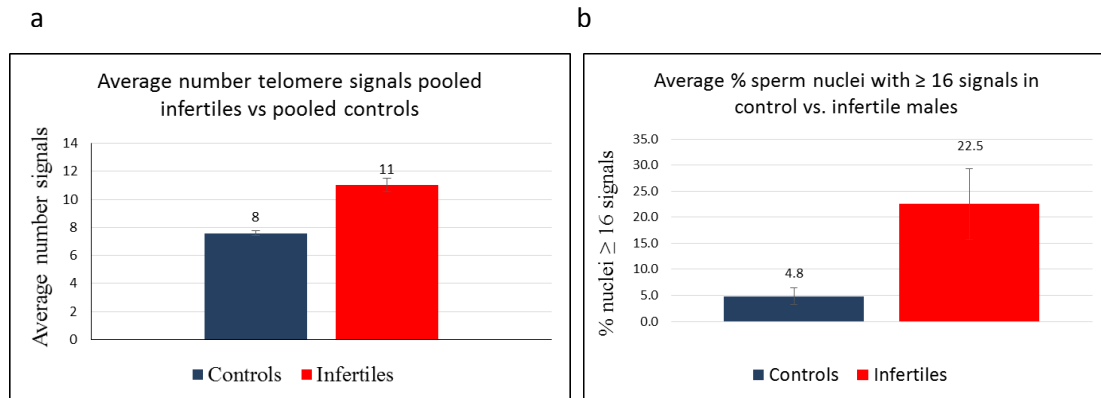


Figure 3.17: Comparison of overall average number of telomere signals (a), and percentage of nuclei with greater than 16 telomere signals (b) in pooled control (blue) and infertile males (red) males. The average number of telomere signals is increased in sperm nuclei of infertile males, and a greater percentage of nuclei make up the subpopulation of sperm cells with a large number of randomly distributed telomere signals in infertile males.

3.3.6 Specific aim 1f. To test the hypothesis that any alteration in nuclear organisation between fertile and infertile males may be related to the degree of chromatin packaging

The above observation showing an association between altered nuclear organisation and male factor infertility is most likely mediated by an increased proportion of cells with randomly distributed telomeres. This leads us to question the mechanism by which this phenomenon arises. One possible candidate might have been a breakdown in the association with H2BFWT however since, in section 3.3.4, we could find no association between this histone variant and the telomeres in normal fertile controls, it does not present a promising avenue to pursue. Another possible candidate is an overall relaxation in the level of chromatin packaging in sperm heads of infertile patients. Chromatin packaging can be assessed by Chromomycin A₃ (CMA3) staining of sperm nuclei as described in section 2.2.5. Since CMA3 competes with protamine binding sites in DNA, a deficiency in protamine within the sperm nucleus is easily identified by positive staining with CMA3. To the best of my knowledge overall chromatin packaging in sperm heads has not been associated with a breakdown in telomere organisation in the sperm heads of infertile males, hence the reason for the hypothesis tested here. In this study, at least 100 images were captured per patient and assessed for positive or negative staining with CMA3 for each infertile patient and control sample. The percentage of positively stained nuclei was then calculated, and results from the pooled infertile group were compared to that obtained from the pooled control

group. A student's t-test was then carried out for statistical analysis. Results can be seen in figure 3.18.

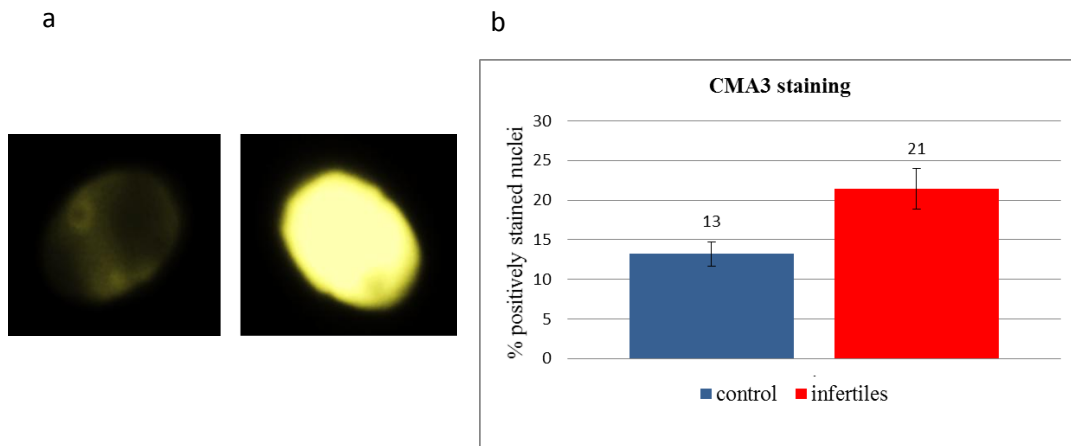


Figure 3.18: Example images of negatively stained (a) and positively stained (b) sperm nuclei after chromomycin A3 (CMA3) staining. b: Graphical representation of the percentage of positively stained sperm nuclei in fertile controls (blue) compared to sperm nuclei of infertile males (red) following CMA3 staining. Infertile males possess a higher percentage of positive CMA3 staining (error bars represent standard error).

As shown in figure 3.18b, infertile males showed a significantly higher percentage of positively stained sperm nuclei than normal control males when a student's t-test was carried out ($p = 0.008$), indicating that a higher proportion of sperm cells contained protamine deficiency and/or histone retention. This in turn is likely to impact on the ability of the sperm nucleus to package its genome correctly, and therefore the above observations supports the hypothesis that the altered distribution and overall increase in the number of telomere signals observed in sperm of infertile males might be related to a lack of chromatin compaction in sperm nuclei of these men.

3.4 Discussion

3.4.1 Telomeres are located at the nuclear periphery in human sperm heads

Data presented here first of all indicates that overall, 2D and 3D approaches to measure telomere distribution generally give similar results, with the majority of signals present at, or near to the nuclear periphery. This indicates that both the in-house developed algorithms that correct for the flattening of a 3D object into a 2D image are able to do so with reasonable accuracy. These results confirm previously published 2D work that telomeres are predominantly localised at the nuclear periphery in the sperm of normal males, as previously demonstrated in humans and many other mammalian species (Zalensky et al., 1995; Zalensky et al., 1993). Although this non-random distribution of telomeres has been well accepted since these earlier studies, conversely 3D analysis of telomere localisation in a study by Hazzouri *et al* 2000 did not observe telomere distribution at the nuclear periphery, but rather found that telomeres were dispersed throughout the nucleus. However, in the Hazzouri study only 13 cells were analysed for telomere distribution, and these were subjected to harsh swelling procedures (1M NaOH for 5 minutes) (Hazzouri et al., 2000). As indicated in section 3.3.2, such swelling conditions drastically alter the natural architecture of the sperm nucleus, and thus conclusions drawn from these experiments should be done so with appreciation of this effect. In the data presented here, in order to preserve the natural architecture of the sperm nucleus, no swelling procedures were performed, therefore results should be indicative of the sperm head in its natural state. It is of course possible that the results presented here might arise due to the preferential binding of the pan-telomere probe to more accessible telomeres at the nuclear periphery, along with a lack of binding to any inaccessible telomeres that might reside in the interior of the nucleus. However, preservation of the natural architecture of the sperm nucleus was preferable over increased probe binding efficiency, given the risk of altering normal telomere interactions and overall nuclear structure when employing swelling techniques. Overall therefore, results presented here are in agreement with the initial findings of a chromocentric model of nuclear organisation in human sperm, which is reiterated given that both 2D and 3D approaches have been employed, and a large number of sperm nuclei have been analysed (~1300 and ~250 respectively).

3.4.2 H2BFWT is also located at the nuclear periphery but not in association with telomeres

In order to understand better the process behind how telomeres are held at the nuclear periphery, a search of the current literature identified H2BFWT as a likely candidate as an anchor molecule (Churikov et al., 2004). However, to the best of my knowledge, confirmation of the presence of H2BFWT in the intact sperm nuclear membrane *in vivo* is missing from this information, and therefore this research set out to address this gap. Results from my experiments confirmed that H2BFWT is present at the nuclear periphery in human sperm nuclei, in agreement with a previous study that showed its isolation from the nuclear membrane fraction of human sperm (Churikov et al., 2004). However despite co-localisation of green fluorescent protein (GFP) tagged recombinant H2BFWT with telomeres when expressed in a Chinese hamster ovarian (CHO) cell line, and an affinity for this histone 2B variant for double stranded telomere repeat sequences (as shown in a previous report) (Churikov et al., 2004), no such observation was confirmed here in human sperm heads. Instead, while telomeres were localised in close proximity to H2BFWT, signals did not overlap and therefore based on this evidence, it is unlikely that H2BFWT interacts with telomeres in order to play a functional role in anchoring telomeres at the nuclear membrane. Of course, this finding could be the result of a technical artefact, given that sperm cells are subject to dehydration and denaturation at 75°C during the FISH protocol prior to IF staining. Therefore it is possible that aspects of the FISH procedure may have disrupted any native interactions between the telomere and H2BFWT. However, unfortunately these conditions are necessary for the detection of telomeres by FISH, and therefore could not be avoided. In future studies, it would be interesting to investigate whether telomeric proteins co-localise with H2BFWT using antibodies raised against each of these targets. Such an experiment would negate the need for harsh treatments in FISH experiments, and might provide further insight into the mechanisms of nuclear organisation in the human sperm nucleus.

3.4.3 Nuclear (telomere) organisation as a marker for male infertility

Results from 2D analysis of telomere distribution provide evidence that chromatin packaging and nuclear organisation appear to be altered in males with compromised

semen parameters. These observations help to explain some conflicting findings from the literature assessing centromere position in relation to male factor infertility: Finch *et al* 2008 showed that 2D analysis of centromere positions of the sex chromosomes were found to be altered in males with severely compromised semen parameters (Finch *et al* 2008). Similarly, centromere positions of chromosomes 15, 18, X and Y were found to be altered in infertile males with high incidence of aneuploidy (Olszewska *et al.*, 2008), and centromere positions of chromosomes 7, 9, X and Y were found to be altered in sperm from carriers of reciprocal translocations (Wiland *et al.*, 2008). Conversely however, in a study assessing all 24 chromosomes, the centromeres were found to remain remarkably stable following 2D analysis, despite compromised spermatogenesis (Ioannou and Griffin, 2010). In addition, 3D analysis of the position of the centromere of chromosome 17 in sperm found no difference in longitudinal distribution among motile versus immotile sperm, but a greater percentage of central radial positioning in motile versus immotile sperm (Alladin *et al.*, 2013). Many of these discrepancies might be explained by the fact that sperm cells are highly heterogeneous in any given ejaculate, with up to 25% inter-individual variation among even fertile men (Alladin *et al.*, 2013; Sadeghi, 2014; Sakkas *et al.*, 1999; Wiland *et al.*, 2008). Added to the data presented here however, a picture begins to emerge of the sperm heads of infertile males where the chromocentre stays largely intact regardless of the degree of infertility or prior treatment; the sex chromosome positions may be altered in certain severe oligoasthenoteratozoospermia (OAT) cases; and individual sperm heads are more likely to show aberrant patterns of telomere distribution.

Given the apparent importance of telomeres in meiotic segregation events during spermatogenesis, it is possible that this finding of differences in telomere localisation is also related to levels of aneuploidy in the sperm associated with infertile males. Indeed it is well documented that sperm of infertile males possess higher incidence of aneuploidy compared to sperm of fertile males (Calogero *et al.*, 2001; Pang *et al.*, 1999; Pfeffer *et al.*, 1999; Tempest and Griffin, 2004; Vegetti *et al.*, 2000). In order to address this question, future studies should assess telomere position in combination with aneuploidy, via FISH experiments using a pan-telomeric probe in combination with chromosome specific probes. Furthermore, in this study only the radial positioning of telomere distribution was analysed. Analysis of longitudinal distribution of telomeres within the sperm nucleus might provide a more detailed insight in the future.

3.4.4 The role of CMA3 staining and telomere distribution

CMA3 staining in this study showed that overall, chromatin packaging was altered in this particular cohort of infertile males compared to controls as indicated by a greater percentage of positively stained sperm nuclei in the infertile cohort. These results are in agreement with many other previous studies, showing that infertile males possess a significantly greater percentage of sperm nuclei with improper chromatin packaging, as identified by a greater percentage of cells positively stained with CMA3 (Iranpour et al., 2000; Kazerooni et al., 2009; Lolis et al., 1996; Salsabili et al., 2009). Since CMA3 is known to bind to GC rich sequences in the minor groove of the DNA helix, which is additionally the binding site for protamine (Berman et al., 1985), a positive CMA3 stain implies a lack of protamine or retention of histones, which ultimately results in improper packaging of DNA within the sperm nucleus. This lack of tight organisation of the paternal genome as highlighted by positive CMA3 staining, has been associated with aberrant semen parameters, poor fertilisation rates and poor embryo quality in humans (Esterhuizen et al., 2000; Iranpour, 2014; Manochantr et al., 2011; Sadeghi et al., 2009; Sakkas et al., 1996; Zandemami et al., 2012). Furthermore, in the mouse model, haploinsufficiency of just one of the two genes (protamine 1 (PRM1) or protamine 2 (PRM2)) is sufficient to cause infertility. Sperm of these mice possess reduced nuclear compaction, increased levels of DNA damage, and although they are able to produce pronuclei following ICSI, few embryos are able to develop to blastocyst stage (Cho et al., 2003; Cho et al., 2001). Taken together therefore, evidence from the protamine deficient mouse model and CMA3 staining experiments in humans in this study and in studies by others, identify that protamine is an essential component of the sperm nuclear architecture. Given the direct correlation between increased DNA damage and protamine deficiency observed in the mouse model (Cho et al., 2003), it would be interesting to perform DNA damage analysis in the sperm of the males assessed in the current investigation.

In this study, the percentage of positively stained sperm in infertile males was lower than that observed in other similar studies (Manochantr et al., 2011; Zandemami et al., 2012). However, this might be explained by the low sample size (13 controls and six infertile males) in this study compared to that of others. Furthermore, previous reports show a heterogeneous nature of CMA3 staining among control and infertile groups (Olszewska et al., 2013; Tavalae et al., 2014). Alternatively, user subjectivity might

additionally explain inter-study discrepancies. For these reasons, the use of CMA3 staining in fertility assessment remains under debate (Agarwal and Said, 2004; Dada et al., 2014).

In the current study, the percentage of sperm nuclei displaying positive CMA3 staining (21%) was very similar to the percentage of sperm nuclei belonging to a subpopulation with abnormally high numbers of telomere signals (22.5%). In future studies it may be possible to devise strategies to ask the question of whether it is the same individual cells that are CMA3 positive and have randomly distributed telomeres. Furthermore, it is interesting to note that upon visual inspection, the telomere staining pattern in this subpopulation of sperm (figure 3.3) is similar to that of sperm treated with 0.5M NaOH (figure 3.6c). In concordance with this, while non-swollen and 10mM DTT swollen sperm shared an identical average number of signals (7), 0.5M NaOH swollen sperm had more than 3.5 times this number, with an average number of 25 telomere signals. In addition, the percentage of sperm nuclei with greater than 16 signals in non-swollen sperm was 5%, whereas this number increased to 10% in 10mM DTT swollen sperm and 99% in 0.5M NaOH swollen sperm. Such observations lend further weight to the notion that improper chromatin packaging might result in abnormal organisation of telomeres within the sperm nucleus. It is possible that a lack of tight packaging of chromatin as identified by positive CMA3 staining, might cause altered telomere-telomere interactions that normally result in telomere dimers and tetramers (Solov'eva et al., 2004; Zalensky et al., 1993). This being the case, a more objective approach in telomere signal assessment might solve the subjectivity issues associated with CMA3 staining assessment in the fertility clinic. However, in order to confirm that improper chromatin packaging does indeed result in telomere signal dispersal, it would be necessary to perform FISH in parallel with CMA3 staining. In future studies, it would be interesting to address whether this is the case.

3.4.5 Differences between 2D and 3D analyses

Paradoxically, information from 3D analysis in this study, while supporting the conclusions about the overall distribution and the effects of swelling by NaOH, did not support the 2D analysis of telomere distribution patterns in infertile males compared to controls. One possible explanation might be sample size, the 3D analysis only assessed 30-50 cells from each patient and control sample and thus the numbers may simply

have not been large enough to see any difference. Manual 3D capture and analysis of telomeres within the sperm nucleus is extremely labour intensive and therefore in this study, sample size was limited to between 30 and 50 cells from six fertile control and five control males. In addition, this might be explained by the fact that prior to 3D analysis, it was necessary to first deconvolve image stacks, which may have resulted in the loss of many of the smaller telomere signals present in the original image. Should telomeres of infertile males exist more frequently as singletons rather than as clusters, it stands to reason that some signals may be smaller and therefore may be removed in the process of deconvolving. Alternatively, this might be due to difficulties experienced in instructing Nemo to distinguish several smaller signals from one larger signal. Finally, it is possible that, given such a small number and technical difficulties involved in accurate 3D measurements, I may have, inadvertently picked the easier cells to analyse.

3.4.6 Conclusions

Taken together, the above findings from this chapter: 1. Confirm peripheral telomere localisation in human sperm using 2D and 3D techniques; 2. Suggest that H2BFWT is not solely and/or directly involved in anchoring the telomere to the nuclear membrane in the sperm nucleus; 3. Identify that telomere staining patterns might act as a marker of male infertility. 4. Indicate that altered telomere staining patterns might be the result of improper chromatin packaging leading to disruption to telomere-telomere interactions (as identified by CMA3 staining, and the effect of artificial swelling procedures on telomere staining patterns).

This study provides the basis upon which further work may be based, addressing the complex issue of nuclear organisation and fertility in males. In future therefore, altered chromatin packaging and nuclear organisation of the sperm head may thus indicate that altered nuclear organisation is a marker of compromised male fertility. Indeed future studies should concentrate on idiopathic male infertility to investigate whether there is a subset of males without overtly compromised semen parameters but nonetheless altered nuclear organisation in the sperm heads, thereby compromising their prospects of procreation. If this is the case, then there is the potential for a future screening test for male infertility based on telomere distribution. As sperm screening test become more and more sophisticated and in demand (e.g. with advanced optics using

intracytoplasmic morphological sperm injection (IMSI) and screening for sperm disomy, and/or markers for DNA integrity e.g. hyaluronic A binding (HAB) antibody) then a simple test based around the position and number of visible telomeres may well find a place in the market.

4 Specific aim 2: To optimise a qRT-PCR approach for assaying telomere length using small quantities of starting material

4.1 Background

The study of telomere length has become increasingly popular since the discovery of its involvement in cellular senescence in the 1960s and 70s (Hayflick and Moorhead, 1961; Olovnikov, 1973; Watson, 1972). Despite its popularity however, much remains to be established from all of the biological systems that involve them. The study of telomere length is particularly challenging when the sample type to be investigated originates from small sample sizes or indeed single cells, since the traditional methodology for telomere length analysis (telomere restriction fragment analysis by southern blotting) requires microgram quantities of DNA. For this reason, it is understandable why data available on telomere lengths in gametes, embryos and newborns, are extremely limited.

In the last decade or so however, analysis of telomere length in small sample sizes has become more feasible with the development of a quantitative real-time polymerase chain reaction (qRT-PCR) approach (Cawthon, 2002, 2009). Indeed since its development, many researchers are moving towards this technology, leading to a noticeable growth in its popularity in recent years. The technique relies on determining the factor by which the DNA sample of interest differs from a reference DNA sample in its ratio of telomere sequence copy number (T) to the copy number of a single copy reference gene (S), referred to as the T/S ratio (Cawthon, 2002, 2009). Since telomere length can be analysed from as little as five nanograms of starting DNA material, the qRT-PCR based approach is well suited to analysis of telomere lengths in small sample sizes from newborns. Furthermore, recent modifications to Cawthon's original protocol have been developed for telomere length analysis in single cells (Treff et al., 2011b; Wang et al., 2013b).

The main disadvantage of the qRT-PCR based approach for telomere length analysis however, is that owing to its highly sensitive nature, it requires careful optimisation in

order to ensure efficient and specific amplification of the sequence of interest and the reference sequence. The efficiency of each reaction can be ascertained by performing the experiment with a serial dilution of DNA and plotting the cycle thresholds of each sample against the log of the DNA concentration. This should lie between 95-105%, and should be approximately equal in both the sequence of interest and the reference sequence amplification reactions. The specificity of the reaction can be ascertained by performing melt curve analysis following the completion of the thermal cycling profile, in which the change in fluorescence signal is plotted against the change in temperature. This identifies the temperature at which the double stranded products dissociate, as represented by a peak in the melt curve. The position of the peak on the plot is dependent upon the size of the product, its GC content and the reaction chemistries. The number of peaks depends on the number of expected amplicons and the specificity of the primers for the sequence of interest. The presence of several peaks usually indicates the amplification of non-specific products and/or the generation of primer complexes, which may interfere with and distort reaction efficiencies. Therefore, it is necessary to check the melting profiles of each product in order to ensure that the products generated match the expected profiles. Due to variations in reaction chemistries and technical specifications of thermal cycling machines, optimisation and validation of even previously published protocols and primer sequences is paramount in order to achieve accurate and reliable data (Gil and Coetzer, 2004). With the above information in mind therefore, the specific aims of this chapter were as follows:

4.2 Specific aims:

- 2a. To optimise a multiplex qRT-PCR assay for telomere length analysis from low quantities of genomic DNA template extracted from whole blood from newborns, using the Rotor-gene Q real-time PCR machine

- 2b. To optimise a singleplex qRT-PCR assay for telomere length analysis from whole genome amplified DNA from single cells using the Rotor-Gene Q real-time PCR machine

- 2c. To verify the faithful representation of telomere and reference sequences after whole genome amplification using the SurePlex DNA amplification kit

4.3 Results

4.3.1 Specific aim 2a. To optimise a multiplex qRT-PCR assay for telomere length analysis from low quantities of genomic DNA template extracted from whole blood from newborns, using the Rotor-gene Q real-time PCR machine

The volume of blood that can be sampled from newborns is very low, therefore it was decided that qRT-PCR offered the most practical approach for telomere length analysis in this study population. It was also decided that a multiplex approach, in which both the telomere and the single copy reference gene are amplified in the same reaction tube, offered more accuracy in average relative telomere length determination, therefore this approach was pursued.

In order to optimise my assay to meet these criteria, several different commercially available mastermixes were trialled, and several different primer concentrations were assessed for their performance. These are outlined in tables 4.1 and 4.2:

Mastermix	Supplier
SYBR® Green JumpStart™ Taq ReadyMix™	Sigma Aldrich
Power SYBR® Green Master Mix	Life Technologies
QuantiTect SYBR® Green PCR Kits	Qiagen
QuantiFast SYBR® Green PCR Kit	Qiagen
Rotor-Gene SYBR® Green PCR Kit	Qiagen
iQ™ SYBR® Green Supermix	Bio-Rad
LightCycler® 480 DNA SYBR Green I Master	Roche
SensiMix™ SYBR® No-ROX Kit	Bioline
SensiFast™ SYBR® No-ROX Kit	Bioline

Table 4.1: Different mastermixes tested for optimisation of multiplex qRT-PCR analysis of average relative telomere length. The mastermix highlighted in bold gave the best performance and therefore this was used in subsequent analyses.

	Primer name			
	Telg	Telc	Hgbd	Hgbu
Primer concentration (nm)	150	150	150	150
	75	75	50	50
	50	50	75	75
	50	50	50	50
	25	25	50	50

Table 4.2: Different primer concentrations trialled (in nm) during optimisation of multiplex qRT-PCR analysis of average relative telomere length. The concentration combination highlighted in bold performed the best and therefore this concentration was used in subsequent analyses.

Overall, the reaction performed the best when using the SensiMix™ SYBR® No-ROX Kit. It was also found that, due to the multiplex nature of this assay, it was necessary to reduce primer concentrations in order to eliminate primer complexes, which resulted in reaction over-efficiencies. For example, the presence of a primer complex was clearly visible in the no template control reaction (NTC) upon melt curve analysis following cycling conditions using 150nm of each primer, evidenced by a third peak in the middle of the graph (figure 4.1). Such an event led to reaction efficiencies of 118% for telomere amplification, and 113% for the reference sequence amplification (depicted in figure 4.2).

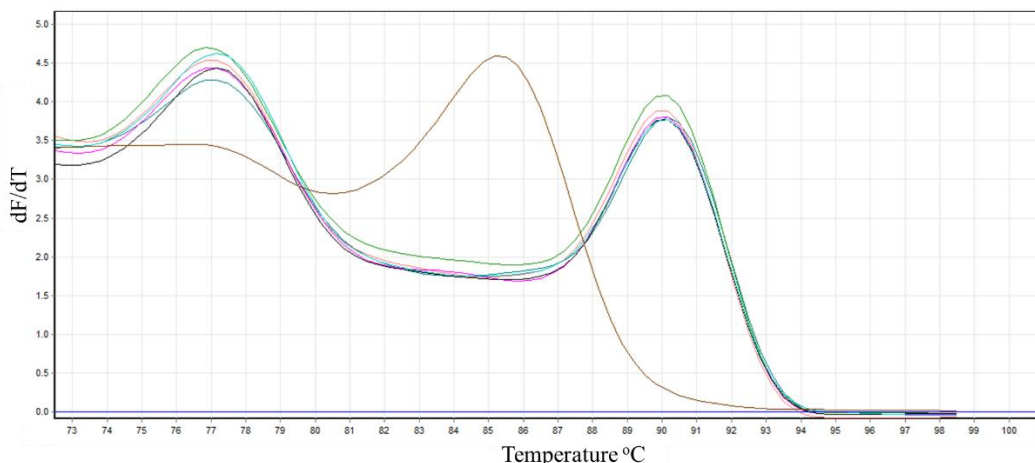


Figure 4.1: Melting curve analysis following cycling conditions using 150nm each telomere and reference sequence primer pair for multiplex qRT-PCR analysis of relative telomere length. The peaks to the far left and right of the graph represent the expected melting profiles of the telomere and single copy reference sequence amplicon respectively, however the peak in the middle represents formation of a primer complex in the no template control reaction.

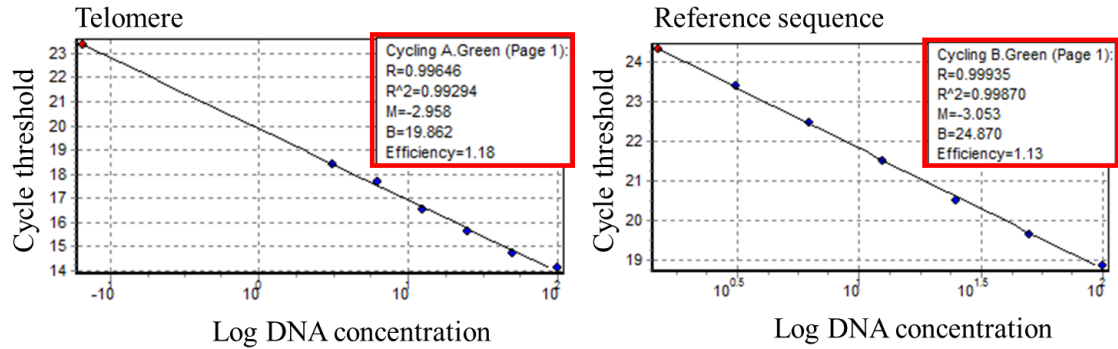


Figure 4.2: Reaction efficiencies (shown in the red boxes) for telomere (left) and reference sequence (right) following multiplex qRT-PCR conditions using 150nm for each telomere and reference sequence primer pair. Both reactions show over-efficiencies (118% for telomere and 113% for reference sequence respectively).

When primer concentrations were reduced to 50nm each, this non-specific peak in the melt curve disappeared (figure 4.3) and the reaction efficiencies fell within acceptable range (102% for telomere amplification and 100% for single copy reference sequence amplification), as shown in figure 4.4. These efficiencies were monitored in every experiment undertaken with patient samples, and proved to be consistently within the acceptable range and approximately equal.

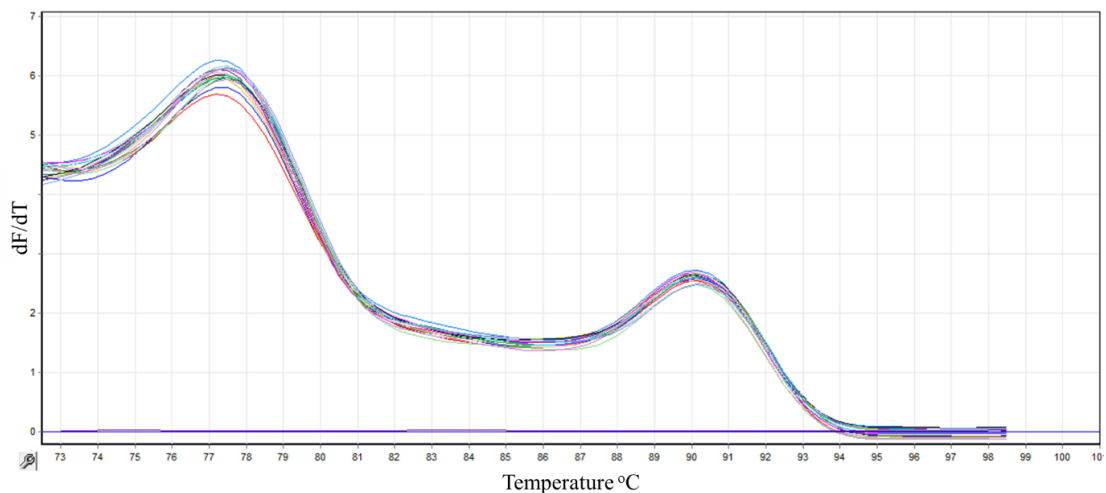


Figure 4.3: Melt curve analysis following thermal cycling for multiplex amplification of the telomere and single copy gene sequences. Both the telomere amplicon peak (left) and the single copy reference sequence amplicon peak (right) are in line with those reported by Cawthon et al 2009.

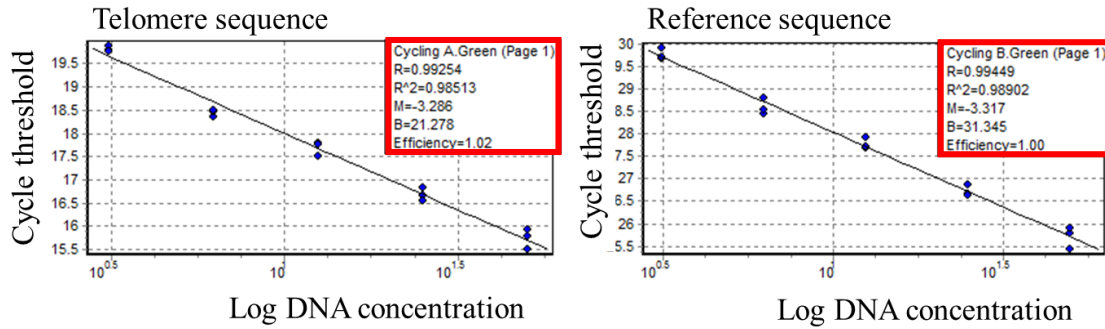


Figure 4.4: Reaction efficiencies (shown in the red box) of telomere amplification (left) and single copy reference sequence amplification (right). Both are within acceptable range (102% and 100% respectively) and approximately equal.

As shown in figure 4.3, only two peaks are visible upon melt curve analysis in the optimised multiplex qRT-PCR reaction, which are in line with the expected melting profiles for the telomere and single copy reference sequence amplicons (Cawthon, 2009). Although the background fluorescence in this graph is high (shown by a high baseline at the far left of the graph), this is likely due to the fact that upon acquisition of fluorescence signal at temperatures below 88°C, the single copy reference sequence amplicon remains double stranded. Therefore, SYBR green remains associated with the single copy reference sequence amplicon, producing a level of background fluorescence signal at these temperatures. This is unlikely to affect any data that is acquired at lower temperatures for telomere amplicon analysis, since the single copy reference sequence cycle threshold is much later than the telomere cycle threshold and therefore at the time of telomere amplicon signal acquisition, no single copy reference sequence amplicons are present. In order to confirm that this is the cause of the high background fluorescence in the melt curve analysis (as opposed to presence of non-specific products) the reaction products were run on a 3% agarose gel (as described in section 2.2.7). The results of this are shown in figure 4.5 on the next page.

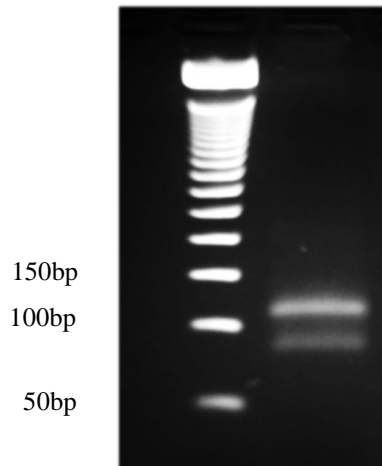


Figure 4.5: Gel electrophoresis of products formed following multiplex qRT-PCR. Two bands are present representing the expected sizes of the telomere and single copy reference sequence amplicons (79bp and 106bp respectively).

Figure 4.5 confirms the presence of only two products, which represent the expected size of the telomere and single copy reference sequence amplicons (79bp and 106bp respectively), as reported by Cawthon et al 2009. Therefore overall, results confirm that the cycling conditions and reaction chemistries utilised in this assay (as described in section 2.2.8) are optimal for sensitive and specific analysis of average relative telomere length using the Rotor-Gene Q real-time PCR machine. Furthermore, intra and inter assay variances were 2.3% and 0.9% respectively, indicating acceptable repeatability and reproducibility.

4.3.2 Specific aim 2b. To optimise a singleplex qRT-PCR assay for telomere length analysis from whole genome amplified DNA from single cells using the Rotor-Gene Q real-time PCR machine

Telomere length analysis from whole genome amplified DNA derived from single cells can be achieved using a singleplex qRT-PCR assay, in which the telomere and reference gene amplification reactions are performed in separate tubes on separate experiment runs. However, it must be assured that firstly, care is taken to optimise a sensitive and efficient assay for relative telomere length analysis, and secondly, that whole genome amplified DNA faithfully represents the original starting material. This section therefore set out to address these points.

Results from specific aim 1 eliminated the use of several commercially available mastermixes and several primer concentration combinations for amplification of the telomere sequence due to poor performance. Therefore the optimisation of reaction conditions for telomere amplification in singleplex qRT-PCR was more straightforward. Three of the best performing mastermixes identified from specific aim 1 were trialled (shown in table 4.3), along with three of the best performing primer concentration combinations (table 4.4). However, optimisation of the reaction designed to amplify the multicopy reference sequence was more complicated and involved identification of a suitable mastermix (from those outlined in table 4.3 that were also compatible with telomere amplification), optimisation of primer concentrations (table 4.5) and optimisation of cycling conditions (table 4.6).

Mastermix	Supplier
Rotor-Gene SYBR® Green PCR Kit	Qiagen
SensiMix™ SYBR® No-ROX Kit	Bioline
SensiFast™ SYBR® No-ROX Kit	Bioline

Table 4.3: PCR mastermixes trialled for qRT-PCR analysis of relative telomere length from WGA DNA. The kit highlighted in bold generated the best reaction performance therefore this was used in subsequent reactions.

Primer concentration (nm)	Primer name	
	Telg	Telc
	200	200
	100	100
	50	50

Table 4.4: Primer concentrations trialled for amplification of the telomere sequence. Details highlighted in bold generated the best performance and were therefore included in all subsequent reactions.

Primer concentration (nm)	Primer name	
	AluF	AluR
	300	300
	200	200
	100	200
	100	100
	50	50

Table 4.5: Primer concentrations trialled for amplification of the multicopy reference sequence. Details highlighted in bold generated the best performance and were therefore included in all subsequent reactions.

Step	Temperatures tested °C	Hold duration time tested
Polymerase activation (as per manufacturer recommendation dependent upon mastermix used)	95	5 mins
		10 mins
Melting	95	15 secs
Annealing	60	60 secs
		30 secs
		15
	64	30
		15
		10
Extension and signal acquisition	70	10 sec
	75	
	77	

Table 4.6: Different cycling conditions attempted for the amplification of the multicopy reference gene for relative telomere length analysis in WGA DNA derived from single cells. Cycling conditions highlighted in bold gave the best reaction performance.

Overall, the Rotor-Gene SYBR® Green PCR Kit performed best when taking into account the reaction efficiencies from both sets of primer pairs. For both telomere and multicopy reference gene amplification, primer concentration at 100nm each was found to generate good reaction efficiency (98% and 103% respectively) as shown in figure 4.6. However this was only the case for the multicopy reference sequence if cycling conditions were set with an annealing temperature at 60°C for 15 seconds and signal acquisition at 77°C. A raised annealing temperature and/or a raised annealing duration and/or a reduced signal acquisition temperature resulted in an over-efficient amplification. An example of this is shown in figure 4.7.

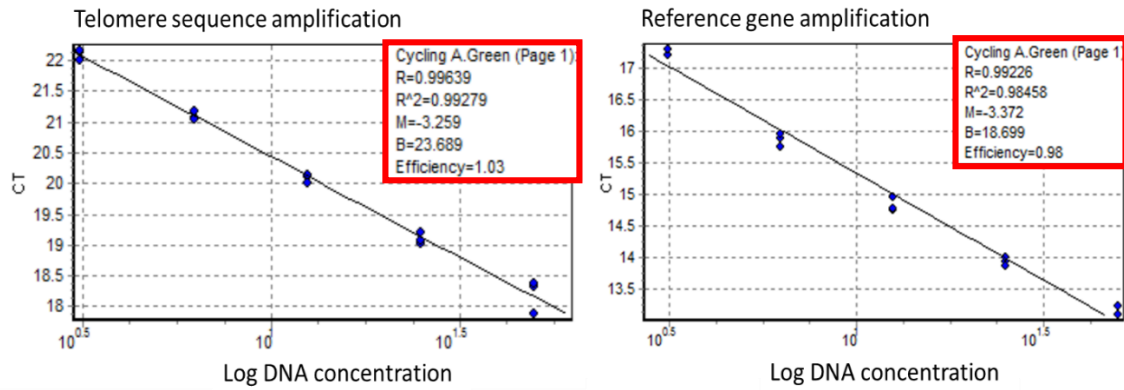


Figure 4.6: Reaction efficiencies (detailed within the red boxes) of telomere amplification (left) and multicopy reference gene (right). Reaction efficiencies are close to 100% and are approximately equal, confirming optimal amplification conditions for quantitative analysis of relative telomere length.

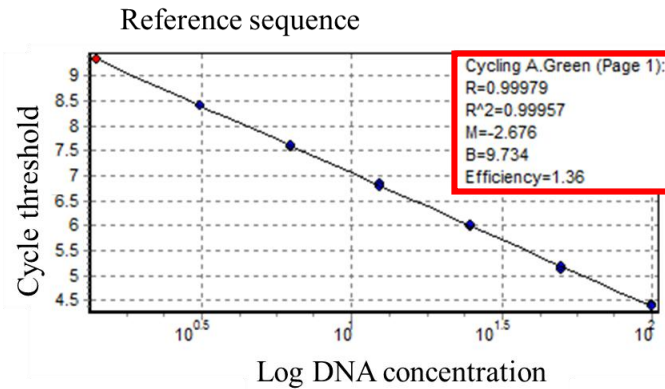


Figure 4.7: An example of poor reaction conditions resulting in an over-efficient reaction of 136% (calculated by the Rotor-Gene Q software and shown in the red box to the top right of the graph) for the multicopy reference sequence. This particular reaction was carried out using the Rotor-Gene SYBR® Green PCR Kit, with primer concentrations at 100nm each and a cycling condition as follows: Polymerase activation at 95°C for 5 mins, melting at 95°C for 15 secs, annealing at 60°C for 60 secs and signal acquisition at 70°C for 10 sec.

Furthermore, in order to confirm the specific amplification of solely the expected products and the absence of primer complexes or non-specific activity, melt curve analysis was performed using the Rotor-gene Q software following each telomere or reference gene reaction. These gave consistent results as outlined in figure 4.8. While both reactions produced melt curves with a raised baseline of background fluorescence intensity at lower temperatures (sometimes indicating the presence of non-specific product formation), a clear peak could be observed at the expected melting temperatures of each of the target products formed (Cawthon, 2009; Nicklas and Buel, 2006).

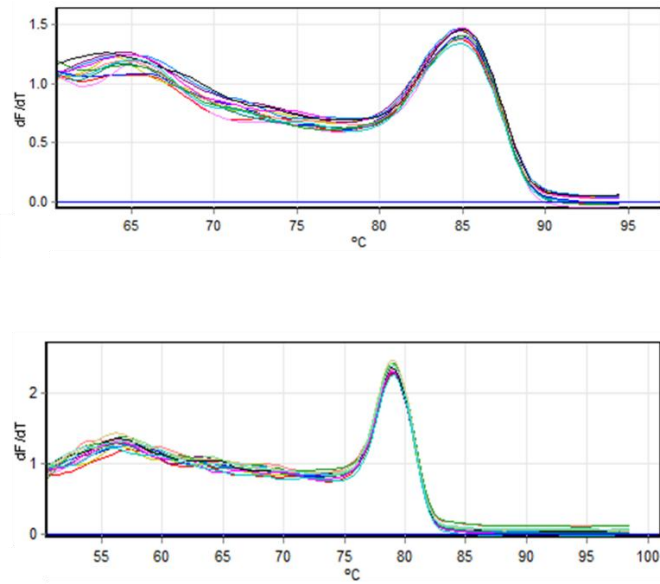


Figure 4.8: Melt curve analysis following amplification of the multicopy reference sequence (top) and the telomere sequence (bottom). On both graphs the y axis represents the change in fluorescence units divided by the change in temperature plotted against the temperature of signal acquisition (°C) on the x axis. Both melt curves indicate a single peak representing specific amplification of a single product.

To ascertain whether the high baseline of fluorescence at lower temperatures in each of the melt curves was due to non-specific product formation (which would indicate that the calculated reaction efficiency might not be entirely attributable to the production of the desired products), both amplicons were run on a 3% agarose gel as described in section 2.2.7. As presented in figure 4.9, this confirmed the presence of a single product at the expected size of the telomere amplicon (79bp) or the reference gene amplicon (127bp).

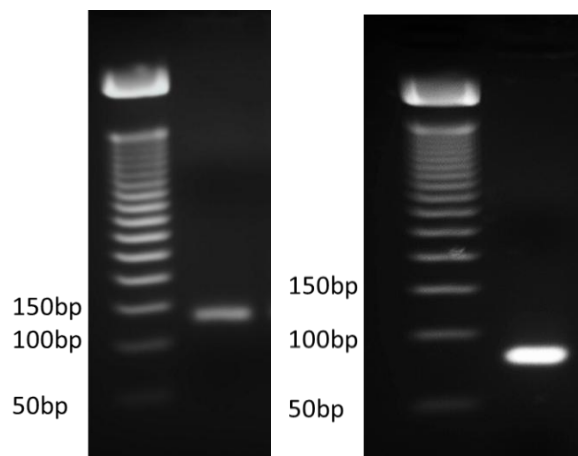


Figure 4.9: Agarose gel electrophoresis of alu reference (left) and telomere (right) PCR products. Both show amplification of a single product that matches the size expected for the amplicon (79bp and 127bp respectively).

Finally, the reproducibility of the assay was assessed by calculating the % covariance within and between experiments. The intra-assay variation was 0.6% and inter-assay variation was 4.6%. Taken together, these results show that I was successful in optimising a qRT-PCR based approach for relative telomere length analysis using whole genome amplified DNA derived from single cells, using the Rotor-Gene Q real-time PCR machine.

4.3.3 Specific aim 2c. Verification of faithful representation of telomere and reference sequences after whole genome amplification using the SurePlex DNA amplification kit

In order to verify the faithful representation of telomere and reference gene sequences following WGA, telomere length was assessed by qRT-PCR in several control DNA samples from known euploid, aneuploid and chaotic cell lines both before and after WGA. A Pearson's correlation coefficient was calculated to assess correlation.

As shown in figure 4.10, the relative telomere length of unamplified DNA correlated well with relative telomere length of WGA DNA (Pearson's correlation coefficient $r = 0.93$, $p = 0.02$).

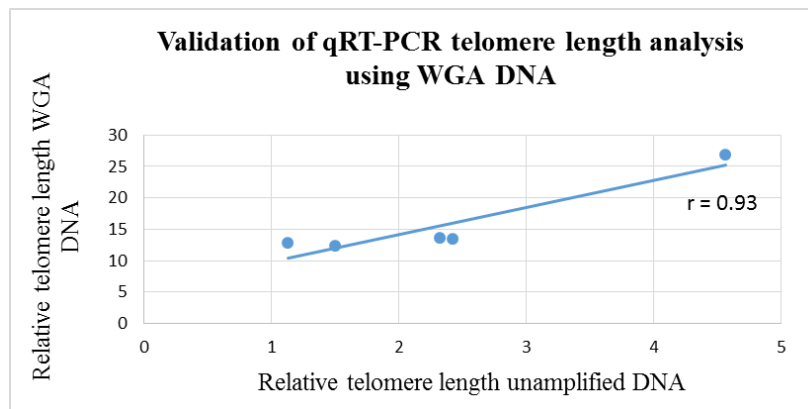


Figure 4.10: Verification of the faithful representation of relative telomere length following whole genome amplification using the SurePlex DNA amplification kit. The graph shows a good correlation between relative telomere length in unamplified DNA and relative telomere length in WGA DNA, indicating acceptable representation of telomeres in the WGA process.

4.4 Discussion

4.4.1 Multiplex qRT-PCR for telomere length analysis

Results from this chapter indicate that the multiplex qRT-PCR protocol for relative telomere length analysis originally published by Cawthon 2009 can be adapted for use with the Rotor-gene Q real-time PCR machine. This was achieved using the Biorad SensiMix™ SYBR No-ROX kit with Cawthon's primer sequences for amplification of the telomere and a single copy reference sequence at a concentration of 50nm each. Both telomere and single copy reference sequence amplification reactions performed at approximately equal efficiencies, which were close to 100%. This is important in the accurate determination of relative telomere length using the calculations described by Cawthon 2009. Furthermore, melt curve analysis and agarose gel electrophoresis were able to confirm the presence of solely the amplicons representing the expected product sizes, which confirms the specificity of the reaction and adds further weight to the accurate determination of relative telomere length in this way. Although melt curve analysis showed a high baseline of background fluorescence at lower temperatures, this is likely to be due to the presence of single copy gene amplicons, which remain double stranded at these temperatures due to their high melting temperature. This does not affect signal acquisition of the telomere amplicon, since the single copy gene does not begin to amplify until several cycles after the telomere amplicon has reached saturation.

While several others have reported the use of the Rotor-gene Q real-time PCR machine (formerly known as the Corbett Rotor-Gene 6000) for relative telomere length analysis (Brouillette et al., 2007; Lee et al., 2014; Mainous III et al., 2010; Salk et al., 2013) the majority of these have utilised Cawthon's earlier published singleplex approach. To the best of my knowledge only one other study has utilised the Rotor-Gene Q real-time PCR machine for relative telomere length analysis using multiplex qRT-PCR (Aini et al., 2014). However, this assay used different primers to those used here (the sequences of which were not published), and the details of the reaction reagents and cycling conditions were absent. Therefore to the best of my knowledge this is the first attempt to utilise the Rotor-gene Q real-time PCR machine and the Biorad SensiMix™ SYBR No-ROX kit to replicate Cawthon's original published protocol using the primers described in this publication. It was important that this optimisation was carried out,

since differences in reaction chemistries and thermal cycling machine specifications means that even well optimised previously published protocols may not perform with the same efficiency in the hands of others (Gil and Coetzer, 2004). The multiplex approach offers several advantages over the alternative singleplex approach including a reduction in the quantity of sample material required, a reduction in assay time and reagents required and improved accuracy due to circumvention of pipetting errors and plate-to-plate variation (Cawthon, 2009). Thus taken together, these results show that the optimised protocol outlined in section 2.2.6 for qRT-PCR analysis of relative telomere length is an accurate and convenient methodology for assessing telomere length in low sample sizes from newborns.

4.4.2 Singleplex qRT-PCR for telomere length analysis in single cells

Telomere length analysis in single cells represents an even more difficult challenge than telomere length analysis from the small sample sizes associated with newborns. Until recently, the only method allowing the possibility for telomere length analysis in single cells was quantitative fluorescence *in situ* hybridisation (QFISH), however, as identified later in chapter 5 and by others, this is prone to producing highly variable results (Lansdorp et al., 1996; Wong and Slijepcevic, 2004) and is therefore not particularly well suited to such studies. However, with the emergence of new technologies in whole genome amplification from single cells, the quantification of telomere length using a qRT-PCR approach has become possible. Indeed other studies have shown that qRT-PCR offers reduced inter and intra-assay variation compared to QFISH (O'Sullivan et al., 2006), indicating improved reliability of the use of this technique. However, it was still necessary to optimise reaction conditions specifically for telomere length analysis of WGA DNA rather than using the same assay developed in specific aim 1 since the use of a single copy reference gene in specific aim 1 is not compatible with WGA DNA. This is because WGA is susceptible to single locus dropout, which could affect the reference sequence.

Formerly, one other study has attempted to develop a qRT-PCR based approach including a pre-amplification step in order to measure telomere length in single cells (Wang et al., 2013a; Wang et al., 2013b). Alternatively, one other study has also

attempted to adapt Cawthon's original protocol for telomere length analysis in WGA DNA using a multicopy reference sequence (Treff et al., 2011b). The latter however was achieved using a different thermal cycling machine and no indication of reaction efficiencies was provided, therefore it was important to perform these optimisation steps in order to ensure an accurate and reliable assay here.

In my experiments, reaction efficiencies for both target (telomere) and reference (alu) sequences were approximately equal and within acceptable range for accurate determination of average relative telomere length. Although melt curve analysis produced a high level of background fluorescence for both amplicons in my experiment, the telomere amplicon melt curve presented here is very similar to that observed previously by Treff *et al* 2011. Unfortunately, no melt curve analysis for the multicopy reference gene is provided in Treff's manuscript, however this was available in a report by Wang *et al* 2013. Wang's melt curve analysis did not show the high background fluorescence seen here, however a considerably higher concentration of primers was used in Wang's experiments, which would have generated more reaction product and therefore reduced the effect of background noise. Regrettably, this was not compatible with my assay, since in my experience, increasing primer concentrations led to the formation of primer complexes resulting in an over-efficient reaction. Nonetheless, gel electrophoresis confirmed amplification of single products with expected sizes from both telomere and multicopy reference amplicons (Cawthon, 2009; Nicklas and Buel, 2006; Treff et al., 2011b; Wang et al., 2013b), indicating high specificity of each reaction. Therefore in summary, results from this section indicate that the cycling conditions and reaction chemistries optimised in this chapter are suitable for telomere length analysis from WGA DNA using the Rotor-Gene Q PCR machine.

4.4.3 Faithful representation of the DNA template following WGA

In addition to optimising reaction conditions for relative telomere length analysis in WGA DNA, it was necessary to confirm that the process of WGA itself using the SurePlex amplification system (Illumina) was able to accurately represent the telomere and reference copy sequences for accurate determination of relative telomere length. Results in section 4.3.3 confirm that qRT-PCR analysis of relative telomere length using WGA DNA correlates well with that of unamplified DNA. These findings are in

agreement with those reported by Treff *et al* 2011, who reported similar correlations using DNA amplified with the GenomePlex single cell WGA4 Kit (Sigma). Thus, experiments conducted in this study, and in that of Treff *et al* 2011 show that whole genome amplification is representative of telomere and multicopy reference genes in the original sample, verifying the use of WGA DNA in relative telomere length analysis in single cells by qRT-PCR. Although Treff *et al* 2011 had already reported accurate representation of relative telomere length using WGA DNA, a different method of WGA was employed to that used in the present study and different cycling conditions were performed for amplification of the telomere and multicopy reference sequence. Therefore it important to validate the protocol optimised in the current study using DNA amplified with the SurePlex WGA technology employed in this study.

4.5 Conclusion

In conclusion therefore I was successful in the fulfilling the three specific aims of this chapter. Moreover, optimisation of each of these assays formed a technology basis from which other chapters in this thesis could proceed. The multiplex qRT-PCR approach optimised in section 4.3.1 is suitable for telomere length analysis in the newborn (chapter 6), and the singleplex qRT-PCR based approach optimised in section 4.3.2 and validated in section 4.3.3 is suitable for use with WGA originating from polar bodies and embryo biopsies (chapter 5).

5 Specific aim 3: To investigate the telomere theory of reproductive ageing in women by addressing a series of hypotheses pertaining to telomere length in first polar bodies and cleavage stage embryos, in relation to maternal age and generation of aneuploidy

5.1 Background

Reproductive ageing in women, evidenced by a sharp decline in the ability to conceive naturally beyond approximately 35 years of age, is well recognised among scientists and clinicians alike. However, the exact causes of reproductive ageing in women remains a subject of investigation (Hassold and Hunt, 2001). Initially, it was believed that an age-related decline in uterine environment leading to a failure to recognise and abort trisomic conceptuses might play a fundamental role in reproductive ageing in women (Aymé and Lippman-Hand, 1982). Since then, it has become clear that it is a decline in the ability of the oocyte to produce a viable pregnancy as oppose to a decline in the uterine environment (Hassold and Hunt, 2001). In support of this, oocytes from women of advanced maternal age (35 years or older) are known to be prone to meiotic errors leading to gains or losses of whole chromosomes (known as aneuploidy), which is the leading cause of pregnancy loss and mental retardation in conceptuses that survive (Hassold and Hunt, 2001).

Several hypotheses have attempted to explain this decline in oocyte potential, including the ‘limited oocyte pool’ hypothesis, which suggests that female fertility declines alongside a depletion in the number of oocytes, as well as a decline in the quality of oocytes (Dorland et al., 1998a; Freeman et al., 2000; Hassold and Hunt, 2001; Munné et al., 2005; Navot et al., 1991). Alternatively, the ‘two hit’ hypothesis explains that a depletion in oocyte quality with age results from the multiple opportune stages for errors to occur in meiosis. That is, errors may occur prenatally during premeiotic mitotic divisions, during early stages of meiosis I in prolonged diplotene (which lasts from fetal life until the onset of puberty at least) or during ovulation in the latter stages of meiosis I and/or early meiosis II. Therefore, bivalents that are susceptible to errors

might arise prenatally during meiosis I (and are therefore age-independent) followed by age dependant abnormal processing of the bivalent (Lamb et al., 1996). More recently however, the telomere theory of reproductive ageing in women has been proposed, which suggests that shortened telomeres in oocytes of women of advanced maternal age render oocytes unable to support fertilisation and embryogenesis. This telomere shortening may be the result of a combination of the end replication problem in mitotically active precursor cells during gestation (Edwards, 1970; Polani and Crolla, 1991), and prolonged exposure to oxidative stress during the interval between oogenesis and ovulation (Passos and von Zglinicki, 2005). Given the important role of telomeres during synapsis, recombination and segregation events during meiosis (which are in turn crucial in ensuring faithful segregation of chromosomes), it is plausible that telomeres may play a role in reproductive ageing in women (Cooper et al., 1998; Dernburg et al., 1995; Keefe et al., 2005; Keefe et al., 2006; Liu et al., 2004; Nimmo et al., 1998). This is highlighted in the mouse model, where telomerase deficient mice appear to mirror the characteristics of this phenomenon (Liu et al., 2002a; Liu et al., 2002b; Liu et al., 2004). Furthermore, women that have given birth to infants affected by trisomy 21 (Down's syndrome) possess shortened telomeres compared to age matched controls (Dorland et al., 1998b; Ghosh et al., 2010).

However, despite a credible rationale for the telomere theory of reproductive ageing in women, very few studies have assessed telomere length in human oocytes or preimplantation embryos. I am aware of little direct evidence that oocyte or embryo telomeres shorten as women age, nor indeed that the telomeres of gametes that undergo segregation errors are shorter than those that do not. This is largely due to restrictions in access to sample material, and the technical challenges of measuring telomeres in single cells. Furthermore, those that have attempted to overcome these hurdles report conflicting data. While Keefe *et al* 2005 showed that oocyte telomere length is predictive of embryo development potential (Keefe et al., 2005), Turner *et al* 2013 found that oocyte telomere length was not associated with IVF outcome (Turner and Hartshorne, 2013). The latter study also found no association between oocyte telomere length and maternal age. In addition, to the best of my knowledge, only one study has assessed telomere length in female gametes and embryos in relation to the presence of aneuploidy. This study showed that telomere length is significantly reduced in aneuploid polar bodies and cleavage stage embryos compared to sibling euploid polar

bodies and cleavage stage embryos respectively from the same IVF cycle (Treff et al., 2011b). However details addressing telomere length in polar bodies and embryos in relation to maternal age were absent. Interestingly, another recent study found that telomere lengths in day 5 embryos derived from women of advanced maternal age are reduced compared to those from younger women (Mania et al., 2014). However in this study, all embryos analysed were aneuploid, and not all embryos reached the same developmental stage. Previous studies have shown that telomerase becomes highly active at the blastocyst stage of development (Wright et al., 2001) leading to an increase in telomere length at this stage (Treff et al., 2011b; Turner et al., 2010), therefore it is possible that the results presented in this study are influenced by developmental stage of the embryo rather than solely on maternal age. The present study was therefore designed to use the qRT-PCR methodology developed in specific aim 2 for relative telomere length analysis in gametes and embryos in order to study the effects of telomere length on reproductive ageing in women.

5.2 Specific aims

Specifically, this study was designed to test the following hypotheses:

- 3a. Telomere length is significantly shorter in first polar bodies from women of advanced maternal age (over the age of 35) compared to their younger counterparts

- 3b. Telomere length is significantly shorter in blastomeres derived from women of advanced maternal age (over the age of 35) compared to their younger counterparts

- 3c. Telomere length is significantly shorter in first polar bodies that are involved in chromosome segregation errors compared to sibling euploid first polar bodies

- 3d. Telomere is length significantly shorter in aneuploid blastomeres compared to euploid blastomeres from sibling embryos

5.3 Results

Anonymised patient details and results of aneuploidy screening (carried out by staff at Care Fertility Nottingham, UK) can be found in tables 5.1 and 5.2 for first polar bodies and blastomeres respectively.

Patient ID	Age	Number of euploid polar bodies assessed	Number of aneuploid polar bodies assessed	Chromosomes involved in aneuploid polar body number 1	Chromosomes involved in aneuploid polar body number 2
1	34	2	1	+4	n/a
2	38	2	2	-16	+4, -15
4	33	2	2	-17	-16
7	41	2	2	+10	+16
35	40	2	2	+22	complex
41	33	2	2	complex	+20
45	31	2	1	+22,+19,+21	n/a
46	42	2	2	-11	+16
50	33	2	0	n/a	n/a
52	26	2	0	n/a	n/a
59	41	2	2	complex	+16,-9,-21
60	37	2	2	+22	+12,+22
66	33	1	2	-4	+16
70	33	1	1	+18,+X	n/a
72	31	2	1	-22	n/a
73	43	2	2	complex	+1,+7,+10
74	47	1	2	+15,+18	+11,+20,+22
75	36	2	2	-2,-8	-22
76	33	2	0	n/a	n/a
80	32	2	1	+11	n/a
82	37	2	2	+15,+21	+21
84	37	2	2	-12,-20	complex
91	32	2	0	n/a	n/a
103	31	2	1	+9	n/a
115	46	1	2	complex	complex

Table 5.1: Anonymised patient details and results of aneuploidy screening in first polar bodies following assessment using the 24 Sure preimplantation genetic screening kit. 'complex' refers to aneuploid results involving four or more chromosomes, 'n/a' is not applicable (i.e. no aneuploid polar body available).

Patient ID	Age	Number of euploid blastomeres assessed	Number of aneuploid blastomeres assessed	Chromosomes involved in aneuploid blastomere number 1	Chromosomes involved in aneuploid blastomere number 2
19	34	2	2	-18, -21	-22
20	43	2	2	XO	dup(13)(q21.31-qter),+16
21	37	2	2	-13,+14	-15
22	41	2	2	-16	complex
24	42	2	2	complex	complex
27	34	2	2	complex	del(11)(q23.3-qter)
33	36	2	2	45;-9	47;+16
34	33	2	2	del(8)(q22.1-qter),-22	-8, del(15)(q25.1-qter)
122	38	2	2	del(1)(p21.1-pter),+22	del(2)(q33.3-qter),-15
123	40	2	2	complex	+19
127	39	2	2	-17,+18	complex
129	42	2	2	+10,+19	complex
130	34	2	2	+13	complex
137	32	2	2	del(6)(p12.1-pter), del(13)(q31.3-qter), del(16)(q11.2-qter)	complex
143	41	2	2	complex	44;-4,-21
144	33	2	2	+14,+22	del(1)(p32.3-pter),-10
163	33	2	2	+5,+21,+22	complex
171	27	2	2	dup(1)(p12-qter),+21	complex
172	34	2	2	complex	-4
188	33	2	2	-5	complex
224	44	1	1	complex	n/a
225	30	2	2	complex	complex

Table 5.2: Patient details and results of aneuploidy screening in blastomeres biopsied from cleavage stage embryos following assessment using the 24 Sure preimplantation genetic screening kit. 'complex' refers to aneuploid results involving four or more chromosomes, 'n/a' is not applicable (i.e. no embryo available), 'del' refers to a deletion with the chromosome involved identified in the first set of brackets and the portion deleted identified in the second brackets, 'dup' refers to a duplication with the chromosome involved identified in the first set of brackets and the portion duplicated identified in the second brackets.

5.3.1 Specific aim 3a. To test the hypothesis that telomere length is significantly shorter in first polar bodies from women of advanced maternal age (over the age of 35) compared to their younger counterparts

Relative telomere length was successfully assessed in two, three or four first polar bodies (depending on availability) from a cohort of women aged 35 or under compared to those of women aged over 35, therefore defined as advanced maternal age (AMA). Polar bodies assessed were made up of a mixture of both euploid and aneuploid samples. Relative telomere length was assessed by a qRT-PCR protocol optimised as part of specific aim 2 (see section 2.2.8). Data from all polar bodies from women under 35 were averaged and compared to mean data from all polar bodies originating from women aged over 35, and analysed for statistical significance using a student's t-test. Results are summarised in figures 5.1 to 5.3:

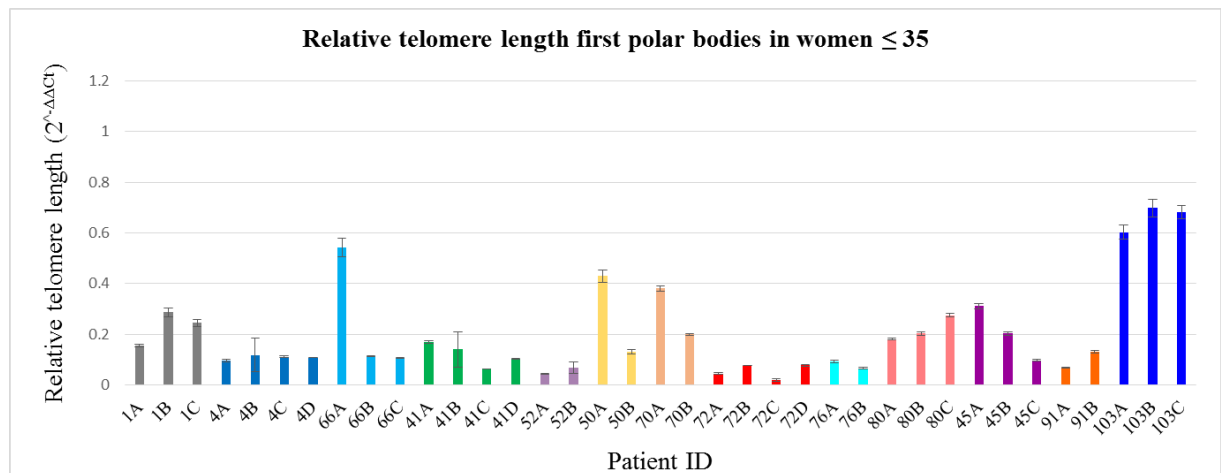


Figure 5.1: Relative telomere lengths in first polar bodies from women under the age of 35. Error bars represent standard error from the mean.

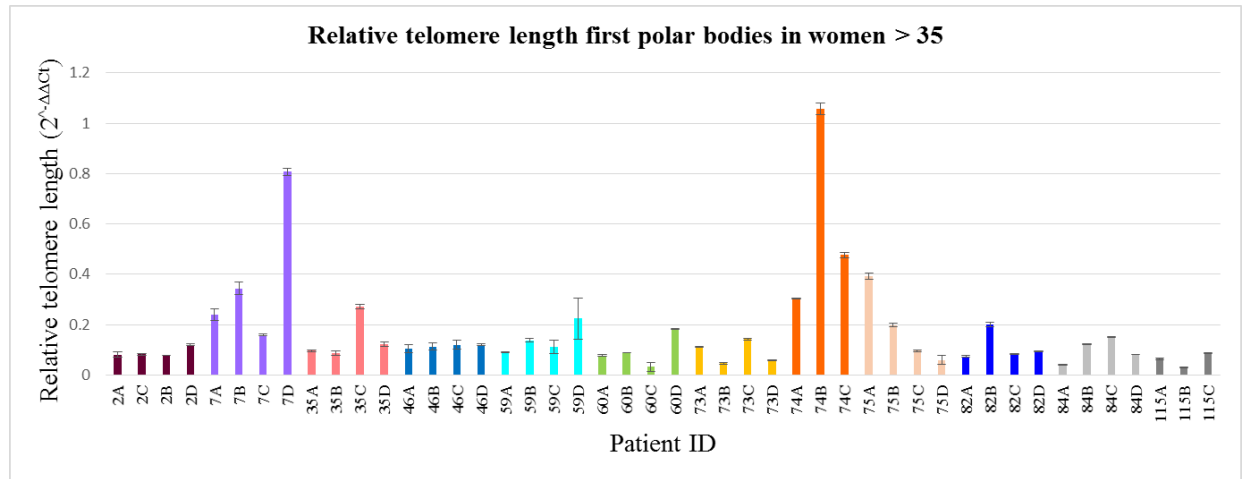


Figure 5.2: Relative telomere lengths in first polar bodies from women aged over 35. Error bars represent standard error from the mean.

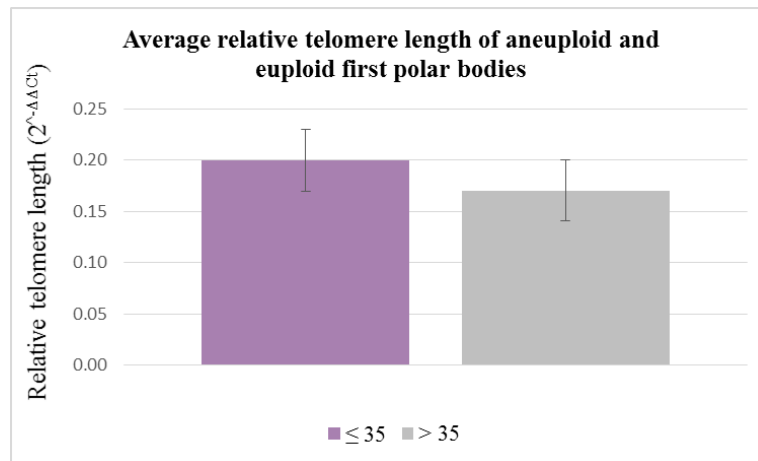


Figure 5.3: Average relative telomere length of all first polar bodies from women 35 years old or under compared to women of advanced maternal age. Results show that telomere length is slightly shorter in first polar bodies from women above 35 years old, however this difference is not statistically significant ($p = 0.48$). Error bars represent standard error from the mean.

Results indicate that relative telomere length in first polar bodies of women of AMA was marginally shorter than that of women 35 years old or under, however this difference was not statistically significant ($p = 0.48$). Indeed, a scatter plot of maternal age versus relative telomere length (shown in figure 5.4) showed no correlation between the two (Pearson’s correlation coefficient $r = 0.07$, $p = 0.52$).

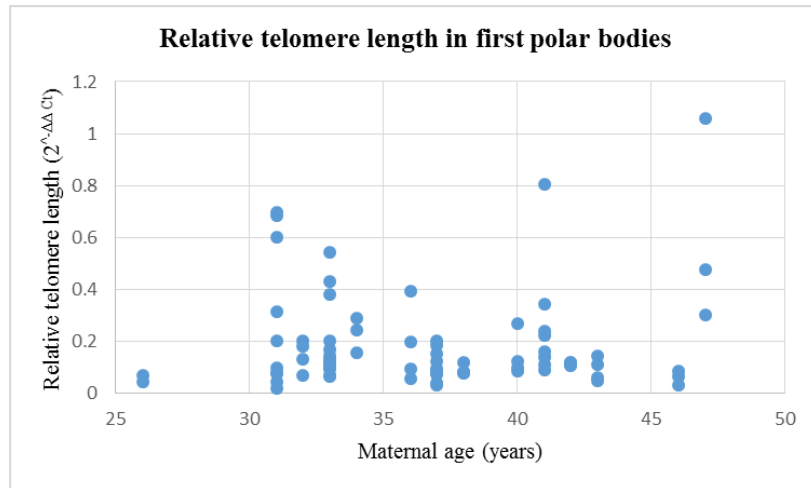


Figure 5.4: Relative telomere lengths of aneuploid and euploid first polar bodies in relation to maternal age. Results indicate no correlation between relative telomere length of first polar bodies and maternal age.

5.3.2 Specific aim 3b. To test the hypothesis that telomere length is significantly shorter in blastomeres derived from women of advanced maternal age (over the age of 35) compared to their younger counterparts

Relative telomere length was assessed in single blastomeres biopsied from a total of 48 embryos from couples in which the woman was 35 years old or under and a total of 42 blastomeres were assessed for telomere length from couples in which the woman was of AMA. Relative telomere length in each blastomere was measured by qRT-PCR (as described in section 2.2.8) from WGA DNA (amplified using the SurePlex DNA amplification kit, Illumina), using the comparative method (Schmittgen and Livak, 2008). From each woman in each cohort an equal number of aneuploid and euploid blastomeres were assessed for relative telomere length (i.e. two aneuploid and two euploid).

As indicated in figures 5.5 to 5.7, results show that relative telomere length in blastomeres biopsied from cleavage stage embryos from couples in which women were 35 years old or under are slightly shorter than those from couples in which women were over the age of 35 (0.20 compared to 0.25 respectively). However, this difference was not statistically significant ($p = 0.37$).

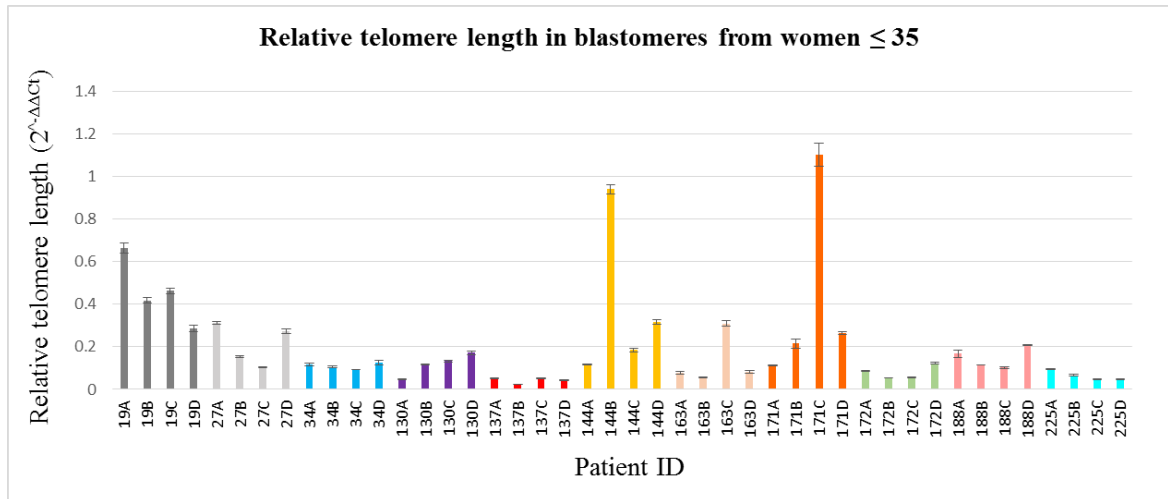


Figure 5.5: Relative telomere length in blastomeres of cleavage stage embryos from women under the age of 35. Error bars represent standard error from the mean.

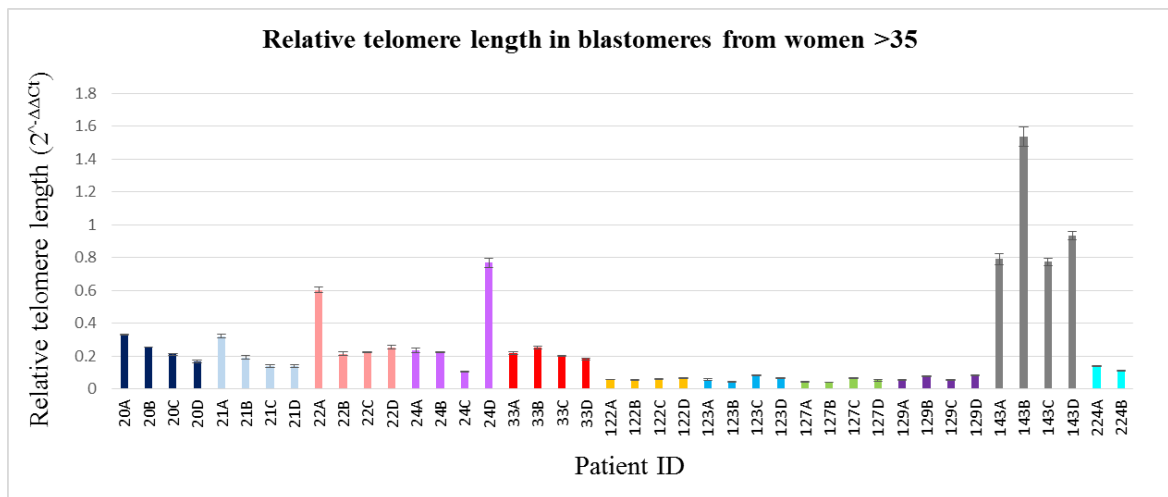


Figure 5.6: Relative telomere length in blastomeres of cleavage stage embryos from women over the age of 35. Error bars represent standard error from the mean.

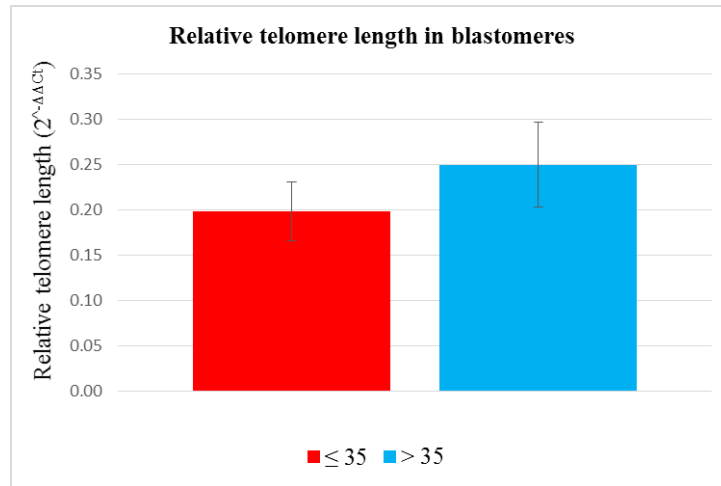


Figure 5.7: Average relative telomere length in all blastomeres from younger women compared to those from women of advanced maternal age. Relative telomere length is slightly shorter in blastomeres derived from couples in which women were younger however this difference was not statistically significant ($p = 0.37$) (bottom). Error bars represent standard error from the mean.

To confirm this finding, relative telomere length measured from each blastomere was plotted against maternal age (figure 5.8). Results showed that, in line with results in figure 5.6, no correlation existed between the two ($r = 0.16$, $p = 0.14$).

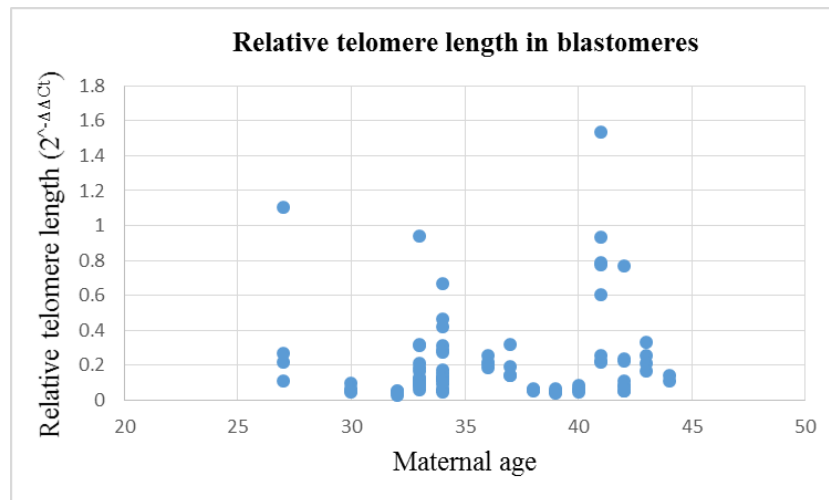


Figure 5.8: Telomere length in blastomeres from cleavage stage embryos in relation to maternal age. Results show no correlation.

Overall, evidence shows that although telomere length appears to be slightly increased in blastomeres derived from cleavage stage embryos from couples in which the woman is of AMA, this difference is not statistically significant and therefore telomere length in the cleavage stage embryo does not appear to be related to maternal age.

5.3.3 Specific aim 3c. To test the hypothesis that telomere length is significantly shorter in first polar bodies that are involved in chromosome segregation errors compared to sibling euploid first polar bodies

In order to study the relationship between telomere length and aneuploidy in first polar bodies, whilst controlling for maternal age and natural variation in inter-individual telomere lengths, a paired analysis was performed by comparing the average telomere length of euploid polar bodies from each woman, to the average telomere length of aneuploid polar bodies from the same women. Average telomere lengths for aneuploid or euploid first polar bodies were calculated from individual telomere lengths of two aneuploid and two euploid first polar bodies respectively. Therefore, only those patients from whom two aneuploid and two euploid first polar bodies were available were included in this analyses (n = 12 women, total of 24 euploid and 24 aneuploid first polar bodies).

Results showed that there was no consistent pattern among telomere lengths of euploid compared to aneuploid polar bodies. While telomere length was shorter in aneuploid polar bodies from some women, it was longer in other women (figure 5.9). Thus overall, the average telomere length of aneuploid first polar bodies (0.13) was almost identical to average telomere length in euploid first polar bodies (0.14) (figure 5.10). Indeed a paired student's t-test revealed no statistically significant difference ($p = 0.80$).

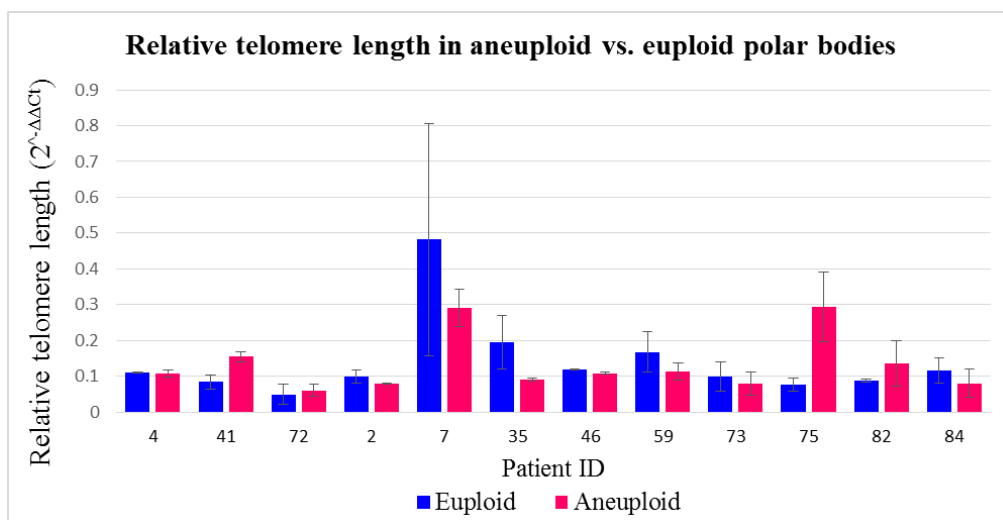


Figure 5.9: Average relative telomere length of two aneuploid first polar bodies compared to two sibling euploid first polar bodies from the same woman. Error bars represent standard error between the two aneuploid or euploid polar bodies assessed.

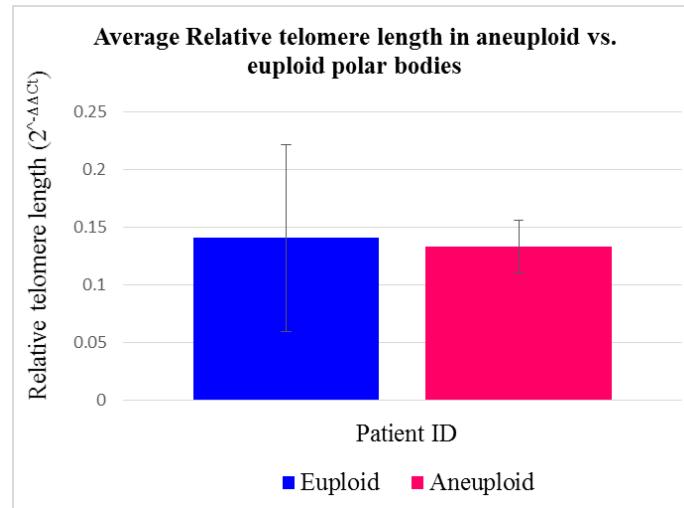


Figure 5.10: Overall average relative telomere length of all aneuploid first polar bodies in comparison to all euploid first polar bodies assessed in all women. Error bars represent standard error among each group.

In summary, results from section 6.3.3 show that telomere length is not different in aneuploid first polar bodies compared to euploid first polar bodies.

5.3.4 Specific aim 3d. To test the hypothesis that telomere length is significantly shorter in aneuploid blastomeres compared to euploid blastomeres from sibling embryos

Telomere length was assessed in blastomeres derived from aneuploid embryos and compared to that of euploid embryos, whilst controlling for natural inter-individual variation in telomere length as well as maternal and paternal age. This was carried out by comparing relative telomere lengths in sibling embryos generated in the same IVF cycle. From each couple, two euploid and two aneuploid embryo samples were available, therefore the average telomere length of the two euploid embryos was compared to the average telomere length of the two aneuploid embryos. A total of 84 embryos from 21 couples were assessed. A paired student's t-test was utilised in order to test for a statistically significant difference in relative telomere length in aneuploid embryos compared to sibling euploid embryos.

Results shown in figure 5.11 indicate that relative telomere length in aneuploid embryos compared to sibling euploid embryos is variable between cases. While some aneuploid embryos possess shorter telomeres than sibling euploid embryos, others

possess longer telomeres. Overall therefore, the average telomere length of aneuploid embryos (0.23) compared to euploid embryos (0.24) was not statistically significantly different ($p = 0.53$). This is illustrated in figure 5.12.

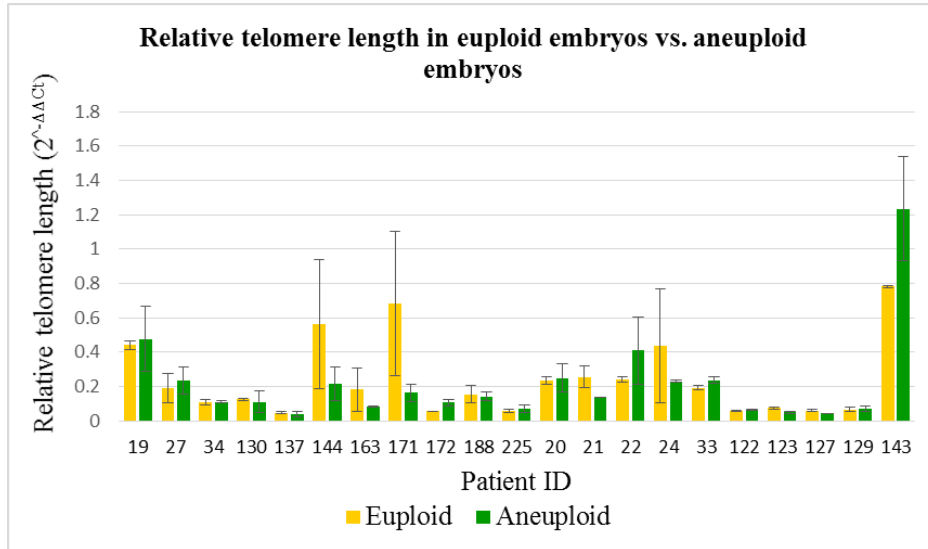


Figure 5.11: Average relative telomere length of blastomeres biopsied from two euploid embryos, compared to average relative telomere length of blastomeres biopsied from two sibling aneuploid embryos generated from the same couple in the same IVF cycle. Error bars represent standard error between the two euploid and two aneuploid blastomeres assessed.

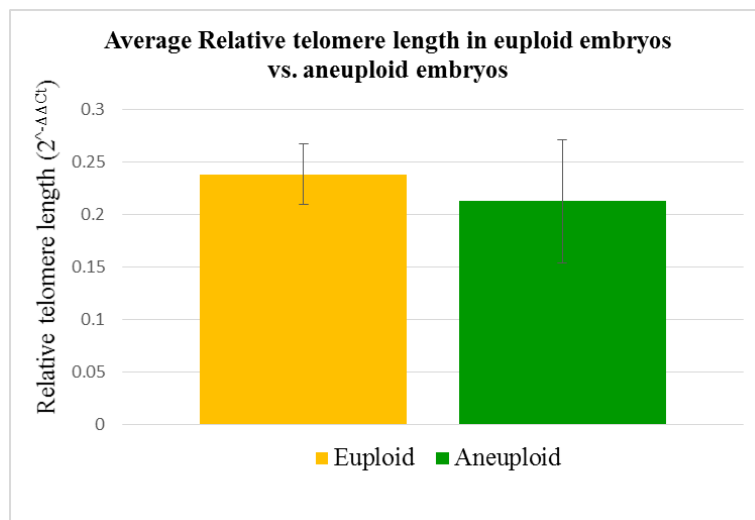


Figure 5.12: Overall average relative telomere length of all euploid and all aneuploid blastomeres assessed from all couples. Error bars represent the standard error within the study group.

5.4 Discussion

5.4.1 Telomere length in relation to maternal age in polar bodies

The results shown in section 5.3.1 indicate that relative telomere length of first polar bodies in younger women is not different to that of women of AMA. Since polar bodies ought to be reflective of the oocyte in terms of genetic complement, this finding is in line with observations using Q-FISH analysis, which found that oocyte telomere length is not correlated with maternal age (Turner and Hartshorne, 2013). Indeed results shown here also conclude that telomere length is not correlated with maternal age. However, in the study by Turner and Hartshorne, immature, mature and degenerate oocytes were included in this analysis, which may have affected the results obtained. Nonetheless, data presented here adds further weight to what is currently published, and additionally offers the benefits of a larger study cohort (82 polar bodies compared to 26 oocytes) and the inclusion of solely polar bodies from good quality oocytes.

Explanation for the above observations include the possible influence of telomere length maintenance by telomerase activity. In support of this, other studies have shown that telomerase is expressed in oocytes at all stages of oogenesis in humans (Wright et al., 2001) and other mammals (Betts and King, 1999; Eisenhauer et al., 1997). Furthermore, it is additionally possible that telomere length may be maintained in the oocyte by mechanisms of alternative lengthening of telomeres, however evidence for this hypothesis is absent in the current literature to the best of my knowledge.

Alternatively, it is important to consider that the above results may be the consequence of a narrow age range in the subjects sampled. Other studies that have observed a relationship between telomere length and chronological age have generally done so with a much broader range of ages (Allsopp et al., 1992; Lansdorp, 2008; Nordfjäll et al., 2009), however in this study the gap between the youngest woman (26) and the oldest woman (47) is only 21 years. The majority of data in this study is from women in their 30s and therefore the low numbers of individuals at the extreme ends of the age range here might additionally skew the overall perception.

In addition, all women included in this study were undergoing fertility treatment, and therefore may not be representative of a normal population. For ethical reasons it is not possible to obtain female gametes from healthy, fertile women and therefore any study

population suffers this limitation. Although it is possible that a proportion of women included in this study were pursuing fertility treatment for male factor infertility and therefore may be considered as healthy and fertile, unfortunately these details were not disclosed. Therefore it is possible that female infertility factors may have influenced the results observed here.

Finally, technical factors may also contribute to the findings obtained in the present study. These may be attributed to the multicopy reference gene used in relative telomere length analysis between subjects. It has previously been documented that inherent differences in copy number of alu repeats exist amongst individuals (Nicklas and Buel, 2006; Otieno et al., 2004). This inter-individual heterogeneity in alu copy number could cause profound effects on subsequent relative telomere length quantification. Traditionally, relative quantitation of telomere length using qRT-PCR takes advantage of a single copy reference gene (Cawthon, 2002, 2009), however it was deemed inappropriate to quantify telomere length in this way in the present study due to the well characterised issues surrounding single locus bias following WGA (Treff et al., 2011a). Use of a multicopy reference gene is thought to reduce susceptibility to this effect (Treff et al., 2011a), however the possibility of under-representation of one or both target sequences cannot be excluded. It will be interesting to see what the future holds for improvements to techniques in WGA and whether these might provide more sensitive measurements in analyses such as those presented here. Indeed, recently a similar but alternative approach to analysis of relative telomere length in single cells by qRT-PCR has been developed. This relies on a pre-amplification step, as opposed to WGA prior to telomere length quantitation (Wang et al., 2013b). Studies comparing the two techniques however have yet to be carried out.

5.4.2 Telomere length in relation to maternal age in embryos

Evidence shown in section 5.3.2 shows that telomere length in cleavage stage embryos is not correlated with maternal age, and therefore embryos derived from women of AMA were not different to those derived from younger women. To the best of my knowledge, this is the first attempt to assess telomere length in relation to maternal age in the cleavage stage embryo (day three post fertilisation), and therefore this study has unveiled some valuable new findings. Interestingly, these findings appear to be specific to the cleavage stage embryo, since observations from a study by Mania *et al* 2014

showed that telomere length is reduced in embryos derived from women of AMA at day five post fertilisation. However all of these embryos were diagnosed as aneuploid and not all embryos developed at the same rate. Mania's study included blastocysts, morulae and arrested embryos, therefore the contributions of aneuploidy and/or developmental delay cannot be excluded from the reduction in telomere length observed (Mania et al., 2014). The latter of these has been related to reduced telomere length in day 3 embryos (Keefe et al., 2005). Furthermore, the study by Mania *et al.* 2014 only studied a total of 35 embryos from 7 couples, whereas in the present study a total of 86 embryos from 22 couples were assessed.

One possible explanation for the increased telomere length observed in embryos from women of AMA here is the paternal contribution to telomere length in the developing embryo. Several studies have previously identified that paternal age is positively correlated with sperm telomere length (Allsopp et al., 1992; Baird et al., 2006; Turner and Hartshorne, 2013) and that telomere length in the offspring is paternally inherited (Kimura et al., 2008; Njajou et al., 2007; Unryn et al., 2005). However, details of paternal age in the present study were not available and therefore could not be assessed in relation to embryo telomere lengths.

Alternatively, mechanisms of telomere lengthening in the developing embryo may explain the results obtained here. Although it is generally accepted that telomerase activity becomes most active at the blastocyst stage of development leading to increased telomere length (Treff et al., 2011b; Turner et al., 2010; Wright et al., 2001), it is possible that recombination based mechanisms of telomere lengthening may play a role in earlier cleavage stage embryos (Liu et al., 2007). Although this has not been demonstrated in human embryos, it has previously been observed in mice (Liu et al., 2007). This being the case, it may be that shortened telomeres are re-set in the cleavage stage embryo irrespective of possible shortened telomeres derived from maternal origin.

Finally, it is important to consider technical aspects in the findings presented here. Alongside the technical aspects related to methodology (described in the previous section), it must also be appreciated that in this experiment it was assumed that a single blastomere from each embryo is representative of the entire embryo. Many studies before this have identified that embryos (and in particular cleavage stage embryos) are

prone to mosaicism (Colls et al., 2007; DeUgarte et al., 2008; Harton et al., 2011), in which daughter cells are not identical. Previous studies have also shown that telomere length is not identical among different blastomeres of the same embryo (Turner and Hartshorne, 2013). Thus it is possible that the blastomeres sampled from the embryos included in this study may not have been reflective of the embryo as a whole. Unfortunately it was not possible to obtain all blastomeres from any embryo in the present study and therefore this phenomenon could not be explored. Although there is some evidence to show that mosaicism is reduced in the blastocyst embryo (Adler et al., 2014; Munné et al., 2005) and therefore some argue that blastocyst biopsy is more representative of the whole embryo, this does not appear to be true in relation to variance in telomere lengths among different daughter cells (Turner and Hartshorne, 2013). For this reason it is unlikely that the stage of development at which embryos were biopsied is likely to have had an effect here.

5.4.3 Telomere length and aneuploidy in first polar bodies compared to sibling euploid first polar bodies

Results from section 5.3.3 illustrate that analysis of relative telomere length in relation to chromosome complement revealed no significant difference between aneuploid and euploid first polar bodies. This observation is in contradiction to that observed by Treff *et al* 2011 whom showed that telomere length is reduced in aneuploid polar bodies compared to sibling euploid polar bodies. However, in Treff's analyses only nine polar bodies were assessed, and these were made up of a mixture of first and second polar bodies (Treff et al., 2011b). Given that one of the proposed contributors to telomere shortening in women of AMA is prolonged exposure to oxidative stress, such an effect may become more apparent following completion of the second meiotic division (Keefe et al., 2007). If this is the case, second polar bodies may be more reflective of the telomere theory of reproductive ageing in women (Passos et al., 2007). That being said, Treff *et al* 2011 noted that relative telomere lengths between first and second polar bodies were not different. In addition, it is generally considered that aneuploidy in oocytes are predominantly the result of errors in meiosis I (Gabriel et al., 2011; Hassold and Hunt, 2001); therefore if dysfunctional telomeres were a potential cause of aneuploidy, it should be evident in first polar bodies.

One possible explanation for the observation found here could be that while shortened telomeres may result in impaired synapsis and recombination events leading to aneuploidy, such an event is likely limited to those chromosomes with critically short telomeres (Hemann et al., 2001b)). Since qRT-PCR analysis cannot determine telomere lengths of individual chromosomes, it is possible that overall relative telomere length is not reflective of critical telomere length sufficient to cause aneuploidy in a selection of chromosomes (Hemann et al., 2001b).

Alternatively, once again, it is possible that telomerase or alternative mechanisms of telomere lengthening may be active in the oocyte, resulting in stable telomere lengths. This being the case, the events leading to aneuploidy must occur by some means other than those directly resulting from shortened telomeres, e.g. inefficient checkpoint mechanisms during meiosis (Burgoyne et al., 2009; Wang and Höög, 2006).

5.4.4 Telomere length and aneuploidy in blastomeres

Results demonstrated in section 5.3.4 show that telomere length is not different in aneuploid embryos compared to sibling euploid embryos. Previous studies have shown that reduced telomere length is associated with chromosome instability (Artandi et al., 2000) and impaired synapsis and recombination in female gametes in the mouse model (Liu et al., 2004; Scherthan, 2007), which is in turn linked to aneuploidy (Liu et al., 2004) in the embryo. However, the results presented in specific aim 3c suggest that telomere shortening is not related to female reproductive ageing in humans. In light of this, it is not surprising that my results also show that telomere shortening is not related to aneuploidy in the cleavage stage embryo.

This finding contradicts that which has previously been shown by Treff *et al* 2011 who showed that telomere length is reduced in aneuploid cleavage stage embryos. However in this study, only 18 embryos (nine aneuploid and nine euploid) from a total of nine couples were assessed, whereas in the current study 84 embryos (42 aneuploid and 42 euploid) from a total of 21 couples were assessed. Thus it is possible that the discrepancies in these data might be due to the limited sample size in Treff's study.

Nonetheless, it is possible that paternal contribution to embryo telomere length (Kimura et al., 2008; Njajou et al., 2007; Unryn et al., 2005), telomerase activity and/or recombination based mechanisms of telomere lengthening in the embryo (Liu et al.,

2007) have overshadowed any effect of telomere reduction in relation to aneuploidy in the present data. Alternatively, it is also possible that the heterogeneity of telomere lengths in individual blastomeres (Turner and Hartshorne, 2013) may render the analysis of one blastomere from each embryo non-representative of the embryo as a whole.

5.5 Conclusion

To the best of my knowledge this is only the second (and largest) study to address telomere length in human female gametes and the first to do the same in human cleavage stage embryos in relation to maternal age. It is also the largest study to address telomere length in female gametes and cleavage stage embryos in relation to chromosome segregation errors.

Analysis of relative telomere length in both first polar bodies and cleavage stage embryos provides no evidence for the involvement of telomere length in reproductive ageing in women. Telomere lengths appear to be similar among first polar bodies independent of maternal age or chromosome complement, and therefore there is no evidence of telomere attrition in female gametes in relation to AMA or the incidence of aneuploidy. Similarly, no difference was observed in telomere lengths among cleavage stage embryos derived from women of AMA in comparison to younger women, nor between aneuploid and euploid embryos. Taken together therefore, results presented here do not support the telomere theory of reproductive ageing in women.

6 Specific aim 4: To test the hypothesis that preterm babies have significantly reduced telomere length by term equivalent age compared their term born counterparts

6.1 Background

Preterm birth, defined as birth at less than 37 completed weeks gestation, accounts for approximately 7.2% of all live births in the UK (Mangham et al., 2009). The incidence of preterm birth is steadily increasing in western countries, and although survival rates are improving, morbidity rates have remained relatively high (Costeloe et al., 2012; Moore et al., 2012), posing a significant public health concern. Alongside the well documented morbidities associated with preterm birth including respiratory and neurodevelopmental sequelae, a number of others are beginning to emerge, which constitute an ‘aged’ phenotype in preterm infants. Compared to healthy term born infants, preterm infants demonstrate altered body fat distribution (Modi et al., 2009; Thomas et al., 2008a; Uthaya et al., 2005; Vasu V and N, 2009), hypertension (Bhat et al., 2012; VanDeVoorde and Mitsnefes, 2014) and insulin resistance (Tinnion et al., 2013). These features are strongly linked with adverse metabolic health and, as such, present complications that persist into adulthood (de Jong et al., 2012; Parkinson et al., 2013; Thomas et al., 2011). This long term morbidity ‘signature’ in the ex-preterm infant is reminiscent of premature ageing in these individuals.

At present, the identification of the long term health outcomes in ex-preterm infants requires careful clinical and developmental follow up, involving a number of tests designed to evaluate a range of biological systems. Given the importance of early recognition of morbidity in this vulnerable patient population, the identification of a novel biomarker that acts as part of a single minimally invasive test could serve as a valuable tool in aiding prognosis. Since telomeres are known to shorten with the process of ageing, and are linked to several disease conditions (discussed in section 1.2) including those mentioned above, telomere length could be a plausible candidate for this role.

Currently very few studies have investigated telomere length in the newborn population, and fewer still in preterm infants (discussed in section 1.8.5). One study by

Friedrich *et al* 2001 found that overall, there was no difference in telomere lengths between preterm and full term infants at the time of birth, however a rapid and significant decline in telomere length was noted in infants born between 27 and 32 weeks gestation (Friedrich *et al.*, 2001). Unfortunately however, this study could not draw this conclusion from longitudinal data that measured telomere length in the same infant more than once. Instead telomere length measurements from different individuals born at different gestational weeks were assessed, and therefore natural inter-individual variation in telomere length cannot be excluded. That being said, a subsequent study that did carry out more than one assessment from each individual, were able to confirm Friedrich's conclusion of consistent reduction in telomere length between 23 and 35 weeks gestation (Holmes *et al.*, 2009). Interestingly this finding was not evident among age-matched fetuses, suggesting that the event of preterm birth itself might impact telomere length in some infants (Holmes *et al.*, 2009). Although these studies combined provide interesting and valuable information on telomere dynamics in this vulnerable study population, to date none have explored telomere length in the preterm infant at term equivalent age. Furthermore, none have assessed telomere lengths in individual chromosomes in newborn infants. Such analysis could provide key insights into the genetic aetiology of the 'aged' phenotype observed in ex-preterm infants. In addition, this information might identify whether telomere length could be utilised as a biomarker and/or a prognostic tool for assessing health outcome in preterm infants, and in turn play a vital role in prompting health management regimes in these individuals. In order to address the gaps in our current knowledge outlined above and in section 1.8.5, the specific aims of this chapter were as follows:

6.2 Specific aims

- 4a. To recruit up to 30 preterm infants and sample their blood at birth and “at term” age and to recruit an equivalent number of term born healthy infants as controls
- 4b. To use the qRT-PCR protocol developed in specific aim 2 to test the hypothesis that the telomeres of preterm infants are significantly shorter than they were at the time that they were born
- 4c. Using the same methodology to test the hypothesis that at term equivalent age, preterm infants have reduced average relative telomere length compared to term born controls
- 4d. To test the hypothesis that, in each of the three groups (preterm at birth; preterm at term; term born controls) overall telomere length correlates to gestational age, birth weight, maternal age, maternal body mass index and/or mode of delivery
- 4e. To test the hypothesis that individual telomeres are prematurely shortened in preterm infants at term equivalent age

6.3 Results

6.3.1 Specific aim 4a. To recruit up to 30 preterm infants and sample their blood at birth and “at term” age and to recruit an equivalent number of term-born healthy infants as controls

In order to address the aims set out in this chapter, preterm infants sampled at birth, preterm infants sampled at term equivalent age, and term born controls were recruited. This was done primarily by staff at the William Harvey Hospital (led by Dr Vimal Vasu) and my personal involvement was to help define the selection criteria, aid in the writing of internal funding to recruit a research nurse and to collect the samples from the hospital. Following informed written parental consent, preterm infants born at less than 32 weeks completed gestation were recruited from the neonatal unit at the William Harvey Hospital. Term born (37-42 weeks gestation) healthy infants were similarly recruited from the postnatal ward at both the William Harvey Hospital and the Queen Elizabeth the Queen Mother Hospital, Margate. This sampling criteria was used as it was deemed more appropriate to assess more extreme cases in this pilot study as a proof of principle. An additional 1ml of blood was drawn during routine blood sampling from preterm infants (up to 48 hours after birth, or at term age). In the case of healthy term born participants, an extra 1ml of blood was drawn if venepuncture was deemed necessary for other clinical reasons (e.g. suspected jaundice, suspected infection). Blood was then stored at room temperature until it was transported to the University of Kent (within 12 hours). In total, 15 preterm infants were recruited and sampled at birth, 10 preterm infants were recruited and sampled at term equivalent age, and 25 term born infants were recruited and sampled at birth. At the time of recruitment, all samples were anonymised by the doctor or nurse taking the sample, by assigning a code to the sample. Thus all samples were “blinded” upon collection so that I had no knowledge of the origin of samples prior to processing. In order to assess average relative telomere lengths in infants, DNA was extracted from 500µl whole blood using a DNA isolation kit for mammalian blood (Roche) as described in section 2.2.11. Clinical details and average relative telomere lengths recorded from each patient are outlined in table 6.1.

Group	Patient ID	Average relative telomere length (T/S ratio)	Gestational age (weeks)	Birth weight (kg)	Mode of delivery	Maternal body mass index (Kg/M ²)	Maternal age (years)
Preterm at birth	1	2.7	27.0	0.9	CS (labour)	-	31
	2	1.0	31.1	1.8	CS (non-labour)	-	20
	4	0.7	29.0	1.1	CS (labour)	30.5	31
	5	2.0	29.0	1.6	Vaginal	26.4	35
	6	1.1	29.0	1.2	Vaginal	26.4	35
	7	1.2	25.0	0.7	Vaginal	-	31
	9	2.8	26.0	0.9	Vaginal	-	36
	10	2.4	26.0	1.1	CS (labour)	-	36
	13	1.3	30.1	1.3	Vaginal	24.3	25
	14	1.2	29.6	0.9	CS (labour)	22.0	25
	15	2.4	25.9	0.8	CS (labour)	-	45
	16	0.6	24.1	0.8	Vaginal	27.7	35
	17	1.5	27.0	0.8	Vaginal	-	27
	18	1.7	27.0	0.9	Vaginal	-	27
5Q	1.2	29.1	1.2	CS (labour)	22.1	20	
Preterm at term equivalent age	8	1.8	27.0	0.9	CS (labour)	-	31
	12	0.9	26.0	1.1	CS (labour)	-	36
	27	1.2	27.6	1.1	Vaginal	19.8	19
	29	0.8	27.4	1.1	Vaginal	20.6	29
	35	1.0	27.1	0.8	CS (labour)	-	32
	37	1.0	30.9	1.1	CS (labour)	25.4	37
	38	1.3	25.3	0.8	Vaginal	25.1	24
	42	1.1	30.9	0.8	CS (non-labour)	-	26
	6Q	1.2	29.1	1.5	CS (non-labour)	25.7	32
	7Q	1.3	29.1	1.0	CS (labour)	25.7	32
Term controls	19	0.8	40.9	5.1	Vaginal	38.1	28
	20	0.8	40.9	3.6	Vaginal	38.2	36
	21	1.2	38.9	4.0	Vaginal	34.9	30
	22	1.3	39.4	3.6	-	18.9	18
	23	0.9	41.4	3.3	CS (labour)	23.3	17
	24	1.3	40.6	3.8	-	21.3	33
	25	1.0	39.7	3.9	CS (labour)	37.2	35
	26	0.8	40.4	3.4	Vaginal	22.8	25
	28	1.0	40.4	3.9	Vaginal	24.2	39
	31	0.9	40.3	3.3	CS (labour)	26.8	29
	32	2.0	40.6	3.9	Vaginal	42.6	37
	33	1.1	37.4	3.5	CS (labour)	37.9	40
	34	0.7	37.4	3.3	CS (labour)	37.9	40
	36	0.8	37.4	2.6	Vaginal	31.5	32
	39	0.7	40.6	4.2	-	21.6	38
	40	1.0	39.3	3.7	CS (labour)	21.0	31
	41	0.4	41.7	3.9	Vaginal	18.4	21
	1Q	1.2	39.4	3.3	-	30.0	-
	2Q	1.3	38.9	-	-	-	-
	3Q	0.6	39.0	3.0	CS (non-labour)	-	-
4Q	0.6	41.9	3.5	Vaginal	32.9	-	
8Q	0.7	38.3	2.3	Vaginal	18.7	-	
9Q	1.3	37.0	2.8	Vaginal	-	-	
10Q	0.5	41.9	3.0	Vaginal	-	-	
11Q	0.4	40.4	3.1	-	-	-	

Table 6.1: Patient information and relative telomere length (T/S ratio). CS (labour) refers to delivery by caesarean section following labour, CS (non-labour) refers to caesarean section in the absence of labour. Where a '-' is present, no information was available.

6.3.2 Specific aim 4b. To use the qRT-PCR protocol developed in specific aim 2 to test the hypothesis that the telomeres of preterm infants are significantly shorter than they were at the time that they were born

Average relative telomere length was assessed by quantitative real-time polymerase chain reaction (qRT-PCR) as described in section 2.2.6 in 15 preterm infants sampled within 48 hours of birth and 10 preterm infants sampled at term equivalent age. Results are shown in figure 6.1 on the next page. The preterm at birth group displayed a range of telomere lengths (T/S ratios) from 0.55 to 2.78, whereas the preterm infants sampled at term equivalent age displayed a range of telomere lengths from 0.76 to 1.77. Despite these differences however, a Shapiro-Wilk test of normality revealed that both groups were normally distributed ($p = 0.249$ for preterm sampled at birth and $p = 0.691$ for preterms sampled at term equivalent age). For this reason, and due to the small sample sizes in each cohort, it was deemed appropriate to compare the means values of the two sample populations. Indeed preterm infants sampled at birth possessed mean telomere length of 1.58 compared to a mean telomere length of 1.16 in preterm infants sampled at term equivalent age. Therefore preterm infants sampled at birth had telomere lengths 1.36x higher than those sampled at term equivalent age. However, a student's t-test revealed that this difference was not significant ($p = 0.10$).

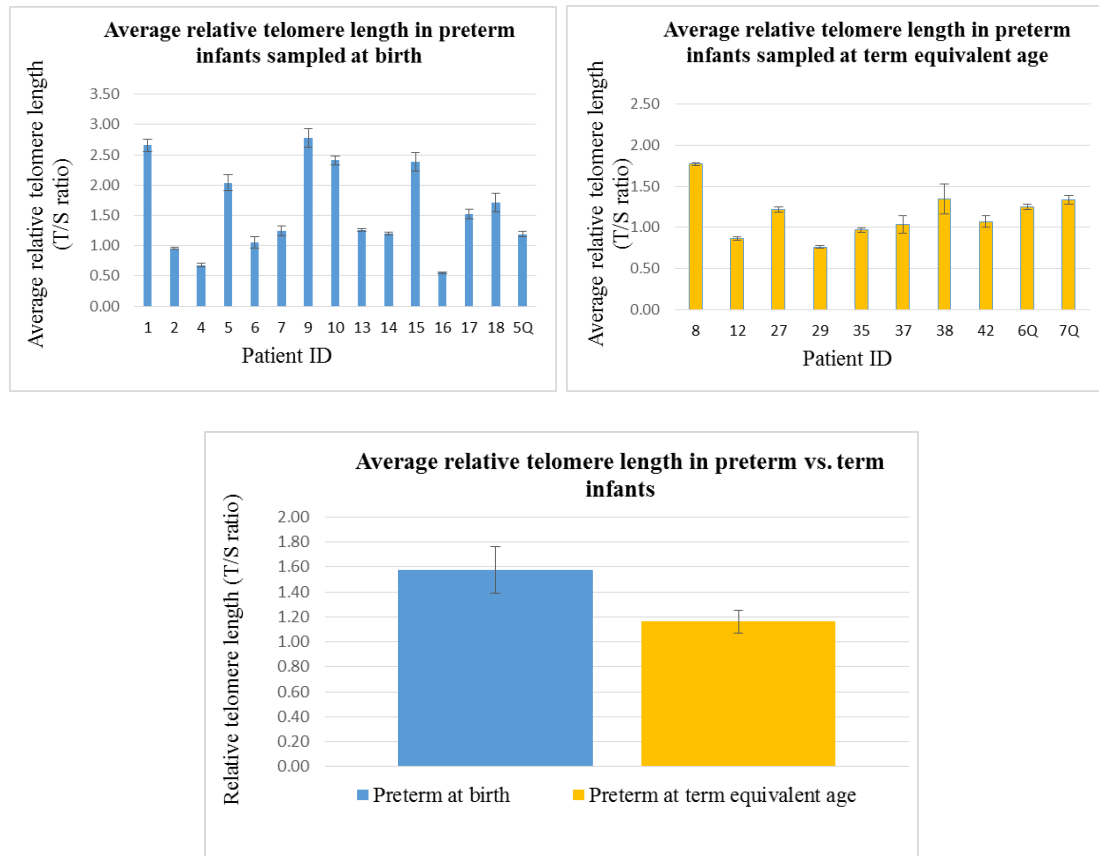


Figure 6.1: Average relative telomere length (as determined by T/S ratio following qRT-PCR) in preterm infants sampled at birth (top left) and preterm infants sampled at term equivalent age (top right). Mean telomere length is longest in preterm infants sampled at birth (bottom), however this difference is not significant ($p = 0.10$). Error bars represent standard error of the mean.

6.3.3 Specific aim 4c. Using the same methodology to test the hypothesis that at term equivalent age, preterm infants have reduced average relative telomere length compared to term born controls

In order to compare average relative telomere lengths in term born babies with that of preterm infants at term equivalent age, again average relative telomere length was assessed by qRT-PCR, this time in 25 term born controls. In term born controls T/S ratios ranged from 0.44 to 1.98 (albeit with the second highest T/S ratio being 1.31). A Shapiro-Wilk test also confirmed normality within this population ($p = 0.13$), and therefore it was deemed appropriate to perform parametric statistical analysis. The mean T/S ratio in term born controls was 0.94 compared to 1.16 in preterm infants sampled at term equivalent age (results shown in figure 6.2). However a student's t-test confirmed that again, this difference was not significant ($p = 0.07$).

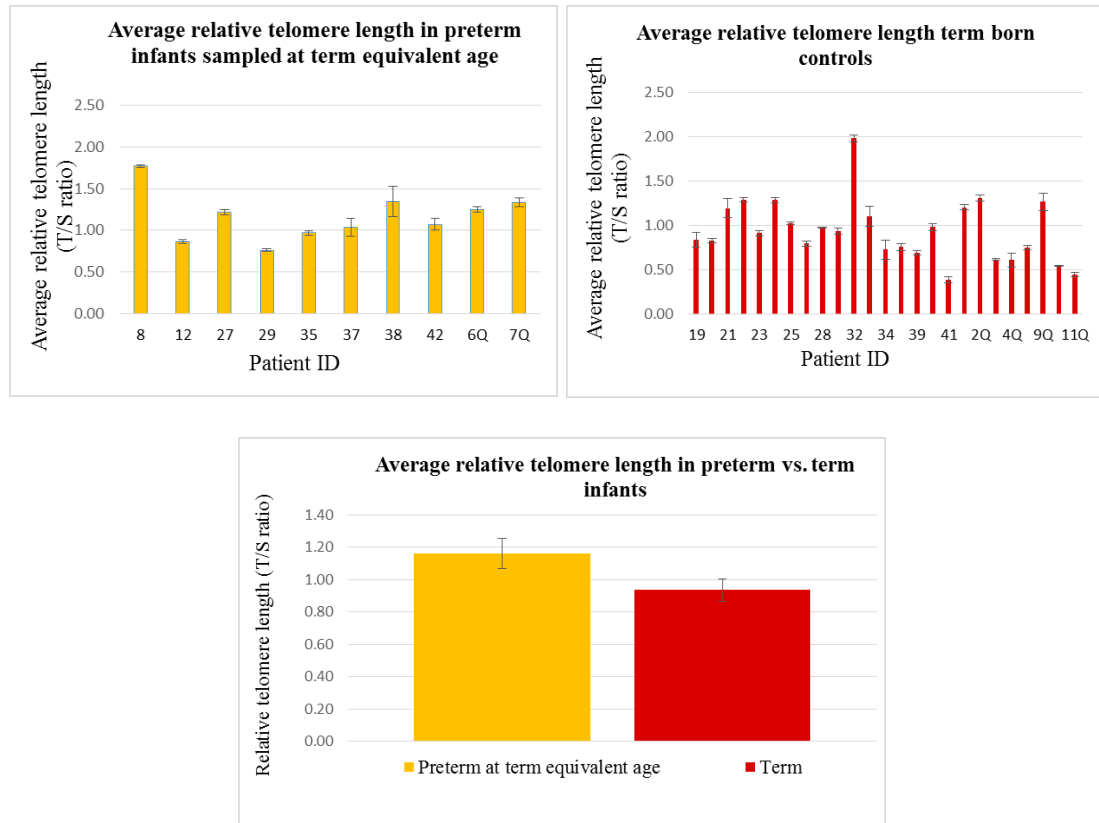


Figure 6.2: Average relative telomere length (as determined by T/S ratio following qRT-PCR) in preterm infants sampled at term equivalent age (top left) compared to term born controls (top right). Mean telomere length is longest in preterm infants (bottom), however this difference is not significant ($p = 0.07$). Error bars represent standard error.

6.3.4 Specific aim 4d. To test the hypothesis that, in each of the three groups (preterm at birth; preterm at term; term born controls) overall telomere length correlates to gestational age, birth weight, maternal age, maternal body mass index and/or mode of delivery

Following measurement of average relative telomere length by qRT-PCR, results were assessed in relation to gestational age, birth weight, maternal age, maternal body mass index (BMI) and mode of delivery in each of the three groups of infants recruited to the study. In all patient cohorts, it was found that telomere length did not correlate with any of the above criteria. These results are illustrated in figures 6.3, 6.4 and 6.5. Furthermore a univariate ANOVA revealed no relationship between telomere length and mode of delivery in any of the study groups ($p = 0.60$ for preterm infants sampled

at birth, $p = 0.94$ for preterm infants sampled at term equivalent age, $p = 0.73$ in term born infants).

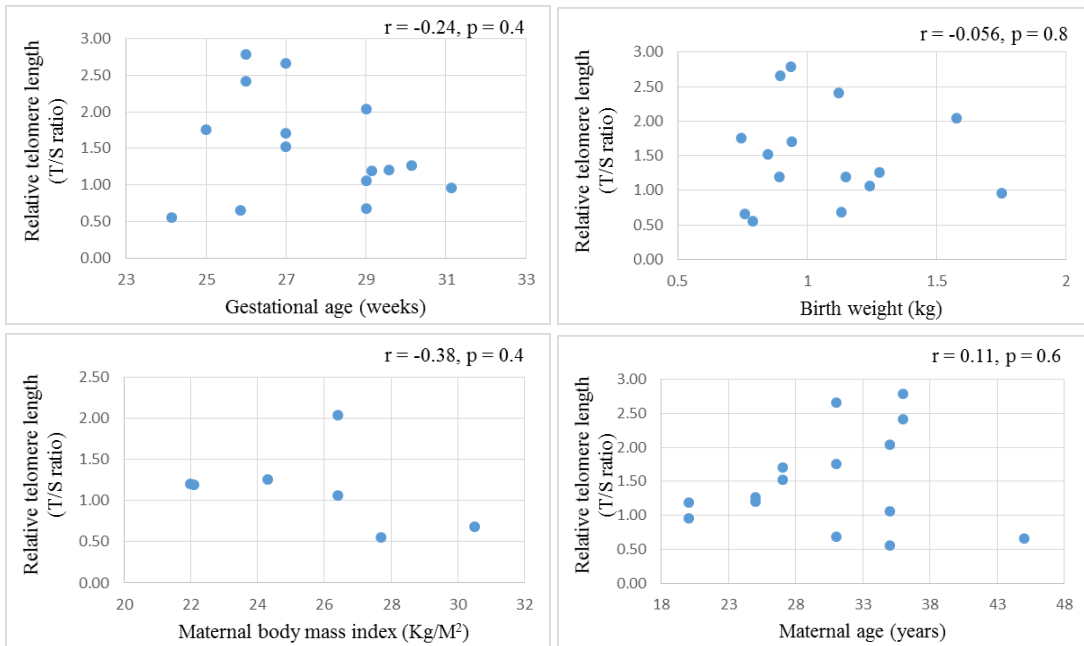


Figure 6.3: Correlation between gestational age (top left), birth weight (top right), maternal body mass index (bottom left) and maternal age (bottom right) with relative telomere length (T/S ratio) as determined by qRT-PCR in preterm infants sampled at birth. No correlation is present amongst any of the variables tested.

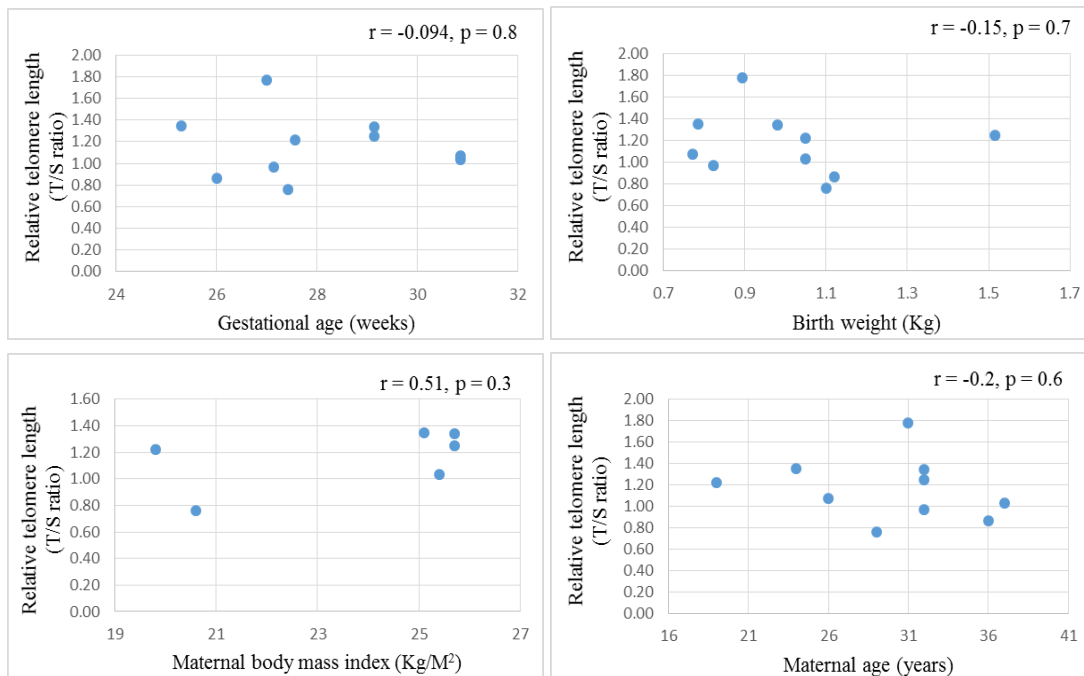


Figure 6.4: Correlation between gestational age (top left), birth weight (top right), maternal body mass index (bottom left) and maternal age (bottom right) with relative telomere length (T/S ratio) as determined by qRT-PCR in preterm infants sampled at term equivalent age. No correlation is present amongst any of the variables tested.

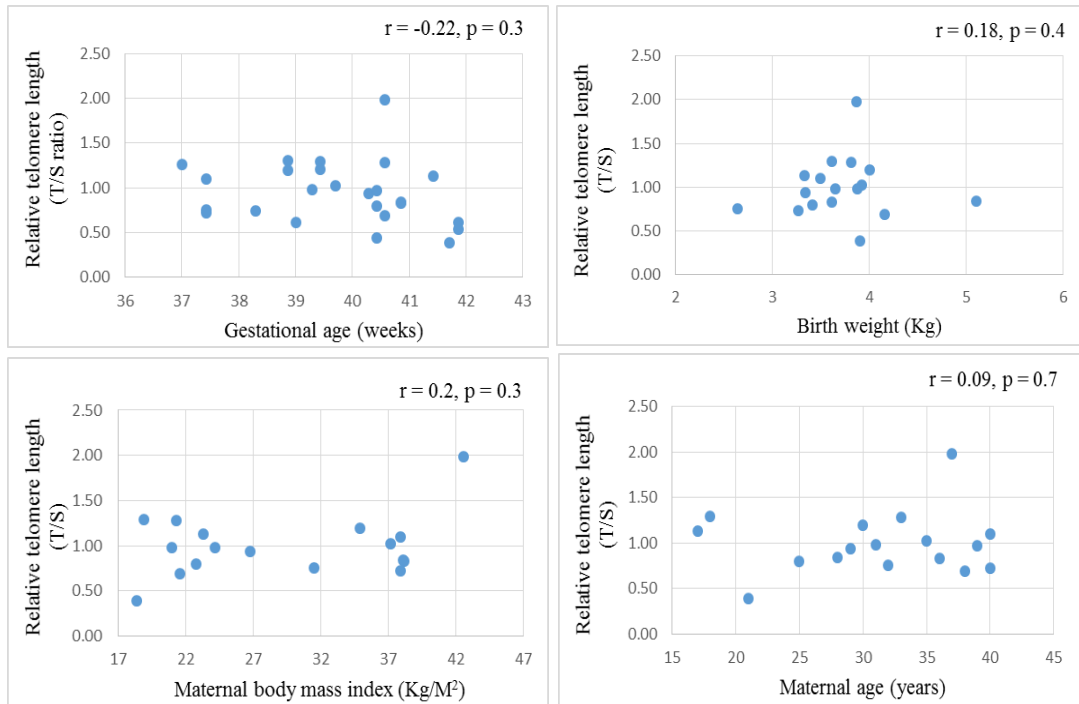


Figure 6.5: Correlation between gestational age (top left), birth weight (top right), maternal body mass index (bottom left) and maternal age (bottom right) with relative telomere length (T/S ratio) as determined by qRT-PCR in term infants. No correlation is present amongst any of the variables tested.

6.3.5 Specific aim 4e. To test the hypothesis that individual telomeres are prematurely shortened in preterm infants at term equivalent age

Telomere length analysis of individual chromosome arms were assessed in all autosomes in order to test the hypothesis that following birth, telomere lengths of specific individual chromosome arms (as yet not identified) are reduced in preterm infants by term equivalent age, leading to reduced telomere lengths compared to term born controls. Sex chromosomes were excluded from this analysis since they do not necessarily represent a homologous pair from which an average measurement of p and q arms can be obtained. Due to the significant work load required for QFISH analysis (as described in section 2.2.16), telomere lengths of individual chromosome arms were assessed in a subset of the group, i.e. five preterm infants sampled at birth, five preterm infants sampled at term equivalent age and five term born controls. At least five metaphase cells hybridised with the telomere specific PNA probe and counterstained with DAPI were captured, karyotyped with the aid of SmartType 2 (Digital Scientific),

and analysed for telomere fluorescence signal intensity using TFL-Telo T/S ratio (see section 2.2.16.6). Figure 6.6 shows an example of a QFISH image and karyotype.

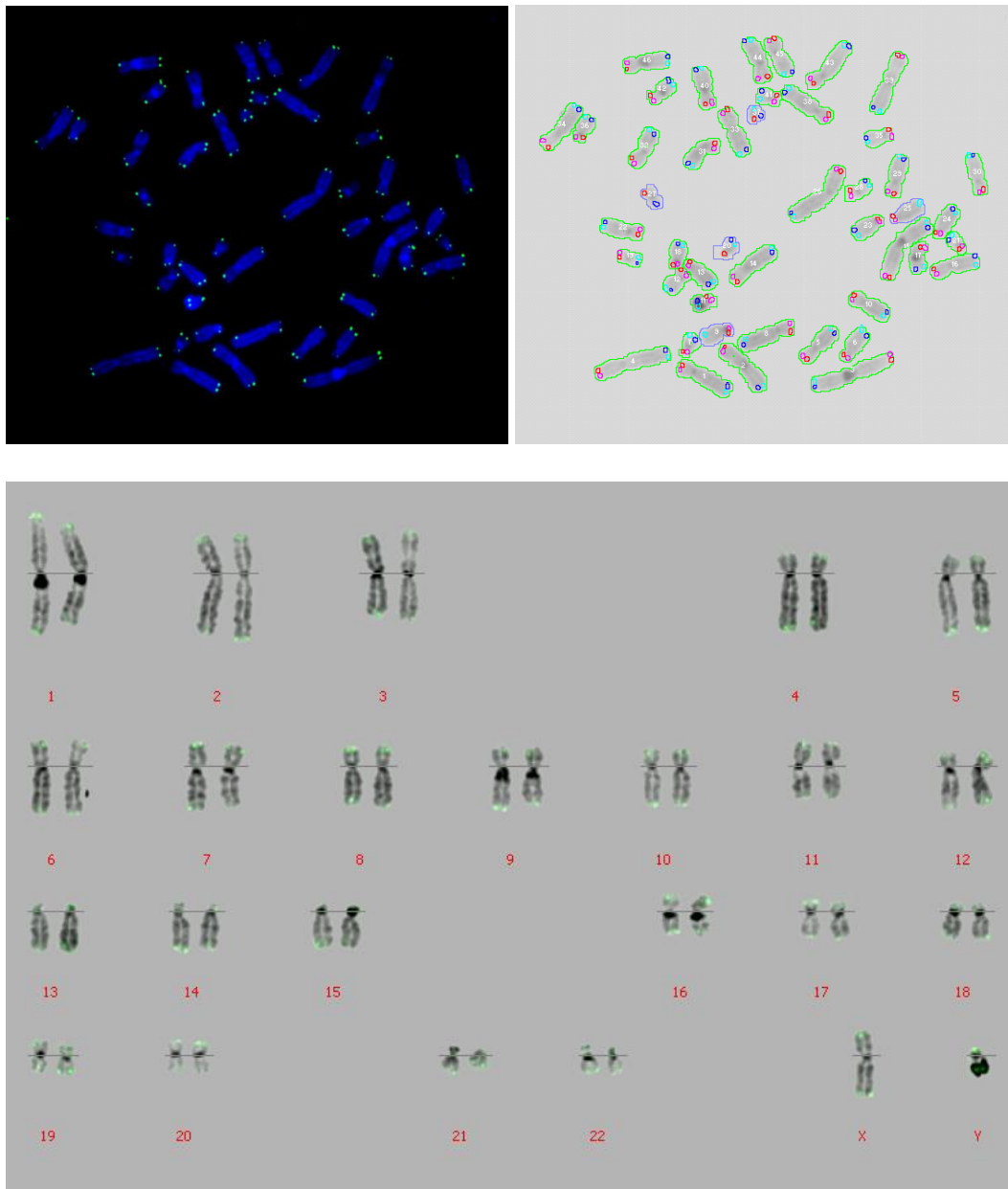


Figure 6.6: Example of an image acquired following QFISH procedures (top left) and detection of chromosomes and telomeres for fluorescence analysis of telomere spots in TFL-Telo (top right). The raw QFISH image was karyotyped with the aid of SmartType 2 (bottom) in order to assign chromosome number to each measured chromosome.

Visual inspection of the overall data demonstrated a consistent pattern in which telomere lengths of individual p and q arms from each chromosome are approximately equal among both preterm groups, and consistently longer in term born controls compared to both preterm groups. However, the level of variation among these

measurements is very high, which is consistent with other published data utilising QFISH for analysis of telomere length (Poon et al., 1999; Wong and Slijepcevic, 2004). This high level of variation meant that despite the observed pattern, a multivariate ANOVA confirmed that telomere length was not statistically different between specific chromosome arms of specific chromosomes within groups, nor between groups ($p = 0.92$). Thus there is no apparent effect of telomere length alteration in any one specific chromosome arm in any of the groups assessed. In other words I could find no evidence to support the hypothesis that any individual telomere(s) were significantly shortened in premature babies. Results are shown in figure 6.7.

In the analysis shown, for the most part, the signal intensities for the term born babies was around twice that of the other two groups. Given that the qRT-PCR results indicated that there was no overall difference between the groups, the two sets of results appear at odds. In point of fact the QFISH was only meant as a means of determining the *relative* lengths of individual p and q arm telomeres compared to one another, within the same patient or group. It is theoretically possible that preparations from term born babies produce higher hybridisation efficiencies for some unbeknownst technical reason that is not related to telomere length. For this reason, in figure 6.8, I manipulated the data so that the mean overall telomere length in each group was the same. This normalisation factor was calculated by dividing the overall average telomere length in all chromosomes from all patients across all groups, by the average telomere length in all chromosome arms from each individual group. In doing so, results further confirmed that, no individual telomere from any particular chromosome was significantly shorter nor longer in any of the groups. This is illustrated in figure 6.8 and confirmed by a multivariate ANOVA ($p = 0.92$).

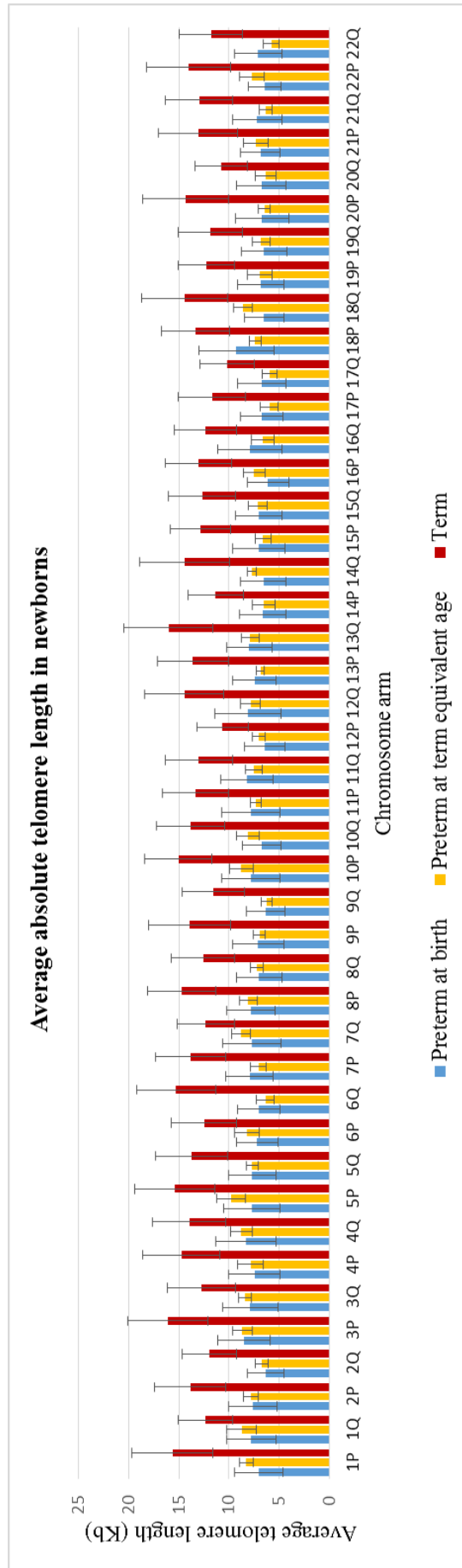


Figure 6.7 Average absolute telomere lengths of individual p and q arms from each chromosome in preterm infants sampled at birth (blue), preterm infants sampled at term equivalent age (yellow) and term born controls (red). Among all individual p and q arms from each chromosome, telomere length is consistently approximately equal between preterm infants sampled at birth and preterm infants sampled at term equivalent age. Similarly, telomere length is consistently longer in term controls compared to both other groups regardless of the chromosome or the chromosome arm. Therefore these results show no chromosome specific effect on telomere length among the different groups. Error bars represent standard error of the mean.

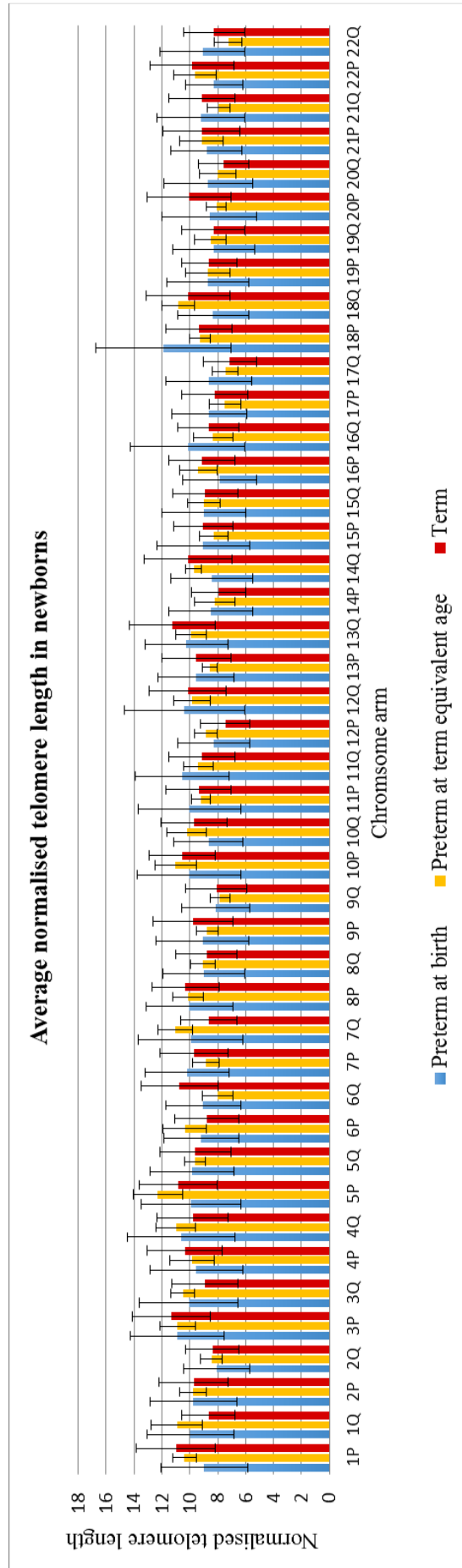


Figure 6.8: Normalised average absolute telomere lengths of individual p and q arms from each chromosome in preterm infants sampled at birth (blue), preterm infants sampled at term equivalent age (yellow) and term born controls (red). Among all groups, telomere lengths of individual p and q arms are similar. Error bars represent standard error of the mean.

6.4 Discussion

6.4.1 Recruitment of preterm infants and term born healthy controls

Over the course of approximately 42 months, a total of 50 patients were recruited and sampled from the William Harvey Hospital (Ashford, Kent) or the Queen Elizabeth Queen Mother Hospital (Margate, Kent). Recruitment of both term and preterm infants to clinical research studies can be challenging. In the population of babies studied, parents were likely to have had concerns about the wellbeing of their baby and so participating in clinical research is often felt to be an additional burden or risk. Nonetheless, I was able to obtain samples from 15 preterm infants sampled at birth, 10 preterm infants sampled at term and 25 term infants sampled at birth. Although the target sample size was not quite reached, the data collected from these patients still represents one of the largest sample sizes in this study population. Moreover, to the best of my knowledge, none have attempted to measure telomere length in the preterm infant at term equivalent age and therefore this data represents a unique contribution to the field of neonatology.

6.4.2 Relative telomere length in preterm infants at birth compared to preterm infants term equivalent age

Results in section 6.4.1 revealed that there is a decline in telomere length from the time of preterm birth to term equivalent age in preterm infants. Although these results were not of statistical significance at the $p = 0.05$ level, they are in keeping with the pattern observed in previously published studies that have shown a rapid decline in telomere length in preterm infants following birth (Friedrich et al., 2001; Holmes et al., 2009; Menon et al., 2012). However, the magnitude of this difference was less pronounced in my own data in comparison to findings from other studies. One possible explanation for this, is that the design of my own study, as well as the numbers recruited were not powerful enough to do so. In the present study it was not possible to sample the same preterm infant at birth and again at term equivalent age, therefore it is possible that natural variation in telomere length (Allsopp et al., 1992; Hastie et al., 1990; Okuda et

al., 2002; Rufer et al., 1999), along with the small sample sizes may have weakened the statistical power of the trends observed here.

Alternatively, it is also possible that other studies may have over-estimated the differences in telomere lengths of preterm infants in relation to gestational age, which may be attributable to technical aspects in measuring telomere length. Other studies (Friedrich et al., 2001; Holmes et al., 2009) have utilised TRF analysis, which is a technique that also measures the highly variable subtelomeric region, and therefore differences in TRF length cannot be solely accountable to differences in true telomere length (Baird et al., 1995; Levy et al., 1992; Mefford and Trask, 2002; Riethman et al., 2005). Furthermore, DNA storage and extraction techniques differ among each of the previously published studies and the study presented here, which has also been shown to effect results obtained from telomere length analysis (Cunningham et al., 2013; Zanet et al., 2013).

In addition, there are several biological factors that may lead to an over-estimation of the magnitude of telomere attrition following preterm birth in other studies. For example, it is possible that a difference in cell type composition among these patients might have had ramifications on the results obtained. Preterm infants have previously been shown to possess altered blood cell composition (Berrington et al., 2005), and it is well known that telomere lengths are not equal among different cell types (Hoffmann et al., 2009; Lansdorp, 2008; Spyridopoulos et al., 2008). Finally, as described in section 1.2.1.5, there are many factors besides replicative history that might affect telomere length. These include genetic, epigenetic and environmental influences, along with exposure to oxidative stress, inflammation or infection, which could influence leukocyte cell turnover rate and in doing so affect telomere length (Aviv et al., 2006).

Alternatively, it is possible that the magnitude of telomere attrition observed in other studies is present only in some individuals. In the present study there was a large range of T/S ratios in the preterm group sampled at birth in which some had very high T/S ratios, whereas in the preterm group sampled at term equivalent age this range was much narrower. With this in mind, it is likely that should the sample size be increased in future work, the overall trend observed here would gain statistical power.

6.4.3 Relative telomere length in preterm infants at term equivalent age compared to term born controls

As shown in figure 6.2, when average relative telomere length was compared in preterm infants sampled at term equivalent age with that of term born controls, although telomere length was slightly longer in the preterm group, this difference was not significantly different. Therefore, although telomere length likely declines following preterm birth based on evidence reported here and by others (Friedrich et al., 2001; Holmes et al., 2009; Menon et al., 2012), this does not result in shorter average telomere length by term equivalent age in the preterm infant compared to term born counterparts. To the best of my knowledge, this is the first study to attempt such a comparison, and therefore this result contributes a novel finding to the field of neonatology.

It is possible that low sample size and the range of aforementioned biological factors impacting individual telomere length might have influenced the results obtained here. Furthermore, it is possible that other medical complications that warranted blood sampling in the term group may have affected their telomere lengths e.g. the presence of infection (Aviv et al., 2006; Ilmonen et al., 2008; Pawelec et al., 2005; Vallejo et al., 2004). However, it is equally likely these results can be explained by the possibility that telomere attrition rate is the same *in utero* as it is *ex utero*. Such an event would lead to similar telomere lengths in the preterm infant at term equivalent age to that of the term born infant, in agreement with data presented here. Although this scenario contradicts what has previously been found by Holmes *et al* 2009, her study included only 5 preterm infants and therefore in light of the findings from the present study, it would be interesting to revisit this in future investigations.

Overall, based on the information from sections 6.3.2, it is unlikely that average relative telomere length can act as a biomarker for the aged phenotype associated with premature birth. However, both sections provide interesting additional information to what it currently known about telomere regulation in this largely under-explored study population.

6.4.4 Correlation of telomere length with gestational age, birth weight, maternal age, maternal BMI and mode of delivery

Previous studies have shown that telomere length in the preterm infant is correlated with gestational age, birth weight and maternal age (Akkad et al., 2006; Friedrich et al., 2001; Holmes et al., 2009; Menon et al., 2012), however in the present study, no such correlations were observed. It is unlikely that this effect is due to telomere maintenance mechanisms *in utero*, since evidence from section 4c shows that telomere lengths in the term born infant are not reduced overall in comparison to telomere lengths in the preterm infant when sampled at birth. Furthermore, a study by Cheng *et al* 2013 showed that telomerase expression gradually decreases in the developing fetus (although this study assessed fetuses between six and 11 weeks gestation) (Cheng et al., 2013b). Based on the data shown in section 4b, the most probable explanation for this finding is the small range in the parameters studied, and the highly heterogeneous nature of telomere lengths in preterm infants, particularly those sampled at birth. This represents a previously unreported finding, which is consistent with the heterogeneous nature of telomere lengths assessed in full term newborns (Lim et al., 2013; Okuda et al., 2002) and other study populations (Allsopp et al., 1992; Hastie et al., 1990; Rufer et al., 1999).

When telomere length was assessed in relation to the same criteria described above in term born controls, results showed that again, telomere length was not correlated with gestational age, birth weight or maternal age. These findings are in partial agreement with others who also found that telomere length was not associated with gestational age or birth weight, but is in disagreement with these other studies in that they did find a correlation between infant telomere length and maternal age (Akkad et al., 2006; Okuda et al., 2002). Given that infant telomere length ought to be influenced by both maternal and paternal contributions, it is perhaps unsurprising that no correlation could be found here, since paternal contribution is ignored. Indeed several studies in the past have highlighted that telomere length in the offspring is paternally inherited (Kimura et al., 2008; Njajou et al., 2007; Unryn et al., 2005), and therefore in future investigations it would be interesting to assess such correlations, and interpret contributions from both parents.

Finally, infant telomere length did not appear to be correlated with maternal BMI or mode of delivery in any of the groups studied. To the best of my knowledge, these factors in relation to infant telomere length have thus far not been explored and therefore represent some interesting new findings. Taken into consideration with the rest of the data presented in this section, these results indicate that overall, in a given population, telomere length remains remarkably stable despite the potential influence of factors known to affect neonatal health outcome. However, the high level of variation among telomere lengths of different individuals suggest that it is unlikely that telomere maintenance mechanisms are involved in this observation. It is therefore possible that the parameters assessed can influence infant telomere length on an individual level, however in order to study this effect, it will be necessary to include much larger sample sizes in future investigations in order to generate meaningful interpretations.

6.4.5 Telomere lengths of individual chromosome arms

Data presented in section 6.3.2 suggest that average relative telomere length is not reduced in preterm infants by term equivalent age compared to term born controls. However others have proposed that analysis of critical telomere length of specific telomeres represents a major contributor to cellular senescence and loss of tissue function associated with ageing (Faragher and Kipling, 1998; Hemann et al., 2001b; Martens et al., 2000; Martens et al., 1998). For this reason, QFISH analysis was performed in a subset of five patients from each group, in order to ascertain whether critical telomere length might act as a marker for the aged phenotype observed in preterm infants.

In general, results from QFISH analysis showed that telomere lengths of p and q arms on each specific chromosome was consistently longest in the term born control group, and approximately equal in both preterm groups. However, statistical analysis revealed that these results were not different from one another within or between the different groups assessed. In order to reduce the influence of the high level of variation in the interpretation of these measurements (as indicated by the large error bars in figure 6.7), results were normalised against this variability as described in section 6.3.5. As shown in figure 6.8, results confirmed the same overall finding, indicating that despite high variability in the results obtained by QFISH, which is well documented by others

(Aubert et al., 2012; Poon et al., 1999; Wong and Slijepcevic, 2004), the overall result is likely reflective of the biological system under assessment.

Of course it is possible that the low sample size, along with the low numbers of metaphase images analysed may contribute to this finding. On account of this, in the future it would prove beneficial to analyse more metaphase cells from a larger number of patients in order to re-visit this topic. Indeed, others recommend that at least 10-20 metaphases are analysed for each individual (Poon et al., 1999; Wong and Slijepcevic, 2004), however due to time restrictions, it was not possible to do this in the present study. Nonetheless, this study represents the first of its kind. To the best of my knowledge no other studies have attempted to measure individual telomere lengths in newborns before, and none have addressed whether any chromosome specific differences exist in telomere lengths between those born prematurely compared to those born at full term.

6.5 Conclusion

On the whole, results from this chapter indicate that while average telomere length is reduced in preterm infants by term equivalent age, this does not render individuals born prematurely with telomeres that are shorter than those of individuals born at full term. Taken together with results from QFISH analysis, neither average telomere length nor telomere lengths of specific chromosome arms are likely to be a suitable biomarker for predicting the morbidities associated with the aged phenotype in preterm infants. These results support findings from other similar studies in this field, and add valuable new preliminary information with regard to telomere length in the preterm infant at term equivalent age.

7 General discussion

Overall, this thesis was largely successful in achieving its specific aims, that is;

1. Nuclear organisation was assessed in the sperm heads of males with severely compromised semen parameters compared to those of normal fertile males, through assaying the position of telomeres and their associated proteins. Evidence presented from these analyses showed that nuclear organisation is altered in the sperm heads of males with compromised semen parameters. Furthermore, it is possible that this might be the result of improper chromatin packaging overall in these sperm nuclei.
2. An experimental means for measuring telomere length from low starting quantities of DNA in small sample sizes from newborns, and from whole genome amplified material derived from single cells was achieved. Previously published protocols for multiplex qRT-PCR analysis of telomere length from genomic DNA, and singleplex qRT-PCR analysis of telomere length from whole genome amplified material were optimised for use with the Rotor-gene Q real-time PCR machine. A search of the literature published at the time of writing indicated that these experiments have not been optimised for use with the Rotor-gene Q real-time PCR machine before, and indeed the singleplex approach for analysis of telomere length in single cells has previously been attempted only once.
3. Telomere length was successfully assessed in relation to reproductive ageing in women, as determined by the relationship between telomere length and maternal age and the incidence of aneuploidy in first polar bodies and cleavage stage embryos. The main outcomes from this research do not support the telomere theory of reproductive ageing in women, as indicated by an absence of telomere attrition in relation to both maternal age and incidence of aneuploidy in first polar bodies and cleavage stage embryos.
4. Using qRT-PCR and QFISH approaches, average telomere length and telomere lengths of specific chromosome arms respectively were assessed in preterm

infants at the time of term equivalent age in comparison to preterm infants at the time of birth and healthy full term infants. qRT-PCR experiments confirmed that average telomere length is reduced in the weeks following preterm birth, however the magnitude of this reduction by term equivalent age was not sufficient to render premature infants with shorter telomeres than healthy full term newborns. In addition, QFISH analysis showed that no specific chromosome arm was reduced in the preterm infant compared to full term controls.

The main outcomes of this work represent many previously under-explored topics in relation to the role of telomeres in human fertility, embryogenesis and early infancy. The significance of the findings from each of the chapters in this thesis are discussed under their respective results sections, and therefore will not be repeated here, however the wider implications of these results will be discussed hereafter.

7.1 Biomarkers of ageing and age-related disorders

Since it was discovered that the proliferative capacity of the cell might be related to telomere shortening as a result of incomplete DNA replication (Hayflick and Moorhead, 1961; Olovnikov, 1973; Watson, 1972), a large collection of studies have attempted to investigate whether this phenomenon is involved in the process of cellular and organismal ageing. While many have showed that telomere shortening is related to the process of ageing *in vitro* and *in vivo* (Allsopp et al., 1992; Cawthon et al., 2003; Frenck et al., 1998; Harley et al., 1990; Hastie et al., 1990; Lindsey et al., 1991; Rufer et al., 1999), others have shown no such relationship (Harris et al., 2012; Honig et al., 2006; Martin-Ruiz et al., 2011; Martin-Ruiz et al., 2005). Therefore the usefulness of telomere length as a biomarker of ageing is still widely debated and largely unknown (Mather et al., 2011; Sanders and Newman, 2013; von Zglinicki, 2012). There are several reasons that have been attributed to this lack of transparency, including those of both practical and biological nature. To summarise, study design, sample size and methodology utilised for measuring telomere length form the main practical considerations, and the high variability in telomere length between individuals due to various genetic, epigenetic and environmental influences form the main biological considerations (Aviv et al., 2006; Mather et al., 2011; Sanders and Newman, 2013). As

a result of these, many have argued that in fact telomere length is not a useful indicator of biological ageing (Aviv et al., 2006; Baird, 2005; Shiels, 2010; von Zglinicki and Martin-Ruiz, 2005), which is further supported by previous observations that senescence may occur in the absence of telomere loss (Hayflick, 1998, 2003). Alternatively, others have argued that N-glycome analysis (Dall'Olio et al., 2013), or cell cycle regulators cyclin dependant kinase inhibitor 2A (CDKN2A) and cyclin dependant kinase inhibitor 1A (CDKN1A) may act as more accurate biomarkers of aging (Gingell-Littlejohn et al., 2013; Koppelstaetter et al., 2008; Pathai et al., 2013).

With the above information in mind, given that results from this thesis suggest that telomere length cannot act as a biomarker for the health outcomes associated with a prematurely aged phenotype in the preterm infant, it would be interesting to pursue the aforementioned alternative biomarkers of ageing in light of these phenotypes (Bhat et al., 2012; Thomas et al., 2008a; Tinnion et al., 2013; Uthaya et al., 2005; VanDeVoorde and Mitsnefes, 2014; Vasu V and N, 2009). Alternatively, evidence has highlighted that abrupt changes in the environment imposed by preterm delivery leads to alterations in the epigenetic profile of the neonate, which in turn alters gene expression patterns and may influence the adult phenotype (Godfrey et al., 2007; Norman, 2010; Nuyt and Alexander, 2009; Ozanne and Constância, 2007). It is also known that the process of ageing and the pathogenesis of age related diseases is related to changes in epigenetic status (Calvanese et al., 2009; D'Aquila et al., 2013; Fraga and Esteller, 2007). For this reason, it would be interesting to investigate the possible influence of epigenetic modification in the preterm infant on neonatal outcome.

Results from this thesis also indicated that telomere length is unlikely to act as a marker for reproductive ageing (in women). This may be reflective of the aforementioned practical and/or biological influences on the data obtained, or alternatively, may indicate that other mechanisms are behind increased aneuploidy rates and the decline in reproductive potential experienced by women of advanced maternal age. Alongside those previously identified (e.g. DNA damage, meiotic checkpoint errors) (Burgoyne et al., 2009; Wang and Höög, 2006), one that was not investigated here is nuclear organisation in the oocyte during maturation, and in particular telomere distribution, which is known to play a key role in synapsis. To the best of my knowledge this has not been previously addressed in humans for practical reasons, however in mice, mutation in SUN1 (which is responsible for guiding telomere led bouquet arrangement

of chromosomes in meiosis) leads to the absence of mature oocytes, and impaired chromosome alignment, recombination and synapsis (Ding et al., 2007). This indicates that telomere distribution may be important in the faithful segregation of chromosomes in the oocyte, and therefore might act as a marker for reproductive ageing in women. Overall therefore, the future of research into novel tools that might identify reproductive ageing in women and aid fertility treatment yields much to be uncovered.

7.2 Diagnostics in male infertility

In addition to improvements in preimplantation genetic screening techniques, the search for improvements in the currently available tools for diagnosis of infertility continues. In 40-50% of couples experiencing reproductive difficulties, a male factor is at least a part of the underlying cause (Sharma et al., 1999). This may arise from genetic, hormonal or physical complications, however in many cases the exact cause is unknown (idiopathic). This has been reported to range anywhere between approximately 15% and 50% of male infertility cases (Irvine, 1998; Kumar et al., 2006; Seli and Sakkas, 2005). Several advances in the detection of novel biomarkers of male infertility have occurred in recent years, including improvements in the detection of Y chromosome anomalies via microarray based technologies (Yuen 2014), analysis of oxidative stress (Benedetti et al., 2012; Chen et al., 2013; Guz et al., 2013; Novotny et al., 2013; Sharma et al., 1999), sperm DNA fragmentation (Sharma et al., 2010), metabolomics (Jayaraman et al., 2014) and proteomics (Amaral et al., 2013; Barazani et al., 2014; Rahman et al., 2013; Xu et al., 2012; Zhao et al., 2007). Despite these advances however, reference ranges are difficult to establish, and therefore much research is still required. As identified in this thesis, nuclear organisation in the sperm head also represents an interesting topic worthy of further investigation in the search for new diagnostic tools. Automation of a method in which objective quantification of telomere distribution signals can be assayed in the sperm nucleus might prove a promising new test in the fertility clinic yet. Furthermore, one topic that was not addressed in this thesis is the subject of telomere length in sperm in relation to male infertility. Indeed other studies have revealed preliminary evidence to show that reduced sperm telomere length is related to male factor infertility (Ferlin et al., 2013; Thilagavathi et al., 2013), however further investigation will be required in the future

to quantify a sperm telomere length threshold from which the infertile male may be identified.

7.3 Does assessment of telomere length or distribution have a role in the future of preimplantation genetic screening (PGS)?

Much of the controversies surrounding the efficacy of PGS and its ability to improve the outcome of fertility treatment remain very active to date (Gleicher et al., 2014; Harper and Harton, 2010; Scott Jr et al., 2013). While the origin of conflicting data regarding PGS efficacy is likely to be in part down to the mosaic nature of the preimplantation embryo (Bielanska et al., 2002; Colls et al., 2007; Hanson et al., 2009; Harton et al., 2011), technical errors in the methodology used are also likely to impact on the diagnosis made (Harper et al., 2010; Mastenbroek et al., 2011; Northrop et al., 2010). As a result, methods of detecting genetic abnormalities are continuously being developed and improved in order to enhance the chances of pregnancy in couples undergoing ART. This raises the question of whether assaying either telomere length (as in chapter 5) or telomere distribution (as in chapter 3) might have a role to play in PGS treatment.

The first technique developed for PGS was FISH, allowing the detection of chromosome copy number of a few chromosomes commonly involved in human aneuploidies (Griffin et al., 1993; Munné et al., 2005). However many found that the application of FISH in PGS actually showed no benefit in enhancing IVF outcome (Delhanty et al., 1993; Mastenbroek et al., 2007; Schoolcraft et al., 2009; Staessen et al., 2004; Staessen et al., 2008). Since this time, the FISH protocol has been adapted for comprehensive aneuploidy screening of all 24 chromosomes (Ioannou et al., 2012; Ioannou et al., 2011), however, the labour intensive and time consuming nature of this protocol render it unsuitable in the PGS setting. Were blastomeres still being screened routinely by FISH then it would have been relatively simple to ask whether telomere distribution was a marker of either aneuploidy and/or compromised developmental potential. In this study I did try to obtain human embryos spread on slides in order to test this hypothesis however time and ethical considerations precluded it.

Currently, with the emergence and continued improvement of WGA techniques in single cells, alternative approaches to PGS have evolved. aCGH procedures were

developed as a fully automated technique capable of screening all 24 chromosomes within a 24 hour time window, allowing fresh transfer of selected embryos and improved accuracy (Hellani et al., 2008; Wells et al., 2008). Evidence shows that use of aCGH in polar bodies, blastomeres or trophoctoderm biopsies has improved pregnancy rate and resulted in successful live births (Fragouli et al., 2010; Geraedts et al., 2011; Yang et al., 2012). Alternatively, a qRT-PCR based approach has been developed for the comprehensive screening of copy number in all chromosomes (Treff and Scott Jr, 2013; Treff et al., 2012). Arguably the most promising development in PGS techniques however, is the ability to detect both single gene disorders and chromosome copy number simultaneously in the form of SNP analysis, which has led to many reports of improved IVF success rates (Brezina et al., 2011; Northrop et al., 2010; Scott Jr et al., 2012; Treff et al., 2010a; Treff et al., 2010b). Detection of genetic errors in this way was the basis for a now commercially available preimplantation genetic diagnosis programme known as Karyomapping. This technique allows detection of trisomies, monosomies, uniparental disomy, deletions, duplications, translocations, and single gene disorders simultaneously, through information gathered from Mendelian inheritance based analysis of SNP arrays from each parent and a reference genome (usually a sibling) (Handyside et al., 2010; Handyside et al., 2009). Finally, many have focused on the application of the now relatively inexpensive next generation sequencing techniques in PGS (Fiorentino et al., 2014; Martín et al., 2013; Treff et al., 2013; Wang et al., 2014; Wells et al., 2014). Nonetheless, despite the development of these novel tools for complete genetic screening in ART, it remains unclear how effective these techniques really are in achieving their goal – that is, in improving IVF success rates (Gleicher et al., 2014; Mastenbroek and Repping, 2014). Thus the emergence of well-rounded and properly conducted randomised clinical trials in the use of PGS remains eagerly awaited in future studies. It is my understanding that several randomised clinical trials are underway at the present time, and therefore the results of these should be at the forefront of our horizon. What is clear from my results in chapter 5 however, is that telomere length may not be a consideration for a new test in PGS.

7.4 The future of telomere studies

Despite the large number of studies investigating telomere biology over the last 50 years, a great deal remains to be unveiled. The tight regulation of their length and structure is highly complex, and how this complex balance might specifically contribute to the process of cellular ageing and the pathogenesis of disease largely continues to be a mystery. Future studies should focus on generating robust reference ranges in order to recognise telomere length as a biomarker for ageing or specific disease conditions (Aviv et al., 2006; Mather et al., 2011; Sanders and Newman, 2013). Furthermore, there is much to be uncovered regarding the epistatic modifications of the telomere sequence, and how this effects the regulation of other genes. The telomere position effect (TPE) (which describes the silencing of genes near the telomeres as a result of epigenetic modifications) has been extensively studied in yeast and *Drosophila* models (Blasco, 2007), however relatively little is known of its mechanisms and effects in mammals, particularly in humans. Indeed, one of the first studies to illustrate TPE in human cells proposed that the alterations in gene expression profiles as a result of TPE may in fact contribute to cell and organ function and in turn the process of ageing and the development of disease (Baur et al., 2001). TPE is able to both regulate, and be regulated by the length of the telomere, however, again, much of the mechanisms surrounding this regulation in mammals is yet to be identified (Blasco, 2007; Dan et al., 2014; Episkopou et al., 2014; García-Cao et al., 2004; Gonzalo et al., 2006). Of particular interest in light of the data presented in this thesis, is the potential involvement of human homologues of the yeast silent information regulator (Sir) proteins in TPE, which are known to co-localise with the telomere at the nuclear periphery (Blasco, 2007; Palladino et al., 1993). This defines an additional functionally relevant role of telomere distribution at the nuclear membrane in telomere length maintenance (Palladino et al., 1993). It would be interesting to ascertain whether similar mechanisms are involved in the human sperm nucleus, and whether this in turn has ramifications for paternal telomere length maintenance and contribution to offspring telomere length. In addition, it is thought that the first part of the paternal genome to respond to oocyte activation signals is the telomeres (Zalenskaya et al., 2000), and therefore it would be interesting to ascertain whether TPE in the paternal genome is important for transcriptional regulation in the zygote.

Furthermore, the direct and indirect molecular pathways involved in the influence of the various genetic and environmental factors on telomere length remain to be established. Likewise it is unclear how telomere length might be inherited and reset in the developing human embryo. While several studies have implicated a paternal inheritance of telomere length (Kimura et al., 2008; Njajou et al., 2007; Unryn et al., 2005), more recent evidence has shown that in fact oocyte telomere length is longer than that of sperm (Turner and Hartshorne, 2013) and that infants born to older mothers possess longer telomeres (Lim et al., 2013). This suggests that telomere length is tightly maintained during oogenesis, which supports the data presented in chapter 5. Current evidence shows that, following fertilisation, telomere length is reset in the embryo predominantly via telomerase activity which increases at the blastocyst stage alongside embryonic genome activation (Treff et al., 2011b; Wright et al., 2001). It has also been shown that TPE plays a role in telomerase regulation in human embryonic stem cells (Zeng et al., 2014), however it is unknown how TPE may regulate expression of other genes during the process of embryogenesis. Interestingly, one study has also mentioned telomere localisation in the embryo, stating that telomeres appear to cluster in varying degrees depending on the stage of development (Turner et al., 2010). This may have implications for telomere lengthening mechanisms and the resetting of telomere length in the embryo, and thus warrants further investigation in the future.

Therefore overall, despite huge advancements in our understanding of the structure and regulation of telomeres over the past 50 years, we are far from fully understanding the contribution of these unique structures to normal and abnormal events in cell biology. This promises a very active future in telomere research, which will likely evolve with the continued improvements in telomere length analysis techniques.

7.5 Future studies arising from this thesis

The work presented in this thesis has helped to address many questions surrounding the involvement of dysfunctional telomeres in fertility and early life complications. However, in light of the observations made from this work, several avenues worthy of further exploration have arisen, and include the following areas:

1. The use of telomere distribution patterns in the diagnosis of male infertility, and the direct impact of altered telomere distribution in the sperm heads of infertile

males. As previously discussed, it is possible that normal telomere distribution at the nuclear periphery in the sperm nucleus plays a functional role in telomere length regulation and in gene expression patterns in the developing offspring via mechanisms of TPE. Further investigations into which proteins are involved in anchoring the telomere at the nuclear membrane within the sperm head, and how these might be involved in maintaining telomere structure would aid such research

2. The investigation of alternative measures of reproductive ageing in female gametes, which might include epigenetic markers or the presence of reactive oxygen species (ROS)
3. The investigation of alternative measures of predicting the ‘aged phenotype’ observed in preterm infants. This might include analysis of epigenetic markers, cell cycle regulators or N-glycome analysis
4. Improvement of telomere length analysis techniques, particularly techniques in the analysis of specific chromosome ends in small sample sizes and single cells. This might identify involvement of critical telomere length of specific chromosomes in reproductive ageing in women, or in the ‘aged phenotype’ observed in preterm infants. Currently available methodologies for this analysis require extensive optimisation in the case of single telomere length analysis (STELA), or produce highly variable results in the case of QFISH. Furthermore, both techniques are extremely labour intensive

7.6 Personal perspectives and concluding remarks

Overall, this thesis has provided some interesting insights into the function of telomeres in nuclear organisation, and telomere length in the process of age-related disorders (i.e. a decline in female reproductive potential with age, and in the pathogenesis of age-related disease conditions associated with premature birth). Despite the credible rationale behind each of the hypotheses tested within this thesis, it is surprising that, in reality, only one of these has proved correct. Results have shown that telomere distribution is highly organised within the sperm nucleus of normal males, and is

disrupted in infertile males. For this reason it is likely that the correct packaging of chromatin within the sperm nucleus, which includes proper organisation of the telomeres is involved in male fertility potential. On the other hand however, results show that telomere length is not involved in the process of ageing in the specific models assessed here. It is my opinion that tight regulation of telomere length within gametes and embryos, and high variation in individual attrition rates in the newborn are likely to be behind these observations. The exact mechanisms involved in the complex interplay between telomere attrition and telomere maintenance, and how these mechanisms may inter-relate with one another remains a mystery that is likely to unfold with future developments. The future of telomere research will certainly remain very active indeed.

8 References

- Achi, M.V., Ravindranath, N., and Dym, M. (2000). Telomere length in male germ cells is inversely correlated with telomerase activity. *Biology of reproduction* 63, 591-598.
- Adaikalakoteswari, A., Balasubramanyam, M., Ravikumar, R., Deepa, R., and Mohan, V. (2007). Association of telomere shortening with impaired glucose tolerance and diabetic macroangiopathy. *Atherosclerosis* 195, 83-89.
- Adams, J., Martin-Ruiz, C., Pearce, M.S., White, M., Parker, L., and Von Zglinicki, T. (2007). No association between socio-economic status and white blood cell telomere length. *Aging cell* 6, 125-128.
- Adler, A., Lee, H.-L., McCulloh, D.H., Ampeloquio, E., Clarke-Williams, M., Wertz, B.H., and Grifo, J. (2014). Blastocyst culture selects for euploid embryos: comparison of blastomere and trophoctoderm biopsies. *Reproductive biomedicine online* 28, 485-491.
- Agarwal, A., and Said, T.M. (2004). Sperm chromatin assessment. *Textbook of ART*, 2nd ed. Taylor & Francis Group, London: UK, 93-106.
- Aini, W., Miyagawa-Hayashino, A., Ozeki, M., Adeeb, S., Hirata, M., Tamaki, K., Uemoto, S., and Haga, H. (2014). Accelerated telomere reduction and hepatocyte senescence in tolerated human liver allografts. *Transplant immunology*.
- Aitken, R., and De Iuliis, G. (2010). On the possible origins of DNA damage in human spermatozoa. *Molecular human reproduction* 16, 3-13.
- Aitken, R.J., and De Iuliis, G.N. (2006). Value of DNA integrity assays for fertility evaluation. *Society of Reproduction and Fertility supplement* 65, 81-92.
- Aitken, R.J., and De Iuliis, G.N. (2007). Origins and consequences of DNA damage in male germ cells. *Reproductive biomedicine online* 14, 727-733.
- Akkad, A., Hastings, R., Konje, J.C., Bell, S.C., Thurston, H., and Williams, B. (2006). Telomere length in small-for-gestational-age babies. *BJOG: An International Journal of Obstetrics & Gynaecology* 113, 318-323.
- Albertson, D.G., Collins, C., McCormick, F., and Gray, J.W. (2003). Chromosome aberrations in solid tumors. *Nature genetics* 34.
- Alder, J.K., Chen, J.J.-L., Lancaster, L., Danoff, S., Su, S.-c., Cogan, J.D., Vulto, I., Xie, M., Qi, X., and Tudor, R.M. (2008). Short telomeres are a risk factor for idiopathic pulmonary fibrosis. *Proceedings of the National Academy of Sciences* 105, 13051-13056.
- Alladin, N., Moskovtsev, S.I., Russell, H., Kenigsberg, S., Lulat, A.G.-M., and Librach, C.L. (2013). The three-dimensional image analysis of the chromocenter in motile and immotile human sperm. *Systems biology in reproductive medicine* 59, 146-152.
- Allshire, R.C., Dempster, M., and Hastie, N.D. (1989). Human telomeres contain at least three types of G-rich repeat distributed non-randomly. *Nucleic acids research* 17, 4611-4627.
- Allsopp, R.C., Vaziri, H., Patterson, C., Goldstein, S., Younglai, E.V., Futcher, A.B., Greider, C.W., and Harley, C.B. (1992). Telomere length predicts replicative capacity of human fibroblasts. *Proceedings of the National Academy of Sciences* 89, 10114-10118.

- Alter, B.P., Baerlocher, G.M., Savage, S.A., Chanock, S.J., Weksler, B.B., Willner, J.P., Peters, J.A., Giri, N., and Lansdorp, P.M. (2007). Very short telomere length by flow fluorescence in situ hybridization identifies patients with dyskeratosis congenita. *Blood* *110*, 1439-1447.
- Amaral, A., Castillo, J., Ramalho-Santos, J., and Oliva, R. (2013). The combined human sperm proteome: cellular pathways and implications for basic and clinical science. *Human reproduction update*, dmt046.
- Ambartsumyan, G., and Clark, A.T. (2008). Aneuploidy and early human embryo development. *Human molecular genetics* *17*, R10-R15.
- Amiard, S., Doudeau, M., Pinte, S., Poulet, A., Lenain, C., Faivre-Moskalenko, C., Angelov, D., Hug, N., Vindigni, A., and Bouvet, P. (2007). A topological mechanism for TRF2-enhanced strand invasion. *Nature structural & molecular biology* *14*, 147-154.
- Anderson, R.A., and Pickering, S. (2008). The current status of preimplantation genetic screening: British Fertility Society Policy and Practice Guidelines. *Human Fertility* *11*, 71-75.
- Antonelli, A., Marcucci, L., Elli, R., Tanzi, N., Paoli, D., Radicioni, A., Lombardo, F., Lenzi, A., and Gandini, L. (2011). Semen quality in men with Y chromosome aberrations. *International journal of andrology* *34*, 453-460.
- Arnoult, N., Van Beneden, A., and Decottignies, A. (2012). Telomere length regulates TERRA levels through increased trimethylation of telomeric H3K9 and HP1alpha. *Nat Struct Mol Biol* *19*, 948-956.
- Artandi, S.E., Chang, S., Lee, S.-L., Alson, S., Gottlieb, G.J., Chin, L., and DePinho, R.A. (2000). Telomere dysfunction promotes non-reciprocal translocations and epithelial cancers in mice. *Nature* *406*, 641-645.
- Aubert, G., Hills, M., and Lansdorp, P.M. (2012). Telomere length measurement—Caveats and a critical assessment of the available technologies and tools. *Mutation Research/Fundamental and Molecular Mechanisms of Mutagenesis* *730*, 59-67.
- Aviv, A., and Aviv, H. (1997). Reflections on telomeres, growth, aging, and essential hypertension. *Hypertension* *29*, 1067-1072.
- Aviv, A., and Aviv, H. (1999). Telomeres and essential hypertension. *American journal of hypertension* *12*, 427-432.
- Aviv, A., Chen, W., Gardner, J.P., Kimura, M., Brimacombe, M., Cao, X., Srinivasan, S.R., and Berenson, G.S. (2009). Leukocyte telomere dynamics: longitudinal findings among young adults in the Bogalusa Heart Study. *American journal of epidemiology* *169*, 323-329.
- Aviv, A., Valdes, A.M., and Spector, T.D. (2006). Human telomere biology: pitfalls of moving from the laboratory to epidemiology. *International journal of epidemiology* *35*, 1424-1429.
- Aydos, S.E., Elhan, A.H., and Tükün, A. (2005). Is telomere length one of the determinants of reproductive life span? *Archives of gynecology and obstetrics* *272*, 113-116.
- Aymé, S., and Lippman-Hand, A. (1982). Maternal-age effect in aneuploidy: does altered embryonic selection play a role? *American journal of human genetics* *34*, 558.
- Azzalin, C.M., Reichenbach, P., Khoriauli, L., Giulotto, E., and Lingner, J. (2007). Telomeric repeat-containing RNA and RNA surveillance factors at mammalian chromosome ends. *Science* *318*, 798-801.

- Baerlocher, G.M., and Lansdorp, P.M. (2003). Telomere length measurements in leukocyte subsets by automated multicolor flow-FISH. *Cytometry Part A* *55*, 1-6.
- Baerlocher, G.M., Vulto, I., de Jong, G., and Lansdorp, P.M. (2006). Flow cytometry and FISH to measure the average length of telomeres (flow FISH). *Nature protocols* *1*, 2365-2376.
- Bai, Y., and Murnane, J.P. (2003). Telomere instability in a human tumor cell line expressing a dominant-negative WRN protein. *Human genetics* *113*, 337-347.
- Bailey, S., Cornforth, M., Kurimasa, A., Chen, D., and Goodwin, E. (2001). Strand-specific postreplicative processing of mammalian telomeres. *Science* *293*, 2462-2465.
- Bailey, S.M., Meyne, J., Chen, D.J., Kurimasa, A., Li, G.C., Lehnert, B.E., and Goodwin, E.H. (1999). DNA double-strand break repair proteins are required to cap the ends of mammalian chromosomes. *Proceedings of the National Academy of Sciences* *96*, 14899-14904.
- Bailey, S.M., and Murnane, J.P. (2006). Telomeres, chromosome instability and cancer. *Nucleic acids research* *34*, 2408-2417.
- Baird, D., Benagiano, G., Cohen, J., Collins, J., Evers, L., Fraser, L., Jacobs, H., Liebaers, I., Tarlatzis, B., and Templeton, A. (2002). Physiopathological determinants of human infertility. *Human Reproduction Update* *8*, 435-447.
- Baird, D.M. (2005). New developments in telomere length analysis. *Experimental gerontology* *40*, 363-368.
- Baird, D.M., Britt-Compton, B., Rowson, J., Amso, N.N., Gregory, L., and Kipling, D. (2006). Telomere instability in the male germline. *Human molecular genetics* *15*, 45-51.
- Baird, D.M., Davis, T., Rowson, J., Jones, C.J., and Kipling, D. (2004). Normal telomere erosion rates at the single cell level in Werner syndrome fibroblast cells. *Human molecular genetics* *13*, 1515-1524.
- Baird, D.M., Jeffreys, A.J., and Royle, N.J. (1995). Mechanisms underlying telomere repeat turnover, revealed by hypervariable variant repeat distribution patterns in the human Xp/Yp telomere. *The EMBO journal* *14*, 5433.
- Baird, D.M., Rowson, J., Wynford-Thomas, D., and Kipling, D. (2003). Extensive allelic variation and ultrashort telomeres in senescent human cells. *Nature genetics* *33*, 203-207.
- Bakkenist, C.J., and Kastan, M.B. (2003). DNA damage activates ATM through intermolecular autophosphorylation and dimer dissociation. *Nature* *421*, 499-506.
- Barazani, Y., Agarwal, A., and Sabanegh Jr, E.S. (2014). Functional Sperm Testing and the Role of Proteomics in the Evaluation of Male Infertility. *Urology* *84*, 255-261.
- Batenburg, N.L., Mitchell, T.R., Leach, D.M., Rainbow, A.J., and Zhu, X.-D. (2012). Cockayne Syndrome group B protein interacts with TRF2 and regulates telomere length and stability. *Nucleic acids research* *40*, 9661-9674.
- Batty, G.D., Wang, Y., Brouillette, S.W., Shiels, P., Packard, C., Moore, J., Samani, N.J., and Ford, I. (2009). Socioeconomic status and telomere length: the West of Scotland Coronary Prevention Study. *Journal of epidemiology and community health* *63*, 839-841.
- Baur, J.A., Zou, Y., Shay, J.W., and Wright, W.E. (2001). Telomere position effect in human cells. *Science* *292*, 2075-2077.

- Bekaert, S., Derradji, H., and Baatout, S. (2004). Telomere biology in mammalian germ cells and during development. *Developmental biology* 274, 15-30.
- Belanger, S.I.N., Christofolini, D.M., Bianco, B., Gava, M.M., Wroclawski, E.R., and Barbosa, C.P. (2009). Male infertility related to an aberrant karyotype, 46, XY, 9ph, 9qh+. *Fertility and sterility* 91, 2732. e2731-2732. e2733.
- Bellon, M., Datta, A., Brown, M., Pouliquen, J.F., Couppie, P., Kazanji, M., and Nicot, C. (2006). Increased expression of telomere length regulating factors TRF1, TRF2 and TIN2 in patients with adult T-cell leukemia. *International journal of cancer* 119, 2090-2097.
- Bendix, L., Horn, P.B., Jensen, U.B., Rubelj, I., and Kolvraa, S. (2010). The load of short telomeres, estimated by a new method, Universal STELA, correlates with number of senescent cells. *Aging cell* 9, 383-397.
- Benedetti, S., Tagliamonte, M.C., Catalani, S., Primiterra, M., Canestrari, F., De Stefani, S., Palini, S., and Bulletti, C. (2012). Differences in blood and semen oxidative status in fertile and infertile men, and their relationship with sperm quality. *Reprod Biomed Online* 25, 300-306.
- Benetos, A., Kark, J.D., Susser, E., Kimura, M., Sinnreich, R., Chen, W., Steenstrup, T., Christensen, K., Herbig, U., and von Bornemann Hjelmberg, J. (2013). Tracking and fixed ranking of leukocyte telomere length across the adult life course. *Aging cell* 12, 615-621.
- Benson, E.K., Lee, S.W., and Aaronson, S.A. (2010). Role of progerin-induced telomere dysfunction in HGPS premature cellular senescence. *Journal of cell science* 123, 2605-2612.
- Berman, E., Brown, S.C., James, T.L., and Shafer, R.H. (1985). NMR studies of chromomycin A3 interaction with DNA. *Biochemistry* 24, 6887-6893.
- Berrington, J., Barge, D., Fenton, A., Cant, A., and Spickett, G. (2005). Lymphocyte subsets in term and significantly preterm UK infants in the first year of life analysed by single platform flow cytometry. *Clinical & Experimental Immunology* 140, 289-292.
- Betts, D.H., and King, W.A. (1999). Telomerase activity and telomere detection during early bovine development. *Developmental genetics* 25, 397-403.
- Bhalla, N., and Dernburg, A.F. (2008). Prelude to a division. *Annual review of cell and developmental biology* 24, 397-424.
- Bhat, R., Salas, A.A., Foster, C., Carlo, W.A., and Ambalavanan, N. (2012). Prospective analysis of pulmonary hypertension in extremely low birth weight infants. *Pediatrics* 129, e682-e689.
- Bianchi, A., and Shore, D. (2007). Increased association of telomerase with short telomeres in yeast. *Genes & development* 21, 1726-1730.
- Bielanska, M., Tan, S.L., and Ao, A. (2002). Chromosomal mosaicism throughout human preimplantation development in vitro: incidence, type, and relevance to embryo outcome. *Human Reproduction* 17, 413-419.
- Biessmann, H., and Mason, J. (1997). Telomere maintenance without telomerase. *Chromosoma* 106, 63-69.
- Biron-Shental, T., Sukenik-Halevy, R., Sharon, Y., Goldberg-Bittman, L., Kidron, D., Fejgin, M.D., and Amiel, A. (2010). Short telomeres may play a role in placental dysfunction in preeclampsia and intrauterine growth restriction. *American journal of obstetrics and gynecology* 202, 381. e381-381. e387.
- Blackburn, E., and Szostak, J. (1984). The molecular structure of centromeres and telomeres. *Annual review of biochemistry* 53, 163-194.
- Blackburn, E.H. (2000). Telomere states and cell fates. *Nature* 408, 53-56.

- Blackburn, E.H., and Gall, J.G. (1978). A tandemly repeated sequence at the termini of the extrachromosomal ribosomal RNA genes in *Tetrahymena*. *Journal of molecular biology* *120*, 33-53.
- Blasco, M.A. (2007). The epigenetic regulation of mammalian telomeres. *Nature Reviews Genetics* *8*, 299-309.
- Blasco, M.a.A., Lee, H.-W., Hande, M.P., Samper, E., Lansdorp, P.M., DePinho, R.A., and Greider, C.W. (1997). Telomere shortening and tumor formation by mouse cells lacking telomerase RNA. *Cell* *91*, 25-34.
- Bochman, M.L., Paeschke, K., and Zakian, V.A. (2012). DNA secondary structures: stability and function of G-quadruplex structures. *Nature Reviews Genetics* *13*, 770-780.
- Bojko, M. (1983). Human meiosis VIII. Chromosome pairing and formation of the synaptonemal complex in oocytes. *Carlsberg Research Communications* *48*, 457-483.
- Bolzer, A., Kreth, G., Solovei, I., Koehler, D., Saracoglu, K., Fauth, C., Müller, S., Eils, R., Cremer, C., and Speicher, M.R. (2005). Three-dimensional maps of all chromosomes in human male fibroblast nuclei and prometaphase rosettes. *PLoS biology* *3*, e157.
- Boué, J., Boué, A., and Lazar, P. (1977). Retrospective and prospective epidemiological studies of 1500 karyotyped spontaneous human abortions. In *Problems of Birth Defects* (Springer), pp. 120-135.
- Boyle, S., Gilchrist, S., Bridger, J.M., Mahy, N.L., Ellis, J.A., and Bickmore, W.A. (2001). The spatial organization of human chromosomes within the nuclei of normal and emerlin-mutant cells. *Human molecular genetics* *10*, 211-219.
- Brenner, C.A., Wolny, Y.M., Adler, R.R., and Cohen, J. (1999). Alternative splicing of the telomerase catalytic subunit in human oocytes and embryos. *Molecular human reproduction* *5*, 845-850.
- Brezina, P.R., Benner, A., Rechitsky, S., Kuliev, A., Pomerantseva, E., Pauling, D., and Kearns, W.G. (2011). Single-gene testing combined with single nucleotide polymorphism microarray preimplantation genetic diagnosis for aneuploidy: a novel approach in optimizing pregnancy outcome. *Fertility and sterility* *95*, 1786. e1785-1786. e1788.
- Bridger, J.M., and Kill, I.R. (2004). Aging of Hutchinson–Gilford progeria syndrome fibroblasts is characterised by hyperproliferation and increased apoptosis. *Experimental gerontology* *39*, 717-724.
- Britt-Compton, B., Rowson, J., Locke, M., Mackenzie, I., Kipling, D., and Baird, D.M. (2006). Structural stability and chromosome-specific telomere length is governed by cis-acting determinants in humans. *Human molecular genetics* *15*, 725-733.
- Brouillette, S.W., Moore, J.S., McMahon, A.D., Thompson, J.R., Ford, I., Shepherd, J., Packard, C.J., and Samani, N.J. (2007). Telomere length, risk of coronary heart disease, and statin treatment in the West of Scotland Primary Prevention Study: a nested case-control study. *The Lancet* *369*, 107-114.
- Brown, W.R.A., MacKinnon, P.J., Villasanté, A., Spurr, N., Buckle, V.J., and Dobson, M.J. (1990). Structure and polymorphism of human telomere-associated DNA. *Cell* *63*, 119-132.
- Bryant, J.E., Hutchings, K.G., Moyzis, R.K., and Griffith, J.K. (1997). Measurement of telomeric DNA content in human tissues. *BioTechniques* *23*, 476-478, 480, 482, passim.

- Bukata, L., Parker, S.L., and D'Angelo, M.A. (2013). Nuclear pore complexes in the maintenance of genome integrity. *Current opinion in cell biology* 25, 378-386.
- Bupp, J.M., Martin, A.E., Stensrud, E.S., and Jaspersen, S.L. (2007). Telomere anchoring at the nuclear periphery requires the budding yeast Sad1-UNC-84 domain protein Mps3. *The Journal of cell biology* 179, 845-854.
- Burgoyne, P.S., Mahadevaiah, S.K., and Turner, J.M. (2009). The consequences of asynapsis for mammalian meiosis. *Nature Reviews Genetics* 10, 207-216.
- Butts, S., Riethman, H., Ratcliffe, S., Shaunik, A., Coutifaris, C., and Barnhart, K. (2009). Correlation of telomere length and telomerase activity with occult ovarian insufficiency. *Journal of Clinical Endocrinology & Metabolism* 94, 4835-4843.
- Calado, R.T., and Young, N.S. (2009). Telomere diseases. *The New England journal of medicine* 361, 2353-2365.
- Calogero, A.E., De Palma, A., Grazioso, C., Barone, N., Romeo, R., Rappazzo, G., and D'Agata, R. (2001). Aneuploidy rate in spermatozoa of selected men with abnormal semen parameters. *Human Reproduction* 16, 1172-1179.
- Calvanese, V., Lara, E., Kahn, A., and Fraga, M.F. (2009). The role of epigenetics in aging and age-related diseases. *Ageing research reviews* 8, 268-276.
- Cawthon, R.M. (2002). Telomere measurement by quantitative PCR. *Nucleic acids research* 30, e47-e47.
- Cawthon, R.M. (2009). Telomere length measurement by a novel monochrome multiplex quantitative PCR method. *Nucleic acids research* 37, e21-e21.
- Cawthon, R.M., Smith, K.R., O'Brien, E., Sivatchenko, A., and Kerber, R.A. (2003). Association between telomere length in blood and mortality in people aged 60 years or older. *The Lancet* 361, 393-395.
- Celli, G.B., Denchi, E.L., and de Lange, T. (2006). Ku70 stimulates fusion of dysfunctional telomeres yet protects chromosome ends from homologous recombination. *Nature cell biology* 8, 885-890.
- Cerone, M.A., Londono-Vallejo, J.A., and Bacchetti, S. (2001). Telomere maintenance by telomerase and by recombination can coexist in human cells. *Human molecular genetics* 10, 1945-1952.
- Cesare, A.J., and Griffith, J.D. (2004). Telomeric DNA in ALT cells is characterized by free telomeric circles and heterogeneous t-loops. *Molecular and cellular biology* 24, 9948-9957.
- Chan, S.R., and Blackburn, E.H. (2004). Telomeres and telomerase. *Philosophical Transactions of the Royal Society of London. Series B: Biological Sciences* 359, 109-122.
- Chan, S.W., Chang, J., Prescott, J., and Blackburn, E.H. (2001). Altering telomere structure allows telomerase to act in yeast lacking ATM kinases. *Current Biology* 11, 1240-1250.
- Chen, S.-j., Allam, J.-P., Duan, Y.-g., and Haidl, G. (2013). Influence of reactive oxygen species on human sperm functions and fertilizing capacity including therapeutical approaches. *Archives of gynecology and obstetrics* 288, 191-199.
- Chen, S.Y., Tsubouchi, T., Rockmill, B., Sandler, J.S., Richards, D.R., Vader, G., Hochwagen, A., Roeder, G.S., and Fung, J.C. (2008). Global analysis of the meiotic crossover landscape. *Developmental cell* 15, 401-415.
- Cheng, E.-H., Chen, S.-U., Lee, T.-H., Pai, Y.-P., Huang, L.-S., Huang, C.-C., and Lee, M.-S. (2013a). Evaluation of telomere length in cumulus cells as a potential biomarker of oocyte and embryo quality. *Human Reproduction* 28, 929-936.

- Cheng, G., Kong, F., Luan, Y., Sun, C., Wang, J., Zhang, L., Jiang, B., Qi, T., Zhao, J., and Zheng, C. (2013b). Differential shortening rate of telomere length in the development of human fetus. *Biochemical and biophysical research communications* 442, 112-115.
- Cherif, H., Tarry, J., Ozanne, S., and Hales, C. (2003). Ageing and telomeres: A study into organ-and gender-specific telomere shortening. *Nucleic acids research* 31, 1576-1583.
- Cherkas, L.F., Hunkin, J.L., Kato, B.S., Richards, J.B., Gardner, J.P., Surdulescu, G.L., Kimura, M., Lu, X., Spector, T.D., and Aviv, A. (2008). The association between physical activity in leisure time and leukocyte telomere length. *Archives of internal medicine* 168, 154-158.
- Cheung, A., and Deng, W. (2008). Telomere dysfunction, genome instability and cancer. *Front Biosci* 13, 2075-2090.
- Cho, C., Jung-Ha, H., Willis, W.D., Goulding, E.H., Stein, P., Xu, Z., Schultz, R.M., Hecht, N.B., and Eddy, E.M. (2003). Protamine 2 deficiency leads to sperm DNA damage and embryo death in mice. *Biology of reproduction* 69, 211-217.
- Cho, C., Willis, W.D., Goulding, E.H., Jung-Ha, H., Choi, Y.-C., Hecht, N.B., and Eddy, E.M. (2001). Haploinsufficiency of protamine-1 or-2 causes infertility in mice. *Nature genetics* 28, 82-86.
- Churikov, D., Siino, J., Svetlova, M., Zhang, K., Gineitis, A., Morton Bradbury, E., and Zalensky, A. (2004). Novel human testis-specific histone H2B encoded by the interrupted gene on the X chromosome. *Genomics* 84, 745-756.
- Ciotti, P., Lagalla, C., Ricco, A., Fabbri, R., Forabosco, A., and Porcu, E. (2000). Micromanipulation of cryopreserved embryos and cryopreservation of micromanipulated embryos in PGD. *Molecular and cellular endocrinology* 169, 63-67.
- Clermont, Y. (1972). Kinetics of spermatogenesis in mammals: seminiferous epithelium cycle and spermatogonial renewal. *Physiological Reviews* 52, 198-236.
- Collins, S.C. (2013). Preimplantation genetic diagnosis: technical advances and expanding applications. *Current Opinion in Obstetrics and Gynecology* 25, 201-206.
- Colls, P., Escudero, T., Cekleniak, N., Sadowy, S., Cohen, J., and Munné, S. (2007). Increased efficiency of preimplantation genetic diagnosis for infertility using “no result rescue”. *Fertility and sterility* 88, 53-61.
- Comhaire, F. (1987). Towards more objectivity in the management of male infertility. The need for a standardized approach. *International journal of andrology*, 1-53.
- Cooke, H.J., and Smith, B.A. (1986). Variability at the telomeres of the human X/Y pseudoautosomal region. In *Cold Spring Harbor symposia on quantitative biology* (Cold Spring Harbor Laboratory Press), pp. 213-219.
- Cooke, S., and Fleming, S.D. (2009). *Textbook of Assisted Reproduction for Scientists in Reproductive Technology* (Vivid Publishing).
- Cooper, J.P., Watanabe, Y., and Nurse, P. (1998). Fission yeast Taz1 protein is required for meiotic telomere clustering and recombination. *Nature* 392, 828-831.
- Costantini, S., Woodbine, L., Andreoli, L., Jeggo, P.A., and Vindigni, A. (2007). Interaction of the Ku heterodimer with the DNA ligase IV/Xrcc4 complex and its regulation by DNA-PK. *DNA repair* 6, 712-722.
- Costeloe, K.L., Hennessy, E.M., Haider, S., Stacey, F., Marlow, N., and Draper, E.S. (2012). Short term outcomes after extreme preterm birth in England:

- comparison of two birth cohorts in 1995 and 2006 (the EPICure studies). *BMJ: British Medical Journal* 345.
- Cowan, C.R., Carlton, P.M., and Cande, W.Z. (2001). The polar arrangement of telomeres in interphase and meiosis. Rabl organization and the bouquet. *Plant Physiology* 125, 532-538.
- Crabbe, L., Jauch, A., Naeger, C.M., Holtgreve-Grez, H., and Karlseder, J. (2007). Telomere dysfunction as a cause of genomic instability in Werner syndrome. *Proceedings of the National Academy of Sciences* 104, 2205-2210.
- Crabbe, L., and Karlseder, J. (2005). In the end, it's all structure. *Current molecular medicine* 5, 135-143.
- Crabbe, L., Verdun, R.E., Haggblom, C.I., and Karlseder, J. (2004). Defective telomere lagging strand synthesis in cells lacking WRN helicase activity. *Science* 306, 1951-1953.
- Craven, R.J., Greenwell, P.W., Dominska, M., and Petes, T.D. (2002). Regulation of genome stability by TEL1 and MEC1, yeast homologs of the mammalian ATM and ATR genes. *Genetics* 161, 493-507.
- Cremer, M., Küpper, K., Wagler, B., Wizelman, L., Hase, J.v., Weiland, Y., Kreja, L., Diebold, J., Speicher, M.R., and Cremer, T. (2003). Inheritance of gene density-related higher order chromatin arrangements in normal and tumor cell nuclei. *The Journal of cell biology* 162, 809-820.
- Cremer, M., von Hase, J., Volm, T., Brero, A., Kreth, G., Walter, J., Fischer, C., Solovei, I., Cremer, C., and Cremer, T. (2001). Non-random radial higher-order chromatin arrangements in nuclei of diploid human cells. *Chromosome research* 9, 541-567.
- Cremer, T., and Cremer, C. (2001). Chromosome territories, nuclear architecture and gene regulation in mammalian cells. *Nature reviews genetics* 2, 292-301.
- Cremer, T., Cremer, C., Baumann, H., Luedtke, E., Sperling, K., Teuber, V., and Zorn, C. (1982). Rabl's model of the interphase chromosome arrangement tested in Chinese hamster cells by premature chromosome condensation and laser-UV-microbeam experiments. *Human genetics* 60, 46-56.
- Cremer, T., and Cremer, M. (2010). Chromosome territories. *Cold Spring Harbor perspectives in biology* 2, a003889.
- Cremer, T., Kurz, A., Zirbel, R., Dietzel, S., Rinke, B., Schrock, E., Speicher, M.R., Mathieu, U., Jauch, A., Emmerich, P., *et al.* (1993). Role of Chromosome Territories in the Functional Compartmentalization of the Cell Nucleus. *Cold Spring Harbor symposia on quantitative biology* 58, 777 <last_page> 792.
- Croft, J.A., Bridger, J.M., Boyle, S., Perry, P., Teague, P., and Bickmore, W.A. (1999). Differences in the localization and morphology of chromosomes in the human nucleus. *The Journal of cell biology* 145, 1119-1131.
- Cronkhite, J.T., Xing, C., Raghu, G., Chin, K.M., Torres, F., Rosenblatt, R.L., and Garcia, C.K. (2008). Telomere shortening in familial and sporadic pulmonary fibrosis. *American journal of respiratory and critical care medicine* 178, 729.
- Cross, J., Brennan, C., Gray, T., Temple, R., Dozio, N., Hughes, J., Levell, N., Murphy, H., Fowler, D., and Hughes, D. (2009). Absence of telomere shortening and oxidative DNA damage in the young adult offspring of women with pre-gestational type 1 diabetes. *Diabetologia* 52, 226-234.
- Cross, J., Temple, R., Hughes, J., Dozio, N., Brennan, C., Stanley, K., Murphy, H., Fowler, D., Hughes, D., and Sampson, M. (2010). Cord blood telomere length, telomerase activity and inflammatory markers in pregnancies in women with diabetes or gestational diabetes. *Diabetic Medicine* 27, 1264-1270.

- Cunningham, J.M., Johnson, R.A., Litzelman, K., Skinner, H.G., Seo, S., Engelman, C.D., Vanderboom, R.J., Kimmel, G.W., Gangnon, R.E., and Riegert-Johnson, D.L. (2013). Telomere length varies by DNA extraction method: implications for epidemiologic research. *Cancer Epidemiology Biomarkers & Prevention*.
- D'Aquila, P., Rose, G., Bellizzi, D., and Passarino, G. (2013). Epigenetics and aging. *Maturitas* 74, 130-136.
- Dada, R., Kumar, B., Kumar, M., Oberoi, A.S., and Shamsi, M.B. (2014). Sperm DNA Damage Assessment: Techniques and Relevance in Male Infertility Diagnostics. *Manual of Cytogenetics in Reproductive Biology*, 135.
- Dall'Olio, F., Vanhooren, V., Chen, C.C., Slagboom, P.E., Wuhler, M., and Franceschi, C. (2013). N-glycomic biomarkers of biological aging and longevity: a link with inflammaging. *Ageing research reviews* 12, 685-698.
- Dan, J., Liu, Y., Liu, N., Chiourea, M., Okuka, M., Wu, T., Ye, X., Mou, C., Wang, L., and Yin, Y. (2014). Rif1 Maintains Telomere Length Homeostasis of ESCs by Mediating Heterochromatin Silencing. *Developmental cell* 29, 7-19.
- Das, U.N. (2004). Metabolic syndrome X: an inflammatory condition? *Current hypertension reports* 6, 66-73.
- Davoli, T., Denchi, E.L., and de Lange, T. (2010). Persistent telomere damage induces bypass of mitosis and tetraploidy. *Cell* 141, 81-93.
- Davy, P., Nagata, M., Bullard, P., Fogelson, N., and Allsopp, R. (2009). Fetal growth restriction is associated with accelerated telomere shortening and increased expression of cell senescence markers in the placenta. *Placenta* 30, 539-542.
- de Jong, F., Monuteaux, M.C., van Elburg, R.M., Gillman, M.W., and Belfort, M.B. (2012). Systematic review and meta-analysis of preterm birth and later systolic blood pressure. *Hypertension* 59, 226-234.
- de Lange, T. (1992). Human telomeres are attached to the nuclear matrix. *The EMBO journal* 11, 717.
- De Lange, T. (1995). Telomere dynamics and genome instability in human cancer. *COLD SPRING HARBOR MONOGRAPH SERIES* 29, 265-294.
- De Lange, T. (2004). T-loops and the origin of telomeres. *Nature Reviews Molecular Cell Biology* 5, 323-329.
- de Lange, T. (2005a). Shelterin: the protein complex that shapes and safeguards human telomeres. *Genes & development* 19, 2100-2110.
- De Lange, T. (2005b). Telomere-related genome instability in cancer. In *Cold Spring Harbor Symposia on Quantitative Biology* (Cold Spring Harbor Laboratory Press), pp. 197-204.
- De Lange, T., Shiue, L., Myers, R., Cox, D., Naylor, S., Killery, A., and Varmus, H. (1990). Structure and variability of human chromosome ends. *Molecular and cellular biology* 10, 518-527.
- de Leon, A.D., Cronkhite, J.T., Katzenstein, A.-L.A., Godwin, J.D., Raghu, G., Glazer, C.S., Rosenblatt, R.L., Girod, C.E., Garrity, E.R., and Xing, C. (2010). Telomere lengths, pulmonary fibrosis and telomerase (TERT) mutations. *PLoS One* 5, e10680.
- De Pauw, E., Verwoerd, N., Duinkerken, N., Willemze, R., Raap, A., Fibbe, W., and Tanke, H. (1998). Assessment of telomere length in hematopoietic interphase cells using in situ hybridization and digital fluorescence microscopy. *Cytometry* 32, 163-169.
- De Ravel, T.J., Devriendt, K., Fryns, J.-P., and Vermeesch, J.R. (2007). What's new in karyotyping? The move towards array comparative genomic hybridisation (CGH). *European journal of pediatrics* 166, 637-643.

- De Vos, A., Staessen, C., De Rycke, M., Verpoest, W., Haentjens, P., Devroey, P., Liebaers, I., and Van de Velde, H. (2009). Impact of cleavage-stage embryo biopsy in view of PGD on human blastocyst implantation: a prospective cohort of single embryo transfers. *Human reproduction* *24*, 2988-2996.
- De Vos, W.H., Houben, F., Hoebe, R.A., Hennekam, R., van Engelen, B., Manders, E.M., Ramaekers, F., Broers, J.L., and Van Oostveldt, P. (2010). Increased plasticity of the nuclear envelope and hypermobility of telomeres due to the loss of A-type lamins. *Biochimica et Biophysica Acta (BBA)-General Subjects* *1800*, 448-458.
- Dechat, T., Gajewski, A., Korbei, B., Gerlich, D., Daigle, N., Haraguchi, T., Furukawa, K., Ellenberg, J., and Foisner, R. (2004). LAP2 α and BAF transiently localize to telomeres and specific regions on chromatin during nuclear assembly. *Journal of cell science* *117*, 6117-6128.
- Decker, M.L., Chavez, E., Vulto, I., and Lansdorp, P.M. (2009). Telomere length in Hutchinson-Gilford progeria syndrome. *Mechanisms of ageing and development* *130*, 377-383.
- Delhanty, J.D., Griffin, D.K., Handyside, A.H., Harper, J., Atkinson, G.H., Pieters, M.H., and Winston, R.M. (1993). Detection of aneuploidy and chromosomal mosaicism in human embryos during preimplantation sex determination by fluorescent in situ hybridisation,(FISH). *Human molecular genetics* *2*, 1183-1185.
- Delhanty, J.D., Harper, J.C., Ao, A., Handyside, A.H., and Winston, R.M. (1997). Multicolour FISH detects frequent chromosomal mosaicism and chaotic division in normal preimplantation embryos from fertile patients. *Human genetics* *99*, 755-760.
- Denchi, E.L., and de Lange, T. (2007). Protection of telomeres through independent control of ATM and ATR by TRF2 and POT1. *Nature* *448*, 1068-1071.
- Deng, W., Tsao, S.W., Guan, X.Y., Lucas, J.N., and Cheung, A.L. (2003). Role of short telomeres in inducing preferential chromosomal aberrations in human ovarian surface epithelial cells: A combined telomere quantitative fluorescence in situ hybridization and whole-chromosome painting study. *Genes, Chromosomes and Cancer* *37*, 92-97.
- der-Sarkissian, H., Bacchetti, S., Cazes, L., and Londoño-Vallejo, J.A. (2004). The shortest telomeres drive karyotype evolution in transformed cells. *Oncogene* *23*, 1221-1228.
- Derijck, A., van der Heijden, G., Giele, M., Philippens, M., and de Boer, P. (2008). DNA double-strand break repair in parental chromatin of mouse zygotes, the first cell cycle as an origin of de novo mutation. *Human molecular genetics* *17*, 1922-1937.
- Dernburg, A.F., Sedat, J.W., Cande, W.Z., and Bass, H.W. (1995). *Cytology of Telomeres*, Vol 29.
- DeUgarte, C.M., Li, M., Surrey, M., Danzer, H., Hill, D., and DeCherney, A.H. (2008). Accuracy of FISH analysis in predicting chromosomal status in patients undergoing preimplantation genetic diagnosis. *Fertility and sterility* *90*, 1049-1054.
- di Fagagna, F.d.A., Hande, M.P., Tong, W.-M., Lansdorp, P.M., Wang, Z.-Q., and Jackson, S.P. (1999). Functions of poly (ADP-ribose) polymerase in controlling telomere length and chromosomal stability. *Nature genetics* *23*, 76-80.

- Diez Roux, A.V., Ranjit, N., Jenny, N.S., Shea, S., Cushman, M., Fitzpatrick, A., and Seeman, T. (2009). Race/ethnicity and telomere length in the Multi-Ethnic Study of Atherosclerosis. *Aging cell* 8, 251-257.
- Ding, X., Xu, R., Yu, J., Xu, T., Zhuang, Y., and Han, M. (2007). SUN1 is required for telomere attachment to nuclear envelope and gametogenesis in mice. *Developmental cell* 12, 863-872.
- Dorland, M., Van Kooij, R., and Te Velde, E. (1998a). General ageing and ovarian ageing. *Maturitas* 30, 113-118.
- Dorland, M., van Montfrans, J., van Kooij, R., Lambalk, C., and te Velde, E. (1998b). Normal telomere lengths in young mothers of children with Down's syndrome. *The Lancet* 352, 961-962.
- Dupont, G. (1998). Link between fertilization-induced Ca²⁺ oscillations and relief from metaphase II arrest in mammalian eggs: a model based on calmodulin-dependent kinase II activation. *Biophysical Chemistry* 72, 153-167.
- Duran, H.E., Simsek-Duran, F., Oehninger, S.C., Jones Jr, H.W., and Castora, F.J. (2011). The association of reproductive senescence with mitochondrial quantity, function, and DNA integrity in human oocytes at different stages of maturation. *Fertility and sterility* 96, 384-388.
- Edwards, R. (1970). Are oocytes formed and used sequentially in the mammalian ovary? *Philosophical transactions of the Royal Society of London. Series B, Biological sciences* 259, 103-105.
- Edwards, R.G. (2005). Genetics of polarity in mammalian embryos. *Reproductive biomedicine online* 11, 104-114.
- Egholm, M., Buchardt, O., Christensen, L., Behrens, C., Freier, S.M., Driver, D.A., Berg, R.H., Kim, S.K., Norden, B., and Nielsen, P.E. (1993). PNA hybridizes to complementary oligonucleotides obeying the Watson-Crick hydrogen-bonding rules. *Nature* 365, 566-568.
- Egozcue, J., Blanco, J., and Vidal, F. (1997). Chromosome studies in human sperm nuclei using fluorescence in-situ hybridization (FISH). *Human reproduction update* 3, 441-452.
- Eisenberg, D.T., Hayes, M.G., and Kuzawa, C.W. (2012). Delayed paternal age of reproduction in humans is associated with longer telomeres across two generations of descendants. *Proceedings of the National Academy of Sciences* 109, 10251-10256.
- Eisenhauer, K.M., Gerstein, R.M., Chiu, C.-P., Conti, M., and Hsueh, A. (1997). Telomerase activity in female and male rat germ cells undergoing meiosis and in early embryos. *Biology of reproduction* 56, 1120-1125.
- Epel, E.S. (2009). Psychological and metabolic stress: a recipe for accelerated cellular aging. *Hormones (Athens)* 8, 7-22.
- Epel, E.S., Blackburn, E.H., Lin, J., Dhabhar, F.S., Adler, N.E., Morrow, J.D., and Cawthon, R.M. (2004). Accelerated telomere shortening in response to life stress. *Proceedings of the National Academy of Sciences of the United States of America* 101, 17312-17315.
- Episkopou, H., Draskovic, I., Van Beneden, A., Tilman, G., Mattiussi, M., Gobin, M., Arnoult, N., Londoño-Vallejo, A., and Decottignies, A. (2014). Alternative Lengthening of Telomeres is characterized by reduced compaction of telomeric chromatin. *Nucleic acids research* 42, 4391-4405.
- Esterhuizen, A., Franken, D., Lourens, J., Prinsloo, E., and Van Rooyen, L. (2000). Sperm chromatin packaging as an indicator of in-vitro fertilization rates. *Human Reproduction* 15, 657-661.

- Evenson, D.P., LARSON, K.L., and Jost, L.K. (2002). Sperm chromatin structure assay: its clinical use for detecting sperm DNA fragmentation in male infertility and comparisons with other techniques. *Journal of Andrology* *23*, 25-43.
- Falchetti, M.L., Pallini, R., Larocca, L.M., Verna, R., and D'Ambrosio, E. (1999). Telomerase expression in intracranial tumours: prognostic potential for malignant gliomas and meningiomas. *Journal of clinical pathology* *52*, 234-236.
- Faragher, R.G., and Kipling, D. (1998). How might replicative senescence contribute to human ageing? *Bioessays* *20*, 985-991.
- Federico, C., Saccone, S., Andreozzi, L., Motta, S., Russo, V., Carels, N., and Bernardi, G. (2004). The pig genome: compositional analysis and identification of the gene-richest regions in chromosomes and nuclei. *Gene* *343*, 245-251.
- Ferlin, A., Raicu, F., Gatta, V., Zuccarello, D., Palka, G., and Foresta, C. (2007). Male infertility: role of genetic background. *Reproductive biomedicine online* *14*, 734-745.
- Ferlin, A., Rampazzo, E., Rocca, M., Keppel, S., Frigo, A., De Rossi, A., and Foresta, C. (2013). In young men sperm telomere length is related to sperm number and parental age. *Human Reproduction* *28*, 3370-3376.
- Finch, K.A., Fonseka, K.G., Abogrein, A., Ioannou, D., Handyside, A.H., Thornhill, A.R., Hickson, N., and Griffin, D.K. (2008). Nuclear organization in human sperm: preliminary evidence for altered sex chromosome centromere position in infertile males. *Human reproduction (Oxford, England)* *23*, 1263-1270.
- Fiorentino, F., Biricik, A., Bono, S., Spizzichino, L., Cotroneo, E., Cottone, G., Kokocinski, F., and Michel, C.-E. (2014). Development and validation of a next-generation sequencing-based protocol for 24-chromosome aneuploidy screening of embryos. *Fertility and sterility* *101*, 1375-1382. e1372.
- Fiorentino, F., Biricik, A., Nuccitelli, A., De Palma, R., Kahraman, S., Sertyel, S., Karadayi, H., Cottone, G., Baldi, M., and Caserta, D. (2008). Rapid protocol for pre-conception genetic diagnosis of single gene mutations by first polar body analysis: a possible solution for the Italian patients. *Prenatal diagnosis* *28*, 62-64.
- Fiorentino, F., Spizzichino, L., Bono, S., Biricik, A., Kokkali, G., Rienzi, L., Ubaldi, F., Iammarrone, E., Gordon, A., and Pantos, K. (2011). PGD for reciprocal and Robertsonian translocations using array comparative genomic hybridization. *Human reproduction* *26*, 1925-1935.
- Fishel, S., Gordon, A., Lynch, C., Dowell, K., Ndukwe, G., Kelada, E., Thornton, S., Jenner, L., Cater, E., and Brown, A. (2010). Live birth after polar body array comparative genomic hybridization prediction of embryo ploidy—the future of IVF? *Fertility and sterility* *93*, 1006. e1007-1006. e1010.
- Fitzpatrick, A.L., Kronmal, R.A., Gardner, J.P., Psaty, B.M., Jenny, N.S., Tracy, R.P., Walston, J., Kimura, M., and Aviv, A. (2007). Leukocyte telomere length and cardiovascular disease in the cardiovascular health study. *American Journal of Epidemiology* *165*, 14-21.
- Foster, H.A., Abeydeera, L.R., Griffin, D.K., and Bridger, J.M. (2005). Non-random chromosome positioning in mammalian sperm nuclei, with migration of the sex chromosomes during late spermatogenesis. *Journal of cell science* *118*, 1811-1820.
- Foster, H.A., and Bridger, J.M. (2005). The genome and the nucleus: a marriage made by evolution. *Genome organisation and nuclear architecture. Chromosoma* *114*, 212-229.

- Fraga, M.F., and Esteller, M. (2007). Epigenetics and aging: the targets and the marks. *Trends in Genetics* 23, 413-418.
- Fragouli, E., Katz-Jaffe, M., Alfarawati, S., Stevens, J., Colls, P., Goodall, N.-n., Tormasi, S., Gutierrez-Mateo, C., Prates, R., and Schoolcraft, W.B. (2010). Comprehensive chromosome screening of polar bodies and blastocysts from couples experiencing repeated implantation failure. *Fertility and sterility* 94, 875-887.
- Freeman, S.B., Yang, Q., Allran, K., Taft, L.F., and Sherman, S.L. (2000). Women with a reduced ovarian complement may have an increased risk for a child with Down syndrome. *The American Journal of Human Genetics* 66, 1680-1683.
- Frenck, R.W., Jr., Blackburn, E.H., and Shannon, K.M. (1998). The rate of telomere sequence loss in human leukocytes varies with age. *Proceedings of the National Academy of Sciences of the United States of America* 95, 5607-5610.
- Friedrich, U., Schwab, M., Griese, E.U., Fritz, P., and Klotz, U. (2001). Telomeres in neonates: new insights in fetal hematopoiesis. *Pediatric research* 49, 252-256.
- Fujisawa, M., Tanaka, H., Tatsumi, N., Okada, H., Arakawa, S., and Kamidono, S. (1998). Telomerase activity in the testis of infertile patients with selected causes. *Human Reproduction* 13, 1476-1479.
- Fulneckova, J. (2014). The Evolution of Telomeres in Algae. In *Plant and Animal Genome XXII Conference (Plant and Animal Genome)*.
- Funabiki, H., Hagan, I., Uzawa, S., and Yanagida, M. (1993). Cell cycle-dependent specific positioning and clustering of centromeres and telomeres in fission yeast. *The Journal of Cell Biology* 121, 961-976.
- Furukawa, S., Fujita, T., Shimabukuro, M., Iwaki, M., Yamada, Y., Nakajima, Y., Nakayama, O., Makishima, M., Matsuda, M., and Shimomura, I. (2004). Increased oxidative stress in obesity and its impact on metabolic syndrome. *Journal of Clinical Investigation* 114, 1752-1761.
- Gabriel, A., Thornhill, A., Ottolini, C., Gordon, A., Brown, A., Taylor, J., Bennett, K., Handyside, A., and Griffin, D. (2011). Array comparative genomic hybridisation on first polar bodies suggests that non-disjunction is not the predominant mechanism leading to aneuploidy in humans. *Journal of medical genetics* 48, 433-437.
- García-Cao, M., O'Sullivan, R., Peters, A.H., Jenuwein, T., and Blasco, M.A. (2004). Epigenetic regulation of telomere length in mammalian cells by the Suv39h1 and Suv39h2 histone methyltransferases. *Nature genetics* 36, 94-99.
- Gardner, J.P., Li, S., Srinivasan, S.R., Chen, W., Kimura, M., Lu, X., Berenson, G.S., and Aviv, A. (2005). Rise in insulin resistance is associated with escalated telomere attrition. *Circulation* 111, 2171-2177.
- Gavory, G., Farrow, M., and Balasubramanian, S. (2002). Minimum length requirement of the alignment domain of human telomerase RNA to sustain catalytic activity in vitro. *Nucleic acids research* 30, 4470-4480.
- Geraedts, J., Montag, M., Magli, M.C., Repping, S., Handyside, A., Staessen, C., Harper, J., Schmutzler, A., Collins, J., and Goossens, V. (2011). Polar body array CGH for prediction of the status of the corresponding oocyte. Part I: clinical results. *Human reproduction* 26, 3173-3180.
- Ghosh, S., Feingold, E., Chakraborty, S., and Dey, S.K. (2010). Telomere length is associated with types of chromosome 21 nondisjunction: a new insight into the maternal age effect on Down syndrome birth. *Human genetics* 127, 403-409.
- Gil, M.E., and Coetzer, T.L. (2004). Real-time quantitative PCR of telomere length. *Molecular biotechnology* 27, 169-172.

- Gillies, C.B. (1989). *Fertility and Chromosome Pairing* (Crc Press).
- Gineitis, A.A., Zalenskaya, I.A., Yau, P.M., Bradbury, E.M., and Zalensky, A.O. (2000). Human Sperm Telomere–Binding Complex Involves Histone H2b and Secures Telomere Membrane Attachment. *The Journal of cell biology* *151*, 1591-1598.
- Gingell-Littlejohn, M., McGuinness, D., McGlynn, L.M., Kingsmore, D., Stevenson, K.S., Koppelstaetter, C., Clancy, M.J., and Shiels, P.G. (2013). Pre-transplant CDKN2A expression in kidney biopsies predicts renal function and is a future component of donor scoring criteria. *PloS one* *8*, e68133.
- Gleicher, N., Kushnir, V.A., and Barad, D.H. (2014). Preimplantation genetic screening (PGS) still in search of a clinical application: a systematic review. *Reproductive Biology and Endocrinology* *12*, 22.
- Godfrey, K.M., Lillycrop, K.A., Burdge, G.C., Gluckman, P.D., and Hanson, M.A. (2007). Epigenetic mechanisms and the mismatch concept of the developmental origins of health and disease. *Pediatric research* *61*, 5R-10R.
- Gonzalez-Suarez, I., Redwood, A.B., Perkins, S.M., Vermolen, B., Lichtensztejin, D., Grotzky, D.A., Morgado-Palacin, L., Gapud, E.J., Sleckman, B.P., and Sullivan, T. (2009). Novel roles for A-type lamins in telomere biology and the DNA damage response pathway. *The EMBO journal* *28*, 2414-2427.
- Gonzalo, S., Jaco, I., Fraga, M.F., Chen, T., Li, E., Esteller, M., and Blasco, M.A. (2006). DNA methyltransferases control telomere length and telomere recombination in mammalian cells. *Nature cell biology* *8*, 416-424.
- Goossens, V., De Rycke, M., De Vos, A., Staessen, C., Michiels, A., Verpoest, W., Van Steirteghem, A., Bertrand, C., Liebaers, I., and Devroey, P. (2008). Diagnostic efficiency, embryonic development and clinical outcome after the biopsy of one or two blastomeres for preimplantation genetic diagnosis. *Human Reproduction* *23*, 481-492.
- Gosden, J., and Hanratty, D. (1993). PCR in situ: a rapid alternative to in situ hybridization for mapping short, low copy number sequences without isotopes. *Biotechniques* *15*, 78-80.
- Gosden, J., and Lawson, D. (1994). Rapid chromosome identification by oligonucleotide-primed in situ DNA synthesis (PRINS). *Human molecular genetics* *3*, 931-936.
- Gottschling, D.E., Aparicio, O.M., Billington, B.L., and Zakian, V.A. (1990). Position effect at *S. cerevisiae* telomeres: reversible repression of Pol II transcription. *Cell* *63*, 751-762.
- Grati, F., Miozzo, M., Cassani, B., Rossella, F., Antonazzo, P., Gentilin, B., Sirchia, S., Mori, L., Rigano, S., and Bulfamante, G. (2005). Fetal and placental chromosomal mosaicism revealed by QF-PCR in severe IUGR pregnancies. *Placenta* *26*, 10-18.
- Greider, C.W., and Blackburn, E.H. (1985). Identification of a specific telomere terminal transferase activity in *Tetrahymena* extracts. *Cell* *43*, 405-413.
- Greider, C.W., and Blackburn, E.H. (1989). A telomeric sequence in the RNA of *Tetrahymena* telomerase required for telomere repeat synthesis. *Nature* *337*, 331-337.
- Gribbin, J., Hubbard, R., and Smith, C. (2009). Role of diabetes mellitus and gastro-oesophageal reflux in the aetiology of idiopathic pulmonary fibrosis. *Respiratory medicine* *103*, 927-931.
- Griffin, D.K., and Finch, K.A. (2005). The genetic and cytogenetic basis of male infertility. *Human Fertility* *8*, 19-26.

- Griffin, D.K., Wilton, L.J., Handyside, A.H., Atkinson, G.H., Winston, R.M., and Delhanty, J.D. (1993). Diagnosis of sex in preimplantation embryos by fluorescent in situ hybridisation. *BMJ: British Medical Journal* *306*, 1382.
- Grodstein, F., van Oijen, M., Irizarry, M.C., Rosas, H.D., Hyman, B.T., Growdon, J.H., and De Vivo, I. (2008). Shorter telomeres may mark early risk of dementia: preliminary analysis of 62 participants from the nurses' health study. *PloS one* *3*, e1590.
- Guan, J.Z., Maeda, T., Sugano, M., Oyama, J.-i., Higuchi, Y., and Makino, N. (2007). Change in the telomere length distribution with age in the Japanese population. *Molecular and cellular biochemistry* *304*, 353-360.
- Guan, J.Z., Maeda, T., Sugano, M., Oyama, J.-i., Higuchi, Y., Suzuki, T., and Makino, N. (2008). A percentage analysis of the telomere length in Parkinson's disease patients. *The Journals of Gerontology Series A: Biological Sciences and Medical Sciences* *63*, 467-473.
- Gué, M., Messaoudi, C., Sun, J.S., and Boudier, T. (2005). Smart 3D-fish: Automation of distance analysis in nuclei of interphase cells by image processing. *Cytometry Part A* *67*, 18-26.
- Guz, J., Gackowski, D., Foksinski, M., Rozalski, R., Zarakowska, E., Siomek, A., Szpila, A., Kotzbach, M., Kotzbach, R., and Olinski, R. (2013). Comparison of oxidative stress/DNA damage in semen and blood of fertile and infertile men. *PloS one* *8*, e68490.
- Haaf, T., and Ward, D.C. (1995). Higher order nuclear structure in mammalian sperm revealed by in situ hybridization and extended chromatin fibers. *Experimental cell research* *219*, 604-611.
- Habermann, F.A., Cremer, M., Walter, J., Kreth, G., von Hase, J., Bauer, K., Wienberg, J., Cremer, C., Cremer, T., and Solovei, I. (2001). Arrangements of macro- and microchromosomes in chicken cells. *Chromosome Research* *9*, 569-584.
- Hande, M.P., Balajee, A.S., Tchirkov, A., Wynshaw-Boris, A., and Lansdorp, P.M. (2001). Extra-chromosomal telomeric DNA in cells from *Atm*^{-/-} mice and patients with ataxia-telangiectasia. *Human molecular genetics* *10*, 519-528.
- Hande, P., Slijepcevic, P., Silver, A., Bouffler, S., van Buul, P., Bryant, P., and Lansdorp, P. (1999). Elongated Telomeres in *scid* Mice. *Genomics* *56*, 221-223.
- Handyside, A., Grifo, J., Prates, R., Tormasi, S., Fischer, J., and Munne, S. (2010). Validation and first clinical application of karyomapping for preimplantation diagnosis (PGD) of Gaucher disease combined with 24 chromosome screening. *Fertility and Sterility* *94*, S79-S80.
- Handyside, A.H., Harton, G.L., Mariani, B., Thornhill, A.R., Affara, N., Shaw, M.-A., and Griffin, D.K. (2009). Karyomapping: a universal method for genome wide analysis of genetic disease based on mapping crossovers between parental haplotypes. *Journal of medical genetics*, jmg. 2009.069971.
- Hanna, C.W., Bretherick, K.L., Gair, J.L., Fluker, M.R., Stephenson, M.D., and Robinson, W.P. (2009). Telomere length and reproductive aging. *Human Reproduction* *24*, 1206-1211.
- Hanson, C., Hardarson, T., Lundin, K., Bergh, C., Hillensjö, T., Stevic, J., Westin, C., Selleskog, U., Rogberg, L., and Wikland, M. (2009). Re-analysis of 166 embryos not transferred after PGS with advanced reproductive maternal age as indication. *Human reproduction*, dep264.
- Haque, F., Lloyd, D.J., Smallwood, D.T., Dent, C.L., Shanahan, C.M., Fry, A.M., Trembath, R.C., and Shackleton, S. (2006). SUN1 interacts with nuclear lamin

- A and cytoplasmic nesprins to provide a physical connection between the nuclear lamina and the cytoskeleton. *Molecular and cellular biology* 26, 3738-3751.
- Hardarson, T., Hanson, C., Lundin, K., Hillensjö, T., Nilsson, L., Stevic, J., Reismer, E., Borg, K., Wikland, M., and Bergh, C. (2008). Preimplantation genetic screening in women of advanced maternal age caused a decrease in clinical pregnancy rate: a randomized controlled trial. *Human reproduction* 23, 2806-2812.
- Harley, C.B., Futcher, A.B., and Greider, C.W. (1990). Telomeres shorten during ageing of human fibroblasts. *Nature* 345, 458-460.
- Harper, J., Coonen, E., De Rycke, M., Fiorentino, F., Geraedts, J., Goossens, V., Harton, G., Moutou, C., Budak, T.P., and Renwick, P. (2010). What next for preimplantation genetic screening (PGS)? A position statement from the ESHRE PGD Consortium Steering Committee. *Human Reproduction* 25, 821-823.
- Harper, J.C., and Harton, G. (2010). The use of arrays in preimplantation genetic diagnosis and screening. *Fertility and sterility* 94, 1173-1177.
- Harper, J.C., and SenGupta, S.B. (2012). Preimplantation genetic diagnosis: state of the art 2011. *Human genetics* 131, 175-186.
- Harris, S.E., Martin-Ruiz, C., von Zglinicki, T., Starr, J.M., and Deary, I.J. (2012). Telomere length and aging biomarkers in 70-year-olds: the Lothian Birth Cohort 1936. *Neurobiology of aging* 33, 1486. e1483-1486. e1488.
- Harton, G., Magli, M., Lundin, K., Montag, M., Lemmen, J., and Harper, J. (2011). ESHRE PGD Consortium/Embryology Special Interest Group—best practice guidelines for polar body and embryo biopsy for preimplantation genetic diagnosis/screening (PGD/PGS). *Human reproduction* 26, 41-46.
- Harton, G.L., Munné, S., Surrey, M., Grifo, J., Kaplan, B., McCulloh, D.H., Griffin, D.K., and Wells, D. (2013). Diminished effect of maternal age on implantation after preimplantation genetic diagnosis with array comparative genomic hybridization. *Fertility and sterility* 100, 1695-1703.
- Hassold, T., Abruzzo, M., Adkins, K., Griffin, D., Merrill, M., Millie, E., Saker, D., Shen, J., and Zaragoza, M. (1996). Human aneuploidy: incidence, origin, and etiology. *Environmental and molecular mutagenesis* 28, 167-175.
- Hassold, T., Chen, N., Funkhouser, J., Jooss, T., Manuel, B., Matsuura, J., Matsuyama, A., Wilson, C., Yamane, J., and Jacobs, P. (1980). A cytogenetic study of 1000 spontaneous abortions. *Annals of human genetics* 44, 151-164.
- Hassold, T., and Hunt, P. (2001). To err (meiotically) is human: the genesis of human aneuploidy. *Nature Reviews Genetics* 2, 280-291.
- Hassold, T., and Hunt, P. (2009). Maternal age and chromosomally abnormal pregnancies: what we know and what we wish we knew. *Current opinion in pediatrics* 21, 703.
- Hastie, N.D., Dempster, M., Dunlop, M.G., Thompson, A.M., Green, D.K., and Allshire, R.C. (1990). Telomere reduction in human colorectal carcinoma and with ageing. *Nature* 346, 866-868.
- Hayflick, L. (1976). The cell biology of human aging. *The New England journal of medicine* 295, 1302.
- Hayflick, L. (1998). How and why we age. *Experimental gerontology* 33, 639-653.
- Hayflick, L. (2003). Living forever and dying in the attempt. *Experimental gerontology* 38, 1231-1241.

- Hayflick, L., and Moorhead, P.S. (1961). The serial cultivation of human diploid cell strains. *Experimental cell research* 25, 585-621.
- Hazzouri, M., Rousseaux, S., Mongelard, F., Usson, Y., Pelletier, R., Faure, A.K., Vourc'h, C., and Sele, B. (2000). Genome organization in the human sperm nucleus studied by FISH and confocal microscopy. *Molecular reproduction and development* 55, 307-315.
- Hellani, A., Abu-Amero, K., Azouri, J., and El-Akoum, S. (2008). Successful pregnancies after application of array-comparative genomic hybridization in PGS-aneuploidy screening. *Reproductive biomedicine online* 17, 841-847.
- Hemann, M.T., Rudolph, K.L., Strong, M.A., DePinho, R.A., Chin, L., and Greider, C.W. (2001a). Telomere dysfunction triggers developmentally regulated germ cell apoptosis. *Molecular biology of the cell* 12, 2023-2030.
- Hemann, M.T., Strong, M.A., Hao, L.-Y., and Greider, C.W. (2001b). The shortest telomere, not average telomere length, is critical for cell viability and chromosome stability. *Cell* 107, 67-77.
- Henson, J.D., Neumann, A.A., Yeager, T.R., and Reddel, R.R. (2002). Alternative lengthening of telomeres in mammalian cells. *oncogene* 21.
- Herbig, U., Jobling, W.A., Chen, B.P., Chen, D.J., and Sedivy, J.M. (2004). Telomere Shortening Triggers Senescence of Human Cells through a Pathway Involving ATM, p53, and p21^{CIP1}, but Not p16^{INK4a}. *Molecular cell* 14, 501-513.
- Herrera, E., Samper, E., Martín-Caballero, J., Flores, J.M., Lee, H.W., and Blasco, M.A. (1999). Disease states associated with telomerase deficiency appear earlier in mice with short telomeres. *The EMBO Journal* 18, 2950-2960.
- Hilliker, A., and Appels, R. (1989). The arrangement of interphase chromosomes: structural and functional aspects. *Experimental cell research* 185, 297-318.
- Hilscher, W. (1974). Kinetics of spermatogenesis and spermatogenesis. *Verhandlungen der Anatomischen Gesellschaft* 68, 39.
- Hiraoka, Y., Agard, D.A., and Sedat, J.W. (1990). Temporal and spatial coordination of chromosome movement, spindle formation, and nuclear envelope breakdown during prometaphase in *Drosophila melanogaster* embryos. *The Journal of cell biology* 111, 2815-2828.
- Hochstrasser, M., Mathog, D., Gruenbaum, Y., Saumweber, H., and Sedat, J.W. (1986). Spatial organization of chromosomes in the salivary gland nuclei of *Drosophila melanogaster*. *The Journal of cell biology* 102, 112-123.
- Hochstrasser, T., Marksteiner, J., and Humpel, C. (2012). Telomere length is age-dependent and reduced in monocytes of Alzheimer patients. *Experimental gerontology* 47, 160-163.
- Hoffmann, J., Erben, Y., Zeiher, A.M., Dimmeler, S., and Spyridopoulos, I. (2009). Telomere length-heterogeneity among myeloid cells is a predictor for chronological ageing. *Experimental gerontology* 44, 363-366.
- Holmes, D.K., Bellantuono, I., Walkinshaw, S.A., Alfirevic, Z., Johnston, T.A., Subhedar, N.V., Chittick, R., Swindell, R., and Wynn, R.F. (2009). Telomere length dynamics differ in foetal and early post-natal human leukocytes in a longitudinal study. *Biogerontology* 10, 279-284.
- Homan, G., Davies, M., and Norman, R. (2007). The impact of lifestyle factors on reproductive performance in the general population and those undergoing infertility treatment: a review. *Human Reproduction Update* 13, 209-223.

- Honig, L.S., Schupf, N., Lee, J.H., Tang, M.X., and Mayeux, R. (2006). Shorter telomeres are associated with mortality in those with APOE ϵ 4 and dementia. *Annals of neurology* *60*, 181-187.
- Hsu, H.-L., Gilley, D., Galande, S.A., Hande, M.P., Allen, B., Kim, S.-H., Li, G.C., Campisi, J., Kohwi-Shigematsu, T., and Chen, D.J. (2000). Ku acts in a unique way at the mammalian telomere to prevent end joining. *Genes & development* *14*, 2807-2812.
- Hull, M., Glazener, C., Kelly, N., Conway, D., Foster, P., Hinton, R., Coulson, C., Lambert, P., Watt, E., and Desai, K. (1985). Population study of causes, treatment, and outcome of infertility. *British medical journal (Clinical research ed.)* *291*, 1693.
- Iannuccelli, E., Mompert, F., Gellin, J., Lahbib-Mansais, Y., Yerle, M., and Boudier, T. (2010). NEMO: a tool for analyzing gene and chromosome territory distributions from 3D-FISH experiments. *Bioinformatics* *26*, 696-697.
- Ijdo, J., Baldini, A., Ward, D., Reeders, S., and Wells, R. (1991). Origin of human chromosome 2: an ancestral telomere-telomere fusion. *Proceedings of the National Academy of Sciences* *88*, 9051-9055.
- Ijdo, J.W., Lindsay, E.A., Wells, R.A., and Baldini, A. (1992). Multiple variants in subtelomeric regions of normal karyotypes. *Genomics* *14*, 1019-1025.
- Ilmonen, P., Kotrschal, A., and Penn, D.J. (2008). Telomere attrition due to infection. *PloS one* *3*, e2143.
- Ioannou, D., Fonseka, K., Meershoek, E., Thornhill, A., Abogrein, A., Ellis, M., and Griffin, D.K. (2012). Twenty-four chromosome FISH in human IVF embryos reveals patterns of post-zygotic chromosome segregation and nuclear organisation. *Chromosome Research* *20*, 447-460.
- Ioannou, D., and Griffin, D. (2010). Male fertility, chromosome abnormalities, and nuclear organization. *Cytogenetic and Genome Research* *133*, 269-279.
- Ioannou, D., Meershoek, E., Thornhill, A., Ellis, M., and Griffin, D. (2011). Multicolour interphase cytogenetics: 24 chromosome probes, 6 colours, 4 layers. *Molecular and cellular probes* *25*, 199-205.
- Iranpour, F.G. (2014). The effects of protamine deficiency on ultrastructure of human sperm nucleus. *Advanced Biomedical Research* *3*, 24.
- Iranpour, F.G., Nasr-Esfahani, M.H., Valojerdi, M.R., and Al-Taraihi, T.M.T. (2000). Chromomycin A3 staining as a useful tool for evaluation of male fertility. *Journal of assisted reproduction and genetics* *17*, 60-66.
- Irvine, D.S. (1998). Epidemiology and aetiology of male infertility. *Human Reproduction* *13*, 33-44.
- Iwama, H., Ohyashiki, K., Ohyashiki, J.H., Hayashi, S., Yahata, N., Ando, K., Toyama, K., Hoshika, A., Takasaki, M., and Mori, M. (1998). Telomeric length and telomerase activity vary with age in peripheral blood cells obtained from normal individuals. *Human genetics* *102*, 397-402.
- Jacobs, E.J., Newton, C.C., Wang, Y., Patel, A.V., McCullough, M.L., Campbell, P.T., Thun, M.J., and Gapstur, S.M. (2010). Waist circumference and all-cause mortality in a large US cohort. *Archives of Internal Medicine* *170*, 1293.
- Jain, D., and Cooper, J.P. (2010). Telomeric strategies: means to an end. *Annual review of genetics* *44*, 243-269.
- Jansen, R.P., Bowman, M.C., de Boer, K.A., Leigh, D.A., Lieberman, D.B., and McArthur, S.J. (2008). What next for preimplantation genetic screening (PGS)? Experience with blastocyst biopsy and testing for aneuploidy. *Human reproduction* *23*, 1476-1478.

- Jayaraman, V., Ghosh, S., Sengupta, A., Srivastava, S., Sonawat, H., and Narayan, P.K. (2014). Identification of biochemical differences between different forms of male infertility by nuclear magnetic resonance (NMR) spectroscopy. *Journal of assisted reproduction and genetics*, 1-10.
- Jennings, C., and Powell, D. (1995). Genome organisation in the murine sperm nucleus. *Zygote (Cambridge, England)* 3, 123-131.
- Johnson, D.S., Cinnioglu, C., Ross, R., Filby, A., Gemelos, G., Hill, M., Ryan, A., Smotrich, D., Rabinowitz, M., and Murray, M.J. (2010). Comprehensive analysis of karyotypic mosaicism between trophectoderm and inner cell mass. *Molecular human reproduction* 16, 944-949.
- Jones, K.T. (2008). Meiosis in oocytes: predisposition to aneuploidy and its increased incidence with age. *Human reproduction update* 14, 143-158.
- Kalmbach, K.H., Fontes Antunes, D.M., Dracxler, R.C., Knier, T.W., Seth-Smith, M.L., Wang, F., Liu, L., and Keefe, D.L. (2013). Telomeres and human reproduction. *Fertility and sterility* 99, 23-29.
- Kalousek, D.K., and Dill, F.J. (1983). Chromosomal mosaicism confined to the placenta in human conceptions. *Science* 221, 665-667.
- Kaminker, P., Plachot, C., Kim, S.-H., Chung, P., Crippen, D., Petersen, O.W., Bissell, M.J., Campisi, J., and Lelièvre, S.A. (2005). Higher-order nuclear organization in growth arrest of human mammary epithelial cells: a novel role for telomere-associated protein TIN2. *Journal of cell science* 118, 1321-1330.
- Kaminker, P.G., Kim, S.-H., Desprez, P.-Y., and Campisi, J. (2009). A novel form of the telomere-associated protein TIN2 localizes to the nuclear matrix. *Cell Cycle* 8, 931-939.
- Kang, S.S., Kwon, T., and Do, S.I. (1999). Akt protein kinase enhances human telomerase activity through phosphorylation of telomerase reverse transcriptase subunit. *Journal of Biological Chemistry* 274, 13085-13090.
- Karlseder, J. (2003). Telomere repeat binding factors: keeping the ends in check. *Cancer letters* 194, 189-197.
- Karlseder, J., Broccoli, D., Dai, Y., Hardy, S., and de Lange, T. (1999). p53- and ATM-dependent apoptosis induced by telomeres lacking TRF2. *Science* 283, 1321-1325.
- Karlseder, J., Hoke, K., Mirzoeva, O.K., Bakkenist, C., Kastan, M.B., Petrini, J.H., and de Lange, T. (2004). The telomeric protein TRF2 binds the ATM kinase and can inhibit the ATM-dependent DNA damage response. *PLoS biology* 2, e240.
- Karlseder, J., Smogorzewska, A., and de Lange, T. (2002). Senescence induced by altered telomere state, not telomere loss. *Science* 295, 2446-2449.
- Kasai, F., Takahashi, E.-i., Koyama, K., Terao, K., Suto, Y., Tokunaga, K., Nakamura, Y., and Hirai, M. (2000). Comparative FISH mapping of the ancestral fusion point of human chromosome 2. *Chromosome Research* 8, 727-735.
- Kastan, M., Lim, D., Kim, S., and Yang, D. (2001). ATM-A key determinant of multiple cellular responses to irradiation. *Acta Oncologica* 40, 686-688.
- Kawanishi, S., and Oikawa, S. (2004). Mechanism of telomere shortening by oxidative stress. *Annals of the New York Academy of Sciences* 1019, 278.
- Kazerooni, T., Asadi, N., Jadid, L., Kazerooni, M., Ghanadi, A., Ghaffaripasand, F., Kazerooni, Y., and Zolghadr, J. (2009). Evaluation of sperm's chromatin quality with acridine orange test, chromomycin A3 and aniline blue staining in couples with unexplained recurrent abortion. *Journal of assisted reproduction and genetics* 26, 591-596.

- Keefe, D., Liu, L., and Marquard, K. (2007). Telomeres and meiosis in health and disease: Telomeres and aging-related meiotic dysfunction in women. *Cellular and Molecular Life Sciences CMLS* 64, 139-143.
- Keefe, D.L., Franco, S., Liu, L., Trimarchi, J., Cao, B., Weitzen, S., Agarwal, S., and Blasco, M.A. (2005). Telomere length predicts embryo fragmentation after in vitro fertilization in women—toward a telomere theory of reproductive aging in women. *American journal of obstetrics and gynecology* 192, 1256-1260.
- Keefe, D.L., and Liu, L. (2008). Telomeres and reproductive aging. *Reproduction, Fertility and Development* 21, 10-14.
- Keefe, D.L., Marquard, K., and Liu, L. (2006). The telomere theory of reproductive senescence in women. *Current Opinion in Obstetrics and Gynecology* 18, 280-285.
- Keltz, M.D., Vega, M., Sirota, I., Lederman, M., Moshier, E.L., Gonzales, E., and Stein, D. (2013). Preimplantation Genetic Screening (PGS) with Comparative Genomic Hybridization (CGH) following day 3 single cell blastomere biopsy markedly improves IVF outcomes while lowering multiple pregnancies and miscarriages. *Journal of assisted reproduction and genetics* 30, 1333-1339.
- Khan, F.H., Ganesan, P., and Kumar, S. (2010). Y Chromosome microdeletion and altered sperm quality in human males with high concentration of seminal hexachlorocyclohexane (HCH). *Chemosphere* 80, 972-977.
- Kilian, A., Bowtell, D.D., Abud, H.E., Hime, G.R., Venter, D.J., Keese, P.K., Duncan, E.L., Reddel, R.R., and Jefferson, R.A. (1997). Isolation of a candidate human telomerase catalytic subunit gene, which reveals complex splicing patterns in different cell types. *Human molecular genetics* 6, 2011-2019.
- Kim, N.W., Piatyszek, M.A., Prowse, K.R., Harley, C.B., West, M.D., Ho, P.d.L., Coviello, G.M., Wright, W.E., Weinrich, S.L., and Shay, J.W. (1994). Specific association of human telomerase activity with immortal cells and cancer. *Science* 266, 2011-2015.
- Kimura, M., Cherkas, L.F., Kato, B.S., Demissie, S., Hjelmborg, J.B., Brimacombe, M., Cupples, A., Hunkin, J.L., Gardner, J.P., Lu, X., *et al.* (2008). Offspring's Leukocyte Telomere Length, Paternal Age, and Telomere Elongation in Sperm. *PLoS Genetics* 4, e37.
- Kinugawa, C., Murakami, T., Okamura, K., and Yajima, A. (2000). Telomerase activity in normal ovaries and premature ovarian failure. *The Tohoku journal of experimental medicine* 190, 231-238.
- Kitada, T., Seki, S., Kawakita, N., Kuroki, T., and Monna, T. (1995). Telomere shortening in chronic liver diseases. *Biochemical and biophysical research communications* 211, 33-39.
- Kleckner, N. (1996). Meiosis: how could it work? *Proceedings of the National Academy of Sciences* 93, 8167-8174.
- Koch, J., Hindkjaer, J., Mogensen, J., Kølvråa, S., and Bolund, L. (1991). An improved method for chromosome-specific labeling of α satellite DNA in situ by using denatured double-stranded DNA probes as primers in a primed in situ labeling (PRINS) procedure. *Genetic Analysis: Biomolecular Engineering* 8, 171-178.
- Koering, C.E., Pollice, A., Zibella, M.P., Bauwens, S., Puisieux, A., Brunori, M., Brun, C., Martins, L., Sabatier, L., and Pulitzer, J.F. (2002). Human telomeric position effect is determined by chromosomal context and telomeric chromatin integrity. *EMBO reports* 3, 1055-1061.
- Kohli, J. (1994). Meiosis: telomeres lead chromosome movement. *Current Biology* 4, 724-727.

- Koppelstaetter, C., Schratzberger, G., Perco, P., Hofer, J., Mark, W., Öllinger, R., Oberbauer, R., Schwarz, C., Mitterbauer, C., and Kainz, A. (2008). Markers of cellular senescence in zero hour biopsies predict outcome in renal transplantation. *Aging cell* 7, 491-497.
- Kosak, S.T., and Groudine, M. (2004). Form follows function: The genomic organization of cellular differentiation. *Genes & development* 18, 1371-1384.
- Koster, A., Leitzmann, M.F., Schatzkin, A., Mouw, T., Adams, K.F., van Eijk, J.T.M., Hollenbeck, A.R., and Harris, T.B. (2008). Waist circumference and mortality. *American journal of epidemiology* 167, 1465-1475.
- Kovacic, J.C., Moreno, P., Hachinski, V., Nabel, E.G., and Fuster, V. (2011). Cellular Senescence, Vascular Disease, and Aging Part 1 of a 2-Part Review. *Circulation* 123, 1650-1660.
- Kruisselbrink, E., Guryev, V., Brouwer, K., Pontier, D.B., Cuppen, E., and Tijsterman, M. (2008). Mutagenic Capacity of Endogenous G4 DNA Underlies Genome Instability in FANCD1-Defective *C. elegans*. *Current Biology* 18, 900-905.
- Kuliev, A., Cieslak, J., and Verlinsky, Y. (2005). Frequency and distribution of chromosome abnormalities in human oocytes. *Cytogenetic and genome research* 111, 193-198.
- Kuliev, A., and Verlinsky, Y. (2004). Meiotic and mitotic nondisjunction: lessons from preimplantation genetic diagnosis. *Human reproduction update* 10, 401-407.
- Kuliev, A., Zlatopolsky, Z., Kirillova, I., Spivakova, J., and Cieslak Janzen, J. (2011). Meiosis errors in over 20,000 oocytes studied in the practice of preimplantation aneuploidy testing. *Reproductive biomedicine online* 22, 2-8.
- Kumar, R., Gautam, G., and Gupta, N.P. (2006). Drug therapy for idiopathic male infertility: rationale versus evidence. *The Journal of urology* 176, 1307-1312.
- Küpker, W., Huber, G., Ludwig, M., and Diedrich, K. (2001). Preimplantation genetic diagnosis in Germany: ethical responsibility and law. *Reproductive biomedicine online* 2, 84-87.
- Kuroda, M., Tanabe, H., Yoshida, K., Oikawa, K., Saito, A., Kiyuna, T., Mizusawa, H., and Mukai, K. (2004). Alteration of chromosome positioning during adipocyte differentiation. *Journal of cell science* 117, 5897-5903.
- Kyo, S., Takakura, M., Kanaya, T., Zhuo, W., Fujimoto, K., Nishio, Y., Orimo, A., and Inoue, M. (1999). Estrogen activates telomerase. *Cancer Research* 59, 5917-5921.
- Kyrion, G., Liu, K., Liu, C., and Lustig, A. (1993). RAP1 and telomere structure regulate telomere position effects in *Saccharomyces cerevisiae*. *Genes & development* 7, 1146-1159.
- Lamb, N.E., Freeman, S.B., Savage-Austin, A., Pettay, D., Taft, L., Hersey, J., Gu, Y., Shen, J., Saker, D., and May, K.M. (1996). Susceptible chiasmate configurations of chromosome 21 predispose to non-disjunction in both maternal meiosis I and meiosis II. *Nature genetics* 14, 400-405.
- Lambert, C.C. (1986). Fertilization-induced modification of chorion N-acetylglucosamine groups blocks polyspermy in ascidian eggs. *Developmental Biology* 116, 168-173.
- Langford, L.A., Piatyszek, M.A., Xu, R., Schold Jr, S.C., Wright, W.E., and Shay, J.W. (1997). Telomerase activity in ordinary meningiomas predicts poor outcome. *Human pathology* 28, 416-420.
- Lansdorp, P.M. (1996). Close encounters of the PNA kind. *Nature biotechnology* 14, 1653-1653.

- Lansdorp, P.M. (2000). Repair of telomeric DNA prior to replicative senescence. *Mechanisms of ageing and development* *118*, 23-34.
- Lansdorp, P.M. (2008). Telomeres, stem cells, and hematology. *Blood* *111*, 1759-1766.
- Lansdorp, P.M., Verwoerd, N.P., van de Rijke, F.M., Dragowska, V., Little, M.T., Dirks, R.W., Raap, A.K., and Tanke, H.J. (1996). Heterogeneity in telomere length of human chromosomes. *Human molecular genetics* *5*, 685-691.
- Lavoie, J., Bronsard, M., Lebel, M., and Drouin, R. (2003). Mouse telomere analysis using an optimized primed in situ (PRINS) labeling technique. *Chromosoma* *111*, 438-444.
- Lavranos, T.C., Mathis, J.M., Latham, S.E., Kalionis, B., Shay, J.W., and Rodgers, R.J. (1999). Evidence for ovarian granulosa stem cells: telomerase activity and localization of the telomerase ribonucleic acid component in bovine ovarian follicles. *Biology of reproduction* *61*, 358-366.
- Le Caignec, C., Spits, C., Sermon, K., De Rycke, M., Thienpont, B., Debrock, S., Staessen, C., Moreau, Y., Fryns, J.-P., and Van Steirteghem, A. (2006). Single-cell chromosomal imbalances detection by array CGH. *Nucleic acids research* *34*, e68-e68.
- Lee, D.-C., Im, J.-A., Kim, J.-H., Lee, H.-R., and Shim, J.-Y. (2005). Effect of long-term hormone therapy on telomere length in postmenopausal women. *Yonsei medical journal* *46*, 471-479.
- Lee, H.-W., Blasco, M.A., Gottlieb, G.J., Horner, J.W., Greider, C.W., and DePinho, R.A. (1998). Essential role of mouse telomerase in highly proliferative organs. *Nature* *392*, 569-574.
- Lee, J., Park, H.S., Kim, H.H., Yun, Y.J., Lee, D.R., and Lee, S. (2009). Functional polymorphism in H2BFWT-5' UTR is associated with susceptibility to male infertility. *Journal of Cellular and Molecular Medicine* *13*, 1942-1951.
- Lee, M., Hills, M., Conomos, D., Stutz, M.D., Dagg, R.A., Lau, L.M., Reddel, R.R., and Pickett, H.A. (2014). Telomere extension by telomerase and ALT generates variant repeats by mechanistically distinct processes. *Nucleic acids research* *42*, 1733-1746.
- Lei, M., Podell, E.R., and Cech, T.R. (2004). Structure of human POT1 bound to telomeric single-stranded DNA provides a model for chromosome end-protection. *Nature structural & molecular biology* *11*, 1223-1229.
- Lei, M., Zaug, A.J., Podell, E.R., and Cech, T.R. (2005). Switching human telomerase on and off with hPOT1 protein in vitro. *Journal of Biological Chemistry* *280*, 20449-20456.
- Lenain, C., Bauwens, S., Amiard, S., Brunori, M., Giraud-Panis, M.-J., and Gilson, E. (2006). The Apollo 5' exonuclease functions together with TRF2 to protect telomeres from DNA repair. *Current biology* *16*, 1303-1310.
- Lestou, V.S., and Kalousek, D.K. (1998). Confined placental mosaicism and intrauterine fetal growth. *Archives of Disease in Childhood-Fetal and Neonatal Edition* *79*, F223-F226.
- Levis, R., Hazelrigg, T., and Rubin, G.M. (1985). Effects of genomic position on the expression of transduced copies of the white gene of *Drosophila*. *Science* *229*, 558-561.
- Levis, R.W. (1989). Viable deletions of a telomere from a *Drosophila* chromosome. *Cell* *58*, 791-801.
- Levis, R.W., Ganesan, R., Houtchens, K., Tolar, L.A., and Sheen, F.-m. (1993). Transposons in place of telomeric repeats at a *Drosophila* telomere. *Cell* *75*, 1083-1093.

- Levy, M.Z., Allsopp, R.C., Futcher, A.B., Greider, C.W., and Harley, C.B. (1992). Telomere end-replication problem and cell aging. *Journal of Molecular Biology* 225, 951-960.
- Li, B., and Lustig, A.J. (1996). A novel mechanism for telomere size control in *Saccharomyces cerevisiae*. *Genes & development* 10, 1310-1326.
- Lichter, P., Cremer, T., Borden, J., Manuelidis, L., and Ward, D. (1988). Delineation of individual human chromosomes in metaphase and interphase cells by in situ suppression hybridization using recombinant DNA libraries. *Human genetics* 80, 224-234.
- Liebaers, I., El Inati, E., Lissens, W., and Viville, S. (2014). Genes and infertility.
- Lim, S.-N., Yahya, Z., Zeegers, D., Moe, T., Kyaw, E.E.P., Yeo, G.S., Hande, M.P., and Tan, E.-C. (2013). Distribution of Telomere Length in the Cord Blood of Chinese Newborns. *British Journal of Medicine & Medical Research* 3.
- Lin, Y., Mahan, K., Lathrop, W.F., Myles, D.G., and Primakoff, P. (1994). A hyaluronidase activity of the sperm plasma membrane protein PH-20 enables sperm to penetrate the cumulus cell layer surrounding the egg. *The Journal of cell biology* 125, 1157-1163.
- Lindsey, J., McGill, N.I., Lindsey, L.A., Green, D.K., and Cooke, H.J. (1991). In vivo loss of telomeric repeats with age in humans. *Mutation Research/DNAging* 256, 45-48.
- Lingner, J., Cooper, J.P., and Cech, T.R. (1995). Telomerase and DNA end replication: no longer a lagging strand problem? *Science* 269, 1533-1534.
- Liu, J., Fox, C.S., Hickson, D.A., May, W.D., Hairston, K.G., Carr, J.J., and Taylor, H.A. (2010). Impact of abdominal visceral and subcutaneous adipose tissue on cardiometabolic risk factors: the Jackson Heart Study. *Journal of Clinical Endocrinology & Metabolism* 95, 5419-5426.
- Liu, L., Bailey, S.M., Okuka, M., Munoz, P., Li, C., Zhou, L., Wu, C., Czerwiec, E., Sandler, L., Seyfang, A., *et al.* (2007). Telomere lengthening early in development. *Nature cell biology* 9, 1436-1441.
- Liu, L., Blasco, M.A., and Keefe, D.L. (2002a). Requirement of functional telomeres for metaphase chromosome alignments and integrity of meiotic spindles. *EMBO reports* 3, 230-234.
- Liu, L., Blasco, M.A., Trimarchi, J.R., and Keefe, D.L. (2002b). An essential role for functional telomeres in mouse germ cells during fertilization and early development. *Developmental biology* 249, 74-84.
- Liu, L., Franco, S., Spyropoulos, B., Moens, P.B., Blasco, M.A., and Keefe, D.L. (2004). Irregular telomeres impair meiotic synapsis and recombination in mice. *Proceedings of the National Academy of Sciences of the United States of America* 101, 6496-6501.
- Lolis, D., Georgiou, I., Syrrou, M., Zikopoulos, K., Konstantelli, M., and Messinis, I. (1996). Chromomycin A3-staining as an indicator of protamine deficiency and fertilization. *International journal of andrology* 19, 23-27.
- Longhese, M.P. (2008). DNA damage response at functional and dysfunctional telomeres. *Genes & development* 22, 125-140.
- Lopes, J., Piazza, A., Bermejo, R., Kriegsman, B., Colosio, A., Teulade-Fichou, M.P., Foiani, M., and Nicolas, A. (2011). G-quadruplex-induced instability during leading-strand replication. *The EMBO journal* 30, 4033-4046.
- Ludérus, M., de Graaf, A., Mattia, E., den Blaauwen, J., Grande, M., de Jong, L., and van Driel, R. (1992). Binding of matrix attachment regions to lamin B1. *Cell* 70, 949-959.

- Luderus, M., van Steensel, B., Chong, L., Sibon, O., Cremers, F., and de Lange, T. (1996). Structure, subnuclear distribution, and nuclear matrix association of the mammalian telomeric complex. *The Journal of cell biology* *135*, 867-881.
- Ludlow, A.T., Zimmerman, J.B., Witkowski, S., Hearn, J.W., Hatfield, B.D., and Roth, S.M. (2008). Relationship between physical activity level, telomere length, and telomerase activity. *Medicine and science in sports and exercise* *40*, 1764.
- Lukasova, E., Kozubek, S., Kozubek, M., Kroha, V., Mareckova, A., Skalnikova, M., Bártová, E., and Slotova, J. (1999). Chromosomes participating in translocations typical of malignant hemoblastoses are also involved in exchange aberrations induced by fast neutrons. *Radiation research* *151*, 375-384.
- Luke, B., and Lingner, J. (2009). TERRA: telomeric repeat-containing RNA. *The EMBO journal* *28*, 2503-2510.
- Mahadevaiah, S.K., Bourc'his, D., de Rooij, D.G., Bestor, T.H., Turner, J.M., and Burgoyne, P.S. (2008). Extensive meiotic asynapsis in mice antagonises meiotic silencing of unsynapsed chromatin and consequently disrupts meiotic sex chromosome inactivation. *The Journal of cell biology* *182*, 263-276.
- Mainous III, A.G., Codd, V., Diaz, V.A., Schoepf, U.J., Everett, C.J., Player, M.S., and Samani, N.J. (2010). Leukocyte telomere length and coronary artery calcification. *Atherosclerosis* *210*, 262-267.
- Makarov, V.L., Hirose, Y., and Langmore, J.P. (1997). Long G tails at both ends of human chromosomes suggest a C strand degradation mechanism for telomere shortening. *Cell* *88*, 657-666.
- Manders, E.M., Kimura, H., and Cook, P.R. (1999). Direct imaging of DNA in living cells reveals the dynamics of chromosome formation. *The Journal of cell biology* *144*, 813-822.
- Mangham, L.J., Petrou, S., Doyle, L.W., Draper, E.S., and Marlow, N. (2009). The cost of preterm birth throughout childhood in England and Wales. *Pediatrics* *123*, e312-327.
- Mania, A., Mantzouratou, A., Delhanty, J.D., Baio, G., Serhal, P., and Sengupta, S.B. (2014). Telomere length in human blastocysts. *Reproductive biomedicine online* *28*, 624-637.
- Manochantr, S., Chiamchanya, C., and Sobhon, P. (2011). Relationship between chromatin condensation, DNA integrity and quality of ejaculated spermatozoa from infertile men. *Andrologia* *44*, 187-199.
- Manuelidis, L., and Borden, J. (1988). Reproducible compartmentalization of individual chromosome domains in human CNS cells revealed by in situ hybridization and three-dimensional reconstruction. *Chromosoma* *96*, 397-410.
- Marella, N.V., Bhattacharya, S., Mukherjee, L., Xu, J., and Berezney, R. (2009). Cell type specific chromosome territory organization in the interphase nucleus of normal and cancer cells. *Journal of cellular physiology* *221*, 130-138.
- Martens, U.M., Chavez, E.A., Poon, S.S., Schmoor, C., and Lansdorp, P.M. (2000). Accumulation of short telomeres in human fibroblasts prior to replicative senescence. *Experimental cell research* *256*, 291-299.
- Martens, U.M., Zijlmans, J.M.J., Poon, S.S., Dragowska, W., Yui, J., Chavez, E.A., Ward, R.K., and Lansdorp, P.M. (1998). Short telomeres on human chromosome 17p. *Nature genetics* *18*, 76-80.
- Martin-Ruiz, C., Jagger, C., Kingston, A., Collerton, J., Catt, M., Davies, K., Dunn, M., Hilkens, C., Keavney, B., and Pearce, S.H. (2011). Assessment of a large

- panel of candidate biomarkers of ageing in the Newcastle 85+ study. *Mechanisms of ageing and development* 132, 496-502.
- Martin-Ruiz, C., Dickinson, H.O., Keys, B., Rowan, E., Kenny, R.A., and Von Zglinicki, T. (2006). Telomere length predicts poststroke mortality, dementia, and cognitive decline. *Annals of neurology* 60, 174-180.
- Martin-Ruiz, C.M., Gussekloo, J., Heemst, D., Zglinicki, T., and Westendorp, R.G. (2005). Telomere length in white blood cells is not associated with morbidity or mortality in the oldest old: a population-based study. *Aging cell* 4, 287-290.
- Martín, J., Cervero, A., Mir, P., Conejero Martinez, J.A., Pellicer, A., and Simón, C. (2013). The impact of next-generation sequencing technology on preimplantation genetic diagnosis and screening. *Fertility and sterility* 99, 1054-1061. e1053.
- Mason, J.M., Frydrychova, R.C., and Biessmann, H. (2008). Drosophila telomeres: an exception providing new insights. *Bioessays* 30, 25-37.
- Mastenbroek, S., and Repping, S. (2014). Preimplantation genetic screening: back to the future. *Human Reproduction*, deu163.
- Mastenbroek, S., Scriven, P., Twisk, M., Viville, S., Van Der Veen, F., and Repping, S. (2008). What next for preimplantation genetic screening? More randomized controlled trials needed? *Human reproduction* 23, 2626-2628.
- Mastenbroek, S., Twisk, M., Van der Veen, F., and Repping, S. (2011). Preimplantation genetic screening: a systematic review and meta-analysis of RCTs. *Human reproduction update* 17, 454-466.
- Mastenbroek, S., Twisk, M., van Echten-Arends, J., Sikkema-Raddatz, B., Korevaar, J.C., Verhoeve, H.R., Vogel, N.E., Arts, E.G., De Vries, J.W., and Bossuyt, P.M. (2007). In vitro fertilization with preimplantation genetic screening. *New England Journal of Medicine* 357, 9-17.
- Masutomi, K., Yu, E.Y., Khurts, S., Ben-Porath, I., Currier, J.L., Metz, G.B., Brooks, M.W., Kaneko, S., Murakami, S., and DeCaprio, J.A. (2003). Telomerase maintains telomere structure in normal human cells. *Cell* 114, 241-253.
- Mather, K.A., Jorm, A.F., Parslow, R.A., and Christensen, H. (2011). Is telomere length a biomarker of aging? A review. *The Journals of Gerontology Series A: Biological Sciences and Medical Sciences* 66, 202-213.
- Mathog, D., Hochstrasser, M., Gruenbaum, Y., Saumweber, H., and Sedat, J. (1983). Characteristic folding pattern of polytene chromosomes in Drosophila salivary gland nuclei. *Nature* 308, 414-421.
- Maxwell, P.H., Coombes, C., Kenny, A.E., Lawler, J.F., Boeke, J.D., and Curcio, M.J. (2004). Ty1 mobilizes subtelomeric Y' elements in telomerase-negative *Saccharomyces cerevisiae* survivors. *Molecular and cellular biology* 24, 9887-9898.
- Mayer, R., Brero, A., Von Hase, J., Schroeder, T., Cremer, T., and Dietzel, S. (2005). Common themes and cell type specific variations of higher order chromatin arrangements in the mouse. *BMC cell biology* 6, 44.
- Mayer, S., Brüderlein, S., Perner, S., Waibel, I., Holdenried, A., Ciloglu, N., Hasel, C., Mattfeldt, T., Nielsen, K., and Möller, P. (2006). Sex-specific telomere length profiles and age-dependent erosion dynamics of individual chromosome arms in humans. *Cytogenetic and genome research* 112, 194-201.
- McClintock, B. (1939). The behavior in successive nuclear divisions of a chromosome broken at meiosis. *Proceedings of the National Academy of Sciences of the United States of America* 25, 405.

- McGee, J.S., Phillips, J.A., Chan, A., Sabourin, M., Paeschke, K., and Zakian, V.A. (2010). Reduced Rif2 and lack of Mec1 target short telomeres for elongation rather than double-strand break repair. *Nature structural & molecular biology* *17*, 1438-1445.
- McGrath, M., Wong, J.Y., Michaud, D., Hunter, D.J., and De Vivo, I. (2007). Telomere length, cigarette smoking, and bladder cancer risk in men and women. *Cancer Epidemiology Biomarkers & Prevention* *16*, 815-819.
- McIlrath, J., Bouffler, S.D., Samper, E., Cuthbert, A., Wojcik, A., Szumiel, I., Bryant, P.E., Riches, A.C., Thompson, A., and Blasco, M.A. (2001). Telomere length abnormalities in mammalian radiosensitive cells. *Cancer research* *61*, 912-915.
- Meaburn, K.J., and Misteli, T. (2008). Locus-specific and activity-independent gene repositioning during early tumorigenesis. *The Journal of cell biology* *180*, 39-50.
- Medicine, P.C.o.t.A.S.f.R. (2004). Smoking and infertility. *Fertility and sterility* *81*, 1181.
- Meerdo, L.N., Reed, W.A., and White, K.L. (2005). Telomere-to-centromere ratio of bovine clones, embryos, gametes, fetal cells, and adult cells. *Cloning and stem cells* *7*, 62-73.
- Mefford, H.C., and Trask, B.J. (2002). The complex structure and dynamic evolution of human subtelomeres. *Nature reviews Genetics* *3*, 91-102.
- Menezo, D.a.l.c.d.Y. (2006). Oocyte capacity to repair DNA damage induced in sperm. *Journal de Gynecologie Obstetrique et Biologie de la Reproduction* *35*, 19-23.
- Mengerink, K.J., and Vacquier, V.D. (2001). Glycobiology of sperm-egg interactions in deuterostomes. *Glycobiology* *11*, 37R-43R.
- Menon, R., Yu, J., Basanta-Henry, P., Brou, L., Berga, S.L., Fortunato, S.J., and Taylor, R.N. (2012). Short fetal leukocyte telomere length and preterm prelabor rupture of the membranes. *PloS one* *7*, e31136.
- Meselson, M., and Stahl, F.W. (1958). The replication of DNA in *Escherichia coli*. *Proceedings of the national academy of sciences* *44*, 671-682.
- Metcalf, J.A., Parkhill, J., Campbell, L., Stacey, M., Biggs, P., Byrd, P.J., and Taylor, A.M.R. (1996). Accelerated telomere shortening in ataxia telangiectasia. *Nature genetics* *13*, 350-353.
- Mewborn, S.K., Puckelwartz, M.J., Abuisneineh, F., Fahrenbach, J.P., Zhang, Y., MacLeod, H., Dellefave, L., Pytel, P., Selig, S., and Labno, C.M. (2010). Altered chromosomal positioning, compaction, and gene expression with a lamin A/C gene mutation. *PloS one* *5*, e14342.
- Meyer-Ficca, M., Muller-Navia, J., and Scherthan, H. (1998). Clustering of pericentromeres initiates in step 9 of spermiogenesis of the rat (*Rattus norvegicus*) and contributes to a well defined genome architecture in the sperm nucleus. *Journal of cell science* *111 (Pt 10)*, 1363-1370.
- Meyne, J., Ratliff, R.L., and MoYzIs, R.K. (1989). Conservation of the human telomere sequence (TTAGGG)_n among vertebrates. *Proceedings of the National Academy of Sciences* *86*, 7049-7053.
- Mikelsaar, R., Nelis, M., Kurg, A., Žilina, O., Korrovits, P., Rätsep, R., and Väli, M. (2012). Balanced reciprocal translocation t(5;13)(q33;q12) and 9q31.1 microduplication in a man suffering from infertility and pollinosis. *Journal of applied genetics* *53*, 93-97.
- Minamino, T., Miyauchi, H., Yoshida, T., Ishida, Y., Yoshida, H., and Komuro, I. (2002). Endothelial cell senescence in human atherosclerosis role of telomere in endothelial dysfunction. *Circulation* *105*, 1541-1544.

- Mitchell, J.R., Wood, E., and Collins, K. (1999). A telomerase component is defective in the human disease dyskeratosis congenita. *Nature* *402*, 551-555.
- Modi, N., Thomas, E.L., Uthaya, S.N., Umranikar, S., Bell, J.D., and Yajnik, C. (2009). Whole body magnetic resonance imaging of healthy newborn infants demonstrates increased central adiposity in Asian Indians. *Pediatric research* *65*, 584-587.
- Moore, T., Hennessy, E.M., Myles, J., Johnson, S.J., Draper, E.S., Costeloe, K.L., and Marlow, N. (2012). Neurological and developmental outcome in extremely preterm children born in England in 1995 and 2006: the EPICure studies. *BMJ (Clinical research ed.)* *345*, e7961.
- Morrish, T.A., Garcia-Perez, J.L., Stamato, T.D., Taccioli, G.E., Sekiguchi, J., and Moran, J.V. (2007). Endonuclease-independent LINE-1 retrotransposition at mammalian telomeres. *Nature* *446*, 208-212.
- Moskovtsev, S.I., Willis, J., White, J., and Mullen, J.B.M. (2010). Disruption of telomere-telomere interactions associated with DNA damage in human spermatozoa. *Systems biology in reproductive medicine* *56*, 407-412.
- Moyzis, R.K., Buckingham, J.M., Cram, L.S., Dani, M., Deaven, L.L., Jones, M.D., Meyne, J., Ratliff, R.L., and Wu, J.R. (1988). A highly conserved repetitive DNA sequence, (TTAGGG)_n, present at the telomeres of human chromosomes. *Proceedings of the National Academy of Sciences of the United States of America* *85*, 6622-6626.
- Mudrak, O., Tomilin, N., and Zalensky, A. (2005). Chromosome architecture in the decondensing human sperm nucleus. *Journal of cell science* *118*, 4541-4550.
- Muller, H. (1938). The remaking of chromosomes. *Collecting net* *13*, 181-195.
- Munné, S., Chen, S., Fischer, J., Colls, P., Zheng, X., Stevens, J., Escudero, T., Oter, M., Schoolcraft, B., and Simpson, J.L. (2005). Preimplantation genetic diagnosis reduces pregnancy loss in women aged 35 years and older with a history of recurrent miscarriages. *Fertility and sterility* *84*, 331-335.
- Munné, S., Gianaroli, L., Tur-Kaspa, I., Magli, C., Sandalinas, M., Grifo, J., Cram, D., Kahraman, S., Verlinsky, Y., and Simpson, J.L. (2007). Substandard application of preimplantation genetic screening may interfere with its clinical success. *Fertility and sterility* *88*, 781-784.
- Munné, S., Sandalinas, M., Escudero, T., Velilla, E., Walmsley, R., Sadowy, S., Cohen, J., and Sable, D. (2003). Improved implantation after preimplantation genetic diagnosis of aneuploidy. *Reproductive biomedicine online* *7*, 91-97.
- Muñoz-Espín, D., and Serrano, M. (2014). Cellular senescence: from physiology to pathology. *Nature reviews Molecular cell biology* *15*, 482-496.
- Muntoni, A., and Reddel, R.R. (2005). The first molecular details of ALT in human tumor cells. *Human Molecular Genetics* *14*, R191-R196.
- Musio, A., and Rainaldi, G. (1997). Cycling-PRINS: A method to improve the accuracy of telomeric sequence detection in mammalian chromosomes. *Mutation Research/Genetic Toxicology and Environmental Mutagenesis* *390*, 1-4.
- Nakamura, T.M., Morin, G.B., Chapman, K.B., Weinrich, S.L., Andrews, W.H., Lingner, J., Harley, C.B., and Cech, T.R. (1997). Telomerase catalytic subunit homologs from fission yeast and human. *Science* *277*, 955-959.
- Nakamura, Y., Hirose, M., Matsuo, H., Tsuyama, N., Kamisango, K., and Ide, T. (1999). Simple, rapid, quantitative, and sensitive detection of telomere repeats in cell lysate by a hybridization protection assay. *Clinical chemistry* *45*, 1718-1724.

- Natarajan, S., and McEachern, M.J. (2002). Recombinational telomere elongation promoted by DNA circles. *Molecular and cellular biology* 22, 4512-4521.
- Navot, D., Bergh, R., Williams, M.A., Garrisi, G.J., Guzman, I., Sandler, B., and Grunfeld, L. (1991). Poor oocyte quality rather than implantation failure as a cause of age-related decline in female fertility. *The Lancet* 337, 1375-1377.
- Neusser, M., Schubel, V., Koch, A., Cremer, T., and Müller, S. (2007). Evolutionarily conserved, cell type and species-specific higher order chromatin arrangements in interphase nuclei of primates. *Chromosoma* 116, 307-320.
- Nicklas, J.A., and Buel, E. (2006). Simultaneous Determination of Total Human and Male DNA Using a Duplex Real-Time PCR Assay. *Journal of forensic sciences* 51, 1005-1015.
- Nielsen, P.E., Egholm, M., Berg, R.H., and Buchardt, O. (1991). Sequence-selective recognition of DNA by strand displacement with a thymine-substituted polyamide. *Science (New York, N.Y.)* 254, 1497-1500.
- Nimmo, E.R., Pidoux, A.L., Perry, P.E., and Allshire, R.C. (1998). Defective meiosis in telomere-silencing mutants of *Schizosaccharomyces pombe*. *Nature* 392, 825-828.
- Njajou, O.T., Cawthon, R.M., Damcott, C.M., Wu, S.H., Ott, S., Garant, M.J., Blackburn, E.H., Mitchell, B.D., Shuldiner, A.R., and Hsueh, W.C. (2007). Telomere length is paternally inherited and is associated with parental lifespan. *Proceedings of the National Academy of Sciences of the United States of America* 104, 12135-12139.
- Nordfjäll, K., Svenson, U., Norrback, K.-F., Adolfsson, R., Lenner, P., and Roos, G. (2009). The individual blood cell telomere attrition rate is telomere length dependent. *PLoS genetics* 5, e1000375.
- Norman, M. (2010). Preterm birth—an emerging risk factor for adult hypertension? In *Seminars in perinatology* (Elsevier), pp. 183-187.
- Northrop, L., Treff, N., Levy, B., and Scott, R. (2010). SNP microarray-based 24 chromosome aneuploidy screening demonstrates that cleavage-stage FISH poorly predicts aneuploidy in embryos that develop to morphologically normal blastocysts. *Molecular human reproduction* 16, 590-600.
- Norwood, D., and Dimitrov, D.S. (1998). Sensitive method for measuring telomere lengths by quantifying telomeric DNA content of whole cells. *BioTechniques* 25, 1040-1045.
- Novo, C.L., and Londoño-Vallejo, J.A. (2013). Telomeres and the nucleus. In *Seminars in cancer biology* (Elsevier), pp. 116-124.
- Novotny, J., Aziz, N., Rybar, R., Brezinova, J., Kopecka, V., Filipcikova, R., Reruchova, M., and Oborna, I. (2013). Relationship between reactive oxygen species production in human semen and sperm DNA damage assessed by Sperm Chromatin Structure Assay. *Biomedical Papers* 157, 383-386.
- Nowell, P.C. (1997). Genetic alterations in leukemias and lymphomas: impressive progress and continuing complexity. *Cancer genetics and cytogenetics* 94, 13-19.
- Nuyt, A.M., and Alexander, B.T. (2009). Developmental programming and hypertension. *Current opinion in nephrology and hypertension* 18, 144.
- O'Callaghan, N.J., and Fenech, M. (2011). A quantitative PCR method for measuring absolute telomere length. *Biological Procedures Online* 13, 3.
- O'Flynn O'Brien, K.L., Varghese, A.C., and Agarwal, A. (2010). The genetic causes of male factor infertility: a review. *Fertility and sterility* 93, 1-12.

- O'Sullivan, J., Risques, R.A., Mandelson, M.T., Chen, L., Brentnall, T.A., Bronner, M.P., MacMillan, M.P., Feng, Z., Siebert, J.R., and Potter, J.D. (2006). Telomere length in the colon declines with age: a relation to colorectal cancer? *Cancer Epidemiology Biomarkers & Prevention* *15*, 573-577.
- Oeseburg, H., de Boer, R.A., van Gilst, W.H., and van der Harst, P. (2010). Telomere biology in healthy aging and disease. *Pflügers Archiv-European Journal of Physiology* *459*, 259-268.
- Ogawa, T., and Okazaki, T. (1980). Discontinuous DNA replication. *Annual review of biochemistry* *49*, 421-457.
- Oh, B.-K., Kim, Y.-J., Park, C., and Park, Y.N. (2005). Up-regulation of telomere-binding proteins, TRF1, TRF2, and TIN2 is related to telomere shortening during human multistep hepatocarcinogenesis. *The American journal of pathology* *166*, 73-80.
- Ohki, R., and Ishikawa, F. (2004). Telomere-bound TRF1 and TRF2 stall the replication fork at telomeric repeats. *Nucleic acids research* *32*, 1627-1637.
- Ohki, R., Tsurimoto, T., and Ishikawa, F. (2001). In vitro reconstitution of the end replication problem. *Molecular and cellular biology* *21*, 5753-5766.
- Ohno, S., Klinger, H., and Atkin, N. (1962). Human oogenesis. *Cytogenetics* *1*, 42-51.
- Oikawa, S., and Kawanishi, S. (1999). Site-specific DNA damage at GGG sequence by oxidative stress may accelerate telomere shortening. *FEBS letters* *453*, 365-368.
- Okazaki, R., Okazaki, T., Sakabe, K., Sugimoto, K., and Sugino, A. (1968). Mechanism of DNA chain growth. I. Possible discontinuity and unusual secondary structure of newly synthesized chains. *Proceedings of the National Academy of Sciences of the United States of America* *59*, 598.
- Okuda, K., Bardeguet, A., Gardner, J.P., Rodriguez, P., Ganesh, V., Kimura, M., Skurnick, J., Awad, G., and Aviv, A. (2002). Telomere length in the newborn. *Pediatric Research* *52*, 377-381.
- Okuda, K., Khan, M.Y., Skurnick, J., Kimura, M., Aviv, H., and Aviv, A. (2000). Telomere attrition of the human abdominal aorta: relationships with age and atherosclerosis. *Atherosclerosis* *152*, 391-398.
- Olovnikov, A.M. (1973). A theory of marginotomy. *Journal of theoretical biology* *41*, 181 <last_page> 190.
- Olszewska, M., Fraczek, M., Huleyuk, N., Czernikiewicz, A., Wiland, E., Boksa, M., Zastavna, D., Panasiuk, B., Midro, A.T., and Kurpisz, M. (2013). Chromatin structure analysis of spermatozoa from reciprocal chromosome translocation (RCT) carriers with known meiotic segregation patterns. *Reproductive biology* *13*, 209-220.
- Olszewska, M., Wiland, E., and Kurpisz, M. (2008). Positioning of chromosome 15, 18, X and Y centromeres in sperm cells of fertile individuals and infertile patients with increased level of aneuploidy. *Chromosome Research* *16*, 875-890.
- Onalan, G., Yilmaz, Z., Durak, T., Sahin, F.I., and Zeyneloglu, H.B. (2011). Successful pregnancy with preimplantation genetic diagnosis in a woman with mosaic Turner syndrome. *Fertility and sterility* *95*, 1788. e1781-1788. e1783.
- Opravil, S., Doyle, M., Sibilia, M., Jenuwein, T., and Biocenter, V. (2001). Loss of the Suv39h Histone Methyltransferases Impairs Mammalian Heterochromatin and Genome Stability. *Cell* *107*, 323-337.

- Otieno, A.C., Carter, A.B., Hedges, D.J., Walker, J.A., Ray, D.A., Garber, R.K., Anders, B.A., Stoilova, N., Laborde, M.E., and Fowlkes, J.D. (2004). Analysis of the Human Alu Ya-lineage. *J. Mol. Biol* 342, 109-118.
- Ourliac-Garnier, I., and Londoño-Vallejo, A. (2011). Telomere Length Analysis by Quantitative Fluorescent In situ Hybridization (Q-FISH). In *Telomeres and Telomerase* (Springer), pp. 21-31.
- Ozanne, S.E., and Constância, M. (2007). Mechanisms of disease: the developmental origins of disease and the role of the epigenotype. *Nature Clinical Practice Endocrinology & Metabolism* 3, 539-546.
- Paavonen, J., and Eggert-Kruse, W. (1999). Chlamydia trachomatis: impact on human reproduction. *Hum Reprod Update* 5, 433-447.
- Palladino, F., Laroche, T., Gilson, E., Axelrod, A., Pillus, L., and Gasser, S. (1993). SIR3 and SIR4 proteins are required for the positioning and integrity of yeast telomeres. *Cell* 75, 543-555.
- Pandey, L., Pandey, S., Gupta, J., and Saxena, A. (2010). Loss of the AZFc region due to a human Y-chromosome microdeletion in infertile male patients. *Genet Mol Res* 9, 1267-1273.
- Pang, M., Hoegerman, S., Cuticchia, A., Moon, S., Doncel, G., Acosta, A., and Kearns, W. (1999). Detection of aneuploidy for chromosomes 4, 6, 7, 8, 9, 10, 11, 12, 13, 17, 18, 21, X and Y by fluorescence in-situ hybridization in spermatozoa from nine patients with oligoasthenoteratozoospermia undergoing intracytoplasmic sperm injection. *Human Reproduction* 14, 1266-1273.
- Panossian, L., Porter, V., Valenzuela, H., Zhu, X., Reback, E., Masterman, D., Cummings, J., and Effros, R. (2003). Telomere shortening in T cells correlates with Alzheimer's disease status. *Neurobiology of aging* 24, 77-84.
- Parada, L.A., and Misteli, T. (2002). Chromosome positioning in the interphase nucleus. *Trends in cell biology* 12, 425-432.
- Parkinson, J.R., Hyde, M.J., Gale, C., Santhakumaran, S., and Modi, N. (2013). Preterm birth and the metabolic syndrome in adult life: a systematic review and meta-analysis. *Pediatrics* 131, e1240-e1263.
- Pasquali, R., Patton, L., and Gambineri, A. (2007). Obesity and infertility. *Current Opinion in Endocrinology, Diabetes and Obesity* 14, 482-487.
- Passos, J.F., Saretzki, G., and von Zglinicki, T. (2007). DNA damage in telomeres and mitochondria during cellular senescence: is there a connection? *Nucleic acids research* 35, 7505-7513.
- Passos, J.o.F., and von Zglinicki, T. (2005). Mitochondria, telomeres and cell senescence. *Experimental gerontology* 40, 466-472.
- Pathai, S., Gilbert, C.E., Lawn, S.D., Weiss, H.A., Peto, T., Cook, C., Wong, T.Y., and Shiels, P.G. (2013). Assessment of candidate ocular biomarkers of ageing in a South African adult population: relationship with chronological age and systemic biomarkers. *Mechanisms of ageing and development*.
- Pavanello, S., Hoxha, M., Dioni, L., Bertazzi, P.A., Snenghi, R., Nalesso, A., Ferrara, S.D., Montisci, M., and Baccarelli, A. (2011). Shortened telomeres in individuals with abuse in alcohol consumption. *International journal of cancer* 129, 983-992.
- Pawelec, G., Akbar, A., Caruso, C., Solana, R., Grubeck-Loebenstein, B., and Wikby, A. (2005). Human immunosenescence: is it infectious? *Immunological reviews* 205, 257-268.
- Pfeffer, J., Pang, M.-G., Hoegerman, S.F., Osgood, C.J., Stacey, M., Mayer, J., Oehninger, S., and Kearns, W.G. (1999). Aneuploidy frequencies in semen

- fractions from ten oligoasthenoteratozoospermic patients donating sperm for intracytoplasmic sperm injection. *Fertility and sterility* 72, 472-478.
- Pfeifer, C., Scherthan, H., and Thomsen, P.D. (2003). Sex-specific telomere redistribution and synapsis initiation in cattle oogenesis. *Developmental biology* 255, 206-215.
- Pfeifer, C., Thomsen, P., and Scherthan, H. (2001). Centromere and telomere redistribution precedes homologue pairing and terminal synapsis initiation during prophase I of cattle spermatogenesis. *Cytogenetic and Genome Research* 93, 304-314.
- Podlevsky, J.D., Bley, C.J., Omana, R.V., Qi, X., and Chen, J.J.-L. (2008). The telomerase database. *Nucleic acids research* 36, D339-D343.
- Polani, P.E., and Crolla, J.A. (1991). A test of the production line hypothesis of mammalian oogenesis. *Human genetics* 88, 64-70.
- Poon, S.S.S., Martens, U.M., Ward, R.K., and Lansdorp, P.M. (1999). Telomere length measurements using digital fluorescence microscopy. *Cytometry* 36, 267-278.
- Puterman, E., Lin, J., Blackburn, E., O'Donovan, A., Adler, N., and Epel, E. (2010). The power of exercise: buffering the effect of chronic stress on telomere length. *PLoS One* 5, e10837.
- Rabl, C. (1885). *Über zelltheilung* (Morphol Jarbuch: W. Engelmann).
- Rahman, M.S., Lee, J.-S., Kwon, W.-S., and Pang, M.-G. (2013). Sperm proteomics: road to male fertility and contraception. *International journal of endocrinology* 2013.
- Ramsden, D.A., and Gellert, M. (1998). Ku protein stimulates DNA end joining by mammalian DNA ligases: a direct role for Ku in repair of DNA double-strand breaks. *The EMBO Journal* 17, 609-614.
- Ranganathan, V., Heine, W.F., Ciccone, D.N., Rudolph, K.L., Wu, X., Chang, S., Hai, H., Ahearn, I.M., Livingston, D.M., and Resnick, I. (2001). Rescue of a telomere length defect of Nijmegen breakage syndrome cells requires NBS and telomerase catalytic subunit. *Current Biology* 11, 962-966.
- Rasmussen, S.W., and Holm, P.B. (1978). Human meiosis II. Chromosome pairing and recombination nodules in human spermatocytes. *Carlsberg research communications* 43, 275-327.
- Raz, V., Vermolen, B.J., Garini, Y., Onderwater, J.J., Mommaas-Kienhuis, M.A., Koster, A.J., Young, I.T., Tanke, H., and Dirks, R.W. (2008). The nuclear lamina promotes telomere aggregation and centromere peripheral localization during senescence of human mesenchymal stem cells. *Journal of cell science* 121, 4018-4028.
- Redon, S., Reichenbach, P., and Lingner, J. (2010). The non-coding RNA TERRA is a natural ligand and direct inhibitor of human telomerase. *Nucleic acids research* 38, 5797-5806.
- Riethman, H. (2009). Human subtelomeric copy number variations. *Cytogenetic and genome research* 123, 244-252.
- Riethman, H., Ambrosini, A., and Paul, S. (2005). Human subtelomere structure and variation. *Chromosome research : an international journal on the molecular, supramolecular and evolutionary aspects of chromosome biology* 13, 505-515.
- Robinson, W., Barrett, I., Bernard, L., Telenius, A., Bernasconi, F., Wilson, R., Best, R., Howard-Peebles, P., Langlois, S., and Kalousek, D. (1997). Meiotic origin of trisomy in confined placental mosaicism is correlated with presence of fetal uniparental disomy, high levels of trisomy in trophoblast, and increased risk of

- fetal intrauterine growth restriction. *American journal of human genetics* *60*, 917.
- Rodríguez, S., Goyanes, V., Segrelles, E., Blasco, M., Gosálvez, J., and Fernández, J.L. (2005). Critically short telomeres are associated with sperm DNA fragmentation. *Fertility and sterility* *84*, 843-845.
- Roeder, G.S. (1997). Meiotic chromosomes: it takes two to tango. *Genes & Development* *11*, 2600-2621.
- Roig, I., Liebe, B., Egozcue, J., Cabero, L., Garcia, M., and Scherthan, H. (2004). Female-specific features of recombinational double-stranded DNA repair in relation to synapsis and telomere dynamics in human oocytes. *Chromosoma* *113*, 22-33.
- Rowley, J.D. (1999). The role of chromosome translocations in leukemogenesis. In *Seminars in hematology*, pp. 59-72.
- Rubio, C., Bellver, J., Rodrigo, L., Bosch, E., Mercader, A., Vidal, C., De los Santos, M.J., Giles, J., Labarta, E., and Domingo, J. (2013). Preimplantation genetic screening using fluorescence in situ hybridization in patients with repetitive implantation failure and advanced maternal age: two randomized trials. *Fertility and sterility* *99*, 1400-1407.
- Rudd, M.K. (2014). Human and Primate Subtelomeres. In *Subtelomeres* (Springer), pp. 153-164.
- Rufer, N., Brümmendorf, T.H., Kolvraa, S., Bischoff, C., Christensen, K., Wadsworth, L., Schulzer, M., and Lansdorp, P.M. (1999). Telomere fluorescence measurements in granulocytes and T lymphocyte subsets point to a high turnover of hematopoietic stem cells and memory T cells in early childhood. *The Journal of experimental medicine* *190*, 157-168.
- Rupnick, M.A., Panigrahy, D., Zhang, C.-Y., Dallabrida, S.M., Lowell, B.B., Langer, R., and Folkman, M.J. (2002). Adipose tissue mass can be regulated through the vasculature. *Proceedings of the National Academy of Sciences* *99*, 10730-10735.
- Russell, L.D., Ettl, R.A., Hikim, A.P.S., and Clegg, E.D. (1993). Histological and histopathological evaluation of the testis. *International journal of andrology* *16*, 83-83.
- Russo, V., Berardinelli, P., Martelli, A., Di Giacinto, O., Nardinocchi, D., Fantasia, D., and Barboni, B. (2006). Expression of telomerase reverse transcriptase subunit (TERT) and telomere sizing in pig ovarian follicles. *Journal of Histochemistry & Cytochemistry* *54*, 443-455.
- Sabourin, M., Tuzon, C.T., and Zakian, V.A. (2007). Telomerase and Tel1p Preferentially Associate with Short Telomeres in *S. cerevisiae*. *Molecular cell* *27*, 550.
- Sadeghi, M.R. (2014). The State of Semen Analysis over Time. *Journal of reproduction & infertility* *15*, 1.
- Sadeghi, M.R., Hodjat, M., Lakpour, N., Arefi, S., Amirjannati, N., Modarresi, T., Jadda, H.H., and Akhondi, M.M. (2009). Effects of sperm chromatin integrity on fertilization rate and embryo quality following intracytoplasmic sperm injection. *Avicenna Journal of Medical Biotechnology* *1*, 173.
- Sadler, T.W. (2011). *Langman's medical embryology* (Lippincott Williams & Wilkins).
- Sakabe, K., and Okazaki, R. (1966). A unique property of the replicating region of chromosomal DNA. *Biochimica et Biophysica Acta (BBA)-Nucleic Acids and Protein Synthesis* *129*, 651-654.

- Sakkas, D., Mariethoz, E., Manicardi, G., Bizzaro, D., Bianchi, P.G., and Bianchi, U. (1999). Origin of DNA damage in ejaculated human spermatozoa. *Reviews of reproduction* 4, 31-37.
- Sakkas, D., Urner, F., Bianchi, P., Bizzaro, D., Wagner, I., Jaquenoud, N., Manicardi, G., and Campana, A. (1996). Sperm chromatin anomalies can influence decondensation after intracytoplasmic sperm injection. *Human Reproduction* 11, 837-843.
- Salk, J.J., Bansal, A., Lai, L.A., Crispin, D.A., Ussakli, C.H., Horwitz, M.S., Bronner, M.P., Brentnall, T.A., Loeb, L.A., and Rabinovitch, P.S. (2013). Clonal expansions and short telomeres are associated with neoplasia in early-onset, but not late-onset, ulcerative colitis. *Inflammatory bowel diseases* 19, 2593-2602.
- Salpea, K., Talmud, P., Cooper, J., Maubaret, C., Stephens, J., Abelak, K., and Humphries, S. (2010). Association of telomere length with type 2 diabetes, oxidative stress and UCP2 gene variation. *Atherosclerosis* 209, 42-50.
- Salpea, K.D., and Humphries, S.E. (2010). Telomere length in atherosclerosis and diabetes. *Atherosclerosis* 209, 35.
- Salsabili, N., Mehraei, A., Jalalizadeh, B., Pourmand, G., and Jalaie, S. (2009). Correlation of sperm nuclear chromatin condensation staining method with semen parameters and sperm functional tests in patients with spinal cord injury, varicocele, and idiopathic infertility. *Urology journal* 3, 32-37.
- Samani, N.J., Boulby, R., Butler, R., Thompson, J.R., and Goodall, A.H. (2001). Telomere shortening in atherosclerosis. *The Lancet* 358, 472-473.
- Samper, E., Goytisolo, F.A., Slijepcevic, P., Van Buul, P.P., and Blasco, M.A. (2000). Mammalian Ku86 protein prevents telomeric fusions independently of the length of TTAGGG repeats and the G-strand overhang. *EMBO reports* 1, 244-252.
- Sanders, J.L., and Newman, A.B. (2013). Telomere Length in Epidemiology: A Biomarker of Aging, Age-Related Disease, Both, or Neither? *Epidemiologic reviews* 35, 112-131.
- Santiso, R., Tamayo, M., Gosálvez, J., Meseguer, M., Garrido, N., and Fernández, J.L. (2010). Swim-up procedure selects spermatozoa with longer telomere length. *Mutation Research/Fundamental and Molecular Mechanisms of Mutagenesis* 688, 88-90.
- Sasaki, M., Honda, T., Yamada, H., Wake, N., Barrett, J.C., and Oshimura, M. (1994). Evidence for multiple pathways to cellular senescence. *Cancer research* 54, 6090-6093.
- Sastre, J., Borrás, C., GARCÍA-SALA, D., Lloret, A., Pallardó, F.V., and Viña, J. (2002). Mitochondrial damage in aging and apoptosis. *Annals of the New York Academy of Sciences* 959, 448-451.
- Savage, S.A., Giri, N., Baerlocher, G.M., Orr, N., Lansdorp, P.M., and Alter, B.P. (2008). TIN2, a Component of the Shelterin Telomere Protection Complex, Is Mutated in Dyskeratosis Congenita. *The American Journal of Human Genetics* 82, 501-509.
- Sbracia, M., Baldi, M., Cao, D., Sandrelli, A., Chiandetti, A., Poverini, R., and Aragona, C. (2002). Preferential location of sex chromosomes, their aneuploidy in human sperm, and their role in determining sex chromosome aneuploidy in embryos after ICSI. *Human Reproduction* 17, 320-324.
- Scherthan, H. (2007). Telomere attachment and clustering during meiosis. *Cellular and molecular life sciences: CMLS* 64, 117-124.

- Scherthan, H., Weich, S., Schwegler, H., Heyting, C., Härle, M., and Cremer, T. (1996). Centromere and telomere movements during early meiotic prophase of mouse and man are associated with the onset of chromosome pairing. *The Journal of cell biology* *134*, 1109-1125.
- Schmitt, J., Benavente, R., Hodzic, D., Hoog, C., Stewart, C.L., and Alsheimer, M. (2007). Transmembrane protein Sun2 is involved in tethering mammalian meiotic telomeres to the nuclear envelope. *Proceedings of the National Academy of Sciences of the United States of America* *104*, 7426-7431.
- Schmittgen, T.D., and Livak, K.J. (2008). Analyzing real-time PCR data by the comparative CT method. *Nature protocols* *3*, 1101-1108.
- Schoeftner, S., and Blasco, M.A. (2009). A 'higher order' of telomere regulation: telomere heterochromatin and telomeric RNAs. *The EMBO journal* *28*, 2323-2336.
- Schoolcraft, W.B., Katz-Jaffe, M.G., Stevens, J., Rawlins, M., and Munne, S. (2009). Preimplantation aneuploidy testing for infertile patients of advanced maternal age: a randomized prospective trial. *Fertility and sterility* *92*, 157-162.
- Schulz, V.P., Zakian, V.A., Ogburn, C.E., McKay, J., Jarzebowicz, A.A., Martin, G., and Edland, S. (1996). Accelerated loss of telomeric repeats may not explain accelerated replicative decline of Werner syndrome cells. *Human genetics* *97*, 750-754.
- Scott Jr, R.T., Ferry, K., Su, J., Tao, X., Scott, K., and Treff, N.R. (2012). Comprehensive chromosome screening is highly predictive of the reproductive potential of human embryos: a prospective, blinded, nonselection study. *Fertility and sterility* *97*, 870-875.
- Scott Jr, R.T., Upham, K.M., Forman, E.J., Zhao, T., and Treff, N.R. (2013). Cleavage-stage biopsy significantly impairs human embryonic implantation potential while blastocyst biopsy does not: a randomized and paired clinical trial. *Fertility and sterility* *100*, 624-630.
- Seifer, D., Gardiner, A., Ferreira, K., and Peluso, J. (1996). Apoptosis as a function of ovarian reserve in women undergoing in vitro fertilization. *Fertility and sterility* *66*, 593-598.
- Seifer, D.B., Charland, C., Berlinsky, D., Penzias, A.S., Haning Jr, R.V., Naftolin, F., and Barker, B.E. (1993). Proliferative index of human luteinized granulosa cells varies as a function of ovarian reserve. *American journal of obstetrics and gynecology* *169*, 1531-1535.
- Seli, E., and Sakkas, D. (2005). Spermatozoal nuclear determinants of reproductive outcome: implications for ART. *Human reproduction update* *11*, 337-349.
- Serrano, A.L., and Andrés, V. (2004). Telomeres and Cardiovascular Disease Does Size Matter? *Circulation research* *94*, 575-584.
- Sfeir, A., Kabir, S., van Overbeek, M., Celli, G.B., and de Lange, T. (2010). Loss of Rap1 induces telomere recombination in the absence of NHEJ or a DNA damage signal. *Science* *327*, 1657-1661.
- Shah, K., Sivapalan, G., Gibbons, N., Tempest, H., and Griffin, D.K. (2003). The genetic basis of infertility. *Reproduction* *126*, 13-25.
- Sharma, R.K., Pasqualotto, F.F., Nelson, D.R., Thomas, A.J., and Agarwal, A. (1999). The reactive oxygen species—total antioxidant capacity score is a new measure of oxidative stress to predict male infertility. *Human Reproduction* *14*, 2801-2807.

- Sharma, R.K., Sabanegh, E., Mahfouz, R., Gupta, S., Thiagarajan, A., and Agarwal, A. (2010). TUNEL as a test for sperm DNA damage in the evaluation of male infertility. *Urology* 76, 1380-1386.
- Shay, J.W. (1995). Aging and cancer: are telomeres and telomerase the connection? *Molecular medicine today* 1, 378-384.
- Shay, J.W. (2003). Telomerase therapeutics: Telomeres recognized as a DNA damage signal. *Clinical cancer research* 9, 3521-3525.
- Shay, J.W., Wright, W.E., and Werbin, H. (1991). Defining the molecular mechanisms of human cell immortalization. *Biochimica et Biophysica Acta (BBA)-Reviews on Cancer* 1072, 1-7.
- Shibuya, H., Ishiguro, K.-i., and Watanabe, Y. (2014). The TRF1-binding protein TERB1 promotes chromosome movement and telomere rigidity in meiosis. *Nature cell biology*.
- Shiels, P.G. (2010). Improving precision in investigating aging: why telomeres can cause problems. *The Journals of Gerontology Series A: Biological Sciences and Medical Sciences* 65, 789-791.
- Shiels, P.G., McGlynn, L.M., MacIntyre, A., Johnson, P.C., Batty, G.D., Burns, H., Cavanagh, J., Deans, K.A., Ford, I., and McConnachie, A. (2011). Accelerated telomere attrition is associated with relative household income, diet and inflammation in the pSoBid cohort. *PLoS One* 6, e22521.
- Shiloh, Y. (1997). Ataxia-telangiectasia and the Nijmegen breakage syndrome: related disorders but genes apart. *Annual review of genetics* 31, 635-662.
- Shoeman, R.L., and Traub, P. (1990). The in vitro DNA-binding properties of purified nuclear lamin proteins and vimentin. *Journal of Biological Chemistry* 265, 9055-9061.
- Simon, N.M., Smoller, J.W., McNamara, K.L., Maser, R.S., Zalta, A.K., Pollack, M.H., Nierenberg, A.A., Fava, M., and Wong, K.-K. (2006). Telomere shortening and mood disorders: preliminary support for a chronic stress model of accelerated aging. *Biological psychiatry* 60, 432-435.
- Simoncini, T., Hafezi-Moghadam, A., Brazil, D.P., Ley, K., Chin, W.W., and Liao, J.K. (2000). Interaction of oestrogen receptor with the regulatory subunit of phosphatidylinositol-3-OH kinase. *Nature* 407, 538-541.
- Skinner, B., Völker, M., Ellis, M., and Griffin, D. (2009). An appraisal of nuclear organisation in interphase embryonic fibroblasts of chicken, turkey and duck. *Cytogenetic and Genome Research* 126, 156-164.
- Slagboom, P.E., Droog, S., and Boomsma, D.I. (1994). Genetic determination of telomere size in humans: a twin study of three age groups. *American journal of human genetics* 55, 876.
- Smith, J.S., Chen, Q., Yatsunyk, L.A., Nicoludis, J.M., Garcia, M.S., Kranaster, R., Balasubramanian, S., Monchaud, D., Teulade-Fichou, M.-P., and Abramowitz, L. (2011). Rudimentary G-quadruplex-based telomere capping in *Saccharomyces cerevisiae*. *Nature structural & molecular biology* 18, 478-485.
- Solov'eva, L., Svetlova, M., Bodinski, D., and Zalensky, A.O. (2004). Nature of telomere dimers and chromosome looping in human spermatozoa. *Chromosome research : an international journal on the molecular, supramolecular and evolutionary aspects of chromosome biology* 12, 817-823.
- Solovei, I., Kreysing, M., Lanctôt, C., Kösem, S., Peichl, L., Cremer, T., Guck, J., and Joffe, B. (2009). Nuclear architecture of rod photoreceptor cells adapts to vision in mammalian evolution. *Cell* 137, 356-368.

- Sotolongo, B., and Ward, W.S. (2000). DNA loop domain organization: the three-dimensional genomic code. *Journal of cellular biochemistry. Supplement Suppl 35*, 23-26.
- Sperling, K., and Luedtke, E.-K. (1981). Arrangement of prematurely condensed chromosomes in cultured cells and lymphocytes of the Indian muntjac. *Chromosoma* 83, 541-553.
- Spyridopoulos, I., Erben, Y., Brummendorf, T.H., Haendeler, J., Dietz, K., Seeger, F., Kissel, C.K., Martin, H., Hoffmann, J., and Assmus, B. (2008). Telomere gap between granulocytes and lymphocytes is a determinant for hematopoietic progenitor cell impairment in patients with previous myocardial infarction. *Arteriosclerosis, thrombosis, and vascular biology* 28, 968-974.
- Staessen, C., Platteau, P., Van Assche, E., Michiels, A., Tournaye, H., Camus, M., Devroey, P., Liebaers, I., and Van Steirteghem, A. (2004). Comparison of blastocyst transfer with or without preimplantation genetic diagnosis for aneuploidy screening in couples with advanced maternal age: a prospective randomized controlled trial. *Human Reproduction* 19, 2849-2858.
- Staessen, C., Verpoest, W., Donoso, P., Haentjens, P., Van der Elst, J., Liebaers, I., and Devroey, P. (2008). Preimplantation genetic screening does not improve delivery rate in women under the age of 36 following single-embryo transfer. *Human reproduction* 23, 2818-2825.
- Stewart, C., and Burke, B. (2014). The missing LINC: A mammalian KASH-domain protein coupling meiotic chromosomes to the cytoskeleton. *Nucleus* 5, 0--1.
- Stewart, S.A., Ben-Porath, I., Carey, V.J., O'Connor, B.F., Hahn, W.C., and Weinberg, R.A. (2003). Erosion of the telomeric single-strand overhang at replicative senescence. *Nature genetics* 33, 492-496.
- Sukenik-Halevy, R., Fejgin, M., Kidron, D., Goldberg-Bittman, L., Sharony, R., Biron-Shental, T., Kitay-Cohen, Y., and Amiel, A. (2009). Telomere aggregate formation in placenta specimens of pregnancies complicated with pre-eclampsia. *Cancer genetics and cytogenetics* 195, 27-30.
- Sun, H.B., Shen, J., and Yokota, H. (2000). Size-Dependent Positioning of Human Chromosomes in Interphase Nuclei. *Biophysical journal* 79, 184 <last_page> 190.
- Takubo, K., Nakamura, K.-I., Izumiyama, N., Furugori, E., Sawabe, M., Arai, T., Esaki, Y., Mafune, K.-I., Kammori, M., and Fujiwara, M. (2000). Telomere shortening with aging in human liver. *The Journals of Gerontology Series A: Biological Sciences and Medical Sciences* 55, B533-B536.
- Takubo, K., Nakamura, K.-I., Izumiyama, N., Sawabe, M., Arai, T., Esaki, Y., Tanaka, Y., Mafune, K.-I., Fujiwara, M., and Kammori, M. (1999). Telomere shortening with aging in human esophageal mucosa. *Age* 22, 95-99.
- Tanabe, H., KüPPER, K., Ishida, T., Neusser, M., and Mizusawa, H. (2004). Inter- and intra-specific gene-density-correlated radial chromosome territory arrangements are conserved in Old World monkeys. *Cytogenetic and genome research* 108, 255-261.
- Tanabe, H., Müller, S., Neusser, M., von Hase, J., Calcagno, E., Cremer, M., Solovei, I., Cremer, C., and Cremer, T. (2002). Evolutionary conservation of chromosome territory arrangements in cell nuclei from higher primates. *Proceedings of the National Academy of Sciences* 99, 4424-4429.
- Tanemura, K., Ogura, A., Cheong, C., Gotoh, H., Matsumoto, K., Sato, E., Hayashi, Y., Lee, H.-W., and Kondo, T. (2005). Dynamic rearrangement of telomeres during spermatogenesis in mice. *Developmental biology* 281, 196-207.

- Tarín, J.J., Pérez-Albalá, S., and Cano, A. (2002). Oral antioxidants counteract the negative effects of female aging on oocyte quantity and quality in the mouse. *Molecular reproduction and development* *61*, 385-397.
- Tatone, C., Amicarelli, F., Carbone, M.C., Monteleone, P., Caserta, D., Marci, R., Artini, P.G., Piomboni, P., and Focarelli, R. (2008). Cellular and molecular aspects of ovarian follicle ageing. *Human reproduction update* *14*, 131-142.
- Tavalae, M., Deemeh, M., Arbabian, M., Kiyani, A., and Nasr-Esfahani, M. (2014). Relationship between fertilization rate and early apoptosis in sperm population of infertile individuals. *Andrologia* *46*, 36-41.
- Tempest, H., and Griffin, D. (2004). The relationship between male infertility and increased levels of sperm disomy. *Cytogenetic and genome research* *107*, 83-94.
- Terasawa, M., Ogawa, H., Tsukamoto, Y., Shinohara, M., Shirahige, K., Kleckner, N., and Ogawa, T. (2007). Meiotic recombination-related DNA synthesis and its implications for cross-over and non-cross-over recombinant formation. *Proceedings of the National Academy of Sciences* *104*, 5965-5970.
- Tesarik, J. (1989). Involvement of oocyte-coded message in cell differentiation control of early human embryos. *Development* *105*, 317-322.
- Therkelsen, A., Nielsen, A., Koch, J., Hindkjaer, J., and Kølvrå, S. (1995). Staining of human telomeres with primed in situ labeling (PRINS). *Cytogenetic and Genome Research* *68*, 115-118.
- Thilagavathi, J., Kumar, M., Mishra, S., Venkatesh, S., Kumar, R., and Dada, R. (2013). Analysis of sperm telomere length in men with idiopathic infertility. *Archives of gynecology and obstetrics*, 1-5.
- Thomas, E.L., Parkinson, J.R., Hyde, M.J., Yap, I.K., Holmes, E., Doré, C.J., Bell, J.D., and Modi, N. (2011). Aberrant adiposity and ectopic lipid deposition characterize the adult phenotype of the preterm infant. *Pediatric research* *70*, 507-512.
- Thomas, E.L., Uthaya, S., Vasu, V., McCarthy, J.P., McEwan, P., Hamilton, G., Bell, J.D., and Modi, N. (2008a). Neonatal intrahepatocellular lipid. *Archives of Disease in Childhood-Fetal and Neonatal Edition* *93*, F382-F383.
- Thomas, P., O' Callaghan, N.J., and Fenech, M. (2008b). Telomere length in white blood cells, buccal cells and brain tissue and its variation with ageing and Alzheimer's disease. *Mechanisms of ageing and development* *129*, 183-190.
- Tinnion, R., Gillone, J., Cheetham, T., and Embleton, N. (2013). Preterm birth and subsequent insulin sensitivity: a systematic review. *Archives of disease in childhood*, archdischild-2013-304615.
- Toutain, J., Prochazkova-Carlotti, M., Cappellen, D., Jarne, A., Chevret, E., Ferrer, J., Idrissi, Y., Pelluard, F., Carles, D., and Maugey-Laulon, B. (2013). Reduced Placental Telomere Length during Pregnancies Complicated by Intrauterine Growth Restriction. *PloS one* *8*, e54013.
- Traversa, M.V., Marshall, J., McArthur, S., and Leigh, D. (2011). The genetic screening of preimplantation embryos by comparative genomic hybridisation. *Reprod Biol* *11*, 51-60.
- Treff, N.R., Fedick, A., Tao, X., Devkota, B., Taylor, D., and Scott Jr, R.T. (2013). Evaluation of targeted next-generation sequencing-based preimplantation genetic diagnosis of monogenic disease. *Fertility and sterility* *99*, 1377-1384. e1376.

- Treff, N.R., and Scott Jr, R.T. (2013). Four-hour quantitative real-time polymerase chain reaction–based comprehensive chromosome screening and accumulating evidence of accuracy, safety, predictive value, and clinical efficacy. *Fertility and sterility* *99*, 1049-1053.
- Treff, N.R., Su, J., Kasabwala, N., Tao, X., Miller, K.A., and Scott Jr, R.T. (2010a). Robust embryo identification using first polar body single nucleotide polymorphism microarray-based DNA fingerprinting. *Fertility and sterility* *93*, 2453-2455.
- Treff, N.R., Su, J., Tao, X., Levy, B., and Scott Jr, R.T. (2010b). Accurate single cell 24 chromosome aneuploidy screening using whole genome amplification and single nucleotide polymorphism microarrays. *Fertility and sterility* *94*, 2017-2021.
- Treff, N.R., Su, J., Tao, X., Northrop, L.E., and Scott, R.T. (2011a). Single-cell whole-genome amplification technique impacts the accuracy of SNP microarray-based genotyping and copy number analyses. *Molecular human reproduction* *17*, 335-343.
- Treff, N.R., Su, J., Taylor, D., and Scott, R.T., Jr. (2011b). Telomere DNA deficiency is associated with development of human embryonic aneuploidy. *PLoS genetics* *7*, e1002161.
- Treff, N.R., Tao, X., Ferry, K.M., Su, J., Taylor, D., and Scott Jr, R.T. (2012). Development and validation of an accurate quantitative real-time polymerase chain reaction–based assay for human blastocyst comprehensive chromosomal aneuploidy screening. *Fertility and sterility* *97*, 819-824. e812.
- Tsakiri, K.D., Cronkhite, J.T., Kuan, P.J., Xing, C., Raghu, G., Weissler, J.C., Rosenblatt, R.L., Shay, J.W., and Garcia, C.K. (2007). Adult-onset pulmonary fibrosis caused by mutations in telomerase. *Proceedings of the National Academy of Sciences* *104*, 7552-7557.
- Tsend-Ayush, E., Dodge, N., Mohr, J., Casey, A., Himmelbauer, H., Kremitzki, C.L., Schatzkamer, K., Graves, T., Warren, W.C., and Grützner, F. (2009). Higher-order genome organization in platypus and chicken sperm and repositioning of sex chromosomes during mammalian evolution. *Chromosoma* *118*, 53-69.
- Tsukamoto, Y., Taggart, A.K., and Zakian, V.A. (2001). The role of the Mre11-Rad50-Xrs2 complex in telomerase-mediated lengthening of *Saccharomyces cerevisiae* telomeres. *Current Biology* *11*, 1328-1335.
- Turner, J., Aprelikova, O., Xu, X., Wang, R., Kim, S., Chandramouli, G.V., Barrett, J.C., Burgoyne, P.S., and Deng, C.-X. (2004a). BRCA1, histone H2AX phosphorylation, and male meiotic sex chromosome inactivation. *Current Biology* *14*, 2135-2142.
- Turner, J.M., Mahadevaiah, S.K., Fernandez-Capetillo, O., Nussenzweig, A., Xu, X., Deng, C.-X., and Burgoyne, P.S. (2004b). Silencing of unsynapsed meiotic chromosomes in the mouse. *Nature genetics* *37*, 41-47.
- Turner, K.J., Vasu, V., Greenall, J., and Griffin, D.K. (2014). Telomere length analysis and preterm infant health: the importance of assay design in the search for novel biomarkers. *Biomarkers in medicine* *8*, 485-498.
- Turner, S., and Hartshorne, G.M. (2013). Telomere lengths in human pronuclei, oocytes and spermatozoa. *Molecular human reproduction*.
- Turner, S., Wong, H.P., Rai, J., and Hartshorne, G.M. (2010). Telomere lengths in human oocytes, cleavage stage embryos and blastocysts. *Molecular human reproduction*.

- Ulaner, G.A., and Giudice, L.C. (1997). Developmental regulation of telomerase activity in human fetal tissues during gestation. *Molecular human reproduction* 3, 769-773.
- Unryn, B.M., Cook, L.S., and Riabowol, K.T. (2005). Paternal age is positively linked to telomere length of children. *Aging cell* 4, 97-101.
- Uringa, E.-J., Youds, J.L., Lisaingo, K., Lansdorp, P.M., and Boulton, S.J. (2010). RTEL1: an essential helicase for telomere maintenance and the regulation of homologous recombination. *Nucleic acids research*, gkq1045.
- Uthaya, S., Thomas, E.L., Hamilton, G., Dore, C.J., Bell, J., and Modi, N. (2005). Altered adiposity after extremely preterm birth. *Pediatric research* 57, 211-215.
- Uziel, O., Singer, J.A., Danicek, V., Sahar, G., Berkov, E., Luchansky, M., Fraser, A., Ram, R., and Lahav, M. (2007). Telomere dynamics in arteries and mononuclear cells of diabetic patients: effect of diabetes and of glycemic control. *Experimental gerontology* 42, 971-978.
- Valdes, A., Andrew, T., Gardner, J.a., Kimura, M., Oelsner, E., Cherkas, L., Aviv, A., and Spector, T. (2005). Obesity, cigarette smoking, and telomere length in women. *The Lancet* 366, 662-664.
- Valdes, A., Deary, I., Gardner, J., Kimura, M., Lu, X., Spector, T., Aviv, A., and Cherkas, L. (2010). Leukocyte telomere length is associated with cognitive performance in healthy women. *Neurobiology of aging* 31, 986-992.
- Vallejo, A.N., Weyand, C.M., and Goronzy, J.J. (2004). T-cell senescence: a culprit of immune abnormalities in chronic inflammation and persistent infection. *Trends in molecular medicine* 10, 119-124.
- Van Voorhis, B.J. (2007). In vitro fertilization. *New England Journal of Medicine* 356, 379-386.
- VanDeVoorde, R.G., and Mitsneces, M.M. (2014). Neonatal Hypertension. In *Kidney and Urinary Tract Diseases in the Newborn* (Springer), pp. 349-361.
- Vanneste, E., Voet, T., Le Caignec, C., Ampe, M., Konings, P., Melotte, C., Debrock, S., Amyere, M., Vikkula, M., and Schuit, F. (2009). Chromosome instability is common in human cleavage-stage embryos. *Nature medicine* 15, 577-583.
- Vasu V, T.E.L., Durighel G, Uthaya S, Bell J D., and N, M. (2009). Abstracts of the 50th Annual Meeting of the European Society for Paediatric Research. October 9-12, 2009. Hamburg, Germany. *Acta paediatrica* (Oslo, Norway : 1992). Supplement 98, 1-278.
- Vasu, V., Thomas, E., Durighel, G., Hyde, M., Bell, J., and Modi, N. (2013). Early nutritional determinants of intrahepatocellular lipid deposition in preterm infants at term age. *International Journal of Obesity* 37, 500-504.
- Vaziri, H., Schächter, F., Uchida, I., Wei, L., Zhu, X., Effros, R., Cohen, D., and Harley, C. (1993). Loss of telomeric DNA during aging of normal and trisomy 21 human lymphocytes. *American journal of human genetics* 52, 661.
- Vegetti, W., Van Assche, E., Frias, A., Verheyen, G., Bianchi, M.M., Bonduelle, M., Liebaers, I., and Van Steirteghem, A. (2000). Correlation between semen parameters and sperm aneuploidy rates investigated by fluorescence in-situ hybridization in infertile men. *Human Reproduction* 15, 351-365.
- Verdun, R.E., Crabbe, L., Haggblom, C., and Karlseder, J. (2005). Functional human telomeres are recognized as DNA damage in G2 of the cell cycle. *Molecular cell* 20, 551-561.
- Verdun, R.E., and Karlseder, J. (2006). The DNA damage machinery and homologous recombination pathway act consecutively to protect human telomeres. *Cell* 127, 709-720.

- Verdun, R.E., and Karlseder, J. (2007). Replication and protection of telomeres. *Nature* *447*, 924-931.
- Verlinsky, Y., and Kuliev, A. (2005). Clinical Outcomes Following Preimplantation Genetic Diagnosis. *Practical Preimplantation Genetic Diagnosis*, 169-173.
- Vicencio, J.M., Galluzzi, L., Tajeddine, N., Ortiz, C., Criollo, A., Tasdemir, E., Morselli, E., Ben Younes, A., Maiuri, M.C., and Lavandro, S. (2008). Senescence, apoptosis or autophagy? *Gerontology* *54*, 92-99.
- Vincent, M., Daudin, M., De, M., Massat, G., Mieusset, R., Pontonnier, F., Calvas, P., Bujan, L., and Bourrouillout, G. (2001). Cytogenetic investigations of infertile men with low sperm counts: a 25-year experience. *Journal of andrology* *23*, 18-22; discussion 44-15.
- von Zglinicki, T. (2012). Will your telomeres tell your future. *BMJ* *344*.
- von Zglinicki, T., and Martin-Ruiz, C.M. (2005). Telomeres as biomarkers for ageing and age-related diseases. *Current Molecular Medicine* *5*, 197-203.
- Von Zglinicki, T., Serra, V., Lorenz, M., Saretzki, G., Lenzen-Gro, bgr, R., Ge, bgr, R., Risch, A., and Steinhagen-Thiessen, E. (2000). Short telomeres in patients with vascular dementia: an indicator of low antioxidative capacity and a possible risk factor? *Laboratory investigation* *80*, 1739-1747.
- Voss, S.R., Kump, D.K., Putta, S., Pauly, N., Reynolds, A., Henry, R.J., Basa, S., Walker, J.A., and Smith, J.J. (2011). Origin of amphibian and avian chromosomes by fission, fusion, and retention of ancestral chromosomes. *Genome research* *21*, 1306-1312.
- Vulliamy, T.J., Marrone, A., Knight, S.W., Walne, A., Mason, P.J., and Dokal, I. (2006). Mutations in dyskeratosis congenita: their impact on telomere length and the diversity of clinical presentation. *Blood* *107*, 2680-2685.
- Waga, S., and Stillman, B. (1998). The DNA replication fork in eukaryotic cells. *Annual review of biochemistry* *67*, 721-751.
- Walne, A.J., Vulliamy, T., Marrone, A., Beswick, R., Kirwan, M., Masunari, Y., Al-Qurashi, F.-h., Aljurf, M., and Dokal, I. (2007). Genetic heterogeneity in autosomal recessive dyskeratosis congenita with one subtype due to mutations in the telomerase-associated protein NOP10. *Human molecular genetics* *16*, 1619-1629.
- Wang, F., Kalmbach, K., Seth-Smith, M., Antunes, D., Liu, L., and Keefe, D. (2013a). Single cell method to measure oocyte telomere length. *Fertility and Sterility* *100*, S233-S234.
- Wang, F., Pan, X., Kalmbach, K., Seth-Smith, M.L., Ye, X., Antunes, D.M., Yin, Y., Liu, L., Keefe, D.L., and Weissman, S.M. (2013b). Robust measurement of telomere length in single cells. *Proceedings of the National Academy of Sciences* *110*, E1906-E1912.
- Wang, H., Chen, H., Gao, X., McGrath, M., Deer, D., De Vivo, I., Schwarzschild, M.A., and Ascherio, A. (2008). Telomere length and risk of Parkinson's disease. *Movement Disorders* *23*, 302-305.
- Wang, H., and Höög, C. (2006). Structural damage to meiotic chromosomes impairs DNA recombination and checkpoint control in mammalian oocytes. *The Journal of cell biology* *173*, 485-495.
- Wang, L., Wang, X., Zhang, J., Song, Z., Wang, S., Gao, Y., Wang, J., Luo, Y., Niu, Z., and Yue, X. (2014). Detection of Chromosomal Aneuploidy in Human Pre-implantation Embryos by Next Generation Sequencing. *Biology of reproduction, biolreprod.* 113.116459.

- Wang, R.C., Smogorzewska, A., and de Lange, T. (2004). Homologous recombination generates T-loop-sized deletions at human telomeres. *Cell* *119*, 355-368.
- Wang, Y.Y., Chen, A.F., Wang, H.Z., Xie, L.Y., Sui, K.X., and Zhang, Q.Y. (2011). Association of shorter mean telomere length with large artery stiffness in patients with coronary heart disease. *The aging male : the official journal of the International Society for the Study of the Aging Male* *14*, 27-32.
- Ward, W.S., Kimura, Y., and Yanagimachi, R. (1999). An intact sperm nuclear matrix may be necessary for the mouse paternal genome to participate in embryonic development. *Biology of reproduction* *60*, 702-706.
- Watfa, G., Dragonas, C., Brosche, T., Dittrich, R., Sieber, C., Alecu, C., Benetos, A., and Nzietchueng, R. (2011). Study of telomere length and different markers of oxidative stress in patients with Parkinson's disease. *The journal of nutrition, health & aging* *15*, 277-281.
- Watson, J.D. (1972). Origin of concatemeric T7DNA. *Nature* *239*, 197-201.
- Webb, C.J., Wu, Y., and Zakian, V.A. (2013). DNA repair at telomeres: Keeping the ends intact. *Cold Spring Harbor perspectives in biology* *5*, a012666.
- Wei, C., and Price, M. (2003). Protecting the terminus: t-loops and telomere end-binding proteins. *Cellular and Molecular Life Sciences CMLS* *60*, 2283-2294.
- Weierich, C., Brero, A., Stein, S., von Hase, J., Cremer, C., Cremer, T., and Solovei, I. (2003). Three-dimensional arrangements of centromeres and telomeres in nuclei of human and murine lymphocytes. *Chromosome research* *11*, 485-502.
- Weipoltshammer, K., Schöfer, C., Almeder, M., Philimonenko, V.V., Frei, K., Wachtler, F., and Hozák, P. (1999). Intranuclear anchoring of repetitive DNA sequences centromeres, telomeres, and ribosomal DNA. *The Journal of cell biology* *147*, 1409-1418.
- Wellinger, R.J., Ethier, K., Labrecque, P., and Zakian, V.A. (1996). Evidence for a new step in telomere maintenance. *Cell* *85*, 423-433.
- Wellinger, R.J., Wolf, A.J., and Zakian, V.A. (1993). *Saccharomyces* telomeres acquire single-strand TG₁₋₃ tails late in S phase. *Cell* *72*, 51-60.
- Wells, D., Alfarawati, S., and Fragouli, E. (2008). Use of comprehensive chromosomal screening for embryo assessment: microarrays and CGH. *Molecular human reproduction* *14*, 703-710.
- Wells, D., Kaur, K., Grifo, J., Glassner, M., Taylor, J.C., Fragouli, E., and Munne, S. (2014). Clinical utilisation of a rapid low-pass whole genome sequencing technique for the diagnosis of aneuploidy in human embryos prior to implantation. *Journal of medical genetics* *51*, 553-562.
- Wentzensen, I.M., Mirabello, L., Pfeiffer, R.M., and Savage, S.A. (2011). The association of telomere length and cancer: a meta-analysis. *Cancer Epidemiology Biomarkers & Prevention* *20*, 1238-1250.
- Wiemann, S., Satyanarayana, A., Tsahuridu, M., Tillmann, H., Zender, L., Klempnauer, J., Flemming, P., Franco, S., Blasco, M., and Manns, M. (2002). Hepatocyte telomere shortening and senescence are general markers of human liver cirrhosis. *FASEB journal: official publication of the Federation of American Societies for Experimental Biology* *16*, 935.
- Wieser, M., Stadler, G., Böhm, E., Borth, N., Katinger, H., Grillari, J., and Voglauer, R. (2006). Nuclear flow FISH: isolation of cell nuclei improves the determination of telomere lengths. *Experimental gerontology* *41*, 230-235.
- Wiland, E., Żegało, M., and Kurpisz, M. (2008). Interindividual differences and alterations in the topology of chromosomes in human sperm nuclei of fertile

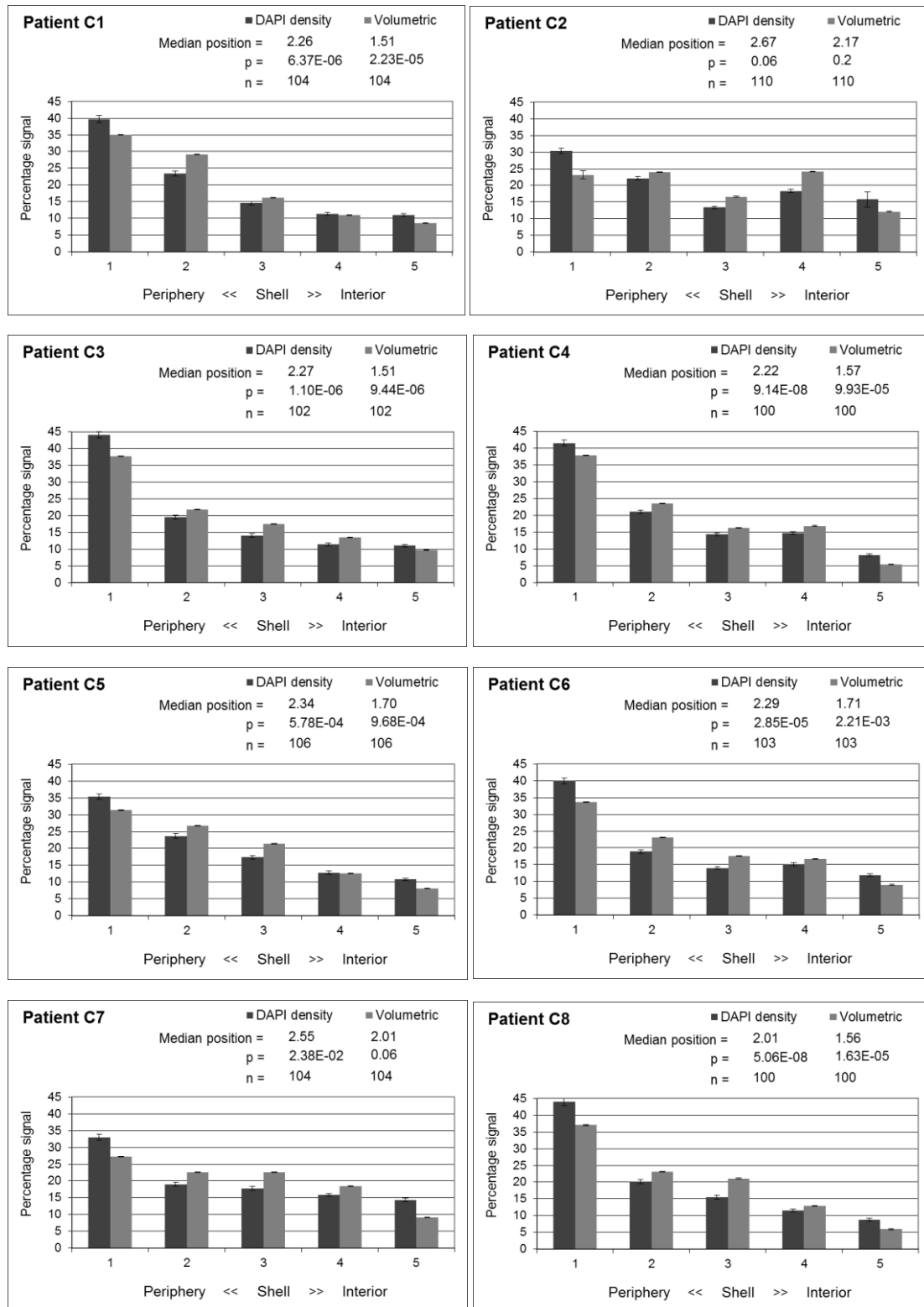
- donors and carriers of reciprocal translocations. *Chromosome research* 16, 291-305.
- Wilkins, L., Tchinda, J., Komminoth, P., and Werner, M. (1997). Single-and double-color oligonucleotide primed in situ labeling (PRINS): applications in pathology. *Histochemistry and cell biology* 108, 439-446.
- Willeit, P., Willeit, J., Brandstätter, A., Ehrlenbach, S., Mayr, A., Gasperi, A., Weger, S., Oberhollenzer, F., Reindl, M., and Kronenberg, F. (2010a). Cellular aging reflected by leukocyte telomere length predicts advanced atherosclerosis and cardiovascular disease risk. *Arteriosclerosis, thrombosis, and vascular biology* 30, 1649-1656.
- Willeit, P., Willeit, J., Mayr, A., Weger, S., Oberhollenzer, F., Brandstätter, A., Kronenberg, F., and Kiechl, S. (2010b). Telomere length and risk of incident cancer and cancer mortality. *Jama* 304, 69-75.
- Williams, R.S., Williams, J.S., and Tainer, J.A. (2007). Mre11-Rad50-Nbs1 is a keystone complex connecting DNA repair machinery, double-strand break signaling, and the chromatin template This paper is one of a selection of papers published in this Special Issue, entitled 28th International West Coast Chromatin and Chromosome Conference, and has undergone the Journal's usual peer review process. *Biochemistry and Cell Biology* 85, 509-520.
- Williamson, J.R., Raghuraman, M., and Cech, T.R. (1989). Monovalent cation-induced structure of telomeric DNA: the G-quartet model. *Cell* 59, 871-880.
- Wolkowitz, O.M., Mellon, S.H., Epel, E.S., Lin, J., Dhabhar, F.S., Su, Y., Reus, V.I., Rosser, R., Burke, H.M., and Kupferman, E. (2011). Leukocyte telomere length in major depression: correlations with chronicity, inflammation and oxidative stress-preliminary findings. *PLoS One* 6, e17837.
- Wong, H.P., and Slijepcevic, P. (2004). Telomere length measurement in mouse chromosomes by a modified Q-FISH method. *Cytogenetic and genome research* 105, 464-470.
- Wright, D.L., Jones, E.L., Mayer, J.F., Oehninger, S., Gibbons, W.E., and Lanzendorf, S.E. (2001). Characterization of telomerase activity in the human oocyte and preimplantation embryo. *Molecular human reproduction* 7, 947-955.
- Wright, W.E., Pereira-Smith, O., and Shay, J. (1989). Reversible cellular senescence: implications for immortalization of normal human diploid fibroblasts. *Molecular and cellular biology* 9, 3088-3092.
- Wright, W.E., Piatyszek, M.A., Rainey, W.E., Byrd, W., and Shay, J.W. (1996). Telomerase activity in human germline and embryonic tissues and cells. *Developmental genetics* 18, 173-179.
- Wright, W.E., and Shay, J.W. (1992). The two-stage mechanism controlling cellular senescence and immortalization. *Experimental gerontology* 27, 383-389.
- Wright, W.E., Tesmer, V.M., Huffman, K.E., Levene, S.D., and Shay, J.W. (1997). Normal human chromosomes have long G-rich telomeric overhangs at one end. *Genes & development* 11, 2801-2809.
- Wu, Y., Xiao, S., and Zhu, X.-D. (2007). MRE11-RAD50-NBS1 and ATM function as co-mediators of TRF1 in telomere length control. *Nature structural & molecular biology* 14, 832-840.
- Xin, H., Liu, D., and Songyang, Z. (2008). The telosome/shelterin complex and its functions. *Genome Biol* 9, 232.
- Xing, J., Ajani, J.A., Chen, M., Izzo, J., Lin, J., Chen, Z., Gu, J., and Wu, X. (2009). Constitutive short telomere length of chromosome 17p and 12q but not 11q and

- 2p is associated with an increased risk for esophageal cancer. *Cancer Prevention Research* 2, 459-465.
- Xu, J., and Yang, X. (2000). Telomerase activity in bovine embryos during early development. *Biology of reproduction* 63, 1124-1128.
- Xu, W., Hu, H., Wang, Z., Chen, X., Yang, F., Zhu, Z., Fang, P., Dai, J., Wang, L., and Shi, H. (2012). Proteomic characteristics of spermatozoa in normozoospermic patients with infertility. *Journal of proteomics* 75, 5426-5436.
- Yamada-Fukunaga, T., Yamada, M., Hamatani, T., Chikazawa, N., Ogawa, S., Akutsu, H., Miura, T., Miyado, K., Tarín, J.J., and Kuji, N. (2013). Age-associated telomere shortening in mouse oocytes. *Reproductive Biology and Endocrinology* 11, 108.
- Yamada, K., Fujita, K., Quan, J., Sekine, M., Kashima, K., Yahata, T., and Tanaka, K. (2010). Increased apoptosis of germ cells in patients with AZFc deletions. *Journal of assisted reproduction and genetics* 27, 293-297.
- Yamada, M., Tsuji, N., Nakamura, M., Moriai, R., Kobayashi, D., Yagihashi, A., and Watanabe, N. (2001). Down-regulation of TRF1, TRF2 and TIN2 genes is important to maintain telomeric DNA for gastric cancers. *Anticancer research* 22, 3303-3307.
- Yamagata, Y., Nakamura, Y., Umayahara, K., Harada, A., Takayama, H., Sugino, N., and Kato, H. (2002). Changes in telomerase activity in experimentally induced atretic follicles of immature rats. *Endocrine journal* 49, 589-595.
- Yamaguchi, H., Calado, R.T., Ly, H., Kajigaya, S., Baerlocher, G.M., Chanock, S.J., Lansdorp, P.M., and Young, N.S. (2005). Mutations in TERT, the gene for telomerase reverse transcriptase, in aplastic anemia. *New England Journal of Medicine* 352, 1413-1424.
- Yan, J., Chen, B.-Z., Bouchard, E.F., and Drouin, R. (2004). The labeling efficiency of human telomeres is increased by double-strand PRINS. *Chromosoma* 113, 204-209.
- Yang, Z., Liu, J., Collins, G.S., Salem, S.A., Liu, X., Lyle, S.S., Peck, A.C., Sills, E.S., and Salem, R.D. (2012). Selection of single blastocysts for fresh transfer via standard morphology assessment alone and with array CGH for good prognosis IVF patients: results from a randomized pilot study. *Molecular cytogenetics* 5, 1-8.
- Yankiwski, V., Marciniak, R.A., Guarente, L., and Neff, N.F. (2000). Nuclear structure in normal and Bloom syndrome cells. *Proceedings of the National Academy of Sciences* 97, 5214-5219.
- Yashima, K., Maitra, A., Rogers, B.B., Timmons, C.F., Rathi, A., Pinar, H., Wright, W.E., Shay, J.W., and Gazdar, A.F. (1998). Expression of the RNA component of telomerase during human development and differentiation. *Cell growth & differentiation: the molecular biology journal of the American Association for Cancer Research* 9, 805-813.
- Ying, H.-q., Scott, M.B., and Zhou-cun, A. (2012). Relationship of SNP of H2BFWT gene to male infertility in a Chinese population with idiopathic spermatogenesis impairment. *Biomarkers* 17, 402-406.
- Youngren, K., Jeanclos, E., Aviv, H., Kimura, M., Stock, J., Hanna, M., Skurnick, J., Bardeguet, A., and Aviv, A. (1998). Synchrony in telomere length of the human fetus. *Human genetics* 102, 640-643.
- Zahler, A.M., Williamson, J.R., Cech, T.R., and Prescott, D.M. (1991). Inhibition of telomerase by G-quartet DNA structures. *Nature* 350, 718-720.

- Zalenskaya, I.A., Bradbury, E.M., and Zalensky, A.O. (2000). Chromatin structure of telomere domain in human sperm. *Biochemical and biophysical research communications* 279, 213-218.
- Zalenskaya, I.A., and Zalensky, A.O. (2004). Non-random positioning of chromosomes in human sperm nuclei. *Chromosome Research* 12, 163-173.
- Zalensky, A., and Zalenskaya, I. (2007). Organization of chromosomes in spermatozoa: an additional layer of epigenetic information? *Biochemical Society Transactions* 35, 609-611.
- Zalensky, A.O., Allen, M.J., Kobayashi, A., Zalenskaya, I.A., Balhorn, R., and Bradbury, E.M. (1995). Well-defined genome architecture in the human sperm nucleus. *Chromosoma* 103, 577-590.
- Zalensky, A.O., Breneman, J.W., Zalenskaya, I.A., Brinkley, B.R., and Bradbury, E.M. (1993). Organization of centromeres in the decondensed nuclei of mature human sperm. *Chromosoma* 102, 509 <last_page> 518.
- Zalensky, A.O., Tomilin, N.V., Zalenskaya, I.A., Teplitz, R.L., and Bradbury, E.M. (1997). Telomere-telomere interactions and candidate telomere binding protein(s) in mammalian sperm cells. *Experimental cell research* 232, 29-41.
- Zandemami, M., Qujeq, D., Akhondi, M.M., Kamali, K., Raygani, M., Lakpour, N., Shiraz, E.S., and Sadeghi, M.R. (2012). Correlation of CMA3 Staining with Sperm Quality and Protamine Deficiency. *Lab Medicine* 43, 262-267.
- Zanet, D.L., Saberi, S., Oliveira, L., Sattha, B., Gadawski, I., and Côté, H.C. (2013). Blood and dried blood spot telomere length measurement by qPCR: assay considerations. *PloS one* 8, e57787.
- Zaug, A.J., Podell, E.R., and Cech, T.R. (2005). Human POT1 disrupts telomeric G-quadruplexes allowing telomerase extension in vitro. *Proceedings of the National Academy of Sciences of the United States of America* 102, 10864-10869.
- Zeichner, S.L., Palumbo, P., Feng, Y., Xiao, X., Gee, D., Sleasman, J., Goodenow, M., Biggar, R., and Dimitrov, D. (1999). Rapid telomere shortening in children. *Blood* 93, 2824-2830.
- Zekry, D., Herrmann, F.R., Irminger-Finger, I., Ortolan, L., Genet, C., Vitale, A.-M., Michel, J.-P., Gold, G., and Krause, K.-H. (2010). Telomere length is not predictive of dementia or MCI conversion in the oldest old. *Neurobiology of aging* 31, 719-720.
- Zeng, S., Liu, L., Sun, Y., Xie, P., Hu, L., Yuan, D., Chen, D., Ouyang, Q., Lin, G., and Lu, G. (2014). Telomerase-mediated telomere elongation from human blastocysts to embryonic stem cells. *Journal of cell science* 127, 752-762.
- Zhang, P., Dilley, C., and Mattson, M.P. (2007). DNA damage responses in neural cells: focus on the telomere. *Neuroscience* 145, 1439-1448.
- Zhao, C., Huo, R., Wang, F.-Q., Lin, M., Zhou, Z.-M., and Sha, J.-H. (2007). Identification of several proteins involved in regulation of sperm motility by proteomic analysis. *Fertility and sterility* 87, 436-438.
- Zhu, X.-D., Küster, B., Mann, M., Petrini, J.H., and de Lange, T. (2000). Cell-cycle-regulated association of RAD50/MRE11/NBS1 with TRF2 and human telomeres. *Nature genetics* 25, 347-352.
- Zhu, X.-D., Niedernhofer, L., Kuster, B., Mann, M., Hoeijmakers, J.H., and de Lange, T. (2003). ERCC1/XPF removes the 3' overhang from uncapped telomeres and represses formation of telomeric DNA-containing double minute chromosomes. *Molecular cell* 12, 1489-1498.

- Zijlmans, J.M.J.M., Martens, U.M., Poon, S.S.S., Raap, A.K., Tanke, H.J., Ward, R.K., and Lansdorp, P.M. (1997). Telomeres in the mouse have large inter-chromosomal variations in the number of T2AG3 repeats. *Proceedings of the National Academy of Sciences* *94*, 7423-7428.
- Zini, A., Fischer, M.A., Sharir, S., Shayegan, B., Phang, D., and Jarvi, K. (2002). Prevalence of abnormal sperm DNA denaturation in fertile and infertile men. *Urology* *60*, 1069-1072.

9 Supplementary data



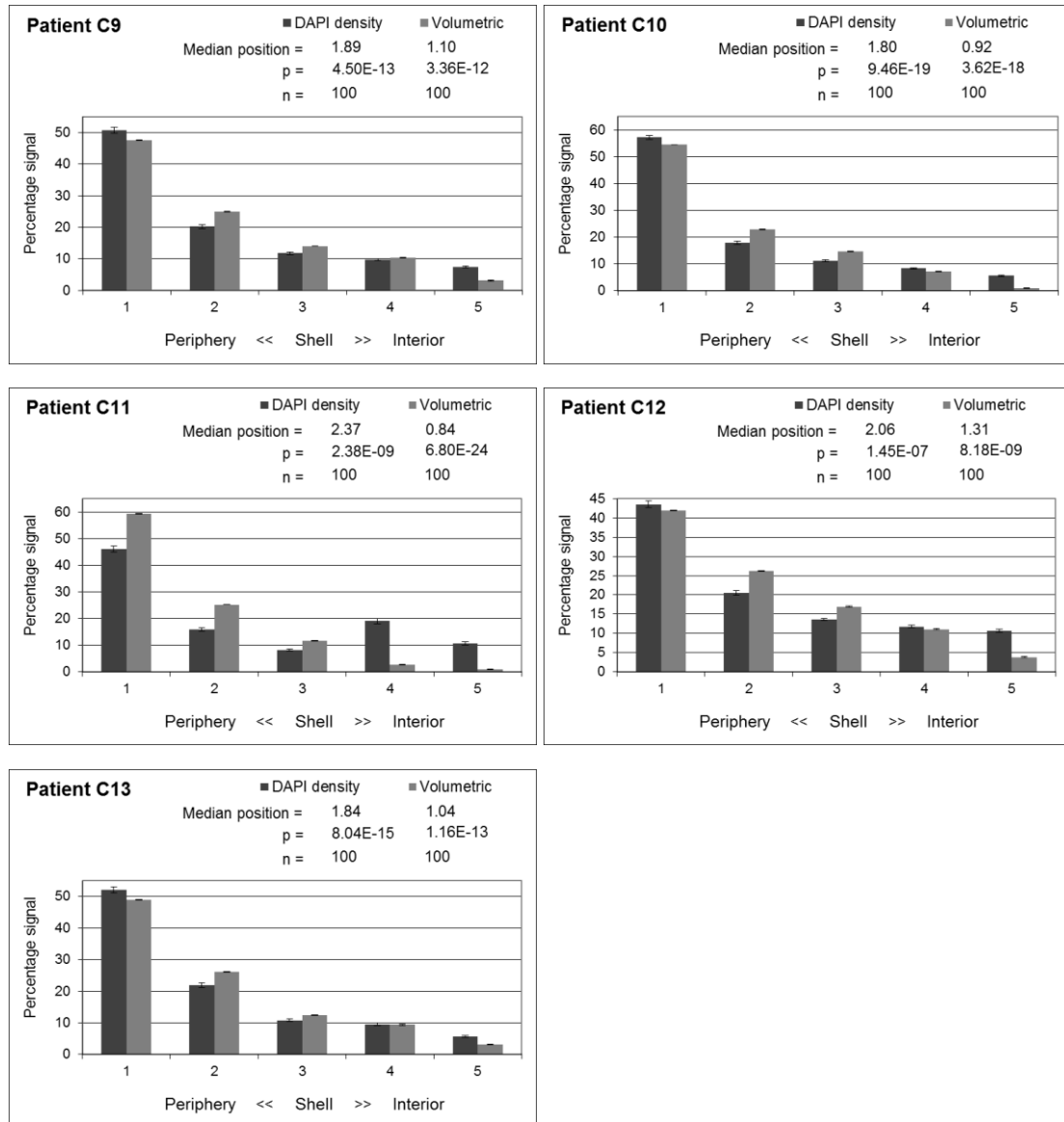


Figure 1: Telomere distribution patterns in the sperm heads of each individual normal fertile male following 2D analysis of FISH signals using DAPI density and volumetric compensation models. Error bars represent the standard error of the mean, n is the number of sperm nuclei analysed, p is the statistical significance of a non-random distribution assessed by Chi² test.

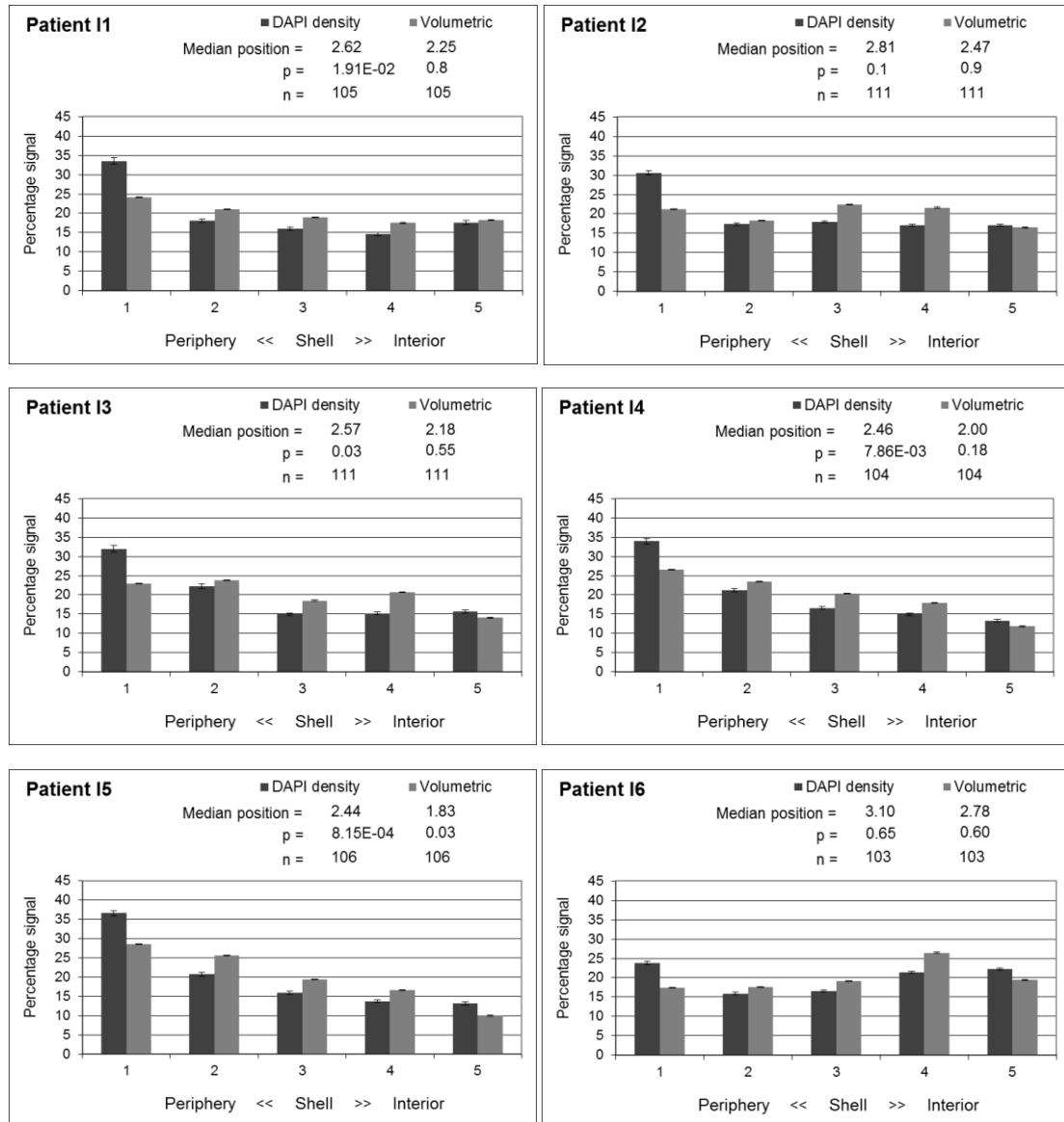


Figure 2: Telomere distribution patterns in the sperm heads of each individual infertile male following 2D analysis of FISH signals using DAPI density and volumetric compensation models. Error bars represent the standard error of the mean, n is the number of sperm nuclei analysed, p is the statistical significance of a non-random distribution assessed by Chi² test.

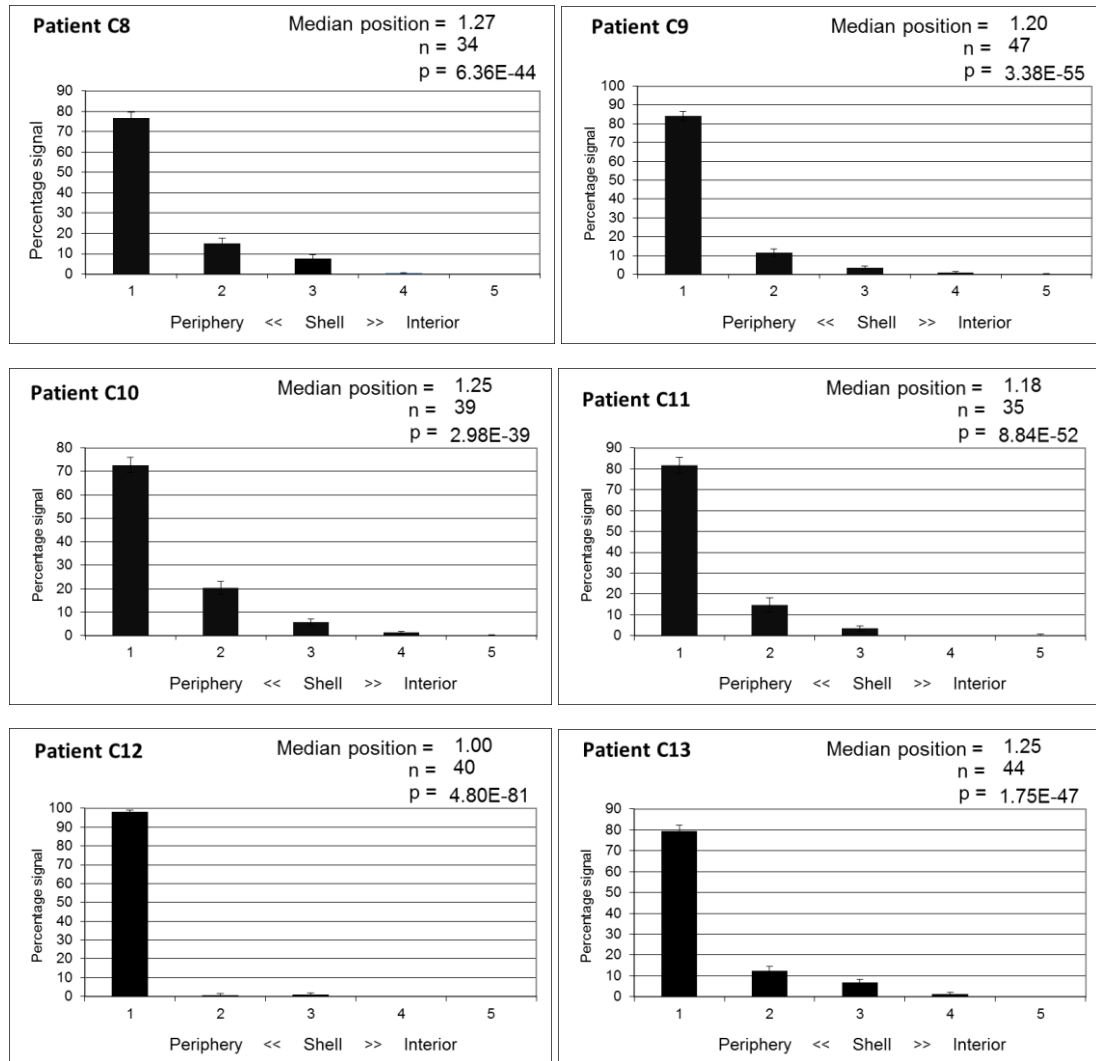


Figure 3: Telomere distribution patterns in the sperm heads of each individual fertile male following 3D analysis of FISH signals. Error bars represent the standard error of the mean, n is the number of sperm nuclei analysed, p is the statistical significance of a non-random distribution assessed by Chi² test.

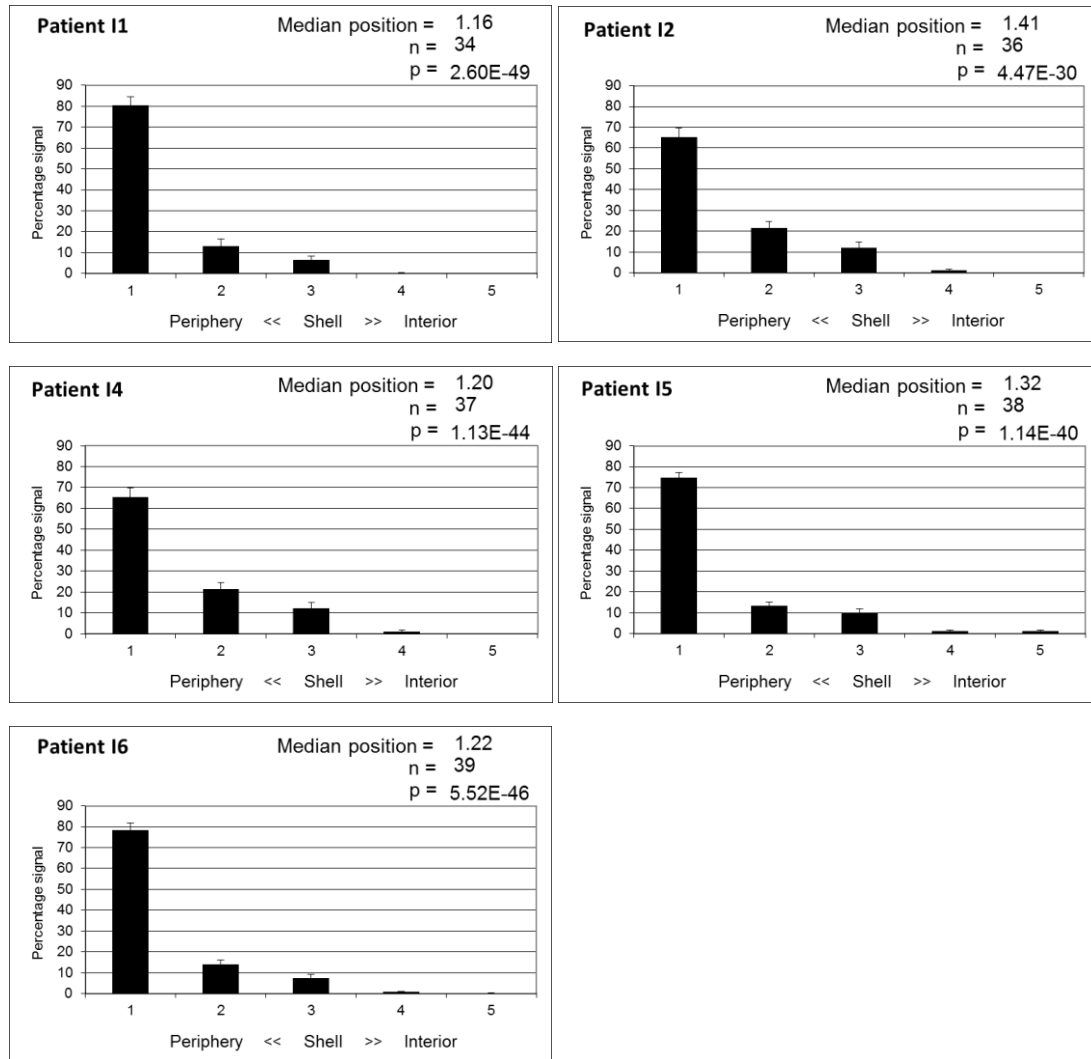


Figure 4: Telomere distribution patterns in the sperm heads of each individual infertile following 3D analysis of FISH signals. Error bars represent the standard error of the mean, n is the number of sperm nuclei analysed, p is the statistical significance of a non-random distribution assessed by Chi² test.

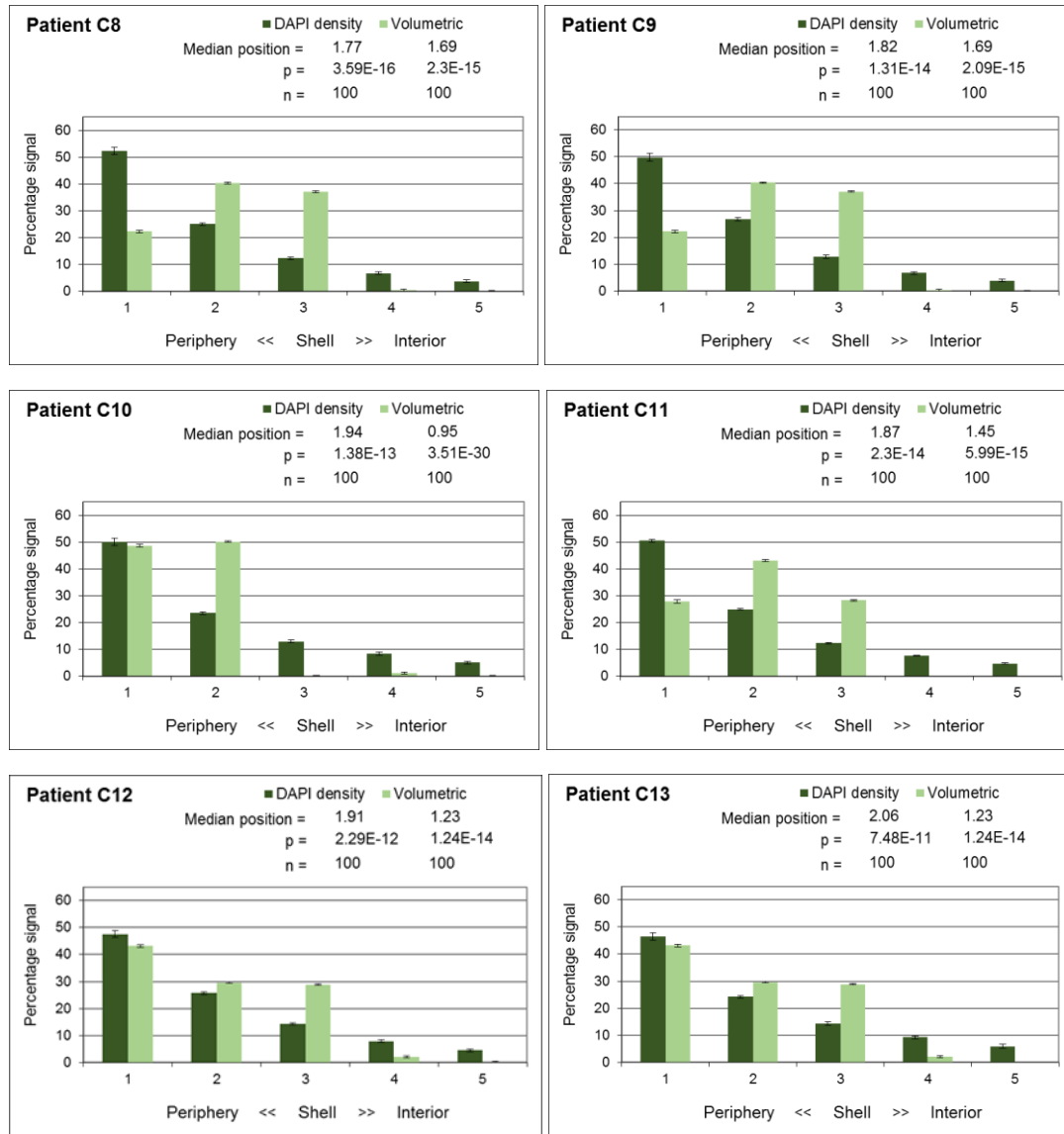


Figure 5: H2BFWT distribution in the sperm heads of each individual normal fertile male following 2D analysis of antibody staining patterns using DAPI density and volumetric compensation models. Error bars represent the standard error of the mean, n is the number of sperm nuclei analysed, p is the statistical significance of a non-random distribution assessed by Chi² test.

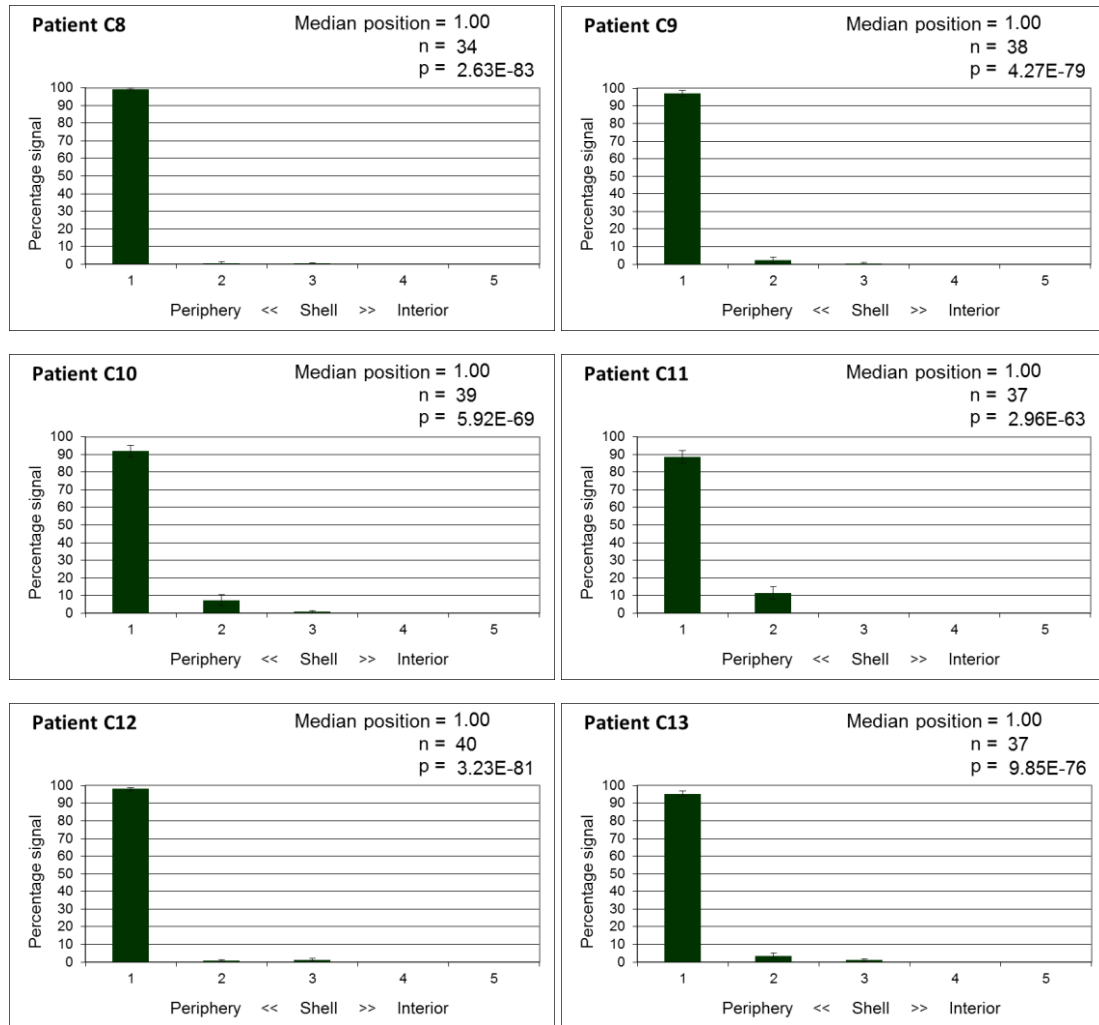


Figure 6: H2BFWT distribution in the sperm heads of each individual normal fertile male following 3D analysis of antibody staining patterns. Error bars represent the standard error of the mean, n is the number of sperm nuclei analysed, p is the statistical significance of a non-random distribution assessed by Chi² test.

10 Publications and activities arising from this thesis

10.1 Publications

Turner KJ, Vasu J, Greenall J, Griffin DK, (2014) Telomere length analysis and preterm infant health: The importance of assay design in the search for novel biomarkers. *Biomarkers in Medicine* 8 (4) 485 – 498.

10.2 Manuscripts in preparation

Turner KJ, Vasu J, Greenall J, George S, Griffin DK. Telomere length in the preterm infant

Turner KJ, Griffin DK. Telomere distribution as a marker of male factor infertility

Turner KJ, Lynch C, Rouse H, Griffin DK. Telomere length is not associated with reproductive ageing in women

10.3 Poster and oral presentations

Oral presentation, International Chromosome Conference, University of Bologna, Bologna, Italy, September 2013. ‘Altered chromatin packaging in male factor infertility’.

Oral presentation, Postgraduate Symposium, University of Kent, Canterbury, UK, July 2013. ‘Altered chromatin packaging in male factor infertility’.

Oral presentation, Neonatal Society Meeting, Canterbury Cathedral Lodge, Canterbury UK, May 2012. ‘Assay optimisation for telomere length analysis in newborn infants’.

Oral presentation, Postgraduate Induction Symposium, University of Kent, Canterbury, UK, September 2011. ‘The role of telomeres in human sperm nuclear organisation’.

Poster presentation, Turner KJ, Griffin DK. International Chromosome Conference, University of Kent, Canterbury, Kent, UK, September 2014. ‘Telomere distribution and nuclear organization in fertile and infertile males’.

Poster presentation, Turner KJ, Vasu V, Greenall J, George S, Lee. Z, Griffin DK. International Chromosome Conference, University of Kent, Canterbury, Kent, UK, September 2014. ‘Premature telomere shortening and its association with preterm birth’.

Poster presentation, Turner KJ, Vasu V, Griffin DK. Postgraduate Symposium, University of Kent, Canterbury, UK, July 2012. ‘Assay optimisation for telomere length analysis in newborn infants’.

Poster presentation, Turner KJ, Griffin DK. Wain Medal Lecture, University of Kent, Canterbury, Kent, UK, October 2012. ‘Chromatin packaging is altered in males with severely compromised semen parameters’.

Poster presentation, Turner KJ, Fonseka KGL, Mirzazadeh F, Ottolini CS, Griffin DKG. Wain Medal Lecture, University of Kent, Canterbury, Kent, UK, October 2011. ‘Human chromonomics: From the spermatozoon and the oocyte, to the embryo and beyond’.